WORLD SCIENTIFIC SERIES ON NONLINEAR SCIENCE

Series A Vol. 54

Series Editor: Leon O. Chua

DYNAMICS OF CROWD-MINDS

PATTERNS OF IRRATIONALITY IN EMOTIONS, BELIEFS AND ACTIONS

Andrew Adamatzky

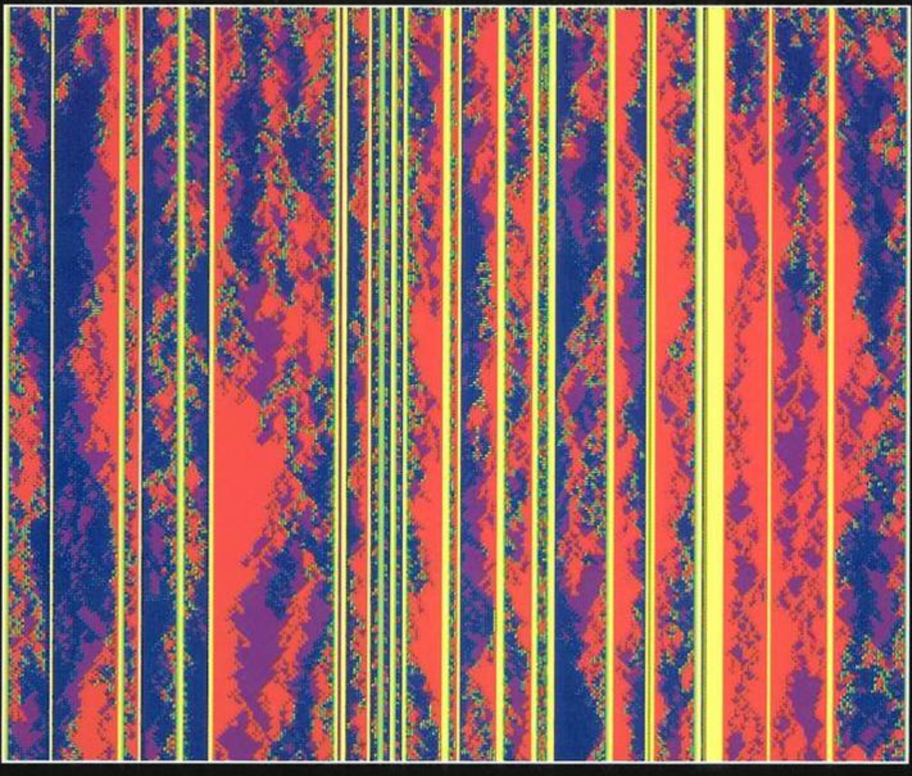

World Scientific

DYNAMICS OF CROWD-MINDS

PATTERNS OF IRRATIONALITY IN EMOTIONS, BELIEFS AND ACTIONS

WORLD SCIENTIFIC SERIES ON NONLINEAR SCIENCE

Editor: Leon O. Chua
University of California, Berkeley

Series A. MONOGRAPHS AND TREATISES

Volume 35: Introduction to Control of Oscillations and Chaos
A. L. Fradkov & A. Yu. Pogromsky

Volume 36: Chaotic Mechanics in Systems with Impacts & Friction
B. Blazejczyk-Okolewska, K. Czolczynski, T. Kapitaniak & J. Wojewoda

Volume 37: Invariant Sets for Windows — Resonance Structures, Attractors, Fractals and Patterns
A. D. Morozov, T. N. Dragunov, S. A. Boykova & O. V. Malysheva

Volume 38: Nonlinear Noninteger Order Circuits & Systems — An Introduction
P. Arena, R. Caponetto, L. Fortuna & D. Porto

Volume 39: The Chaos Avant-Garde: Memories of the Early Days of Chaos Theory
Edited by Ralph Abraham & Yoshisuke Ueda

Volume 40: Advanced Topics in Nonlinear Control Systems
Edited by T. P. Leung & H. S. Qin

Volume 41: Synchronization in Coupled Chaotic Circuits and Systems
C. W. Wu

Volume 42: Chaotic Synchronization: Applications to Living Systems
E. Mosekilde, Y. Maistrenko & D. Postnov

Volume 43: Universality and Emergent Computation in Cellular Neural Networks
R. Dogaru

Volume 44: Bifurcations and Chaos in Piecewise-Smooth Dynamical Systems
Z. T. Zhusubaliyev & E. Mosekilde

Volume 45: Bifurcation and Chaos in Nonsmooth Mechanical Systems
J. Awrejcewicz & C.-H. Lamarque

Volume 46: Synchronization of Mechanical Systems
H. Nijmeijer & A. Rodriguez-Angeles

Volume 47: Chaos, Bifurcations and Fractals Around Us
W. Szemplińska-Stupnicka

Volume 48: Bio-Inspired Emergent Control of Locomotion Systems
M. Frasca, P. Arena & L. Fortuna

Volume 49: Nonlinear and Parametric Phenomena
V. Damgov

Volume 50: Cellular Neural Networks, Multi-Scroll Chaos and Synchronization
M. E. Yalcin, J. A. K. Suykens & J. P. L. Vandewalle

Volume 51: Symmetry and Complexity
K. Mainzer

Volume 52: Applied Nonlinear Time Series Analysis
M. Small

Volume 53: Bifurcation Theory and Applications
T. Ma & S. Wang

WORLD SCIENTIFIC SERIES ON
NONLINEAR SCIENCE

Series Editor: Leon O. Chua

DYNAMICS OF CROWD-MINDS

PATTERNS OF IRRATIONALITY IN EMOTIONS, BELIEFS AND ACTIONS

Andrew Adamatzky
University of the West of England, Bristol, UK

World Scientific

NEW JERSEY • LONDON • SINGAPORE • BEIJING • SHANGHAI • HONG KONG • TAIPEI • CHENNAI

Published by

World Scientific Publishing Co. Pte. Ltd.
5 Toh Tuck Link, Singapore 596224
USA office: 27 Warren Street, Suite 401-402, Hackensack, NJ 07601
UK office: 57 Shelton Street, Covent Garden, London WC2H 9HE

British Library Cataloguing-in-Publication Data
A catalogue record for this book is available from the British Library.

DYNAMICS OF CROWD-MINDS

ISBN 981-256-286-9

Printed in Singapore by Mainland Press

This book is dedicated to those
who made my life good.

Preface

Mental dynamics of a large mass of believing emotional entities, crowd-minds, acting at the edge of, or sometimes far beyond, rationality, was a subject of psychological studies in the last hundred years. As early as 1895 a similarity between crowds and spatially distributed physical systems was implicitly brought up by Gustave Le Bon, who was a friend of Henri Poincare, and thus might have got a physical influence on his social theories [Le Bon (1994)]. However, phenomena of collective irrationality have never been studied from physics, mathematics and computer-science points of view. In the book we try to fill the gap, and thus develop and study computational and automaton models of a crowd-mind.

What is a crowd-mind? The crowd-mind emerges when formation of a crowd causes fusion of individual minds into one collective mind. In the crowd-mind "derationalized by passion, deactualized by memory, ideas and purposes are reborn as irrational beliefs and symbols" [Moscovici (1985)]. Members of a crowd lose their individuality. The deindividuation results in emotional, impulsive and irrational behavior, self-catalytic activities, memory impairment, perceptual distortion and hyper-responsiveness to local neighbors; ultimately, this leads to "distortion of traditional forms and structures" [Zimbardo (1969)]. As Everett Dean Martin wrote in 1920

> "... the crowd-mind is a phenomenon which should best be classed with dreams, delusions, and the various forms of automatic behavior" [Martin (1920)].

Rephrasing Ortega y Gasset, we can say that the crowd-mind does "not care to give reasons or even to be right", and this brings forward a key feature of the crowd-mind — the right not to be reasonable: "the reason of unreason" [Ortega y Gasset (1985)]. Serge Moscovici indicates three notable

symptoms of losing personality in favor of crowd mentality: decrease of intellectual component, increase of emotional component and disregard for personal profit [Moscovici (1985)].

A collective delusion emerges when thought disorder interacts with disturbances of affect [Winters and Neale (1983)]. The delusion may be seen as a symptom of mental disorder or at least collective divergence from the norm [Moscovici (1985)]. Collective behavior of crowd-minds is highly non-linear because of mutual actions between delusive thinking, emotional contagion and also "collective movements and collective outburst" [Smelser (1962)]. In the book we study the non-linearity of crowd-minds using cellular automata, algebraic structures, artificial-chemistry paradigms and mobile automata on lattices.

Andrew Adamatzky
February 2005

Contents

Preface vii

1. Crowding Minds 1

1.1 Non-linear psychology and sociodynamics 1
1.2 Crowds 4
1.3 Quasi-chemistry and cellular automata 8
1.4 Dual interpretation 13
1.5 Emotions, beliefs and actions 13

2. Patterns of Affect 23

2.1 Artificial chemistry of emotions 23
2.2 Happiness and sadness 25
2.3 Anger, fear and happiness 28
2.4 Happiness, anger, confusion and fear 32
2.5 Happiness, anger, confusion and sadness 35
2.6 Emotional abuse therapy 41
2.7 Affectons 48
2.7.1 Affectons in random environment 54
2.7.2 Reflecting singletons 57
2.7.3 Coupled affectons 58
2.7.3.1 Deterministic dynamic 58
2.7.3.2 Probabilistic dynamic 60
2.7.3.3 Unreachable emotional states 60
2.7.3.4 Longest transitions 62
2.8 Wicked feelings 62

3. Doxastic Dynamics at the Edge of Irrationality 67

3.1 On doxastic states and their binary compositions 69
3.2 Non-sense functors 74
3.3 Reflective agents 77
3.4 Stirred crowds 78
3.5 Non-stirred crowds 81
3.5.1 Development of doxatons from H-configuration . . . 83
3.5.2 Development of doxatons from Q-configuration . . . 86
3.5.3 Collective based on algebras of non-sense 90
3.5.3.1 Developing from H-configuration 90
3.5.3.2 Development of naive agents from Q-configuration 92
3.5.3.3 Development of contradicting agents from Q-configuration 93
3.5.3.4 Development of conservative agents from Q-configuration 94
3.5.3.5 Development of anxious agents from Q-configuration 94
3.6 Interacting doxastic worlds 96
3.7 Doxastic chemistries 99
3.7.1 Doxastic reactions 100
3.7.2 Rationalizing doxastic mixtures 102
3.8 Future is delusion 105

4. Normative Worlds 111

4.1 Norms 112
4.2 Properties of $\langle \mathbb{D}, \odot_N \rangle$ 113
4.3 Normalizing doxatons 116
4.4 Normalization of reflecting doxatons 118
4.5 Solutions of normalized doxatons 119
4.6 Quiescent states and sets 120
4.7 On stable neighborhoods 121
4.8 Homogeneity of doxaton local functions 121
4.9 Evolving from the homogeneous configurations 123
4.10 Fate of the singleton 124
4.10.1 Ignorant singleton 124
4.10.2 Doubting singleton 126

4.10.3 Delusional singleton . . . 130
4.10.4 Misbelieving singleton . . . 133
4.10.5 Singleton that knows . . . 137
4.11 Evolving from the random configuration . . . 143
4.12 Consequences of normalization . . . 145

5. Dynamically Non-trivial Logics 151

5.1 Artificial chemistry of logics: the model . . . 152
5.2 Non-trivially behaving systems . . . 153
5.3 Oscillatory logic $\langle T* \rangle$ . . . 158
5.3.1 Stirred reactors . . . 158
5.3.2 Thin-layer reactors . . . 162
5.4 Bifurcatory logic $\langle *T \rangle$ . . . 165
5.4.1 Stirred reactor . . . 165
5.4.2 Thin-layer reactor . . . 168
5.5 Emergence of complexity . . . 170
5.5.1 Static complexity of interaction rules . . . 171
5.5.2 Complexity of connectives . . . 174
5.6 Niche of non-triviality . . . 174

6. Morphology of Irrationality 181

6.1 Interval sensitivity . . . 182
6.2 Morphological classification . . . 185
6.2.1 Hyper-sociality: $\mathcal{C}$-class . . . 186
6.2.2 Autistic dissolution: $\mathcal{S}$-class . . . 188
6.2.3 Segregation: $\mathcal{H}$-class . . . 188
6.2.4 Socialization: $\mathcal{P}$-class . . . 190
6.2.5 Brewing of structure: $\mathcal{Y}$-class . . . 190
6.2.6 Structuring crowds: $\mathcal{L}$-class . . . 190
6.2.7 Ordered crowds: $\mathcal{F}$-class . . . 190
6.3 Time, size and order . . . 192
6.3.1 Size . . . 193
6.3.2 Convergence . . . 194
6.3.3 Order . . . 195
6.4 Rational choice and threshold of activation . . . 198
6.5 Upshots of unrest . . . 200
6.6 Boosting degree of unreason . . . 202
6.6.1 New faces of irrational morphology . . . 205

6.6.2 Density-based description 205
6.6.3 Necessary conditions 210
6.6.4 Fine structure of morphologies of irrational crowds . 210
6.6.4.1 $\mathcal{C}$-class 211
6.6.4.2 $\mathcal{S}$-class 211
6.6.4.3 $\mathcal{G}$-class 212
6.6.4.4 $\mathcal{P}$-class 213
6.6.4.5 $\mathcal{L}$-class 213
6.6.4.6 $\mathcal{W}$-class 215
6.6.4.7 $\mathcal{B}$-class 215
6.6.4.8 $\mathcal{M}$-class 216
6.6.5 Hierarchies of irrationality, hostility and unrest . . . 216
6.7 Controlling irrational crowds 220
6.7.1 Negation 220
6.7.2 (Con/Dis)junction of classes 221
6.8 Schizophrenia on a lattice 222

Epilogue 225

Glossary 227

Acknowledgments 231

Bibliography 233

Index 249

Chapter 1

Crowding Minds

In the book we exploit paradigms of non-linear psychology, artificial life and sociodynamics to simulate, analyze and characterize spatio-temporal dynamics of massive pools of mental entities, i.e. non-trivial dynamics of crowd-minds. In this chapter we give an informal introduction to the paradigms discussed, methods and techniques used, and provide a brief outline of the book's contents.

1.1 Non-linear psychology and sociodynamics

In 1949 Rashevsky proposed

> "... to construct a mathematical system of social sciences by starting with some plausible postulates about the interactions of two or more individuals. In principle these postulates should be derived from the equations of the mathematical biology of the central nervous system" [Rashevsky (1949)].

This idea was developed half-a-century later in physics-based approaches to sociology and collective intelligence. Results in pedestrian dynamics give us a good example of how social systems can be interpreted in physical terms. Thus, Helbing [Helbing (1992); Helbing *et. al* (1998)] successfully applied principles of molecular dynamics to the paradigm of social force. As Moscovici wrote

> "Physicists began to speak of crowds of molecules and to refer to such phenomena as mass phenomena. Thus we find the "same" atomization in nature and in society, a social image of "crowds" common to various branches of learning, a similar concern for a "science of confusion". For this is indeed a physics of confusion since all physical systems, all gases, tend towards confusion when the activity of some power is transformed into heat" [Moscovici (1985)].

Attractive analogies between reaction–diffusion, morphogenesis and pattern formation in social insect societies are made in [Bonabeau (1997); Bonabeau *et. al* (1998a)]. Dynamics of opinion formation [Kacperski and Hołyst (1999); Plewczyński (1998)] is another field where techniques of nonlinear physics are flourishing. As is reasonably highlighted in [Plewczyński (1998)], classical mathematical models of individual attitude change lead to entire uniformity of opinions in a collective of many persons (as in the case of a majority classification problem or voting). These models assume, sometimes implicitly, global interaction between the individuals, as in stirred solutions of reagents. Unfortunately, such situations quite rarely occur in the real world, which is ambiguous, uncertain and contradictory (see also [Axelrod (1997); Axelrod (1986)]).

New generations of models represent space–time dynamics of individual opinions. The models consider evolution towards stable clusters of individuals, who share minority opinions [Plewczyński (1998)]. Thus, for example, Plewczyński [Plewczyński (1998)] describes the social changes in a collective, with lattice topology, of individuals by a nonlinear Schrödinger equation by analogy with a superfluid and a weakly interacting Bose gas in an external potential. The approach proved to be fruitful not only in dynamics of opinions [Kacperski and Hołyst (1999); Plewczyński (1998)] but also in attitude change [Nowak *et. al* (1990)].

Studies of dynamics of excitation in a stadium give us probably the most impressive examples of physics-based interpretation of crowd dynamics. Thus, from video footage of people's behavior at a stadium it was derived that excitation waves travel with a speed of around 22 seats/sec and a wave width of around 6–12 m (15 seats) [Farkas *et. al* (2003)]. Further, the local behavior of participants can be interpreted in terms of a chemically

excitable medium with the following reaction set [Nagatami (2003)]:

$$\begin{aligned}&\text{Passive } + \text{Activated } \mapsto 2 \cdot \text{Activated}\\&\text{Activated } \mapsto \text{Refractory}\\&\text{Refractory } \mapsto \text{Passive.}\end{aligned}$$

Other examples of physics of mentality include the Hameroff–Penrose theory of consciousness based on dynamics of quantum coherent superpositions [Hameroff (2001); Hameroff *et. al* (2002); Hameroff and Penrose (1996); Hameroff (1998)] and dynamics of intelligence [Zak (1998); Zak *et. al* (1997)].

The non-linear physics approaches are reinforced by automaton-based computational techniques, exemplified by cellular-automaton models of artificial societies and emergence of societal structure in collectives of simple agents [Epstein and Axtell (1996); Gilbert and Conte (1995)] and populations of interacting finite automata [Axelrod (1997); Doran (1998); Jager *et. al* (2001)].

These and other results in physical interpretation of collective dynamics in groups, crowds and societies led to the formation of the new discipline of sociophysics [Helbing (1995b); Weidlich (2003); Stauffer and Kułakowski (2002)], with the first dedicated conference held in 2002 [Sociophysics (2002)]. In his overview of sociophysics [Stauffer (2002)], Stauffer mentions pioneering results on a physics-based approach to social dynamics, which include dynamics of social segregation [Schelling (1971)], social imitation and opinion formation [Callen and Shapero (1974)]. We also refer to early papers on physics-based market analysis [Beckman (1971)] (in this particular paper the term "social physics" is introduced explicitly). More recent fields developed in sociophysics include social percolation [Proykova and Stauffer (2002); Goldenberg *et. al* (2000); Solomon *et. al* (2000)], belief and rumor propagation [Kabashima (2002); Galam (2002)], pedestrian dynamics [Helbing (1992); Helbing (1993); Helbing *et. al* (1998); Helbing (1991); Helbing and Molnár (1995); Helbing *et. al* (2000); Burstedde *et. al* (2001); Kirchner and Schadschneider (2002)], traffic simulation [Mahmassani (1990); Mahmassani *et. al* (1990); Helbing (1995a); Wolf (1999); Visser and Nagel (2001); Helbing *et. al* (2002)], opinion formation and voting [Weidlich (1991); Babinec (1997); Kacperski and Hołyst (1999); Kacperski and Hołyst (2000); Alves *et. al* (2002)], and formation of cultural domains [Castelano *et. al* (2000)], active Brownian particles and swarm dynamics [Schimansky-Geier *et. al* (1995); Schweitzer and Schimansky-Geier (1994); Ebeling *et. al* (1999); Holyst *et. al*

(2000); Ebeling and Schweitzer (2002)].

Battlefield simulation is yet another emerging field of sociophysics; a brilliant overview is provided by Ilachinski [Ilachinski (2004)]. Some analogs between chemical and physical instabilities and dynamics of combatant masses can be found in [Clements and Hughes (2004)]. There mathematical modeling of the Battle of Agincourt [Clements and Hughes (2004)] shows that instability of the battle front led to loss of the French and Burgundian army in favor of the English army:

> "The Battle of Agincourt was lost ... by the greater army because of its excessive zeal for combat leading to sections of it pushing through the ranks of the weaker army only to be surrounded and isolated" [Clements and Hughes (2004)].

In parallel with non-linear dynamics of societies, a field of dynamical, non-linear, psychology flourished [Lewis and Haviland-Jones (2000); Mayne and Ramsey (2001); Abraham (1992); Sulis and Combs (1996); Butz (1997)] on a fertile soil of Minsky's "mind as a society of many agents" [Minsky (1988)], Dawkins's memes as an evolving space–time configuration of global mental states [Dawkins (1976)] and Dennet's theory of consciousness as a space–time configuration of a many-agent collective [Dennet (1991)]. Foundations of non-linear analysis of social and psychological systems were laid in [Abraham and Gilgen (1995); Guastello (1995); Vallacher and Nowak (1994)], and a mathematical analysis of consciousness (see e.g. [Goertzel (1996)]). Amongst pioneering works, we also mention mathematical models of emotions [Lettvin and Pitts (1943); Colby and Gilbert (1964)] and a cybernetic model of persecutory delusions [Melges and Fougerousse (1966)].

1.2 Crowds

In the book we exploit the science of crowds.

> "If we think of crowds as large numbers of people we typically imagine them as packed together in close proximity to each other. "(Too) many people in (too) little space" may serve as a preliminary schema signifying some basic communalities between phenomena of crowds and of crowding" [Kruse (1986)].

Talking about formation of crowds, Everett Dean Martin wrote:

> "The complex of ideas becomes a closed system, a world in itself. Conflicting facts of experience are discounted and denied by all the cunning of an insatiable, unconscious will. The fiction then gets itself substituted for the true facts of experience; the individual has "lost the function of the real". He no longer admits its disturbing elements as correctives. He has become mentally unadjusted — pathological" [Martin (1920)].

Why are crowds more interesting than groups? Smelser outlines three basic differences between small groups and collectives [Smelser (1962)]: (a) in a small group an individual can personally control a scene of operation, (b) while in the collective there is a sense of "transcending power", (c) the communication in small groups is global, and it is local in large groups, (d) small groups are mobilized by "direct machinery" and in large groups by incitation and agitation. In contrast to groups, see e.g. [Klein (1956)], crowds have no structure whatsoever (apart from topological order imposed on spatially extended models), no hierarchies and often no leadership. Also, high group cohesiveness and physiological arousal of crowd members will "shut down the self-regulation of behavior through private self-awareness reduction" and "enhance the likelihood that the individual's acts will be influenced by environmental stimuli ..." [Prentice-Dunn and Rofers (1989)].

Crowds are unique phenomena, whose studies may bring impressive results and fruitful discoveries. This is because the behavior of each person in a crowd can be reduced to a level of an abstract finite machine - due to the deindividuation process, and spatio-temporal dynamics of crowds may expose non-trivial modes and regimes — due to irrationality of crowd global behavior. This is why a crowd psychology is sometimes attributed to a "science of the irrational" [Moscovici (1985)].

A derationalization — when an individual joins a crowd he loses his rationality [Graumann (1985)] — happens because of deindividuation. Amongst several characteristics of crowd formation developed by Martin [Martin (1920)], we would like to highlight that a crowd is a mental phenomenon occurring simultaneously with gatherings, where repressed impulses are released and thinking is primitivised (individuals become more automaton-like).

"The crowd-mind is then not mere excess of emotion on the part of people who have abandoned "reason"; crowd behavior is in a sense psychopathic and has many elements in common with somnambulism, the compulsion neurosis and even paranoia" [Martin (1920)].

Why do people behave in crowds differently? Possible processes involved in deindividuation and irrationalization are listed in [Marx and McAdam (1994)]: (a) a large number of people within each other's view, (b) illusion of unanimity produced by group pressure, (c) diffusion of responsibilities, (d) anonymity ("In an impersonal sea of faces, the individual may come to feel that he or she cannot be called to account for the behavior in question" [Marx and McAdam (1994)]), (e) solidarity, (f) social facilitatio and (g) immediacy ("Some persons may become so immersed in the crowd that they respond more immediately and less reflectively to stimuli and suggestions for behavior than is usually the case" [Marx and McAdam (1994)]).

In the book we follow the idea of "pre-experimentalists" of group mind theory, by classification in [Turner (1987)], including Le Bon [Le Bon (1994)], Freud [Freud (1921)] and McDougall [McDougall (1921)], who explained unique features of crowds by three processes [Turner (1987)]:

- deindividuation: "the anonymity of crowd members and the sense of invincible power produced by being in a crowd lead to a diffusion of their feelings of personal responsibility, a loss of personal identity" [Turner (1987)],
- contagion: "actions and emotions spread through the crowd through a form of mutual imitation, leading to uniformity and homogeneity in which personal differences disappear" [Turner (1987)],
- suggestibility: "acceptance of influence on irrational grounds because some kind of emotional tie to and submissive attitude to a person or group" [Turner (1987)].

Deindividuation leads to automatic, delusive and irrational behavior. What is deindividuation?

"... deindividuation ... is a state of affairs in a group where members do not pay attention to other individuals *qua* individuals and, correspondingly, the members do not feel they are being singled out by others ... such state of affairs results in a reduction of inner restraints in the members" [Festinger *et. al* (1952)].

In 1969 Zimbardo [Zimbardo (1969)] outlined basic precedents for dein-

dividuation: (a) anonymity, (b) shared and diffused responsibility, (c) high group size, (d) temporal distortion (expansion of present and distantiating of past and future), (e) arousal, sensory input overload, reliance upon non-cognitive interactions, (f) unstructured situation, altered states of consciousness and (g) enhancement of affective–proprioceptive feedbacks.

In certain cases deindividuation caused by crowding arousal, diffused responsibility and reduced self-awareness may result in disinhibited and sometimes violent behavior [Prentice-Dunn and Rofers (1989)]:

> "Like the paranoiac, every crowd is potentially if not actually homicidal in its tendencies. But whereas with the paranoiac the murderous hostility remains for the greater part an unconscious "wish fancy", and it is the mechanisms which disguise it or serve as a defense against it which appear to consciousness, with the crowd the murder-wish will itself appear to consciousness whenever the unconscious can fabricate such defense mechanisms as will provide it with a fiction of moral justification" [Martin (1920)].

Deindividuation could also be considered as a defense against a threatening environment, as opposed to individuation desirable in a supportive social climate [Ziller (1964); Zimbardo (1969)].

Crowds are also irrational because changes in emotional arousal in crowds lead to derationalization [Kaufman (1999)]:

> "... too much emotional intensity causes the person to be so aroused that thinking and physical self-control become disorganized"[Kaufman (1999)].

Changing attitudes may be another reason for irrationality:

> "... The deeds of crowd members are not rationally controlled, because the thought process in crowds is used only to serve the prepotent interests, not to direct them ..." [Allport (1924)].

Association between a crowd and abnormality was also highlighted by Freud in his work on group psychology and the ego [Graumann (1985)].

Another explanation of a crowd's irrationality may lie in the mental regression of crowd members to childhood.

"He himself may be but a miserable clod, but the glory of his crowd reflects upon him. ... In the finality of his crowd-faith there is escape from responsibility and further search. He is willing to be commanded. He is a child again. He has transferred his repressed infantilism from the lost family circle to the crowd. There is a very real sense in which the crowd stands to his emotional life *in loco parentis*" [Martin (1920)].

Crowd-minds are also seen as substrates of unconsciousness:

"Simply that ideas and purposes, especially those contrived by science and rationality, have to undergo a series of metamorphoses before they can be accepted by the crowd. Once transformed into formulae, images, and similes they cease to be part of the conscious mind and enter the realm of the unconscious. Derationalized by passion, deactualized by memory, ideas and purposes are reborn as irrational beliefs and symbols" [Moscovici (1985)].

1.3 Quasi-chemistry and cellular automata

All through the book we use cellular-automaton and mobile finite automaton models and a paradigm of artificial chemistry.

Adopting an automaton approach we consider agents, affective and doxastic entities, as minimalist structures, atoms of emotions and cognition. Several attempts to build a framework of knowledge and belief automata have been successfully made before; see e.g. [Manevitz (1989)]. Emergent properties of automata networks were considered to be a possible tool to manage uncertainty; see [Ligomenidas (1991)]. One of recent examples of how someone can use finite automata when dealing with terminological representational languages is given in [Baader (1996)]. A cellular-automata-based interpretation of knowledge, belief and action distributed among agents is proposed in [Adamatsky (1995b); Adamatzky (1998b); Adamatzky (1998c); Adamatzky (1995a); Adamatzky (1999)]; there problems of the approximation, or reconstruction, of functions of local evolution of epistemic, doxastic and action components from the given set of global configurations of mental states are discussed.

Automaton models were already proved to be successful models of artificial collectives in the 1940s when discrete spaces of finite-state machines were employed to imitate social segregation (see [Hegselmann and Flache

(1998)]); in the 1950s chains of finite and locally interacting automata were studied in a context of game theory (see [Tsetlin (1973)]). A recent boost in automaton models of social behavior is due to development of paradigms of artificial societies [Epstein and Axtell (1996)], particularly automata models of growing societies [Gilbert and Conte (1995)] and populations of finite automata [Axelrod (1997); Doran (1998)], social impact on opinion formation [Nowak *et. al* (1990)] and automaton interpretation of logic [Schaller and Svozil (1996); Svozil and Zapatrin (1996)]. Hereby, we mention that even some of the connectionist models are rooted in cellular-automata semantics; see e.g. [Read and Miller (1998)].

Artificial societies is yet another field where automata models gained success. This deals with emergence of societal structure in collectives of simple agents [Epstein and Axtell (1996)]. The research focuses mainly on automata models of growing societies [Gilbert and Conte (1995)] and populations of interacting finite automata [Axelrod (1997)]. Behavior of automaton models of agent collectives becomes even richer, and obtains a sense of artificial social life [Bainbridge *et. al* (1994)], when agents are made believable [Hadley (1991a)], emotional context of belief is taken into account [Frank (1998)] or mutual belief is analyzed [Tuomela (1996)]. Thus, for example, it is verified in computer experiments with populations of mobile automata, competing for resources, that a collective misbelief, when co-existing in space and time with a collective belief, may increase survivability of the entire population [Doran (1998)].

Automaton models of crowd-minds seem to be capable for perfectly grasping intrinsic processes of crowd mental dynamics because crowds exhibit lower levels of control and have shorter time scales with more discrete and concrete standards:

> "... the crowd does not think in order to solve problems. To the crowd-mind, as such, there are no problems. It has closed its case beforehand" [Martin (1920)].

Members of a crowd "are impulsive and respond with little foresight", they are "inextricably wrapped up in the cues of the moment" [Prentice-Dunn and Rofers (1989)].

A cogitoid — a computational model of cognition, where knowledge is represented by a lattice of concepts and associations between the concepts [Wiedermann (1998b)] — is yet another example of "automaton mentality". It is demonstrated in [Wiedermann (1998b)] that cogitoids realize

basic behavioral patterns including Pavlovian conditioning. In the cogitoid the concepts, like automaton states, can be represented by quantities of strength, non-negative integers, and by qualities, integers, whereas associations between the concepts possess a weight [Wiedermann (1998a)].

Several fundamental postulates, which support vitality of finite-automata models of consciousness are provided in [Alexander (1997a)], where a model of artificial consciousness is built on the basis of automaton models of neural networks. In automaton neural models in [Alexander (1997b)] consciousness is represented in the firing patterns of neurons: as soon as every neuron can be simulated by an automaton, up to some degree of correctness, the theory converges to a representation of consciousness in terms of finite state machines. There are some remarkable connections with cogitoids [Wiedermann (1998a)]; for example, when concepts are encoded by inner neurons.

Micro-tubules, which form neuron skeletons and indeed are simulated in cellular automata when every tubulin unit is represented by a cell, form a physical basis of the OR theory of consciousness [Hameroff and Penrose (1996); Hameroff (1998)]. It is claimed that consciousness occurs in multi-component systems, which are capable of developing and maintaining quantum coherent superpositions. Every superposition lasts until some event, e.g. exceeding of a threshold, occurs. The coherent state collapses after that. Thus, streams of self-collapsing particles represent a flow of consciousness. So, a subject of consciousness is seen as a massively parallel collective of very simple particles acting coherently.

A paradigm of computational chemistry — molecules represent computational processes — was firstly brought into effective action in a context of self-maintenance of a system and the autopoiesis [Varela *et. al* (1974); McMullin and Varela (1997)]. A molecule in computational chemistry is a symbolic representation of an operator, the molecule's behavior is the operator's action, and a chemical reaction is an evaluation of the functional application [Fontana and Buss (1996)]. Also, a chemical abstract machine — a stirred solution defined by a molecule algebra and rules of molecules' interaction — was invented in [Berry and Boudol (1992)] to realize a paradigm of interaction between molecules in algebraic process calculi [Berry and Boudol (1992)]. In Berry–Boudol's universe a state of a concurrent system is seen as a stirred solution, where molecules of reagents interact with each other according to some specified reaction rules. The process is parallel because all pairs of molecules can interact at once. To set up an architecture of a specific machine, one defines a molecule algebra

and rules of interaction between the molecules. Recently, the artificial-chemistry paradigm emerged and formed a new field concentrating on such issues as self-organization and complexity, and non-standard computation; see an overview in [Dittrich *et. al* (2001)]) and an application of a chemical paradigm to simulate evolution of knowledge and emotions in [Adamatzky (2001c); Adamatzky (2002b)]. So, by representing mental states of agents as chemical species, we can design a quasi-chemistry-like reaction between the mental states. The idea has been around for some time and, already in 1967, while talking about social context of riots in the black ghetto of Milwaukee, Slesinger used somewhat chemical terminology:

> "... to distinguish between possible catalytic events leading to the outbreak of a civil disturbance and the presence of underlying social, economic, and political conditions which seem to be necessary before the catalyst can precipitate a reaction" [Slesinger (1968)].

To study artificial chemistry of well-stirred reactors in computational experiments we numerically integrate systems of first-order ordinary differential equations [Press *et. al* (1993)]. We represent thin-layer reactors, where chemical species and micro-volumes interact locally, as systems of partial differential equations, and also model these reaction–diffusion systems as cellular neural (non-linear) networks [Chua (1998)]), as well as cellular automata.

A cellular automaton is an array of uniform finite automata, which update their states in parallel, and each automaton calculates its next state depending on states of its closest neighbors (see e.g. [Toffoli and Margolus (1987); Ilachinski (2001)]); we experiment with a one-dimensional cellular automaton, each cell of which updates its state depending on states of its left and its right neighbors.

Using differential equations, cellular non-linear networks and cellular automata we can therefore represent quasi-chemical reactions between belief states and emotion states in the three following ways. Let a set of reactions be

$$X + Y \to^{k_1} 2Z$$
$$Z \to^{k_2} X,$$

with reagents X, Y and Z and reaction rates k_1 and k_2. This may be interpreted as follows: a person expressing affective or doxastic state X meets a person expressing state Y, they observe each other's expressions and change their affective or doxastic states to state Z. Thus the dynamic

of affective or doxastic species in a well-stirred reactor can be simulated as

$$\begin{aligned}
\dot{x} &= -k_1 xy + k_2 z = \varphi(x, y, z) \\
\dot{y} &= -k_1 xy = \psi(x, y) \\
\dot{z} &= k_1 xy - k_2 z = \phi(x, y, z),
\end{aligned}$$

where x, y and z are concentrations of affective or doxastic states X, Y and Z.

The space–time dynamic of doxastic or affective reagent concentrations can also be modeled in a one-dimensional cellular neural (non-linear) network as

$$\begin{aligned}
\dot{x}_i &= \varphi(x_i, y_i, z_i) + D_x(x_{i+1} + x_{i-1} - 2x_i) \\
\dot{y}_i &= \psi(x_i, y_i) + D_y(y_{i+1} + y_{i-1} - 2y_i) \\
\dot{z}_i &= \phi(x_i, y_i, z_i) + D_z(z_{i+1} + z_{i-1} - 2z_i),
\end{aligned}$$

where i is a space index, and D_x, D_y and D_z are diffusion coefficients of affective or doxastic state reagents. In a cellular-automaton model every cell has two neighbors, left and right, takes three states X, Y and Z and updates its states by the following rule. A cell being in state Z takes state X. A cell changes its current state X (Y) to state Z if there is at least one neighbor in state Y (X). If c_i^t is a state of cell c_i at time t, then the cell's state-transition rule looks as follows:

$$c_i^{t+1} = \begin{cases} X \text{ if } c_i^t = Z, \\ Z \text{ if } [(c_i^t = X) \text{ and } ((c_{i-1}^t = Y) \text{ or } (c_{i+1}^t = Y))] \text{ or} \\ \qquad [(c_i^t = Y) \text{ and } ((c_{i-1}^t = X) \text{ or } (c_{i+1}^t = X))]. \end{cases}$$

Amongst these three models only the cellular-automaton one can be probabilistic, when, due to specifics of reactions simulated, a cell takes different states, corresponding to the same configuration of the cell's neighborhood, with certain probabilities.

In some cases, we used a chemical kinetics simulator [CKS], working on principles of discrete stochastic simulation. A chemical reactor there is portrayed as a system of discrete particles where each particle represents a certain amount of reagents; an interaction of reagent pools is simulated via interaction of particles.

1.4 Dual interpretation

In the book we allow for a dual interpretation of dynamics of emotional and cognitive collectives. First, we can talk about our models as representing dynamics of beliefs, emotions and irrational behavior of human crowds, where every person is reduced to a simple automaton or a chemical species. Second, we sometimes adopt a representation of the human mind as a collective of simple "mental" entities, affective and doxastic quanta.

A multi-agent representation of the human mind has a long history. We can find artificial intelligence, biological and philosophical backgrounds of a multi-agent mind in Minsky's ideas of mind as a society of many agents [Minsky (1988)], Dawkins's memes, ideas and beliefs, which diffuse in the noosphere and represent some kind of evolving space–time configuration of global mental states [Dawkins (1976)] and Dennet's theory of consciousness as a space–time configuration of a many-agent collective [Dennet (1991)]. Recent results in the field include Wiedermann's cogitoid [Wiedermann (1998b)], Hameroff–Penrose's OR theory of consciousness [Hameroff and Penrose (1996); Hameroff (1998)] and Alexander's artificial neural consciousness [Alexander (1997b)]. The processes of crowd dynamics can be interpreted in terms of an individual's mental dynamics:

> "The crowd-self ... is analogous in many respects to "compulsion neurosis", "somnambulism", or "paranoic episode". Crowd ideas are "fixations"; they are always symbolic; they are always related to something repressed in the unconsciousness" [Martin (1920)].

1.5 Emotions, beliefs and actions

In the book we aim to demonstrate rich spatio-temporal dynamics of crowds at three basic levels of cognitive behavior – emotions, beliefs and actions. They are discussed in a "natural order", from emotions to beliefs to actions:

> "... thinking, no matter how well articulated, is not sufficient for action. ... Emotions are prime candidates for turning a thinking being into an actor" [Frijda *et. al* (2000)].

Space–time dynamics of emotions in large-scale collectives is studied in the second chapter; this is followed by non-linear models of belief development in "unregulated" crowd-minds and crowd-minds constrained by

norms. The first three forthcoming chapters build up a computational theory of disordered mentality expressed in terms of affects and cognition. Then we introduce logical systems derived from space–time dynamics of crowd-minds, to speculate about possible logics behind irrationality. Finally, we establish morphological correlates of irrational behavior, and uncover surprising facts about morphological complexity of irrationality.

In the second chapter we study affective mixtures. An affective mixture is a theoretical construct which represents emotions spreading and reacting one with another as a massive pool of locally interacting entities. Molecules of the affective mixture correspond to basic emotions – happiness, anger, fear, confusion and sadness — which diffuse and react with each other by quasi-chemical laws. In computational experiments with affective solutions, in well-stirred and thin-layer reactors, we uncover and classify varieties of behavioral modes and regimes determined by particulars of emotion interactions. We test applicability of affective solutions in an idealized situation of emotional abuse therapy. Results outlined in the chapter indicate that a paradigm of affective solutions offers an unconventional but promising technique for designing, analyzing and interpreting integral and spatio-temporal dynamics of mass moods in crowds.

The second chapter is structured as follows. We introduce an artificial chemistry of emotions, a theoretical paradigm, a vision of emotions as abstract chemical species interacting with each other by certain rules similar to quasi-chemical reactions. Several reaction schemes involving happiness, sadness, anger, fear and confusion are analyzed in detail, and spatio-temporal dynamics of the affective quasi-chemical mixtures is studied in cellular-automaton models. A case of emotional abuse therapy is provided as an example of possible practical applications of theoretical findings on behavior of affective mixtures. The second chapter is completed with discussions of affectons — finite-automata models of emotional interactions. An affecton is an emotional automaton which takes states from a set of basic emotions — happiness, anger, confusion, anxiety and sadness, and updates its state depending on its current state and a state of its input (which is also a state-emotion). We define several classes of emotional automata and study dynamics of reflecting affectons and automata in a random environment; we also analyze behavior of coupled affectons using their global state-transition graphs. These toy models of emotional automata are based on our early results in automata models of and algebraic approaches to the study of cognition — simulation of hierarchical groups of believers [Adamatzky (1998c)] and cellular-automaton and artificial-chemistry

models of doxastic evolution [Adamatzky (2001d); Adamatzky (2001a); Adamatzky (2001c)]. In the second chapter we concentrate rather on formal properties of emotional automata and try not to draw any common-sense consequences from results of our studies. Finite-automata models discussed in the chapter should be considered as a preliminary step towards a full-scale formal theory of emotional interactions.

Why do we develop a formal theory of emotional interactions? First, emotions are a basis of cognition [Bates (1994); Chalmers (1996); Goleman (1996); Picard (1997)]. Emotions form a unique primary, fast, component of intelligent response to an external stimulus; beliefs constitute the secondary, slow, component [Eckman (1992); Goleman (1996)]. Therefore, formal models of emotions must be incorporated in mathematical models of computation and cognition. Second, emotions rather than knowledge govern behavior of crowds, which are better in feelings than in reasoning [Graumann and Moscovici (1985); Le Bon (1994); McPhail (1991)]. This is why emotions have to be taken into account in designing mathematical models of social dynamics and in developing algorithms of decentralized computing. Third, robotics lacks architectures of truly emotional robots, that do not simply express but also experience and communicate their emotions to other robots and humans [Breazeal and Scassellati (1999); McCarthy (1979); Scheeff *et. al* (2000)].

Do emotions really interact? They do not interact *per se* but via their carriers, persons. Emotions are contagious in a sense that emotional perturbations spread in groups and collectives (most members of which but a few are assumed to be initially in a "no-emotions" state!):

> "The precipitating stimuli arise from one individual, act upon ... one or more other individuals, and yield corresponding or complementary emotions ... in these individuals" [Hatfield *et. al* (1992); Hatfield *et. al* (1994)].

The contagion may be based on imitation and facial mimicry, which cause an affective feedback from facial receptors and neurons [Hatfield *et. al* (1992); Hatfield *et. al* (1994)]; sometimes the contagion is seen as a mechanism of physiological synchronization [Levenson and Ruef (1997)]. However, surprisingly few publications deal with interaction between emotions; see e.g. [Hatfield *et. al* (1994); Levy and Nail (1993); Marsden (1998)]. We know that persons in certain emotional states would more likely to change their emotions when they encounter persons in other

emotional states, for example

> "It is happy people who are most receptive to others and most likely to catch their moods; the unhappy seem relatively oblivious to other' feelings and to contagion" [Hatfield *et. al* (1994)].

This means that a matrix of binary interaction of emotions may have quite a non-trivial form. Particulars of emotional interaction are usually dependent on emotions' strength, context of emotional interaction and vectors of interpersonal relationships, for example:

> "Angry faces sometimes stimulate fear as well as anger; another's fear may put us at ease" [Hatfield *et. al* (1994)].

What is a minimal computation model of emotional interactions? Given a finite set of emotional states one need only to define a binary composition of emotions to construct a minimalist model. The model would already represent how someone's emotion is changed when he or she interacts with someone else. To make the representation more close to reality one can say that the finite set of emotional states is a state set of a finite automaton and the binary composition is the automaton's state-transition function. This will also allow us to study linked evolution of emotions in automaton collectives.

Most examples of emotional developments, discussed in the second chapter, exhibited affective dynamics at the edge of pathology. Pathology is one of the key consequences of crowding; either it is a crowding of persons or a crowding of thoughts in our brains. We continue the theme of near-pathological mentality of crowd-minds in the third chapter of the book. There we use a conventional belief state to derive states of knowledge, misbelief, delusion, doubt and ignorance, and to construct and study non-trivial compositions of the doxastic states. We show that the compositions truly reflect "abnormalities" of crowd behavior, and that quasi-chemical and finite-automaton models of doxastic collectives express intriguing spatio-temporal dynamics.

Several interesting algebraic properties of the doxastic compositions are studied, and deterministic derivatives of the compositions are analyzed in terms of naive, conservative, anxious and contradictory agents. We study discrete dynamics of reflecting agents and stirred pools of agents in terms of finite automata. We show that non-stirred, or ordered, collectives of agents exhibit in their evolution the richest possible range of space–time

phenomena from competing domains of regular patterns to random trees and triangles. They are analyzed in detail, including the possible influence of algebraic properties of doxastic compositions on space–time patterns of doxastic derivatives that emerge in the evolution of agent collectives. We also determine products of so-called interacting doxastic worlds, where every world is an element of a Boolean of the set of doxastic states, to enforce our insight in domains of attracting and impossible worlds.

To study well-stirred pools of doxastic entities we also adopt an artificial-chemistry approach. Five derivatives of belief — knowledge, misbelief, delusion, ignorance and doubt — are considered to be reactants of an abstract chemical solution. These quasi-chemical species react one with another by certain rules obtained though an unconventional interpretation of a belief update. Several types of reaction systems are studied in computational experiments with the doxastic solutions. A global dynamic of doxastic chemical solutions is also interpreted from a common-sense point of view. Non-stirred pools of doxastic "quanta" are simulated in lattices of doxatons — finite automata which take states of knowledge, misbelief, delusion, ignorance and doubt.

Such diverse fields of artificial intelligence as distributed intelligence, social dynamics, artificial society and collective mind and consciousness deal with believing agents. Despite being so long under the scope of philosophy, logic and computing sciences, only recently was a belief started to be considered as not ideal and believers themselves as not omnipotent. Some non-classical logics and computational models began to incorporate a fallible belief in their framework; see [O'Hara *et. al* (1995); Fagin and Halpern (1988); Gärdenfors (1990)]. Recent research proves that agents can recognize other agents' mental states, including beliefs and intentions [Tambe *et. al* (1998)]. A non-standard, and sometimes even pathological, interaction between people's mental states in developing crowd situations [Le Bon (1994); Smelser (1962)], collective delusions and hysterias got a "proper" formal interpretation just recently; see e.g. [Summers and Markusen (1999); McPhail (2001)]. However, despite the success of non-traditional approaches to researching a collective belief, a diversity of doxastic states was almost left out of consideration. Quite typically, only belief and knowledge are employed in commonly used logical or computation models. The importance of delusion, misbelief, doubt and ignorance was unfairly underestimated.

A context of the doxastic states' updating is also a missing point of modern research. Realistically, a behavior of individuals is governed by a

pleiad of momentary mental states, which undoubtedly include emotions, intentions, dreams, desires and imaginations. More often than is usually expected, the mental states, and beliefs in particular, are updated irrationally or even pathologically. A reversibility of knowledge and imperfect evolution of collective beliefs is also quite a common phenomenon. Thus, for example, it was shown that a false belief may be successfully spread in a social group if supported by falsified judgements or self-fulfilling processes [Burns and Gomolinska (2001)]. Also, in situations of an emotional contagion [Hatfield *et. al* (1994)], we could possibly talk about a cognitive contagion, where one or another state of belief acts upon several individuals of a collective and, as a result, invokes complementary doxastic states. Thus third chapter uncovers and exploits the diversity of the doxastic states and particulars of space–time dynamics of locally interacting doxastic entities.

Norms are the most likely instrument for dealing with abnormal behavior. So, in the fourth chapter, we discuss how norms may influence the space–time dynamic of doxastic components of artificial crowds. A mental state of an agent is characterized by the agent's belief in some proposition and a truth value of the proposition in the agent's local vicinity. Doxastic compositions derived in the third chapter are mainly indeterministic; however, we can make them deterministic by applying norms. These norms are expressed as priority orders over doxastic states. In computer experiments with space–time evolution of well-stirred mixtures and lattices of doxatons we demonstrate how norms and initial conditions can influence the behavior of abstract collectives of simple agents. A set of findings, discussed in the fourth chapter, include controllable diffusion of doxastic states and formation of stationary patterns of doxastic states.

Conventional logics do not work in crowds because deindividuation leads to emergence of an abnormal collective mind, which becomes irrational due to cognitive and affective overload. In the fifth chapter we develop a logical basis for irrationality of crowd thinking. We "breed" logical systems which behave non-trivially when interpreted in terms of dynamical systems. We construe three-valued logical systems as pools of abstract chemical species; logical variables, involved in chemical reactions, are catalyzed by logical connectives. Then we study global and space–time dynamics of these "logical" chemical reactors. We derive a family of combinatorial systems $\langle\{T,F,*\},\wedge\rangle$, where T, F and $*$ are truth values, $\wedge$ is a commutative binary operator and $\wedge$ acts as a Boolean conjunction on $\{T,F\}$; $*\wedge*=*$, $T\wedge*=a$ and $F\wedge*=b$, with $a,b\in\{T,F,*\}$. We look at nine combinatorial systems of the family, specified by values of a and b, and derive

from each member $\langle ab \rangle$ of the family an artificial-chemical system, where interactions between reactants T, F and $*$ are governed by $\wedge$. In computational experiments with well-stirred reactors, we show that all systems but $\langle T* \rangle$ and $\langle *T \rangle$ exhibit a dull behavior and converge to their only stable points. In a reactor of the system $\langle T* \rangle$, catalyzed by $\wedge$, concentrations of reactants oscillate while a reactor of the system $\langle *T \rangle$ finishes its evolution in one of two stable points. Thus we call the models of $\langle T* \rangle$ and $\langle *T \rangle$ oscillatory and bifurcatory systems. Further, we enrich the systems with a negation connective, define additional connectives via $\neg$ and $\wedge$ and undertake a detailed study of the integral dynamic of the artificial stirred chemical reactors and of the space–time dynamic of thin-layer non-stirred chemical reactors derived from the logical connectives. We demonstrate that thin-layer reactors exhibit a rich space–time dynamic ranging from breathing patterns and mobile localizations to fractal structures. A primitive hierarchy of connectives' phenomenological complexity of non-trivially behaving logical systems is constructed therefor.

In the sixth chapter we uncover morphological consequences of irrational behavior. There we study collectives of mobile agent-automata, inhabiting a two-dimensional lattice. For every step of discrete time an agent-automaton decides if it moves at random or stays in its current node depending on a number of occupied neighboring nodes. Agents behave irrationally because they do not simply dislike to stay in neighborhoods with "density" exceeding a certain threshold but an agent moves if the number of other agent-automata in its neighborhood belongs to some specified interval or, in more complex models, a set of integer numbers. Eventually, all agent-automata find their appropriate positions and stop moving; a stationary global pattern of resting agents is finally formed. The morphology of these patterns of resting agents is studied in the sixth chapter. We define a degree of irrationality of an agent's behavior in terms of lower and upper boundaries of an action interval or a structure of an activation set; then we build a mapping between irrationality of agents' behavior and morphology of stationary patterns formed by the agents. Thus, we are making the first step towards a morphological theory of irrationality.

Natural collective phenomena, for example movement of crowds of pedestrians and the impressive nest formations of social insects, provide us with an existence proof that sophisticated constructions may be built by swarms of relatively simple artificial agents. The constructions often appear to have required impressive control and coordination — yet each agent in the collective does not appear to be provided with an internal world model

or blueprint for the complete construction. These macroscopic structures emerge as the consequence of interaction of agents, carrying out simple rules based upon the local state of the world, which includes the interaction between agents and the growing structure. In the sixth chapter we characterize structures emerging in pools of irrationally behaving agents.

Considering the sixth chapter in a context of pattern formation in massive pools of discrete entities, we would like to provide several reasons for this subject to be so important. First, discrete models offer an alternative to conventional methods of numerical solutions of partial differential equations, an alternative which is so attractive because we can control parameters of behavior of each entity of the model and virtually program global behavior via local interactions of elements [Toffoli and Margolus (1991)]. Impressive results in distributed building in collectives of simple mobile agents [Bonabeau (1997)] and in design of smart matter [Hogg and Huberman (1998)] prove the viability of the discrete approach. Second, discrete models are fully scalable. They describe equally well reaction–diffusion systems [Schimansky-Geier *et. al* (1995)], externally driven granular material [Melo *et. al* (1995)] and crowds of pedestrians [Helbing (1991)]. Third, a selfishness and also irrationality, or even a state far from mental equilibrium, of an elementary entity can be accounted for during simulation. This may be particularly useful in situations when behavior of an entity, e.g. agent, violates physical laws. Thus, for instance, self-driven particles [Vicsek *et. al* (1995)] are not especially common in physics; however, they have many real biological and sociological counterparts. A fluid-like dynamic of pedestrians [Helbing (1992)] is, probably, the best example. The pedestrian dynamic together with micro-simulation of pedestrian crowds forms a new sub-discipline, at the edge of physics, computer science and sociology — *sociodynamics* [Helbing (1991)]. A concept of active Brownian particles, i.e. diffusing particles that generate a self-consistent field, offers another example [Schimansky-Geier *et. al* (1995); Ebeling *et. al* (1999); Ebeling and Schweitzer (2002)]. The concept, applied to real phenomena of cell migration, gas discharges and catalytic surfaces, where only a few particles form a stable macroscopic structure, demonstrates that a continuous description is not appropriate and the discrete nature of the phenomena must be employed. A vibrating granular material is last but not least an example in the raw of discrete models with emergent properties. It is shown that various kinds of two-dimensional patterns are formed in a vertically vibrated thin granular layer [Melo *et. al* (1995)]. A transition between different classes of patterns may

be observed when the amplitude of vibration is changed while the frequency of vibration is kept fixed. Experimental and simulation studies report a wide range of patterns: hexagons, standing waves, labyrinthine patterns, stripes and localized structures [Umbanhowar *et. al* (1996); Strassburger and Rehberg (2000)].

* * *

As Marx and McAdam noted

> "The field of collective behavior is like the elephant in Kipling's fable of the blind persons and the elephant. Each person correctly identifies a separate part, but all fail to see the whole animal. The logic involves emergent group behavior in settings where cultural guidelines are non-specific, inadequate, in dispute, or lacking altogether" [Marx and McAdam (1994)].

We hope that models and paradigms developed in the book will contribute towards building of a coherent mathematics- and physics-based theory of collective mentality.

Chapter 2

Patterns of Affect

How do emotions unfold in massive pools of simply interacting entities? What would happen to a happy missionary surrounded by sad islanders? What would be a reaction of your colleagues if you start crying in your office? What would locals in a pub do to you if you become aggressive? The missionary will become sad, your colleagues will be confused and you are likely to be beaten by the locals. We can easily predict ultimate outcomes of emotional disturbances; however, anticipation of a fine dynamic of affects — particularly in spatially extended media at the edge of affective disorder — becomes a non-trivial task. Mathematical and computer models of emotions [Lettvin and Pitts (1943); Colby and Gilbert (1964); Gottman (1997); Marin and Sappington (1994); Chandra (1997)], developed so far, are mainly about decision making and statistical analysis of neural network analogies of emotion formation, and are barely applicable to crowds or even small groups. The missing link — from emotions in the small to affect in the massive — is restored in this chapter, in studies of "automatic, unintentional and mostly inaccessible to conversant awareness" [Hatfield *et. al* (1992)] instances of interactions between emotions in a quasi-chemical sense [Adamatzky (2002c); Adamatzky (2004); Adamatzky (2002b)]. So, we develop a concept of artificial chemistry of emotions and then analyze dynamics of affective mixtures.

2.1 Artificial chemistry of emotions

Artificial chemistry of emotions represents emotions as molecules of abstract "chemical" species. The molecules react with each other, they "disappear", multiply or are transformed to other types of molecules, and thus other emotions, as a result of their interactions. Chemical reactions in affec-

tive solutions are derived from real-world-like laws of interactions between emotions.

Emotions spread and interact in crowds and collectives similarly to molecules diffusing and reacting in chemical mixtures. Emotional contagion is a natural pre-requisite for reaction and diffusion in affective solutions:

> "The precipitating stimuli arise from one individual, act upon (i.e. are perceived and interpreted by) one or more other individuals, and yield corresponding or complementary emotions ... in these individuals" [Hatfield *et. al* (1994)].

From three types of emotional contagion — consciousness analysis, unconditional responses and mimicry — discussed in [Hatfield *et. al* (1994)], we select unconditional, and somewhat momentary, emotional responses as a basis of interaction between affective reactants:

> "When someone yells and screams at you, generally you do not think, "Well, that must be anger, rather than fear; I will try to understand it", at least not at that moment and perhaps never. Instead you flinch, cower, or yell back" [Planalp (1999)].

In computational experiments we will try to incorporate all possible answers to the question:

> "When is the emotion caught the same as, complementary to, or opposite from the emotion expressed?" [Hatfield *et. al* (1992)].

Some of the affective reactions studied are selected due to their interesting dynamics, while others do reflect real-life interactions. There are experimental findings on diffusion and reaction of emotions; see e.g. a detailed account of modern research in communication of emotions in [Andersen and Guerrero (1998)]. Appraisals of facial, vocal, physiological and other clues [Planalp (1999)], facial muscle response [Lundqvist (1995)] is one of the most accessible ones, demonstrate that emotional contagion is indeed a reality, with measurable speed [Wild *et. al* (2001)]. In experimental conditions, sad faces evoke sadness, surprised faces — surprise, anger — fear and disgust, while happy faces evoke happiness and surprise [Lundqvist (1995)].

We exploit an artificial paradigm to simulate emotional diffusion and interaction in crowd-minds:

"Now the crowd is in a sense a "transference phenomenon". In the temporary crowd or mob this transference is too transitory to be very evident, though even here I believe there will generally be found a certain *esprit de corps*" [Martin (1920)].

We design models of affective chemistry with five reacting emotions: happiness (H), anger (A), fear (F), sadness (S) and confusion (C). The first four species are basic [Oatley (1992)] culture-independent [Wild *et. al* (2001)] emotions. Confusion is valuable because it may reflect [Moscovici (1985)] a high state of disorder, e.g. a crowd throws itself into a confusion during outbursts of a collective mood.

Also, these affective reactants represent a convincing sampling of quadrants of the circumplex model of emotions [Russell (1980)], and thus may be seen as sufficient representatives of an affective universe. We do not specify how exactly carriers of emotions recognize affective states of their corresponding neighbors; we assume that visual and verbal means of communication [Heise and Weir (1999)] may be implicitly employed.

In computational experiments we analyze development of affective mixtures, whose initial concentration profiles may be interpreted as follows. Carriers of emotions are initially presented with a momentary event or a situation, a kind of affective disturbance. They reacted to the situation and expressed their emotions. Then they developed "autonomously". We study affective media synthetically, by considering binary mixtures at first and then an increasing number of affective species in the mixtures.

2.2 Happiness and sadness

Happiness H and sadness S are emotions of unlike phases, so it looks reasonable to start with a very simple model of their binary interactions. Let us design a set of possible reactions and exemplify each of the proposed reactions. When happiness interacts with sadness the happiness is transformed into sadness:

$$H + S \rightarrow 2S,$$

as demonstrated in three excerpts below:

"But ah! by constant heed I know
How oft the sadness that I show
Transforms thy smiles to looks of woe ..." [Beattie (1998)],

"For so your doctors hold it very meet,
Seeing too much sadness hath congeal'd your blood,
And melancholy is the nurse of frenzy" [Shakespeare (1997a)],

"ARMADO. How canst thou part sadness and melancholy, my tender Juvenal?" [Shakespeare (1997b)].

We see that sadness is highly contagious and happiness is volatile:

"It is happy people who are most receptive to others and most likely to catch their moods; the unhappy seem relatively oblivious to others' feelings and to contagion" [Hatfield *et. al* (1994)].

We may assume that H is a resting state of an emotion carrier but S is unstable and thus recovers back to H:

$$\begin{aligned} H + S &\to^{k_1} 2S, \\ S &\to^{k_2} H. \end{aligned} \tag{2.1}$$

If a drop of sadness is added to a stirred solution of happiness then reactions develop leading to a stationary concentration profile: $h = \frac{k_2}{k_1}$ and the rest, $h_0 + s_0 - \frac{k_2}{k_1}$, is S. When a small amount of sadness is applied to a thin layer of happiness, the sadness diffuses and increases in concentration until it reaches the maximum concentration of $h_0 - \frac{k_2}{k_1}$; this corresponds to a decrease of happiness $h = \frac{k_2}{k_1}$. The reaction rate k_1 reflects a degree of susceptibility to sadness; k_2 may be seen as a rate of recovery from grief. The ratio $\frac{k_2}{k_1}$ represents an overall degree of optimism in the affective solution, governed by Eq. (2.1).

In a cellular-automaton model of reactions (2.1) a cell in a happy state becomes sad if one of its neighbors is sad, the sad cell then takes a happy state independently of states of their neighbors. As we see in an example of cellular-automaton configurations shown in Fig. 2.1, an initial disturbance spreads in a thin layer filling the space with checker-board pattern of happiness and sadness. An affective medium perturbed by sadness will be thrown into mass grief if $s_0 + h_0 \geq \frac{k_2}{k_1}$.

In some situations happiness may produce sadness:

$$2H \to S + H,$$

for example

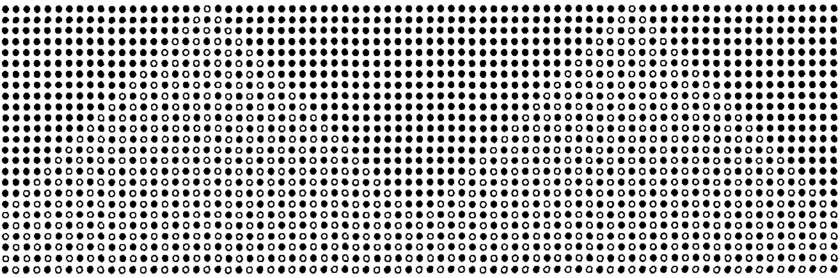

Fig. 2.1 Space–time dynamics of cellular-automaton model of the reaction scheme (2.1). Two "drops" of sadness are applied to a thin layer of happiness. Happiness is • and sadness is ◦. Time arrows downward.

> "... the smile of the beautiful companion has always the same underlying sadness when it responds to Lady Janet's hearty laugh" [Collins (1999b)].

The sadness could also recover back to happiness:

$$S + H \rightarrow 2H,$$

for example

> "Vernal delight and joy, able to drive
> All sadness but despair: now gentle gales
> Fanning their odoriferous wings dispense ..." [Milton (1999)].

These two reactions combined into the reaction

$$2H \rightleftharpoons_{k_2}^{k_1} H + S \tag{2.2}$$

show happiness dissociating to sadness and happiness, and also contagion of sadness by happiness. The reaction may be determined by a vector of interpersonal or dependency relationships between carriers of emotions. A ratio of stationary concentrations of happiness to sadness is proportional to the ratio $\frac{k_2}{k_1}$ of reconciliation (k_2) to estrangement (k_1) rates.

In the cellular-automaton model of Eq. (2.2) a cell in a happy state becomes sad if one of its neighbors is happy; a sad cell becomes happy if one of its neighbors is happy; otherwise the cell does not change its state. Sadness is a quiescent state (like a substrate) and happiness is a diffusing reagent (Fig. 2.2).

There is also evidence of auto-catalytic growth of sadness, for example

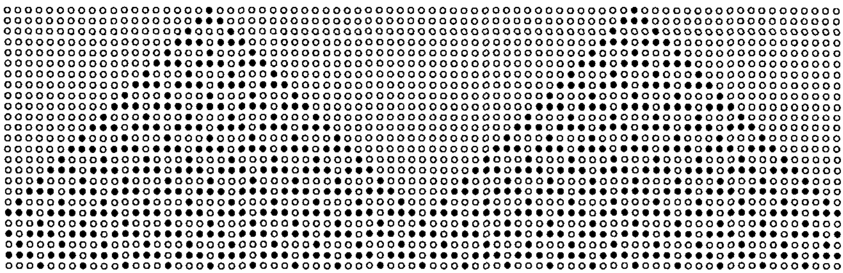

Fig. 2.2 Space–time dynamics of cellular-automaton model of the reaction scheme (2.2). Two "drops" of happiness are applied to a thin layer of sadness. Happiness is • and sadness is ∘. Time arrows downward.

> "... she felt herself strongly infected with the sadness which seemed to magnify her own ..." [Dumas (1998b)].

Such a development, however, does not bring us too interesting dynamics.

2.3 Anger, fear and happiness

Happiness (joy), anger and fear are three emotions basic in the historical context of social studies (see [McPhail (1991)] for further references). Joyous, hostile and fearful masses and crowds are most typical phenomena of collective emotions [McPhail (1991)]. Interactions between these species are open to equivocal readings:

> "Angry faces sometimes stimulate fear as well as anger; another's fear may put us at ease" [Hatfield *et. al* (1994)].

The saying above gives us the first three possible reactions of the scheme:

$$\begin{aligned} &H + A \to^{k_1} 2A, \\ &H + A \to^{k_2} F + A, \\ &F + A \to^{k_3} F + H, \\ &F + 2H \to^{k_4} 3H; \end{aligned} \tag{2.3}$$

the fourth reaction demonstrates that fear may transform into happiness in a "happy" environment.

Either anger or fear is the first instant reaction to somebody else's anger. Recognition of happiness and fear is not instant and takes some time; recov-

ery from fear to happiness is a lengthy process. These particulars of non-symbolic, and often non-communicative, affective interactions determine hypothetical values of reaction rates: $k_1 = 0.1$ (aggressiveness, fearlessness), $k_2 = 0.1$ (fearfulness), $k_3 = 0.09$ and $k_4 = 0.005$ (recoverability). If

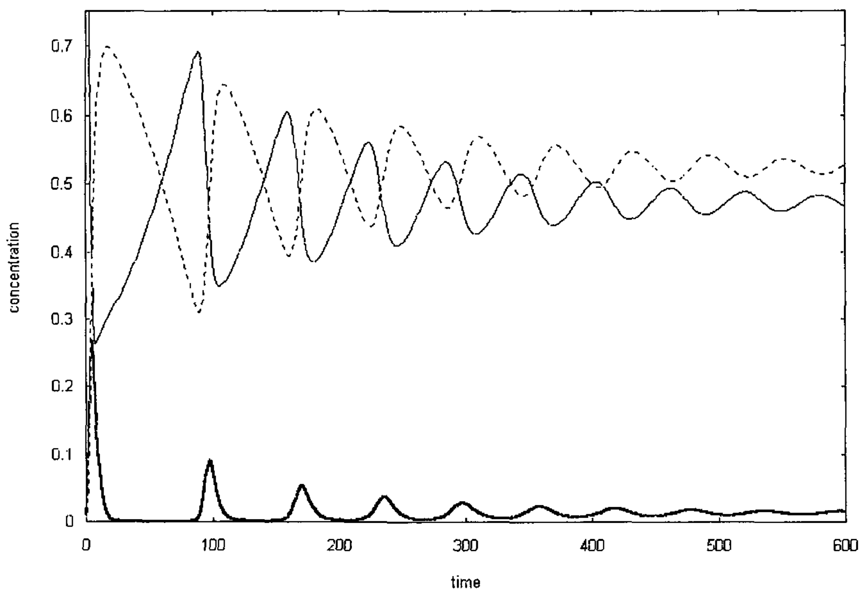

Fig. 2.3 Dynamic of happiness (thin solid line), anger (thick solid line) and fear (dotted line) in a well-stirred reactor with reaction set (2.3); initial concentrations are $h_0 = 1.0$, $a_0 = 0.1$ and $f_0 = 0.0$.

we add a small amount of anger to a solution of happiness, governed by reaction (2.3), concentrations of all three reagents exhibit damped oscillations, as shown in Fig. 2.3. This corresponds to oscillations of extreme emotions in experiments with evolving emotional intelligence [El-Nasr *et. al* (2001)]. Eventually, the dynamics of the mixture drifts towards small-amplitude, low-frequency oscillations. A transient period — aging of an affective reactor — observed in Fig. 2.3 may also correspond to aging of individuals: "emotions become increasingly salient with age" and "older people experience relatively low rates of psychological disorders" [Carstensen (1995)].

Stationary concentrations reached in the reactor's development satisfy the conditions $a^* = \frac{k_4 k_1}{k_2 k_3} h^{*2}$ and $f^* = \frac{k_1}{k_3} h^*$. In a stationary affective liquid (2.3) a ratio of anger to fear is proportional to the ratio of recoverability to fearfulness multiplied by the degree of happiness.

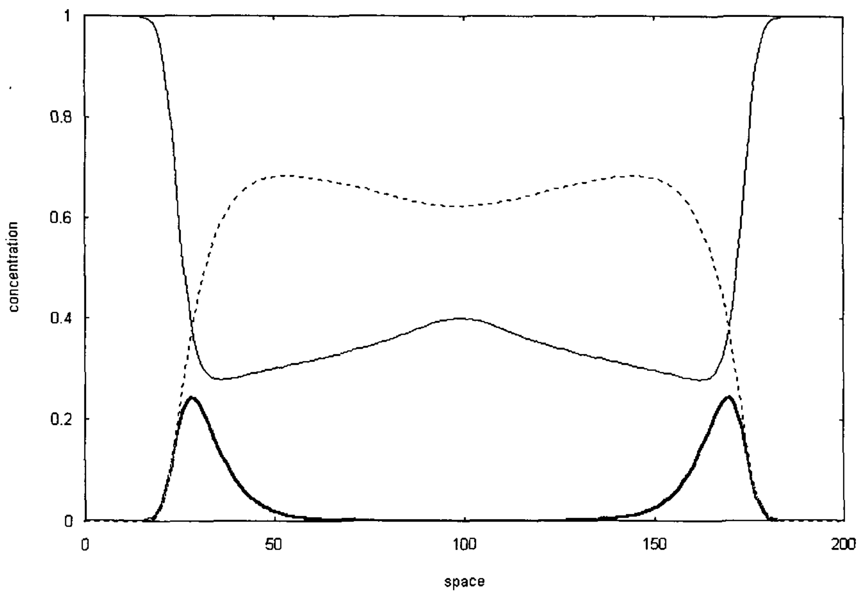

Fig. 2.4 Concentrations of happiness (thin solid line), anger (thick solid line) and fear (dotted line) in a thin-layer affective reactor, governed by Eq. (2.3), at 4000th step of simulation.

When we apply a small amount of anger to a thin-layer solution of happiness, the happiness decreases in concentration; anger and fear grow (Fig. 2.4). The drop of anger splits into two daughter drops traveling in opposite directions. Fronts of decreasing happiness and increasing fear move in unison with the wave fronts of anger (Fig. 2.5). In a reactor with periodic boundary conditions the wave fronts eventually collide and annihilate (Fig. 2.5). When the first wave fronts have gone away from the site of the original disturbance, the smaller wave fronts are generated, because there is still some anger left; then lesser wave fronts are generated until the affective species are distributed uniformly with the ratio of reagent concentrations as described earlier.

To simulate the affective reactor in a cellular automaton we can simplify the scheme (2.3) and substitute the last two reactions of the scheme (2.3) by reactions $A \to H$ and $F \to H$. Thus, in the automaton model of reactions (2.3), a happy cell takes either anger or fear (with probability $\frac{1}{2}$) if one of its neighbors is angry; angry and fearful cells recover to the happy state.

When a small amount of anger is applied to a thin layer of happiness,

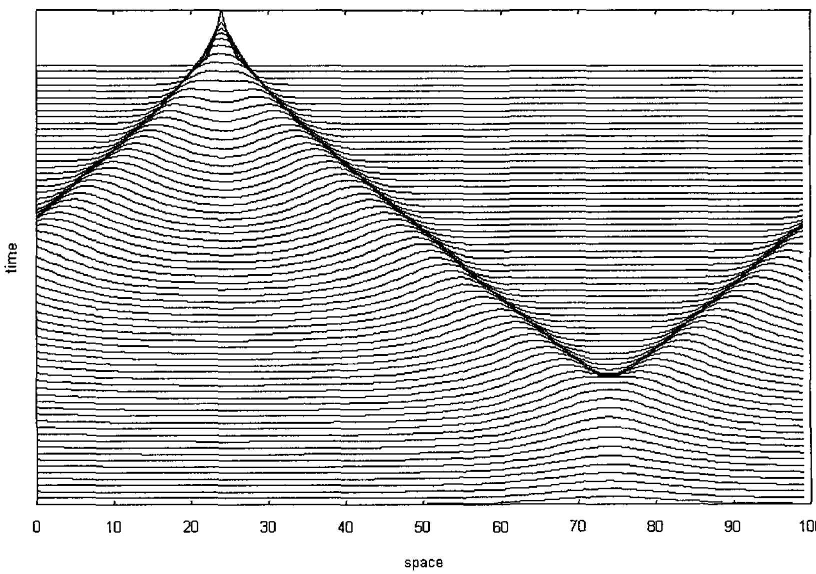

Fig. 2.5 Traveling wave fronts of anger in a thin-layer affective reactor, governed by Eq. (2.3), periodic boundary conditions. Time arrows downward.

wave patterns of anger and fear are formed as

$\cdots H \cdots HAHFH \cdots H \cdots$	traveling leftward,
$\cdots H \cdots HFHAH \cdots H \cdots$	traveling rightward.

Due to the stochasticity of the transition ('#' means any state)

$$(AHA), (AH\#), (\#HA) \to \langle A, F \rangle,$$

a wave may abruptly annihilate; see the first wave from the right in Fig. 2.6, or even reverse its motion; see the second wave from the right in Fig. 2.6. In cellular-automaton models anger–fear waves are rarely annihilated as the result of collision; rather, two waves form immobile or mobile bound states or one of the interacting waves is canceled by the other.

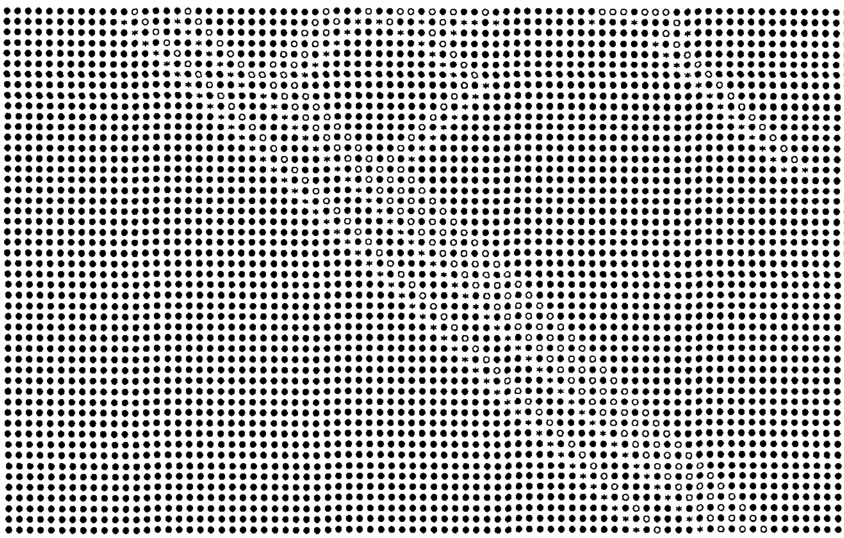

Fig. 2.6 Space–time dynamics of a cellular-automaton model of simplified reaction scheme (2.3). The reactor starts its evolution in a uniform state of happiness with a few drops of anger, arbitrarily applied to the medium. Happiness is $\bullet$, anger is $\circ$ and fear is $*$. Time arrows downward.

2.4 Happiness, anger, confusion and fear

The following set of reactions is inspired by emotional architectures based on evaluation, activation and a sense of potency [Morgan and Heise (1988)]:

$$\begin{array}{ll} H + A \rightarrow^{k_1} A, & H + 2A \rightarrow^{k_2} F, \\ A + 2H \rightarrow^{k_3} C, & A + 2F \rightarrow^{k_4} H, \\ C \rightarrow^{k_5} H, & C + A \rightarrow^{k_6} F, \\ F + H + A \rightarrow^{k_7} C, & F \rightarrow^{k_8} C, \\ F + A \rightarrow^{k_9} F, & F + H \rightarrow^{k_{10}} H, \end{array} \tag{2.4}$$

The first and second reactions of Eqs. (2.4) represent a "flight or fight" choice. The third and fourth reactions show how anger of a single affective carrier may evolve. So, the first four reactions may be seen as related to, talking in terms of [Morgan and Heise (1988)], differentiation of emotions by activation and potency, where for example local potency of happiness is inversely proportional to the concentration of anger in the local vicinity of the happiness. The fifth and tenth reactions of Eqs. (2.4) show that confusion and fear recover to happiness; happiness is seen here as a "ground state".

The seventh and eighth reactions reflect recovery of fear to confusion.

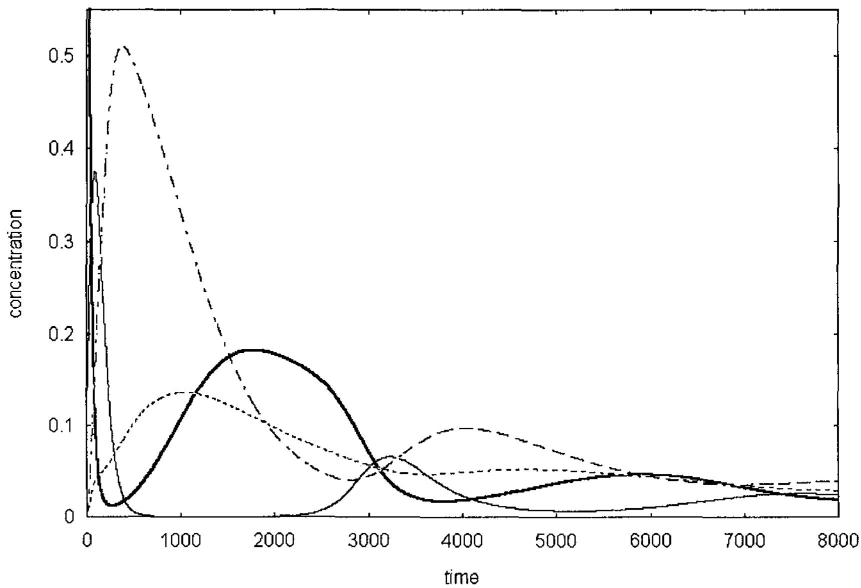

Fig. 2.7 Dynamic of happiness (thick solid line), anger (thin solid line), confusion (dotted line) and fear (dot-dashed line) in a well-stirred reactor with reaction set (2.4); initial concentrations are $h_0 = 0.9$, $a_0 = 0.1$, $f_0 = 0.0$ and $c_0 = 0.0$, reaction rates are $k_1 = 0.1$, $k_2 = 0.1$, $k_3 = 0.01$, $k_4 = 0.001$, $k_5 = 0.001$, $k_6 = 0.01$, $k_7 = 0.05$, $k_8 = 0.001$, $k_9 = 0.05$ and $k_{10} = 0.01$.

What happens if we drop some amount of anger in a well-stirred reactor (2.4) filled with pure happiness? The reactor exhibits a short-time outburst of fear (Fig. 2.7) followed by an outburst of confusion; happiness decreases in concentration, and hence recovers later.

> "Emotion sometimes seems to come out of nowhere, to hit you with full force, then to be over as quickly as it came .... It feels like a freight train of emotion hitting you (or perhaps sweeping you off your feet ..." [Planalp (1999)].

Concentrations of all reagents undergo damped oscillations until they all reach the same stationary level (Fig. 2.7). This may demonstrate that the affective system (2.4) is non-psychopathic, i.e. does not suffer from emotional deficiency and low reactivity [Partick and Zempolich (1998)]. Affective dynamics in Fig. 2.7 shows a drastic resemblance to emotional

changes experienced by survivors of disasters: disbelief and confusion are followed by anger and disappointment, then disillusion and finally (but not necessarily) happiness [Stein and Myers (1999)].

The reaction scheme (2.4) allows for constructing a deterministic cellular-automaton model of a thin-layer reactor as follows. A happy cell becomes angry if there is exactly one angry neighbor. The happy cell takes a state of fear if there are two angry neighbors. An angry cell becomes confused if there are more happy cells than angry cells in its neighborhood. If there are two fearful cells in the neighborhood of an angry cell the angry cell takes the state of happiness. A confused cell becomes happy if there are no angry neighbors, and the cell takes a state of fear if there is at least one angry neighbor. A cell in a state of fear takes a state of confusion if there is one happy and one angry neighbor or if there are neither happy nor angry neighbors. The fearful cell becomes happy if there is at least one happy neighbor and no angry neighbors. Any initial configuration which includes happiness will evolve to a configuration where most cells are in the state of happiness (Fig. 2.8) with a few domains of stationary localizations in the form

$$\begin{array}{c} \dots \\ \cdots HFACH \cdots \\ \cdots HCAFH \cdots \\ \dots \end{array} \tag{2.5}$$

The localized patterns consist of at least one angry cell surrounded by two neighbors which alternate their states between fear and confusion. As we can see in Fig. 2.8 the domains (2.5) can be canceled by traveling localizations

$$\begin{array}{c} \dots \\ \cdots HHHAAFHH \cdots \\ \cdots HACCCHHH \cdots \\ \cdots HAAFHHHH \cdots \\ \dots \end{array} \tag{2.6}$$

Traveling across a layer the localization (2.6) locally switches elements of the layer to anger, followed by fear, followed by confusion, followed by happiness (Fig. 2.8). When an affective solution (2.4) is locally perturbed by anger, traveling localizations (2.6) and immobile domains (2.5) are generated during a very short transient period of a quasi-chaotic dynamic. Some immobile domains and traveling localizations are annihilated in col-

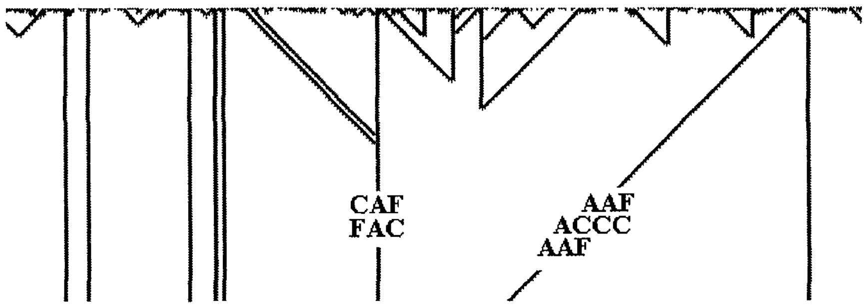

Fig. 2.8 Space–time configuration of cellular-automaton model of a thin-layer reactor (2.4), which starts its evolution in a random configuration of happiness, anger, confusion and sadness. Cells in a state of happiness are white pixels, other states are shown by gradations of gray. Exact configurations of exemplary stationary and mobile localizations are provided. Time arrows downward.

lisions with other traveling localizations; however, a few domains survive and persist in the system indefinitely.

2.5 Happiness, anger, confusion and sadness

From literature analysis we could extract the following set of most common types of affective reactions between happiness, anger, confusion and sadness:

(1) $H + A \to^{k_1} C + A$:

> "Anne blushed a second time, and turned aside under the pretext of taking her pen from her desk again, but in reality to conceal her confusion from her son. "Really, Philip", she said, "you seem to discover expressions for the purpose of embarrassing me, and your anger blinds you while it alarms me; reflect a little" [Dumas (1998a)].

> "... although she did not look, she could feel Martin's anger like a flame beside her. She was aware that Aunt Anne and Mr. Warlock were, like some beings from another world, distant from the general confusion. Her one passionate desire was to get up and leave the place ..." [Walpole (2003)].

(2) $H + A \to^{k_2} S + A$:

"Be careful, be very careful, not to wake his anger against yourself, for peace and happiness depend on keeping his respect. Watch yourself, be the first to ask pardon if you both err, and guard against the little piques, misunderstandings, and hasty words that often pave the way for bitter sorrow and regret..." [Alcott (2000)].

(3) $H + A \rightarrow^{k_3} S + H$:

"His eyes grew less stern, less cold; a look of sadness came upon his face. His love was stronger than he suspected. Mademoiselle de Verneuil, satisfied with these faint signs ..." [de Balzak (1972)].

(4) $H + S \rightarrow^{k_4} H + A$:

"The sight of their own hard lot and of their weakness, which is daily contrasted with the happiness and power of some of their fellow-creatures, excites in their hearts at the same time the sentiments of anger and of fear: the consciousness of their inferiority and of their dependence irritates ..." [de Tocqueville (1998)].

(5) $H + S \rightarrow^{k_5} C + S$:

"They are gay without knowing any very sufficient reason for being so, and when sadness is, as it were, proposed to them, things fall away from under their feet, they are helpless and find no stay" [Meynell (1999)].

(6) $H + S \rightarrow^{k_6} A + S$:

"And when Ortiz and Navarro joined the circle, the story of the fall of the Alamo was told again, and Luis forgot his own happiness, and wept tears of anger and pity for the dead heroes" [Barr (1995)].

(7) $H + S \rightarrow^{k_7} 2S$: discussed earlier.

(8) $A + C \rightarrow^{k_8} 2A$:

"... which were deprived of their heads by cruel men, despoiled of their wealth, the pious driven, like thee, from their homes; fear everywhere, everywhere robbery and confusion: all this ruin might have angered another temper" [Lang (1996)].

(9) $A + S \rightarrow^{k_9} C + S$:

"Motionless and trembling, the girl stood clinging to the bars, to catch his words if he spoke. Seeing him so depressed, disheartened, and pale, she believed herself to be the cause of his sadness. Her anger changed to pity, her pity to tenderness, and she suddenly knew that it was not revenge alone which had brought her there" [de Balzak (1972)].

(10) $2H \rightarrow^{k_{10}} A + H$:

"Why are you jealous of the sudden reveries which overtake me in the midst of our happiness? Why show the pretty anger of a petted woman when silence grasps me?" [de Balzak (1998)].

(11) $3H \rightarrow^{k_{11}} C + A + H$:

"Roger was filled with confusion and anger. A hoax on the part of some of the Corn Cob Club, he thought to himself. He flushed painfully to recall the simplicity of his glee" [Morley (1994)].

(12) $2H \rightarrow^{k_{12}} H + S$:

"The old order was changing rapidly to give place to the new, as Anne felt with a little sadness threading all her excitement and happiness" [Montgomery (1992)].

"But it was not because he was particularly proud this morning, as is the wont of bridegrooms, for his happiness was of a kind that had little reference to men's opinion of it. There was a tinge of sadness in his deep joy; Dinah knew it, and did not feel aggrieved" [Eliot (1996)].

"... Monsieur Mazarine had only taken delight in overwhelming me with sadness and grief, and in exposing my health and my life to his most unreasonable caprice, and in making me pass the best ..." [Molloy (1999)].

(13) $2A \rightarrow^{k_{13}} A + C$:

"... wondered whether she had behaved badly in jumping up to meet him. As she considered this her anger and her confusion at her anger increased" [Walpole (2003)].

(14) $2A \rightarrow^{k_{14}} C + S$:

"Since she had been speaking of M. Van Klopen, Mlle. Lucienne seemed to have lost her tone of haughty assurance and imperturbable coolness; and it was with a look of mingled confusion and sadness that she went on" [Gaboriau (1999)].

(15) $A \rightarrow^{k_{15}} S$:

My anger has left me, my sadness returned, and once more the tears flow. Whom can I curse, whom can I judge, when we are all alike unfortunate?" [Morley (1994)].

"This fit of hot anger was succeeded by a sudden sadness, by the darkening passage of a thought that ran over the scorched surface of his heart ..." [Conrad (1998)].

(16) $A \rightarrow^{k_{16}} C$:

"... and the marquis's anger gradually changed to anxiety. "What can have happened?" he thought" [Gaboriau (1995)].

(17) $2C \rightarrow^{k_{17}} S + A$:

"My state of mind is truly indescribable. Grief mingles with anger, when I tell you that my sweet Euneece has disappointed me, for the first time since I had the happiness of knowing and admiring her" [Collins (1999a)].

Let us discuss stable sets of reactions. A set is stable if no reagents initially absent in the set are produced. Set $\{H, S\}$ was already discussed earlier in this chapter; sets $\{H, C\}$, $\{H, A\}$ and $\{S, A\}$ are not present in a stable form. Set $\{A, C\}$ employs reactions 8, 13 and 16. In a discrete model of a thin-layer reactor with reactions 8, 13 and 16, cells update their states by the following rule. If there are angry and confused cells in the neighborhood of an angry cell then the angry cell remains angry. If there are only angry neighbors the cell either remains angry or becomes confused with probability $\frac{1}{2}$; otherwise the angry cell takes the state of confusion. A confused cell becomes angry if there are angry neighbors in its close vicinity. The states of anger and confusion, see Fig. 2.9, co-exist indefinitely in the reactor's evolution, and the space–time dynamic of the discrete model looks rather chaotic. Consider a well-stirred affective mixture governed by

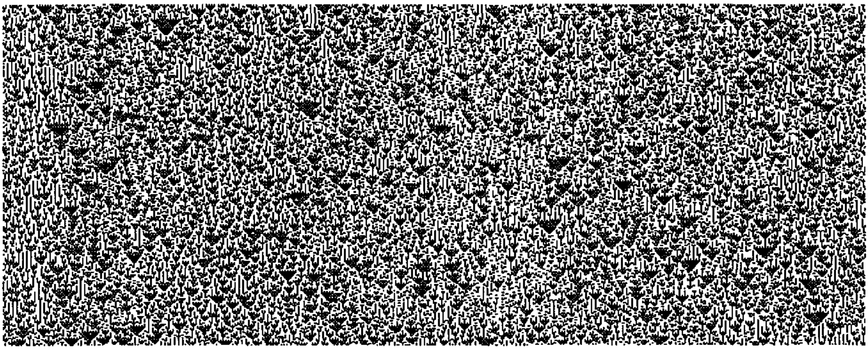

Fig. 2.9 Space–time dynamics of cellular-automaton model of the thin-layer mixture governed by reactions 8, 13 and 16. Anger is shown by white pixels, confusion is black; $n = 800$, $t = 250$.

reactions 8, 13 and 16. Let initially the mixture contains only anger. Then the mixture evolves (we can ignore the reaction $A \rightarrow C$) towards a global state of dominating confusion if the rate of remorse prevails over the rate of confusion ($k_8 < k_{13}$) or anger ($k_8 > k_{13}$). Qualitatively, the set $\{H, C, A\}$ may be reduced to $\{C, A\}$.

The set $\{H, S, C\}$ is determined by reactions 5, 7 and 12. Assuming reaction rates $k_5 = k_7 = k_{12} = 0.1$ and that the initial solution contains only happiness, we find that happiness vanishes and the final concentrations of confusion and sadness satisfy $c^* = \frac{1}{3}h^0$ and $c^* = \frac{7}{10}h^0$. The cellular-automaton model of $\{H, S, C\}$ behaves differently. A happy cell takes a state of confusion (with probability $\frac{1}{4}$) or sadness (with probability $\frac{3}{4}$) if there is a sad neighbor; the happy cell remains happy (with probability $\frac{1}{2}$ or becomes sad (with probability $\frac{1}{2}$) if there are only happy or confused cells in its neighborhood. A confused cell does not change its state. An initially random configuration evolves to a pattern comprising stationary domains of happiness, confusion and sadness; see Fig. 2.10.

Set $\{H, S, A\}$ includes eight reactions: 2, 3, 4, 6, 7, 10, 12 and 15. Assume that anger reacts with happiness twice as fast as happiness reacts with sadness (e.g. because angry faces are recognized faster than sad or happy faces [Hanses *et. al* (1988)]) and that anger very slowly recovers to sadness. Then we can use the following reaction rates: $k_2 = 0.1$, $k_3 = 0.1$, $k_4 = 0.05$, $k_6 = 0.05$, $k_7 = 0.05$, $k_{10} = 0.05$, $k_{12} = 0.05$ and $k_{15} = 0.001$. In experiments with such mixtures we find that an initially happy solution exhibits outbursts of anger and sadness. The anger then declines, while sadness becomes dominating in the solution (Fig. 2.11). In a cellular-

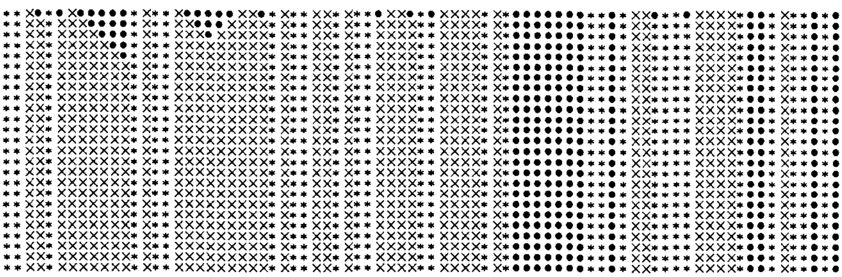

Fig. 2.10 Space–time dynamics of a cellular-automaton model of the reactions 5, 7 and 12. The initial configuration features a random distribution of happiness, sadness and confusion, $n = 80$, $t = 25$. Happiness is $\bullet$, confusion is $*$ and sadness is $\times$. Time arrows downward.

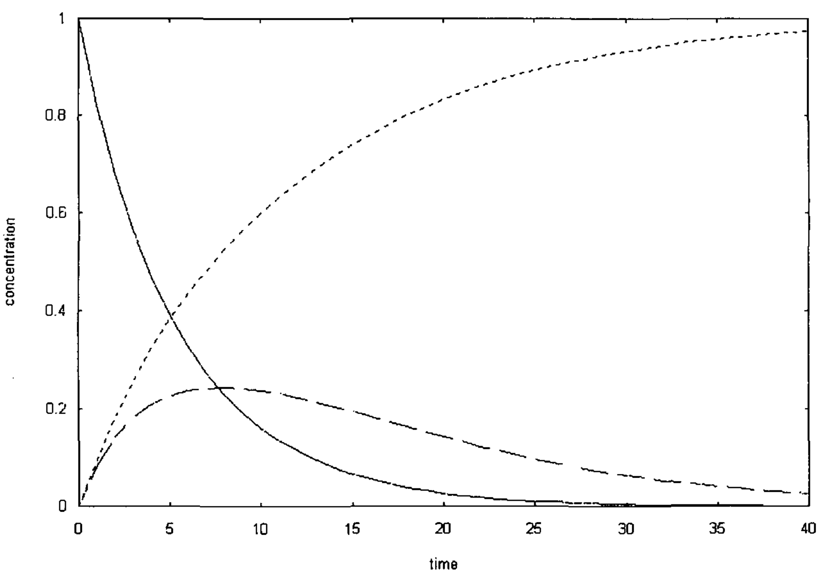

Fig. 2.11 Dynamics of concentrations of happiness (solid line), anger (dashed line) and sadness (dotted line) in a well-stirred affective reactor governed by reactions 2, 3, 4, 6, 7, 10, 12 and 15.

automaton model of reaction set $\{H, A, S\}$, cells behave as follows. An angry cell becomes sad unconditionally. A sad cell becomes angry if there is at least one happy neighbor. A happy cell undergoes a deterministic transition to sadness if there are only angry cells in the cell's neighborhood.

The happy cell switches to an angry or remains in a happy state with probability $\frac{1}{2}$ if its neighborhood contains only happy or only sad cells. If there are sad and angry cells in the neighborhood of the happy cell the cell becomes sad with probability $\frac{3}{4}$ or angry with probability $\frac{1}{4}$. A space–time configuration (Fig. 2.12) of a cellular automaton simulating the reaction mixture $\{H, A, S\}$ is characterized by long-living domains of happiness. In these domains, cells which are not happy change their states cyclically: $\cdots S \rightarrow A \rightarrow S \rightarrow A \cdots$.

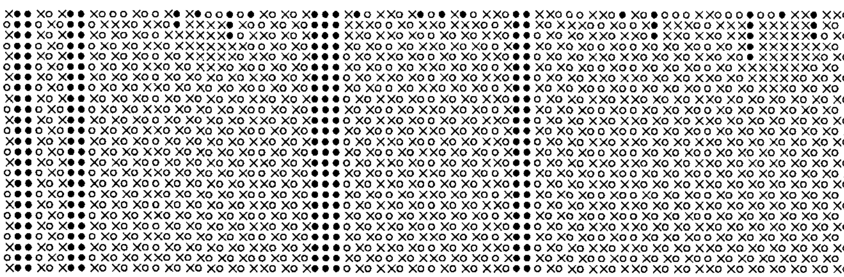

Fig. 2.12 Space–time dynamics of cellular-automaton model of the reactions 2, 3, 4, 6, 7, 10, 12 and 15. The initial configuration features a random distribution of happiness, anger and sadness, $n = 80$, $t = 25$. Happiness is $\bullet$, anger is $\circ$ and sadness is $\times$. Time arrows downward.

Affective solutions governed by reactions 8, 9, 13, 16 and 17 of the set $\{A, C, S\}$ show an auto-catalytic growth of sadness (unless $k_{17} = 0$), and a decline in anger; confusion reaches a stationary concentration meanwhile.

Happiness is never generated in the entire reaction scheme; the happiness either dissociates into other reactants or acts as a catalyst. This means that if ever happiness is present initially in an affective solution, its concentration will decrease until the happiness completely vanishes (so there is no point in considering the set $\{H, A, C, S\}$).

2.6 Emotional abuse therapy

Our paradigm of affective solutions is a toy model reflecting, up to some degree of accuracy, real-life phenomena. This is useful, however, in demonstrating principal trends in affective developments, as we show in the following example of an emotional abuse. The emotional abuse, particularly its demeaning form, is characterized by a typical patterned behavior, where

aggression is followed by contrition, then happiness and then recurrent aggression [Loring (1994)]. In the course of an abusive relationship an abuser "alternates between positive, kindly responses and negative, abusive reactions" and a victim "continues to seek attachment with an abuser who has withdrawn his affection" (a kind of anxious attachment) [Loring (1994)].

The following set of affective reactions seems to grasp perfectly the content of emotional abuse:

$$\begin{array}{ll} 2H \to^{k_1} H + A & \texttt{aggression,} \\ H + A \to^{k_2} S + A & \texttt{victimization,} \\ S + A \to^{k_3} S + H & \texttt{pleasing,} \\ S + H \to^{k_4} 2H & \texttt{contrition.} \end{array} \tag{2.7}$$

In the model we consider a high level of aggression, $k_1 = 0.1$, intermediate values of victimization and contrition, $k_2 = k_4 = 0.05$, and a miniscule degree of pleasing, $k_3 = 0.001$. Initially, a pure solution of happiness experiences an abrupt fall in the concentration of happiness, an outburst and a subsequent decline of anger associated with a smooth growth of sadness. The reaction solution reaches its quasi-stable state, where stationary concentrations of happiness and sadness are expressed via the concentration of anger (a^*) as follows: $s^* = \frac{k_2}{k_4}a^*$ and $h^* = \sqrt{\frac{k_3 k_2}{k_1 k_4}}a^*$.

A cellular-automaton model represents local dynamics of an affective solution (2.7) a bit differently from that in a well-stirred reactor. A happy cell becomes aggressive if at least one of its neighbors is happy and neither neighbor is aggressive. A happy cell takes a state of sadness if at least one of its neighbors is aggressive. An angry cell becomes happy if at least one of its neighbors is sad. A sad cell takes the happy state if there are happy cells in the cell's neighborhood. If a thin-layer reactor starts in a uniform state of happiness, then it evolves to a stationary state of uniform anger. A random initial configuration, where all three affective states are present, gives rise to a fractal dynamic, as shown in Fig. 2.13. As soon as domains of happy states are formed they initiate outbursts of anger. The domains of anger, bounded by sadness, then gradually vanish until the outburst of violence is repeated.

The stationary concentration profile in the "abusive" well-stirred solution (2.7) perfectly satisfies the common-sense finding:

> "... as long as the other partner continues to be submissive, the other partner's anger will grow" [Loring (1994)].

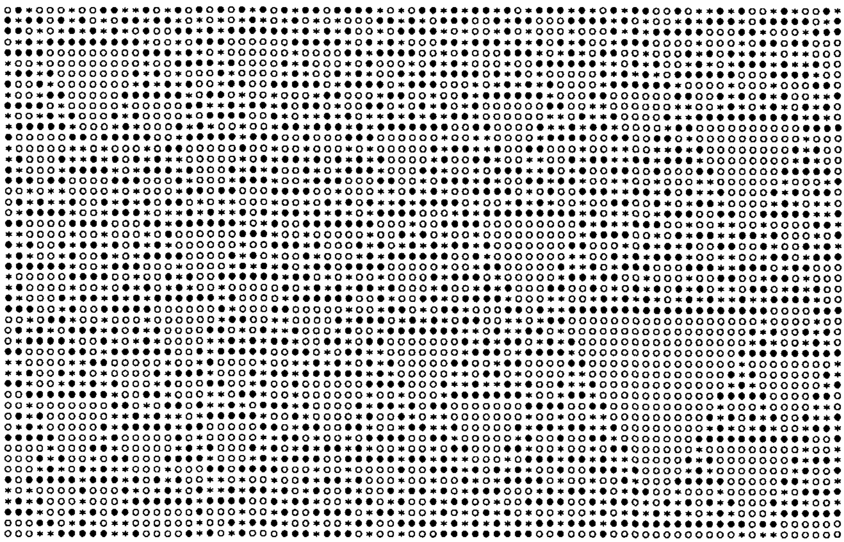

Fig. 2.13 Space–time dynamics of cellular-automaton model of the reaction scheme (2.7). The reactor starts its evolution in a random configuration of happiness, anger and sadness. Happiness is $\bullet$, anger is $\circ$ and sadness is $*$. Time arrows downward.

When detachment of a victim from his or her abuser is impossible, two types of therapy may be considered. "Tit for tat" would be the first approach,

> Anger is better than laughter: because by the sadness of the countenance the mind of the offender is corrected [The Holy Bible].

$$
\begin{array}{ll}
2H \to^{k_1} H + A & \texttt{aggression,} \\
H + A \to^{k_2} 2A & \texttt{retaliation,} \\
2A \to^{k_3} A + C & \texttt{remorse,} \\
C + H \to^{k_4} 2H & \texttt{reconciliation,} \\
C + A \to^{k_5} 2C & \texttt{remorse.}
\end{array}
\qquad (2.8)
$$

When the victim is angry the abuser becomes confused; see reaction $2A \to A + C$. The confusion is a common therapeutic tool [Paar (1992)] used to move an "individual closer to a bifurcation point, from which the individual may either fall back to old patterns (the therapy fails) or moves on to new ones (the therapy succeeds with a bifurcation to a new attractor)" [Abraham (1992)].

In numerical experiments with an affective solution (2.8) we use reaction rates corresponding to rates of the solution (2.7): $k_1 = 0.1$, $k_2 = 0.05$, $k_3 = 0.002$, $k_4 = 0.05$ and $k_5 = 0.001$. An example of abuse therapy in an

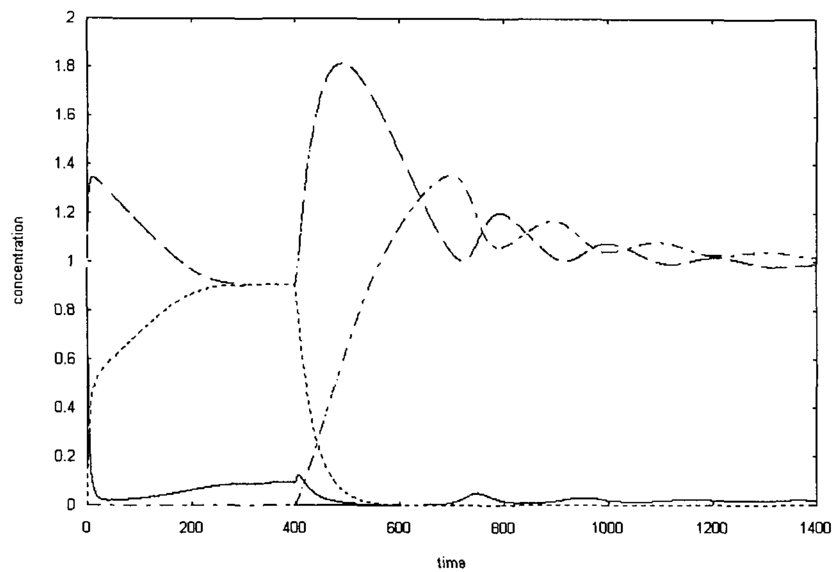

Fig. 2.14 Dynamics of an affective liquid in the course of abuse therapy. The liquid is "purely" abusive, reaction scheme (2.7), until the 400th step of simulation, then therapy, reaction scheme (2.8), is applied. Development of concentrations of happiness (solid line), anger (dashed line), sadness (dotted line) and confusion (dash-dotted line) is shown over time.

affective solution is shown in Fig. 2.14. We started with an abusive solution, determined by reactions (2.7); then, when the concentration dynamic reached its stationary state — where sadness co-exists with aggression — we started a course of "therapy", determined by reactions (2.8). The "therapy" may be seen as an application of a certain catalyst that changes the course of the reaction from scheme (2.7) to scheme (2.8). In numerical experiments, at the beginning of the therapy course we observed an outburst of anger, associated with decline of sadness and growth of confusion; see Fig. 2.14. This was followed by damped oscillations of anger and confusion, until the new stationary state is reached.

In a cellular-automaton model of a thin-layer reactor (2.8) a happy cell takes a state of anger if at least one of its neighbors is happy or angry; an angry cell becomes confused if either of its neighbors is angry or confused;

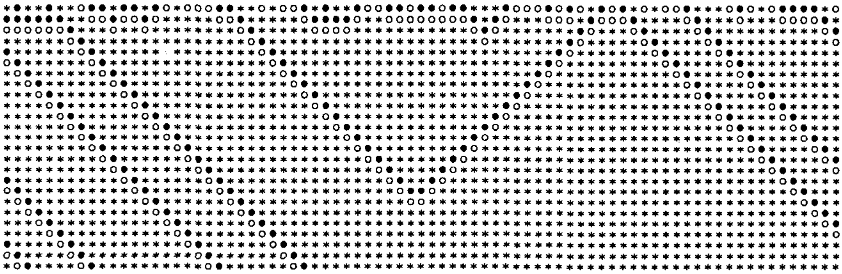

Fig. 2.15 Space–time dynamics of cellular-automaton model of the reaction scheme (2.8). The reactor starts its evolution in a random configuration of happiness, anger and confusion. Happiness is $\bullet$, anger is $\circ$ and confusion is $*$. Time arrows downward.

a confused cell becomes happy if either of the cell's neighbors is happy. The automaton lattice jumps to a state of uniform confusion (all cells are in the state C) if its initial configuration does not contain confusion. If the initial random configuration contains happiness, anger and confusion the majority of the cells take the state of confusion; however, waves of happiness and anger develop (Fig. 2.15). Each wave has a front of happiness and a tail of anger: $\cdots CAHC \cdots$ (rightward) and $\cdots CHAC \cdots$ (leftward). The waves annihilate when they collide (Fig. 2.15).

As we can see in examples of well-stirred (Fig. 2.14) and cellular-automaton (Fig. 2.15) models, the "tit for tat" therapy, reactions (2.8), does not work as perfectly as we would want it to. The therapy (2.8) makes affective carriers confused but not happy. Behavior at the edge of irrationality, or emergent behavior, is rarely absolutely suppressible:

> "As Talleyrand said to Napoleon: "You can do everything with bayonets, Sire, except sit on them". And ruling is not a matter of seizing power, but the easy exercise of it" [Ortega y Gasset (1985)].

To make both partners responsible for abusive behavior may be yet another therapeutic approach:

$$\begin{aligned} &2H \to^{k_1} H + A, \\ &H + A \to^{k_2} S + C, \\ &S + H \to^{k_3} 2H, \\ &C + H \to^{k_4} 2H, \\ &S + A \to^{k_5} 2S, \\ &C + A \to^{k_6} 2C. \end{aligned} \tag{2.9}$$

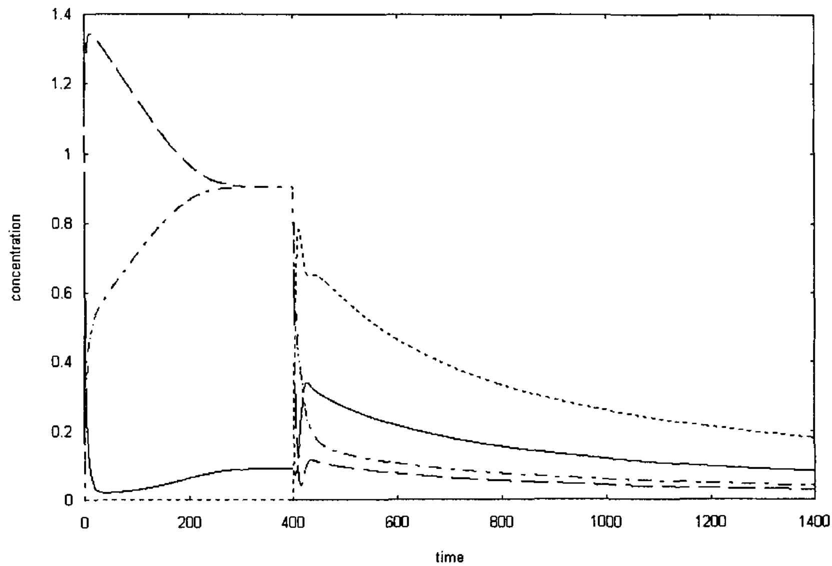

Fig. 2.16 Dynamics of an affective liquid in the course of "both parties" fault therapy. The liquid is "purely" abusive, reaction scheme (2.7), until the 400th step of simulation, then therapy is applied, reaction scheme (2.9). Development of concentrations of happiness (solid line), anger (dashed line), sadness (dotted line) and confusion (dash-dotted line) is shown over time. The following reaction rates are used in experiments: $k_1 = 0.1$, $k_2 = 0.1$, $k_3 = 0.05$, $k_4 = 0.05$, $k_5 = 0.07$ and $k_6 = 0.07$.

The dynamic of a well-stirred reactor during the second therapeutic approach is shown in Fig. 2.16. The therapy does not simply decrease the level of anger but makes happiness the second dominating reagent in the affective solution; however, confusion still prevails.

An example of a space–time configuration of a cellular-automaton model of a thin-layer reactor (2.9) is shown in Fig. 2.17. This dynamics is determined by the following cell state transition rules. Confused and sad cells become happy if there is a happy neighbor. If there is a happy neighbor and no angry neighbor of a happy cell, the cell becomes angry. If there are happy and angry neighbors of a happy cell, the cell takes an angry state with probability $\frac{1}{2}$ and confused and sad states with probability $\frac{1}{4}$. An angry cell takes a state of confusion (sadness) if there are confused (sad) neighbors and no happy or sad (confused) neighbors. The cell takes the state of sadness (confusion) with probability $\frac{2}{3}$ and the state of confusion (sadness) with probability $\frac{1}{3}$ if there are only happy and confused (sad) neighbors. If there are both sad and confused cells or only happy cells in

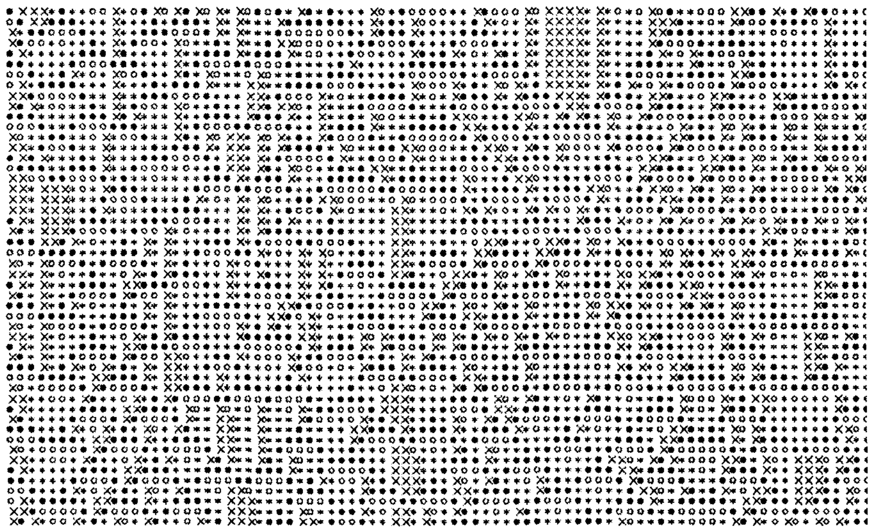

Fig. 2.17 Space–time dynamics of cellular-automaton model of the reaction scheme (2.9). The reactor starts its evolution in a random configuration of happiness, anger and confusion. Happiness is •, anger is ∘, confusion is $*$ and sadness is $\times$. Time arrows downward.

the neighborhood of an angry cell, the cell takes the state of confusion or sadness, each with probability $\frac{1}{2}$.

When started in a random configuration containing all four affective states, the model reveals waves of happiness, long-living domains of sadness and confusion, and momentary outbursts of anger. All affective states look equally present in the evolution of the cellular-automaton model; however, global concentration dynamics (Fig. 2.18) shows that happiness and, slightly less, confusion prevail in the reactor. Overall, the model may demonstrate that in certain conditions violence is indeed a good solution, in some cases even when applied to authorities. As one youth said of police after the St. Paul's riot in Bristol was over:

> "... they will never again treat us with contempt ... they will respect us now" [Reicher (1987)].

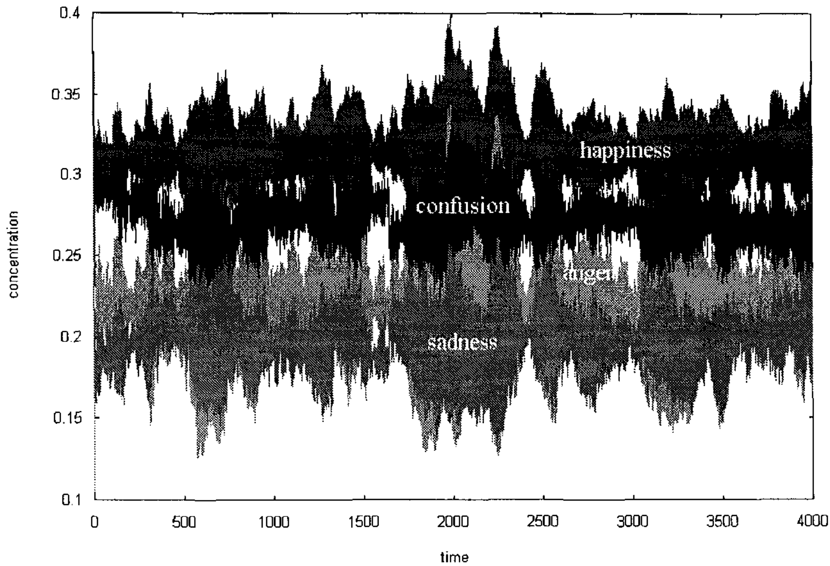

Fig. 2.18 Concentration dynamics of affective reagents in cellular-automaton model of thin-layer reactor (2.9), see also Fig. 2.17. The reactor started its development in a random configuration.

2.7 Affectons

In the rest of the chapter we adopt a more formal approach to affective dynamics and consider dynamics of finite-automata models of emotions. An emotional automaton — *affecton* — is a tuple $\langle \mathbf{E}, f \rangle$, where elements of a finite set $\mathbf{E}$ represent emotional states and a function $f : \mathbf{E} \times \mathbf{E} \to \mathbf{E}$ calculates the next automaton state from its current state and its input state (both states are elements of $\mathbf{E}$). Affectons evolve in a discrete time, measured in generations or updates of automaton states. If an automaton takes the state s^t at time step t and its input state is y^t, then it takes the state s^{t+1} calculated as $s^{t+1} = f(s^t, y^t)$, $s^t, s^{t+1}, y^t \in \mathbf{E}$. The set $\mathbf{E}$ includes the following emotional states: ζ (happiness), α (anger), κ (confusion), σ (sadness) and ξ ("a currently experienced distress at an apprehended future threat" [Mullen (1997)]). We avoid using formal definitions of the emotional states in the present chapter; we appeal rather to common-sense notation that can be found elsewhere, see e.g. [Amelie (1980); French and Wettstein (1999); Hillman (1992); Izard *et. al* (1998); Kenny (1994); Lewis and Haviland-Jones (2000); Lyons (1980)] to name but few. Alternative

constructs of emotions can be found in [Marchant (1999)], where logical representations of emotions are derived from combinations of actions and appraisals. Most of the published works stick closely to the classical St. Augustine's representation:

> "Love, then, yearning to have what is loved, is desire; and having and enjoying it, is joy; fleeing what is opposed to it, it is fear; and feeling what is opposed to it, when it has befallen it, it is sadness" [Saint Augustine (2000)].

When defining binary interactions of emotions, tabular representations of f, we assume that carriers of emotions are discrete, i.e. subjects or persons. This allows us to explain some, not immediately obvious, results of compositions by appealing to a vector of interpersonal relations between subjects i and j: $i \overset{a \quad b}{\longleftrightarrow} j$, where $a, b \in \{0, +, -\}$ mean neutral, e.g. "do not care"; positive, e.g. "like"; and negative, e.g. "dislike" or "disgust", attitudes experienced by one person, i or j, towards another, j or i. We define and characterize nine classes of affectons, state-transition tables of which are shown in Fig. 2.19. The signature of the vector may be determined by many factors; the most commonly known include dependence, e.g. "powerless is more likely to attend to emotions of those who have power over them" [Hatfield *et. al* (1992)]. There are also instances of counter mimicry [Lanzetta and Englis (1989)], which could be linked to emphatic solidarity [Heise (1998)] in competing groups.

Let us discuss state-transition tables of affectons from different classes. Entries of the forms $\{s_1, s_2\}$ and $\{s_1, s_2, s_3\}$ at the intersection of the row x and the column y mean that if an automaton takes the state x at time step t and its input state is y then the automaton takes one of the states s_1, s_2 or s_1, s_2, s_3 with the same probability $\frac{1}{2}$ or $\frac{1}{3}$. A detailed treatment of the various classes of affectons is provided below.

$\mathcal{HAC}$ affecton

$$
\begin{array}{cc|ccc}
 & & & y^t & \\
 & s^{t+1} & \zeta & \alpha & \kappa \\
\hline
 & \zeta & \zeta & \kappa & \zeta \\
s^t & \alpha & \kappa & \alpha & \alpha \\
 & \kappa & \zeta & \alpha & \kappa
\end{array}
$$

The automaton $\mathcal{HAC}$ represents somewhat a "positive" kind of emotional interaction. Thus, when a happy subject meets an angry one they both become confused by the fact that their emotional states are in unlike phases, $f(\zeta,\alpha) = f(\alpha,\zeta) = \kappa$. The confusion is excited by happiness and anger, $f(\kappa,\zeta) = \zeta$ and $f(\kappa,\alpha) = \alpha$.

$\mathcal{HAC}_1$ *affecton*

	s^{t+1}	y^t: ζ	α	κ
	ζ	ζ	κ	ζ
s^t	α	κ	α	ζ
	κ	α	α	$\{\zeta,\alpha\}$

In certain moments of real life a confused subject may become angry when he meets a happy subject while the happy subject remains happy. For example, see the quotation for reaction 11, Sec. 2.5. The composition $f(\kappa,\zeta) = \alpha$ and $f(\zeta,\kappa) = \zeta$ could be also determined by the negative vector of interpersonal relations $i \overset{--}{\longleftrightarrow} j$. This may explain why $f(\alpha,\kappa) = \zeta$ and $f(\kappa,\alpha) = \alpha$ — when an angry subject meets a confused subject the angry subject becomes happy, because he does not like the confused one; and, the confused subject becomes angry, because he is embarrassed by the situation and does not fancy the angry subject, see for example

> "... a client may feel angry and aggressive ... about some event ..., but then feel anxious ... about having been angry and aggressive ..." [Chadwick *et. al* (1996)].

$\mathcal{HAC}_2$ *affecton*

	s^{t+1}	y^t: ζ	α	κ
	ζ	$\{\zeta,\alpha\}$	κ	ζ
s^t	α	κ	$\{\alpha,\kappa\}$	α
	κ	ζ	α	κ

Let us consider now a non-standard self-interaction of happiness and anger; they are based on interpersonal relation vectors with negative components.

If one of the subjects does not like another and two happy subjects meet, then one of them is infuriated while the other remains happy: $f(\zeta,\zeta) = \alpha$ and $f(\zeta,\zeta) = \zeta$, see for example reaction 4 in Sec. 2.5. By analogy, when both subjects are angry, the first subject does not change his anger while the second one becomes confused, $f(\alpha,\alpha) = \alpha$ and $f(\alpha,\alpha) = \kappa$.

$\mathcal{HAC}_3$ *affecton*

$$
\begin{array}{cc|ccc}
 & & & y^t & \\
 & s^{t+1} & \zeta & \alpha & \kappa \\
\hline
 & \zeta & \zeta & \{\zeta,\alpha,\kappa\} & \zeta \\
s^t & \alpha & \{\zeta,\alpha,\kappa\} & \alpha & \kappa \\
 & \kappa & \alpha & \kappa & \kappa
\end{array}
$$

In the model $\mathcal{HAC}_3$ we assume that a happy subject makes the confused one angry. However, the angry subject is confused in the interaction with the confused subject. As to the interaction of anger and happiness, one can exploit various configurations of the interpersonal relations vector. If the vector is two-way positive, $i \overset{++}{\longleftrightarrow} j$, both subjects become confused. The two-way negative vector $i \overset{--}{\longleftrightarrow} j$ makes the emotions "freeze": the happy subject is still happy to see the angry subject angry, and the angry subject is angry because the happy subject is happy. Following [Planalp (1999)], we could explain this by a feeling of "schadenfreude", expressing the situation when one takes "pleasure in another's misfortune" [Planalp (1999)]. Adopting the vectors $i \overset{+-}{\longleftrightarrow} j$ and $i \overset{-+}{\longleftrightarrow} j$, we can produce the states of happiness, anger and confusion as a result of emotional interactions.

$\mathcal{HAN}$ *affecton*

$$
\begin{array}{cc|ccc}
 & & & y^t & \\
 & s^{t+1} & \zeta & \alpha & \xi \\
\hline
 & \zeta & \zeta & \alpha & \alpha \\
s^t & \alpha & \alpha & \{\alpha,\xi\} & \alpha \\
 & \xi & \xi & \alpha & \xi
\end{array}
$$

Let anxiety interact with happiness and anger. Amongst a dozen realistic scenarios we have chosen the one that gives a non-trivial dynamic to the model $\mathcal{HAN}$. A happy subject becomes angry when it encounters an angry

one. An anxious person also takes the state of anger when he meets an angry person. The angry one does not change its state. Anger and anxiety are produced in the reaction between anxiety and anger. Why? Firstly, the happy subject does not like to see signs of anxiety and thus becomes agitated; the anxious subject remains anxious. Secondly, we can assume that the anxious subject becomes embarrassed and then angry when he sees the happy subject; at the same time the happy subject becomes anxious because he made someone else feel awkward. The composition $f(\alpha, \alpha) = \alpha$ and $f(\alpha, \alpha) = \xi$ may be determined by the interpersonal relation vector $i \overset{+-}{\longleftrightarrow} j$: when two angry persons interact one becomes anxious while the other remains angry.

$\mathcal{HACS}$ affecton

	s^{t+1}	y^t: ζ	α	κ	σ
	ζ	ζ	κ	κ	κ
s^t	α	κ	α	α	α
	κ	α	κ	κ	κ
	σ	α	σ	α	σ

The model $\mathcal{HACS}$ employs four emotional states — in addition to the usual happiness, anger and confusion a sadness is added. The following scheme of interaction is adopted. When a happy person meets a sad one the happy one becomes confused, e.g. he could feel guilty for being happy when others are confused, and the sad one becomes angry, e.g. he is upset that somebody is happy when he himself is sad. For an example, see the reaction 3 in Sec. 2.5. Both happy and angry persons become confused when they meet one another. When sadness interacts with confusion the sadness is transformed to anger but the confusion remains unchanged. The sadness composed with sadness may also produce sadness, for example

> "... she felt herself strongly infected with the sadness which seemed to magnify her own ..." [Dumas (1998b)].

And yet another example of the composition $\sigma = f(\sigma, \sigma)$ is:

> "And so with a new sorrow I sorrowed for my sorrow and was wasted with a twofold sadness ..." [Saint Augustine (2002)].

$\mathcal{HACS}_1$ *affecton*

s^t \ s^{t+1}	y^t: ζ	α	κ	σ
ζ	ζ	σ	ζ	κ
α	κ	α	α	κ
κ	ζ	α	κ	κ
σ	κ	κ	σ	σ

Sometimes happy and sad persons become confused when they encounter one another. This may occur because the happy person is ashamed of his happiness when his counterpart is sad and the sad person is confused because he may be embarrassed to be sad, see for example the reaction 5 in Sec. 2.5. This model conforms to a two-way positive vector of interpersonal relations. So, one can demonstrate that when a happy person meets an angry one the happy one is saddened by the anger of another subject and the angry person becomes confused because he expressed anger in an inappropriate situation. The confused person becomes happy when he encounters happiness. When the sad person interacts with the angry one they both become confused. The confusion itself is easily infected by anger.

$\mathcal{HACS}_2$ *affecton*

s^t \ s^{t+1}	y^t: ζ	α	κ	σ
ζ	ζ	$\{\zeta, \kappa\}$	ζ	κ
α	$\{\alpha, \kappa\}$	α	κ	κ
κ	α	κ	κ	κ
σ	ζ	κ	σ	σ

The $\mathcal{HACS}_2$ model is similar to the one previously discussed in all but the interaction of happiness with anger, confusion with happiness, and sadness with happiness. The happy person makes the confused one angry, independently of their interpersonal relationships. The confused person makes the angry one confused, e.g. when $i \overset{++}{\longleftrightarrow} j$. Interaction of happiness with anger is adopted from the model $\mathcal{HAC}_3$ with the only difference that composition of the emotional states is asymmetric.

$\mathcal{HACS}_3$ *affecton*

		y^t			
	s^{t+1}	ζ	α	κ	σ
	ζ	ζ	σ	ζ	σ
s^t	α	κ	α	α	κ
	κ	ζ	α	κ	κ
	σ	κ	σ	σ	σ

Let, as in the model $\mathcal{HACS}_1$, a confused person become angry when he interacts with an angry person; and, he become happy when he encounters happiness. However, in the model $\mathcal{HACS}_3$ sadness is not changed in the interaction with happiness or anger. Interaction with the sad person confuses both happy and angry subjects, see e.g. Sec. 2.2. Both confusion and sadness are generated in the interaction of anger with sadness, see for example the reaction 10 in Sec. 2.5.

2.7.1 *Affectons in random environment*

We define a random environment as an infinite string Ω of elements from $\mathbf{E}$; any element of $\mathbf{E}$ occurs in Ω with the probability $1/|\mathbf{E}|$. Each moment of discrete time an affecton gets a symbol ω^t from Ω. The automaton updates its state depending on its current state and the state of its input as $s^{t+1} = f(s^t, \omega^t)$. The automaton's behavior in the random environment is characterized by a distribution π of probabilities for the automaton to be in the state a.

The distribution π can be derived from stochastic matrices of state transitions (Fig. 2.19). An entry m_{ab} of the stochastic matrix $\mathbf{M}$ (the matrix is stochastic because $m_{ab} > 0$ for any a and b from $\mathbf{E}$ and $\sum m_{ab} = 1$ for any $a \in \mathbf{E}$) gives a probability for an affecton (which works in the random environment Ω) to update its state $s^0 = a$ to state $s^t = b$, $t > 0$. Every class $\mathcal{C}$ of affectons can be determined by a finite-automaton's state set $\mathbf{E}$ and matrix $\mathbf{M}_{\mathcal{C}}$. Space and time of the process are discrete and its transition-probability matrix is constant (time independent); therefore, the studied process is a stationary (homogeneous) Markov chain. There are only two proper *closed sub-sets* in the chains, specific for affecton classes. They are $\{\alpha, \xi\}$ in the class $\mathcal{HAN}$; and $\{\zeta, \alpha, \kappa\}$ in the classes $\mathcal{HACS}$ and $\mathcal{HACS}_2$. So far, the only chains determined by the classes $\mathcal{HAC}$, $\mathcal{HAC}_1$, $\mathcal{HAC}_2$, $\mathcal{HAC}_3$, $\mathcal{HACS}_1$ and $\mathcal{HACS}_3$ are irreducible; their states are recurrent and

s^t \ s^{t+1}	ζ	α	κ
ζ	$\frac{2}{3}$	0	$\frac{1}{3}$
α	0	$\frac{2}{3}$	$\frac{1}{3}$
κ	$\frac{1}{3}$	$\frac{1}{3}$	$\frac{1}{3}$

(a) $\mathbf{M}_{\mathcal{HA}\mathcal{C}}$

s^t \ s^{t+1}	ζ	α	κ
ζ	$\frac{2}{3}$	0	$\frac{1}{3}$
α	$\frac{1}{3}$	$\frac{1}{3}$	$\frac{1}{3}$
κ	$\frac{1}{6}$	$\frac{5}{6}$	0

(b) $\mathbf{M}_{\mathcal{HA}\mathcal{C}_1}$

s^t \ s^{t+1}	ζ	α	κ
ζ	$\frac{1}{2}$	$\frac{1}{6}$	$\frac{1}{3}$
α	0	$\frac{1}{2}$	$\frac{1}{2}$
κ	$\frac{1}{3}$	$\frac{1}{3}$	$\frac{1}{3}$

(c) $\mathbf{M}_{\mathcal{HA}\mathcal{C}_2}$

s^t \ s^{t+1}	ζ	α	κ
ζ	$\frac{7}{9}$	$\frac{1}{9}$	$\frac{1}{9}$
α	$\frac{1}{9}$	$\frac{4}{9}$	$\frac{4}{9}$
κ	0	$\frac{1}{3}$	$\frac{2}{3}$

(d) $\mathbf{M}_{\mathcal{HA}\mathcal{C}_3}$

s^t \ s^{t+1}	ζ	α	ξ
ζ	$\frac{1}{3}$	$\frac{2}{3}$	0
α	0	$\frac{5}{6}$	$\frac{1}{6}$
ξ	0	$\frac{1}{3}$	$\frac{2}{3}$

(e) $\mathbf{M}_{\mathcal{HA}\mathcal{N}}$

s^t \ s^{t+1}	ζ	α	κ	σ
ζ	$\frac{1}{4}$	0	$\frac{3}{4}$	0
α	0	$\frac{3}{4}$	$\frac{1}{4}$	0
κ	0	$\frac{1}{4}$	$\frac{3}{4}$	0
σ	0	$\frac{1}{2}$	0	$\frac{1}{2}$

(f) $\mathbf{M}_{\mathcal{HA}\mathcal{CS}}$

s^t \ s^{t+1}	ζ	α	κ	σ
ζ	$\frac{1}{2}$	0	$\frac{1}{4}$	$\frac{1}{4}$
α	0	$\frac{1}{2}$	$\frac{1}{2}$	0
κ	$\frac{1}{4}$	$\frac{1}{4}$	$\frac{1}{2}$	0
σ	0	0	$\frac{1}{2}$	$\frac{1}{2}$

(g) $\mathbf{M}_{\mathcal{HA}\mathcal{CS}_1}$

s^t \ s^{t+1}	ζ	α	κ	σ
ζ	$\frac{5}{8}$	0	$\frac{3}{8}$	0
α	0	$\frac{3}{8}$	$\frac{5}{8}$	0
κ	0	$\frac{1}{4}$	$\frac{3}{4}$	0
σ	$\frac{1}{4}$	0	$\frac{1}{4}$	$\frac{1}{2}$

(h) $\mathbf{M}_{\mathcal{HA}\mathcal{CS}_2}$

s^t \ s^{t+1}	ζ	α	κ	σ
ζ	$\frac{1}{2}$	0	0	$\frac{1}{2}$
α	0	$\frac{1}{2}$	$\frac{1}{2}$	0
κ	$\frac{1}{4}$	$\frac{1}{4}$	$\frac{1}{2}$	0
σ	0	0	$\frac{1}{4}$	$\frac{3}{4}$

(i) $\mathbf{M}_{\mathcal{HA}\mathcal{CS}_3}$

Fig. 2.19 Stochastic matrices of affecton state transitions.

the processes so far are ergodic.

A stationary probability distribution δ (calculated from the Chapman–Kolmogorov equation) for affectons acting in a random environment Ω specifies, by elements $\delta(a)$ of the distribution δ, a probability for an affecton to be in state a if the affecton evolves in the environment Ω and its initial states, in every trial of development, is chosen with probability $|\mathbf{E}|^{-1}$. Tables $\mathbf{D}_{\mathcal{C}}$ representing the distribution δ, for each class $\mathcal{C}$, are shown in Fig. 2.20.

s	$\rho(s)$
ζ	$\frac{1}{3}$
α	$\frac{1}{3}$
κ	$\frac{1}{3}$

(a) $\mathbf{D}_{\mathcal{HAC}}$

s	$\rho(s)$
ζ	$\frac{4}{9}$
α	$\frac{11}{36}$
κ	$\frac{1}{4}$

(b) $\mathbf{D}_{\mathcal{HAC}_1}$

s	$\rho(s)$
ζ	$\frac{6}{23}$
α	$\frac{8}{23}$
κ	$\frac{9}{23}$

(c) $\mathbf{D}_{\mathcal{HAC}_2}$

s	$\rho(s)$
ζ	$\frac{1}{6}$
α	$\frac{1}{3}$
κ	$\frac{1}{2}$

(d) $\mathbf{D}_{\mathcal{HAC}_3}$

s	$\rho(s)$
ζ	0
α	$\frac{2}{3}$
ξ	$\frac{1}{3}$

(e) $\mathbf{D}_{\mathcal{HAN}}$

s	$\rho(s)$
ζ	0
α	$\frac{1}{2}$
κ	$\frac{1}{2}$
σ	0

(f) $\mathbf{D}_{\mathcal{HACS}}$

s	$\rho(s)$
ζ	$\frac{2}{9}$
α	$\frac{2}{9}$
κ	$\frac{4}{9}$
σ	$\frac{1}{9}$

(g) $\mathbf{D}_{\mathcal{HACS}_1}$

s	$\rho(s)$
ζ	0
α	$\frac{2}{7}$
κ	$\frac{5}{7}$
σ	0

(h) $\mathbf{D}_{\mathcal{HACS}_2}$

s	$\rho(s)$
ζ	$\frac{1}{6}$
α	$\frac{1}{6}$
κ	$\frac{1}{3}$
σ	$\frac{1}{3}$

(i) $\mathbf{D}_{\mathcal{HACS}_3}$

Fig. 2.20 Tables of stationary probability distribution δ for classes of emotional automata.

An automaton of the class $\mathcal{HAC}$ takes all three states — happiness, anger and confusion — with the same probability, so no emotional trends in the affecton's behavior are observed (Fig. 2.20a).

Only anger α and confusion κ have non-zero entries in the distribution δ in all affecton classes. They are the only states with positive entries of the distribution matrices in the classes $\mathcal{HACS}$, where $\delta(\alpha) = \delta(\kappa)$, and $\mathcal{HACS}_2$, where $\delta(\kappa) > \delta(\alpha)$ (Fig. 2.20f and h). All three emotional states have positive probabilities in δ,

$$\delta(\zeta) > \delta(\alpha) > \delta(\kappa)$$

in the class $\mathcal{HAC}_1$, and

$$\delta(\kappa) > \delta(\alpha) > \delta(\zeta)$$

in the classes $\mathcal{HAC}_2$ and $\mathcal{HAC}_3$ (Fig. 2.20c and d).

An affecton of the class $\mathcal{HAN}$ can be found only in the state of anxiety ξ (with the probability $\frac{1}{3}$) or in the state of anger α (with the probability $\frac{2}{3}$) (Fig. 2.20e).

In the classes $\mathcal{HACS}_1$ and $\mathcal{HACS}_3$ automaton states may be ordered according to their stationary distribution probabilities as follows (Fig. 2.20g and i):

$$\delta(\kappa) > \delta(\zeta) = \delta(\alpha) > \delta(\sigma)$$

in the class $\mathcal{HACS}_1$ and

$$\delta(\kappa) = \delta(\sigma) > \delta(\zeta) = \delta(\alpha)$$

in the class ($\mathcal{HACS}_3$).

2.7.2 *Reflecting singletons*

Usually a subject can recognize his own emotional state and, quite possibly, change his emotion as the result of his reflections. Let us look what would happen — how do emotions develop in such a situation? — if an emotional subject is left alone, deprived of any external emotional influences: $y^t = s^t$ and thus $s^{t+1} = f(s^t, s^t)$.

All states in classes $\mathcal{HAC}$, $\mathcal{HAC}_3$, $\mathcal{HACS}$, $\mathcal{HACS}_1$ and $\mathcal{HACS}_3$ are idempotents. Therefore, singletons do not change their initial states. In the class $\mathcal{HAC}_1$ only states ζ and α are idempotents. So, if an affecton starts its development in the state of confusion κ it takes the state either of happiness ζ or anger α, with the same probability $\frac{1}{2}$; the affecton remains in the chosen state forever.

The class $\mathcal{HAC}_2$ has the only idempotent — the state of confusion κ. In the class $\mathcal{HAC}_2$, an affecton, starting its evolution in the state ζ or α, takes the state ζ or α at time step t with the probability $1/(2^t)$; in a long run the affecton takes the stable state κ.

The affecton from class $\mathcal{HAN}$ keeps its original states α and ξ; if it started its evolution in the state α the automaton retains this state with the probability $1/(2^t)$.

A state of sadness σ is idempotent in all models:

"... Softer expressions followed this, and then again recurred the tender sadness which had sat upon him during his drive along the highway that afternoon ..." [Hardy (1994)].

2.7.3 *Coupled affectons*

In previous sections we studied the behavior of affectons in a random environment and affectons reflecting on their own emotions. How do affectons interact with each other? To keep it simple, we consider only couples of affectons. We "hard wire" two automata, one to the other, $y_A^t = s_B^t$ and $y_B^t = s_A^t$, as follows: $s_A^{t+1} = f(s_A^t, s_B^t)$ and $s_B^{t+1} = f(s_B^t, s_A^t)$. The system is autonomous and there are no external inputs to coupled affectons. Thus, one can construct a phase space — a graph of global state transitions — that essentially characterizes any class of coupled affectons. For any particular class, a global state transition space is represented by a graph, nodes of which are elements of the set $\mathbf{E}^2$, and an arc connecting two nodes $\langle s_A^t, s_B^t\rangle$ and $\langle s_A^{t+1}, s_B^{t+1}\rangle$ symbolizes the transition $\langle s_A^t, s_B^t\rangle \to \langle s_A^{t+1}, s_B^{t+1}\rangle$.

Global transitions of affecton couples, discussed here, are space invariant, so we can consider a generalized version of a transition graph. Namely, we represent configurations ab and ba by one node ab, $a, b \in \mathbf{E}$. We discuss dynamics of deterministic and stochastic affectons, and unreachable configurations and longest paths of non-repeated nodes in global transition graphs.

2.7.3.1 *Deterministic dynamic*

The automata of classes $\mathcal{HAC}$, $\mathcal{HACS}$, $\mathcal{HACS}_1$ and $\mathcal{HACS}_3$ are deterministic, so each node of their global transition graphs (Fig. 2.21) has an output degree of at most one. The input degree is bounded by a number of nodes in a graph. Therefore, couples of automata may finish their evolution only in a fixed point — a stationary configuration, or an attractor — a cyclic sequence of the global states. Deterministic graphs of global transitions of affecton couples are shown in Fig. 2.21.

The structure of a global transition graph of $\mathcal{HAC}$ is as follows. Duples of happiness and confusion $\zeta\kappa$ evolve to happiness $\zeta\zeta$, happiness and anger $\zeta\alpha$ finish their evolution in a state of shared confusion $\kappa\kappa$; a couple of angry and happy states $\alpha\zeta$ develops to an entirely angry duple $\alpha\alpha$ (Fig. 2.21a).

A graph of couples from the class $\mathcal{HACS}$ has four isolated nodes, which are stationary configurations. Three of them include couples of same-state

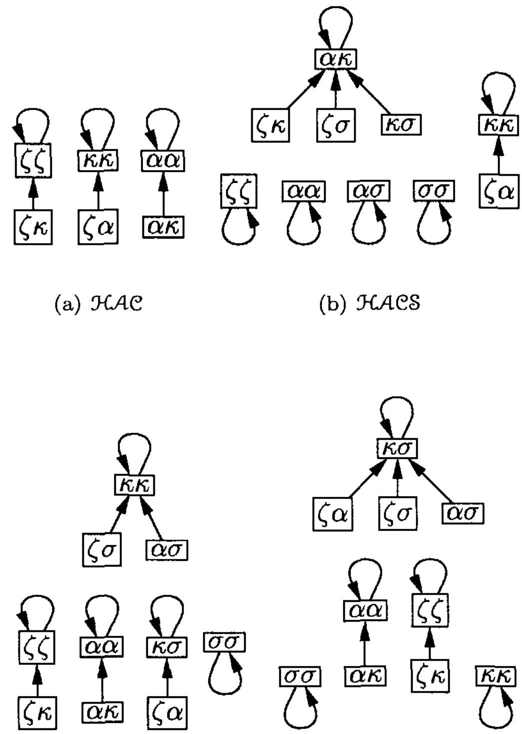

(a) $\mathcal{HAC}$ (b) $\mathcal{HACS}$

(c) $\mathcal{HACS}_1$ (d) $\mathcal{HACS}_3$

Fig. 2.21 Graphs of global transitions of affecton couples of classes $\mathcal{HAC}$ (a), $\mathcal{HACS}$ (b), $\mathcal{HACS}_1$ (c) and $\mathcal{HACS}_3$ (d).

affectons — $\zeta\zeta$, $\alpha\alpha$ and $\sigma\sigma$ — happy, angry and sad (Fig. 2.21b) and the fourth consists of anger and confusion $\alpha\kappa$. A couple of sad and angry affectons $\sigma\alpha$ takes a stationary state of shared confusion $\kappa\kappa$, while couples of happy and confused $\zeta\kappa$, or happy and sad $\zeta\sigma$, or sad and confused $\sigma\kappa$ automata evolve to a stationary state, where one affecton is confused and the other is angry $\kappa\alpha$ (Fig. 2.21b).

In classes $\mathcal{HACS}_1$ and $\mathcal{HACS}_3$, configurations of two happy automata $\zeta\zeta$, two confused automata $\kappa\kappa$, two angry automata $\alpha\alpha$ and configurations of confused and sad automata are attracting fixed points in the evolution (Fig. 2.21c and d); they attract almost all other states of affecton couples.

There are a few isolated nodes in the graphs of $\mathcal{HACS}_1$ and $\mathcal{HACS}_3$: couples of two sad automata $\sigma\sigma$ and two confused automata $\kappa\kappa$; the latter is present only in the class $\mathcal{HACS}_3$ (Fig. 2.21c and d). A pair of happy and confused automata $\zeta\kappa$ evolves to a stationary happiness $\zeta\zeta$, and a pair of angry and confused automata $\alpha\kappa$ — to a stationary anger $\alpha\alpha$. If one of the affectons is sad and another is either angry or happy, the pair from the class $\mathcal{HACS}_1$ takes a stationary state of total confusion $\kappa\kappa$ (Fig. 2.21c) or a combination of sadness and confusion $\sigma\kappa$ in the model $\mathcal{HACS}_3$ (Fig. 2.21d).

2.7.3.2 *Probabilistic dynamic*

Binary compositions defined by tables of automaton state transitions in the models $\mathcal{HAC}_1$ and $\mathcal{HAC}_3$ are symmetric; so are global transition graphs of affecton pairs (Fig. 2.22).

Totally happy and totally angry couples — $\zeta\zeta$ and $\alpha\alpha$ — are absorbing global states in the model $\mathcal{HAC}_1$ (Fig. 2.22a). Starting its evolution in any global state, an affecton couple eventually falls in a state of either total happiness or total anger; a transition to one of these global states occurs with the same probability $\frac{1}{2}$. Obviously, initially angry or happy couples do not change their states. There is yet another absorbing state — shared confusion $\kappa\kappa$ — in the model $\mathcal{HAC}_3$ (Fig. 2.22c). Automaton couples of the class $\mathcal{HAC}_2$ spend a significant part of their time in the states $\alpha\xi$ and $\alpha\kappa$, but ultimately finish their evolution in the state of total confusion $\kappa\kappa$ (Fig. 2.22b).

A happy couple remains happy in the class $\mathcal{HAN}$. All other emotional configurations finish evolution in a sub-set of the configurations "angry–angry", "angry–anxious" and "anxious–angry". A couple switches between these global configurations at random (Fig. 2.22d).

Automaton couples from the class $\mathcal{HACS}_2$ behave straightforwardly: they remain in their initial states of shared happiness $\zeta\zeta$, anger $\alpha\alpha$, sadness $\sigma\sigma$ or confusion and sadness $\kappa\sigma$. All other initial states are absorbed by the state of total confusion $\kappa\kappa$ (Fig. 2.22e).

2.7.3.3 *Unreachable emotional states*

A configuration c of an automaton collective is called unreachable if there is no configuration that is transformed to the configuration c by applying automaton state transition rules to entities of the collective. Unreachable configurations never appear in the evolution of an autonomous system — they can be only artificially introduced in the system. Let $\mathbf{U}(\mathcal{C})$ be a set of

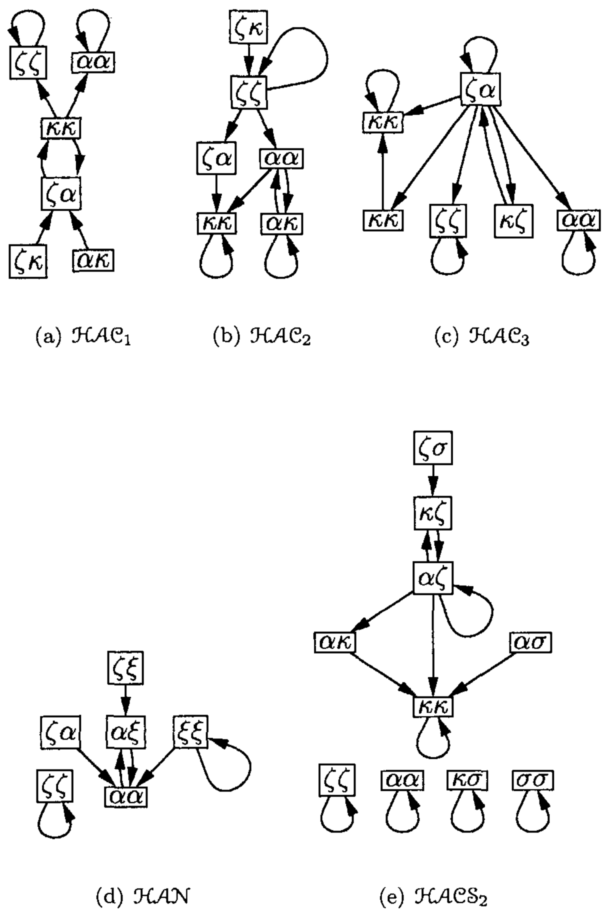

Fig. 2.22 Graphs of global state transitions of affecton couples of classes $\mathcal{HAC}_1$ (a), $\mathcal{HAC}_2$ (b), $\mathcal{HAC}_3$ (c), $\mathcal{HAN}$ (d) and $\mathcal{HACS}_2$ (e).

unreachable configurations of affecton couples of the class $\mathcal{C}$. Then affecton classes are characterized by the following sets of unreachable configurations:

$$\begin{aligned}
\mathbf{U}(\mathcal{HAC}_3) &= \emptyset,\\
\mathbf{U}(\mathcal{HAN}) &= \{\zeta\alpha\},\\
\mathbf{U}(\mathcal{HAC}_2) &= \{\zeta\kappa\},\\
\mathbf{U}(\mathcal{HAC}_1) &= \{\zeta\kappa, \alpha\kappa\},\\
\mathbf{U}(\mathcal{HACS}_2) &= \{\zeta\sigma, \alpha\sigma\},
\end{aligned}$$

$$\begin{aligned}\mathbf{U}(\mathcal{HAC}) &= \{\zeta\alpha, \zeta\kappa, \alpha\kappa\},\\ \mathbf{U}(\mathcal{HACS}) &= \{\zeta\alpha, \zeta\kappa, \zeta\sigma, \kappa\sigma\},\\ \mathbf{U}(\mathcal{HACS}_1) &= \{\zeta\alpha, \zeta\kappa, \zeta\sigma, \alpha\kappa, \alpha\sigma\},\\ \mathbf{U}(\mathcal{HACS}_3) &= \{\zeta\alpha, \zeta\kappa, \zeta\sigma, \alpha\kappa, \alpha\sigma\}.\end{aligned}$$

The class $\mathcal{HAC}_3$ has no unreachable configurations. The classes $\mathcal{HACS}_1$ and $\mathcal{HACS}_3$ have a maximal, amongst all studied classes, number of unreachable configurations: three of the configurations include happiness ζ as one of their states and two others comprise anger α and either confusion κ or sadness σ.

2.7.3.4 *Longest transitions*

Typically, the longer a system's transition from an initial state to a stationary configuration, or an attracting cycle, the richer the behavior of the system. To assess this type of richness of an affecton class one should calculate a longest path of non-repeated nodes in a global transition graph of affecton couples. Generally, the more unreachable configurations there are in a class, the less probably affecton couples of the class would exhibit a rich behavior in their evolution (see e.g. [Wuensche and Lesser (1992)]). $\mathcal{HACS}_2$ could be considered as a behaviorally richest class because a global transition graph of its affecton couples has a maximum path of four non-repeated nodes length; two "less rich" classes $\mathcal{HAC}_1$ and $\mathcal{HAC}_2$ have longest paths of three nodes.

2.8 Wicked feelings

In the chapter we studied several toy models of collective non-linear dynamics of emotions in massive pools of simple entities. Emotions were simulated as abstract molecules in well-stirred and thin-layer affective solutions — abstractions of human crowds, where there are

> "... too many people in too little space ..." [Kruse (1986)].

In the models of affective solutions carriers of emotions never acted, they only changed their emotions as a result of observing emotions of other carriers. Emotions are considered as abstract entities without any connection to goals, desires and achievements. On one side, this makes our models less realistic and thus may avert practitioners; on the other side, this allows for detailed studies of affective dynamics, without unnecessary troubling

with unimportant details.

In computational experiments with continuous and discrete models we uncovered a wide range of behavioral modes of affective solutions and varieties of reactions to local perturbations of affective reagent concentrations. We shown that even very simple reaction schemes involving few emotions may lead to rich space–time dynamics of affective solutions. We employed an affective chemistry paradigm in a simulation of emotional abuse and showed that this theoretical framework allows for a quite unconventional but fruitful representation of reality. Our models may be seen as non-linear system analogs of emphatic consciousness that arises due to emotional synchronization and resonance [Heise (1998)]; however, the emotional resonance observed in the chapter is purely "mechanical" — not determined by symbolic interaction and collateral action of emotion carriers. In certain cases various modes of space–time and integral dynamics of affective mixtures, uncovered in the chapter, meet most dynamical criteria of psychopathology [Mullen (1997)]:

- poverty of emotional response, particularly flattering, when the subject is aware of potential meaning but unable to experience corresponding emotion
- anhedonia, inability to experience pleasure
- incongruity, inappropriate emotional response
- rigidity of emotional responses
- lability, "sudden short-lived but often intense changes in feeling may occur in response to minor events"
- apathy
- ambivalence, co-existing of contradictory emotions, "ambivalence refers to the relatively mundane experience of having a mixture of apparently contradictory emotions about someone or something that tend to alternate rapidly"
- alexithymia, "virtual inability to recognize or verbalize emotional experiences" [Mullen (1997)].

Experimenting with cellular non-linear networks and cellular automata, we demonstrated that for some reaction schemes a thin layer of affective liquid exhibits traveling waves, typical for excitable chemical media. We know that wave-front velocity in a thin-layer chemical medium is around 1–2 mm/sec. What is the wave speed in affective solutions? Wild *et al.* [Wild *et. al* (2001)] have shown that presentation of pictorial emotional expressions during 500–1000 msec evokes a similar (to

presented emotions) emotional response in human respondents. Assuming that the size of human comfortable personal space is around 0.5–1 m, we get a speed of affective wave fronts equal to 1–2 m/sec. The value is significantly less than the velocity of excitation waves in real human masses, since for example those recorded at a stadium can reach 6–12 m/sec, equivalent to about 22 persons/sec [Farkas *et. al* (2002); Farkas *et. al* (2003)]. This is possibly because excitation in football crowds does not actually involve recognition of emotions but just reactions to actions (shouting, jumping up) of nearest neighbors.

We aimed rather to ignite an interest in non-linear dynamics of emotions in spatially extended systems by showing scoping experiments with affective systems. We took emotions out of their "natural" habitat of circumstances, intentions, actions, interpersonal relations, achievements and social norms. We envisage that further studies will enrich the computational models with real-life traits. Emotions determine a social structure of a collective, synchronize social dynamic and lead to formation of coherent actions [Heise and O'Brien (1993); Planalp (1999)]. Therefore, in future, it would be reasonable to couple affective solutions with effective solutions, and to develop novel reaction schemes comprising interactions between affective and effective reagents. This formalism would properly reflect functional roles of emotions in action generations, namely quasi-chemical reactions may interpret emotions as action goals, tendencies and generators of goal-desires [Reisenzein (1996); Reisenzein (1998)].

Moreover, the chapter contributes to the development of a formal theory of emotional interactions and collective emotions, a theory of affective computing, simulation of artificial collectives and societies and design of emotional controllers for robots. Further formal development could concentrate around the following three points. First, a real-life verification of basic types of emotional interactions is necessary. For example, transformations anger $\rightarrow$ {disgust, fear}, fear $\rightarrow$ disgust and sadness $\rightarrow$ sadness are experimentally observed [Wild *et. al* (2001)]; however, they were not included in our models. Wild–Erb–Bartels experiments [Wild *et. al* (2001)] uncovered the following scattering of affective states:

- a happy face evokes happiness (with probability $\frac{1}{2}$), surprise ($\frac{1}{3}$), sadness ($\frac{1}{15}$), anger ($\frac{1}{15}$), disgust ($\frac{1}{15}$) and fear ($\frac{1}{15}$),
- a sad faces evokes sadness (with probability $\frac{1}{3}$), surprise ($\frac{1}{3}$), anger ($\frac{1}{6}$), fear ($\frac{1}{6}$), happiness ($\frac{1}{15}$) and disgust ($\frac{1}{15}$).

Our models of reaction kinetics and diffusion in affective media did not incorporate different diffusion coefficients of different emotions; this could be studied in the future and we expect interesting findings there. It was experimentally shown that happy faces are recognized faster than sad faces but slower than angry faces [Leppänen *et. al* (2003)], so the diffusion coefficients D could be ordered as

$$D_{\text{anger}} \gg D_{\text{happiness}} \gg D_{\text{sadness}}.$$

Second, the concept of affectons could be evolved to a full-scale model of computation coupled with emotions. This may take a form similar to a cogitoid — a computational model of cognition — where knowledge is seen as a lattice of concepts and associations between the concepts [Wiedermann (1998a); Wiedermann (1998b)].

Third, affectons will play an important role in representing a human mind as a collective of simple interacting entities, like Minsky's society of mind [Minsky (1988)] and Dennet's space–time configurations of agent collectives [Dennet (1991)].

Why are affective reactions not less important than doxastic reactions in crowds? Three symptoms, seen as having just a historical value by some modern scholars, are highlighted by Moscovici [Moscovici (1985)]: increase of emotional reactions, decrease in intellectual reactions and decrease in irrationalization and irresponsibility. So, emotions are not simply indispensable in cognition, collective knowledge and development of social structure (see e.g. [Barbalet (2000)]) — emotions govern cognition. This may indicate yet another route of further studies: to couple affective dynamics [Adamatzky (2002c); Adamatzky (2002b)] with dynamics of knowledge dynamics [Adamatzky (2001d); Adamatzky (2002c); Adamatzky (2004); Adamatzky (2002b)].

It is a widely accepted fact that

> ... consequence of emotional contagion is attentional, emotional and behavioral synchrony ... [Hatfield *et. al* (1992)].

Yes, this could happen in some situation; however, most frequently, as we have shown in the chapter, contagion leads to formation of a complicated heterogeneous emotional structure, emergence of domains of alike emotions, spreading and interaction of affective waves:

"... while the behavior caused by emotional states can be irrational, the emotional process itself is largely explicable in rational, scientific terms" [Kaufman (1999)].

Chapter 3

Doxastic Dynamics at the Edge of Irrationality

Since the late 1980s — when ideas of evolving belief [Kraus and Lehmann (1988)] emerged in a context of discourse — it became appropriate to consider belief as a dynamical entity, which is not ideal but incomplete, changing as a result of observations (see [Friedman and Halperd (1996)]). Believers are now seen as not omnidoxastic, they are slaves of their fluctuating mental states, means of communication and levels of reasoning. If, for example, a current observation of a phenomenon contradicts or just does not fit the previous observations (and thus previous beliefs) of a believer, then either the old belief was wrong or the world has changed. In the first case, the believer revises his belief; in the second, he updates his belief; or, just does it both ways [Friedman and Halperd (1996)]. Sometimes [Yager *et. al* (1992)] interaction between observation and belief, as a degree of compatibility of the belief to the observation, is incorporated into the belief models; alternatively, belief is ascribed to an agent's imagination in a context of previous experiences [Paris and Vencovska (1993)]. A model of fallible belief [O'Hara *et. al* (1995)], based on non-normal logics, looks like a most attractive alternative to conventional paradigms.

Two cardinal models of belief, without logical omniscience, were offered in the middle of the 1980s by Levesque [Levesque (1984)] and by Fagin and Halpern [Fagin and Halpern (1988)]. Dynamics of belief is also considered in Hadley's computational model [Hadley (1988)], where agents revise their beliefs without any constraints on the agents' representation language. Or else, one can manipulate sets of assumptions, to revise agents' beliefs, as manifested in [Martin and Shapiro (1988)]. Dubois and Prade [Dubois and Prade (1992)] offer a family of belief functions relevant to incomplete knowledge to analyze beliefs in a statistical framework. Gaspar's model [Gaspar (1991)] is even more close to reality: agents are imperfect reasoners, they

base their judgements on incomplete and, possibly incorrect, knowledge; the agents revise their beliefs depending on information obtained from other agents. Ideas from [Gaspar (1991)] contributed to our models of collective beliefs, which will be discussed further.

Usually, there are several levels of reasoning [Minsky (1988)]: agents can reason about beliefs of other agents and remain syntactically neutral when they express other agents' beliefs. Thus, Hadley [Hadley (1991b)] employs the concepts of knowledge, where a notion of truth incorporates cognitive concepts. The operators of belief revision and updating can be identified syntactically [Del Val (1993)]. Actually, even the beliefs of agents in the collectives can be represented by logical theories [Giunchiglia *et. al* (1993)] and then reasoning about agents' beliefs may be crystallized in another logical theory; a classification of the main forms of non-logical omniscience is an advantage of such an approach. The intelligent interaction in collectives also requires an agent to recognize other agents' mental states, including beliefs and intentions [Tambe *et. al* (1998)].

A theory of collective belief suffers from poor representation of varieties of doxastic states: usually only belief and knowledge are employed in theoretical and computational studies, while the richness of delusion, misbelief, doubt and ignorance is often ignored. Behaviors of quasi-realistic agents are often determined by a cluster of mental states, including emotions, intentions, dreams, desires, beliefs and imaginations. The mental states interweave one with another. Therefore, when agents interact and update their mental states depending on their own previous mental states and the states of other agents, the result of one particular state's update is influenced by spatio-temporal dynamics of other mental states. Very often mental states develop irrationally, if not pathologically. This is particularly evident in crowd conditions, where deindividuation [Zimbardo (1969)] of persons comprising the crowd results in emotional, impulsive and irrational behavior, with perceptual distortions, hyper-responsiveness to neighboring agents, and self-catalytic dynamics. "Distortion of traditional forms and structures" [Zimbardo (1969)] in crowds contorts architectonics of belief update functions, thus making it impossible to apply common-sense reasoning and conventional inferences.

> "The crowd-mind consists ... of a disturbance of the function of real. *The crowd is the creature of belief*" [Martin (1920)].

The models of such non-sensible developments are studied in the present chapter.

3.1 On doxastic states and their binary compositions

Let $\mathbb{A}$ be a finite set of agents and $\mathbb{P}$ be a set of propositions. For an agent i from $\mathbb{A}$ and a proposition p, $\beta_i p$ means that the agent i believes p. Agents can be either mobile or static. If the agents are mobile we model them as a stirred agent-chemicals reactor. If agents are static we order them in a chain and consider them as non-stirred, or thin-layer reactors. An agent can sense other agents being in its local — temporary (in stirred reactors) or constant (in chains) — vicinity. A proposition p may be true or false referring to the local agent neighborhood. We write $\lambda_i p$ when p is true in the neighborhood of i. We take belief as a primary cognitive state, or an atom of cognition. The following "compound" states are derived from belief:

(1) Knowledge, κ, is the justified belief: $\kappa_i p \rightarrow \beta_i p \wedge \lambda_i p$,

(2) Doubt, δ, is the so familiar feeling of uncertainty, an agent doubts p when he neither believes nor disbelieves p: $\delta_i p \rightarrow \neg\beta_i p \wedge \neg\beta_i \neg p$,

(3) Misbelief, μ, is a wrong belief, or a false opinion, referring to the local vicinity: $\mu_i p \rightarrow \beta_i p \wedge \lambda_i \neg p$,

(4) Delusion, ϵ, is an erroneous belief, which is usually defined as the fixed belief that cannot be justified: $\epsilon_i p \rightarrow \beta_i p \wedge \neg\lambda_i p \wedge \neg\lambda_i \neg p$. Delusion is generally considered a belief that does not correspond to "the way things are" [Snyder (1991)]. See also the logical definition of delusion in [Gerasimova (1989)]. In some cases we can also consider delusions as conclusions from arguments whose validity could not be determined [Franceschi (2003)]. Sometimes delusions are means for overcoming social exclusion, a kind of "exploitative mimicry" [Hagen (1995)].

(5) Ignorance: $\iota_i p \rightarrow \neg\beta_i p \wedge \neg\beta_i \neg p \wedge \neg\lambda_i p \wedge \neg\lambda_i \neg p$, agent i is in the state of ignorance when it neither believes nor disbelieves p and there is no information about p in the local vicinity of i; some formalization related to ignorance is presented in [Kraus and Perlis (1989)].

Let the only proposition p be on the horizon of agents of $\mathbb{A}$; then we can say that agent i takes a doxastic state ϑ, $\vartheta \in \mathbb{D} = \{\kappa, \delta, \mu, \epsilon, \iota\}$, if one of the conditions 1–5 occurs. In this model an epistemic set is a singleton, because this set cannot be expanded or retracted, no old beliefs can be given up

and no new belief can be taken on board (those interested in more widely acceptable theories of belief revision are referred to the excellent book by Gärdenfors [Gärdenfors (1990)]).

The complete state of an agent i can be represented by the tuple (s_i, v_i) of its belief in p and the truth state of proposition p in the agent's vicinity, where

$$s_i = \begin{cases} 0 & \text{if} \quad \beta_i \neg p, \\ 1 & \text{if} \quad \beta_i p \wedge \beta_i \neg p, \\ 2 & \text{if} \quad \beta_i p. \end{cases}$$

Similarly, we can determine v_i and λ_i. The correspondence between tuples of $\{0,1,2\} \times \{0,1,2\}$ and doxastic states is pretty straightforward. Hereinafter, we mean elements of $\mathbb{D}$ when we talk about doxastic states of the agents.

Let (s_i, v_i) and (s_j, v_j) be states of agents i and j, and let the agents be neighbors. Then we suggest that agent i changes its state tuple depending on the first, i.e. doxastic, component of its state and both components of agent j's state. So, agent i updates its state as follows:

$$s_i \leftarrow s_i \diamond (s_j, v_j),$$

where composition $\diamond$ is defined by the matrix

$$\begin{array}{c} \\ 0 \\ 1 \\ 2 \end{array} \begin{array}{c} \begin{array}{ccccccccc} (0,0) & (0,1) & (0,2) & (1,0) & (1,1) & (1,2) & (2,0) & (2,1) & (2,2) \end{array} \\ \left(\begin{array}{ccccccccc} 0 & 0 & 1 & 0 & 0 & 1 & 1 & 1 & 1 \\ 0 & 0 & 1 & 1 & 1 & 1 & 1 & 2 & 2 \\ 1 & 1 & 1 & 1 & 2 & 2 & 1 & 2 & 2 \end{array} \right) \end{array}. \tag{3.1}$$

Agent i meets another agent j and i compares j's belief and the truth state in j's vicinity with its own, agent i's, belief, and then i modifies its belief as an outcome of this comparison. Meantime the second component, v_i, remains unchanged.

The composition $\diamond$ (3.1) is pathological, or irrational, in a sense that i is much more concerned with the state of j's local world than with the state of its own vicinity.

This composition well reflects loss of rationality in crowd dynamics:

"Each individual on his own behaves rationally and yet when he joins up with others he ceases to do so and his behavior becomes unpredictable" [Moscovici (1985)].

An epiphenomenon of the composition may be seen in

"... outbursts of crowds as outbursts of madness fomented by blind delusions and showing obvious signs of delirium, hallucination, and a total loss of self-control ..." [Moscovici (1985)].

With the help of composition $\diamond$ we derive the following mappings:

$$\{0,1,2\} \times \{0,1,2\} \to \{0,1,2\}$$

and

$$\odot : \quad \mathbb{D} \times \mathbb{D} \to \mathbb{G}.$$

Set $\mathbb{G}$ is a proper sub-set of a Boolean $B(\mathbb{D})$ of set $\mathbb{D}$.

The matrix form of $\odot$ is shown below:

$$\begin{array}{c} \\ \kappa \\ \epsilon \\ \mu \\ \delta \\ \iota \end{array} \begin{array}{c} \begin{array}{ccccc} \kappa & \epsilon & \mu & \delta & \iota \end{array} \\ \begin{pmatrix} \{\kappa,\delta\} & \{\kappa,\delta\} & \{\delta\} & \{\kappa,\delta\} & \{\kappa\} \\ \{\epsilon,\iota\} & \{\epsilon,\iota\} & \{\iota\} & \{\epsilon,\iota\} & \{\epsilon\} \\ \{\mu,\delta\} & \{\mu,\delta\} & \{\delta,\iota\} & \{\mu,\delta\} & \{\mu\} \\ \{\mu,\kappa\} & \{\mu,\kappa\} & \{\delta\} & \{\delta\} & \{\delta\} \\ \{\epsilon\} & \{\epsilon\} & \{\iota\} & \{\iota\} & \{\iota\} \end{pmatrix} \end{array}. \tag{3.2}$$

A realistic explanation of the composition $\odot$ could be in affective influence of agents' doxastic development as exemplified by the two following quotations:

"Emotions influence beliefs. ... People's emotions ... determine what they think, and what they think is true ... A belief may persist in the face of evidence that contradicts it. The belief renders that evidence powerless. It is ignored or dismissed; arguing appears useless. Furthermore, a person holding a belief may accept information as credible that would appear doubtful to other people ..." [Frijda and Mesquita (2000)].

and

"When it comes to the issue of emotional importance, convincing someone to change his or her existing beliefs to be a virtually hopeless undertaking" [Frijda *et. al* (2000)].

The composition $\odot$ represents a belief update far from mental equilibrium:

> "... every action of the mind which operates with calmness and tranquillity is regarded as reason ..." [Barbalet (2000)].

The crowding phenomenon lies beneath this — individual minds become more irrational when density of the mass of individuals increases [Kruse (1986)].

The matrix of $\odot$ is derived from the matrix of $\diamond$ and the mapping

$$\{0,1,2\} \times \{0,1,2\} \to \{\kappa, \epsilon, \mu, \delta, \iota\}.$$

This is because every duplex of elements of the set $\{0,1,2\}$ can be put into correspondence to one, uniquely determined, doxastic element from the set $\mathbb{D} = \{\kappa, \epsilon, \mu, \delta, \iota\}$.

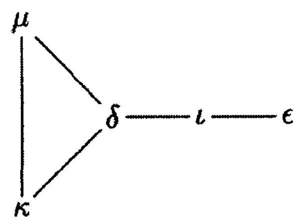

Fig. 3.1 T relation; the links $x\ T\ x$ are not shown.

From the matrix form (3.1) of $\diamond$ we see that any set from $\mathbb{G}$ has at least one and at most two elements. What doxastic states of $\mathbb{D}$ are generated in pairs in $\odot$? Let states s_1 and s_2 be in a relation T if there are two such elements z_1 and z_2 of $\mathbb{D}$ so that $z_1 \odot z_2 = \{s_1, s_2\}$. Relation T is symmetrical; its graph representation is shown in Fig. 3.1. The graphical form makes it clear that knowledge, doubt and misbelief can be generated in pairs.

> Doubt can be born as a pair with ignorance but ignorance is necessarily accompanied by delusion.

This reduces differences between non-bizarre (they could be true) and systematized (they may form a coherent logical system and even integrate recent events) types of delusion [Hagen (1995)].

Ignorance and delusion cannot be born together with misbelief and knowledge.

We call the mapping $\odot$ deterministic if a singleton is produced. Thus, for example, $\kappa \odot \mu = \{\delta\}$ is deterministic. In this case we can write simply $\kappa \odot \mu = \delta$. We apply algebraic terminology to the deterministic components of the mapping $\odot$.

Now we can use the mapping $\odot$ to define the basic rule for the updating agent's states. Let s_i and s_j be doxastic states of agents i and j, and let agents j and i be neighbors. Then agent i changes its doxastic state by the rule: $s_i := s_i \odot s_j$. Hereinafter in the book we will deal with finite-automaton models of agents — doxatons.

A doxaton is a finite automaton $\langle \mathbb{S}, \mathbb{I}, \gamma \rangle$ where sets of states $\mathbb{S}$ and $\mathbb{I}$ of inputs are equal $\mathbb{D}$; and, $\gamma : \mathbb{S} \times \mathbb{I} \to \mathbb{S}$.

All entries of ι's column of the matrix (3.2) are different; therefore, if doxaton i meets doxaton j and doxaton j is in a state of ignorance, the doxaton i does not change its doxastic states. Ignorance is the only right identity; therefore the state of doxaton j may not be substituted by the state of doxaton i (see ι's row of the matrix (3.2)).

Ignorance is a right identity for $\odot$.

There are no left identities and no zeros in $\odot$: the doxatons do not simply accept doxastic states of their counterparts; however, they cannot keep their own states unchanged.

Only doubt and ignorance are idempotents.

This also follows from the matrix (3.2).

$\langle \{\delta, \iota\}, \odot \rangle$ is an associative and non-commutative algebra, every element of which is a right zero and a left identity.

The set $\{\delta, \iota\}$ is stable under $\odot$. Everything else follows from the matrix (3.2).

Knowledge is the minimal generator.

The product of κ with itself gives us the set $\{\kappa, \delta\}$; $\delta \odot \kappa$ produces an additional element μ; so, we have $\{\kappa, \delta, \mu\}$ at this stage. The next iteration of the compositions adds ι, as a product of μ with itself. The fifth element, ϵ, is the product of ι and κ. In such a way the whole set $\mathbb{D}$ can be generated from κ. Therefore, we can say that we need at least two doxatons, both in states of knowledge, to generate the entire spectrum of the doxastic states.

3.2 Non-sense functors

What happens if we ignore the second component — the truth state v_i of doxaton i's vicinity — of an agent's complete state i? We may suggest a probabilistic interpretation of $\diamond$. This new mapping $\star$ assigns the stochastic (all elements of a vector summed to 1) vector to every duplex of truth values. This is a vector of order three. The z's entity of the vector is a probability of truth value $z \in \mathbb{Q} = \{0, 1, 2\}$. The mapping is as follows:

$$\star : \mathbb{Q} \times \mathbb{Q} \to \mathbb{P} \subset [0,1]^3,$$

where $\mathbb{P} = \{(p_1, p_2, p_3) | p_1, p_2, p_3 \in [0,1] \text{ and } \sum_{i=1,2,3} p_i = 1\}$, and p_i is a probability of truth value i. The $\star$ is represented in the following matrix form:

$$\begin{array}{c} \\ 0 \\ 1 \\ 2 \end{array} \begin{array}{c} \begin{array}{ccc} 0 & 1 & 2 \end{array} \\ \begin{pmatrix} (\frac{2}{3}, \frac{1}{3}, 0) & (\frac{2}{3}, \frac{1}{3}, 0) & (0, 1, 0) \\ (\frac{2}{3}, \frac{1}{3}, 0) & (0, 1, 0) & (0, \frac{1}{3}, \frac{2}{3}) \\ (0, 1, 0) & (0, \frac{1}{3}, \frac{2}{3}) & (0, \frac{1}{3}, \frac{2}{3}) \end{pmatrix} \end{array}. \tag{3.3}$$

To derive exotic functors of truth values, we define a deterministic version of $\star$ by choosing only those entries of vectors of the matrix (3.3) which have maximal probabilities. Every vector has just one maximal probability, so we get a deterministic matrix:

$$\begin{array}{c} \\ 0 \\ 1 \\ 2 \end{array} \begin{array}{c} \begin{array}{ccc} 0 & 1 & 2 \end{array} \\ \begin{pmatrix} 0 & 0 & 1 \\ 0 & 1 & 2 \\ 1 & 2 & 2 \end{pmatrix} \end{array}. \tag{3.4}$$

Let the matrix (3.4) represents functor $*$.

$\langle *, \mathbb{Q} \rangle$ is a commutative algebra with an identity.

As follows from the matrix (3.4) the 1, or non-sense, is a two-side identity.

Set $\{0, 2\}$ is a minimal generator of the algebra $\langle *, \mathbb{Q}\rangle$.

Elements 0 and 2 are idempotents and $0 * 2 = 1$.

What are the sensible relatives of functor $*$? We assume that agent i changes its state s_i by the rule: $s_i := s_i \phi s_j$, where ϕ is some specified functor and s_j is a state of another agent in the vicinity of the agent i. Four functors are straightforwardly derived. The agents using the functors in their development to update their doxastic states are called naive, conservative, anxious or contradictory agents.

- Naive agent. Naive agent i changes its state to non-sense if its state contradicts beliefs of its neighbor j. If agent i takes a non-sense state, 1, and agent j does not, then agent i takes the next state as s_j. The functor $*_N$ is represented by the matrix

$$\begin{array}{c c} & \begin{array}{ccc} 0 & 1 & 2 \end{array} \\ \begin{array}{c} 0 \\ 1 \\ 2 \end{array} & \begin{pmatrix} 0 & 0 & 1 \\ 0 & 1 & 2 \\ 1 & 2 & 2 \end{pmatrix} \end{array}. \tag{3.5}$$

  The functors $*$ and $*_N$ are identical. This means that the functor of naivety is a "maximalist" version of the probabilistic functor $*$.

- Conservative agent. A conservative agent preserves its doxastic states. The agent does not change its belief if its counterpart is in a non-sense state; neither does it change its non-sense state if its neighbor is in state 0 or 2. The agent i takes a non-sense state 1 only if its current state contradicts the state of its neighbor j, i.e. $s_i = 0$ and $s_j = 2$, or $s_i = 2$ and $s_j = 0$. The functor $*_C$ is represented as follows:

$$\begin{array}{c c} & \begin{array}{ccc} 0 & 1 & 2 \end{array} \\ \begin{array}{c} 0 \\ 1 \\ 2 \end{array} & \begin{pmatrix} 0 & 0 & 1 \\ 1 & 1 & 1 \\ 1 & 2 & 2 \end{pmatrix} \end{array}. \tag{3.6}$$

- Anxious agent. An anxiety is usually seen as resulting from some emotional conflicts, the nature of which is unfamiliar to an agent.

A feeling of apprehension makes the agent willing to reconsider its beliefs. The agent can even change its state to the "opposite" one when its neighbor is in the non-sense state. The matrix of the functor $*_A$ is shown below:

$$\begin{array}{c c} & \begin{array}{ccc} 0 & 1 & 2 \end{array} \\ \begin{array}{c} 0 \\ 1 \\ 2 \end{array} & \begin{pmatrix} 0 & 2 & 1 \\ 0 & 1 & 2 \\ 1 & 0 & 2 \end{pmatrix} \end{array}. \tag{3.7}$$

- Contradicting agent. Agent i takes state 2 or 0 if its neighbor, agent j, is in state 0 or 2, respectively. If agent i is in state 1 it adopts the state of agent j. The matrix of the contradicting functor $*_{CN}$ is as follows:

$$\begin{array}{c c} & \begin{array}{ccc} 0 & 1 & 2 \end{array} \\ \begin{array}{c} 0 \\ 1 \\ 2 \end{array} & \begin{pmatrix} 2 & 0 & 0 \\ 2 & 1 & 0 \\ 2 & 2 & 0 \end{pmatrix} \end{array}. \tag{3.8}$$

The results discussed below are derived from the structure of the matrices (3.5)–(3.8); we will use this to explain some features of the space–time dynamics of the agent collectives. Let $\mathbb{Q}$ be a set $\{0, 1, 2\}$ of agent states; then

> $\langle *_A, \mathbb{Q}\rangle$ and $\langle *_C, \mathbb{Q}\rangle$ are non-commutative and non-associative algebras; every element of the algebras is idempotent.

The loss of regularity is remarkable for such a distortion of rationality. Unfortunately, there are no two-side identities in these algebras:

> a non-sense state 1 is a right identity of algebra $\langle *_C, \mathbb{Q}\rangle$ and it is a left identity of algebra $\langle *_C, \mathbb{Q}\rangle$.

The common feature of algebras $\langle *_N, \mathbb{Q}\rangle$, $\langle *_C, \mathbb{Q}\rangle$ and $\langle *_A, \mathbb{Q}\rangle$ is that every element is idempotent. Both naive and conservative algebras have the same proper stable sets: $\{0, 1\}$ and $\{1, 2\}$, respectively. There are no proper stable sets in the algebra of anxiety, i.e. the set $\mathbb{Q}$ itself is a minimal stable set. The situation with the generators is quite similar. Both $\langle *_C, \mathbb{Q}\rangle$ and $\langle *_N, \mathbb{Q}\rangle$ have the same minimal generator $\{0, 2\}$. There are no minimal generators in $\langle *_A, \mathbb{Q}\rangle$. The algebra $\langle *_{CN}, \mathbb{Q}\rangle$ has no identities and no zeros;

it is also non-commutative and non-associative; however, this algebra has two minimal generators, $\{0,1\}$ and $\{1,2\}$, and one idempotent, the state 1.

The structure of sub-algebras is responsible for attributes of stationary configurations and homogeneous domains and thus determines outcomes of the spatio-temporal development of agent collectives.

The algebra $\langle *_N, \mathbb{Q}\rangle$ has two proper sub-algebras: $\langle *_N, \{0,1\}\rangle$ and $\langle *_N, \{1,2\}\rangle$. They are Abelian groups.

Commutativity and associativity of these sub-algebras follow from the composition table of $*_N$. Each of the sub-algebras has a zero and an identity. They are 0 and 1, and 2 and 1, respectively.

Algebra $\langle *_C, \mathbb{Q}\rangle$ has two sub-algebras: $\langle *_N, \{0,1\}\rangle$ and $\langle *_N, \{1,2\}\rangle$. They are commutative semi-groups.

Moreover, every element of each semi-group is a right identity and a left zero.

Algebra $\langle *_{CN}, \mathbb{Q}\rangle$ is anticommutative.

3.3 Reflective agents

We call agent (and its finite automaton) i reflective if it updates its state depending only on its own state: $s_i := s_i \phi s_i$, i.e. it does not interact with its neighbors. Let $\phi \equiv \odot$; then a state-transition graph of a doxaton

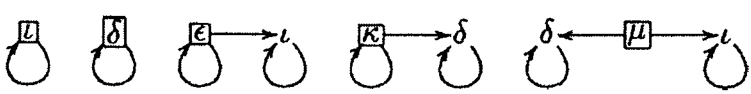

Fig. 3.2 A state-transition graph of a reflecting doxaton. Sometimes a product $s_i \odot s_i$ is not a singleton. In this case the doxaton takes one, arbitrarily chosen, element of $s_i \odot s_i$ as its next state. All possible transitions are shown by arcs. The initial states are framed.

looks as shown in Fig. 3.2. Ignorance and doubt are idempotents of $\langle \odot, \mathbb{Q}\rangle$. Therefore, a doxaton will be in its initial state forever if it starts development in ι or δ. If doxaton i takes the ϵ or κ state initially, $t = 0$, then it will keep this state at the tth step of its development with probability $(2t)^{-1}$ and will take state ι or δ, respectively, with probability $1 - (2t)^{-1}$.

All elements of $\mathbb{Q}$ are idempotents for $*_N, *_C$ and $*_A$. Therefore agents, which employ these functors to updates their states, fall into the fixed point of the development immediately after the start. Initial states of agents are their final states. A reflecting behavior of contradicting agents is a bit more interesting. While starting its development in state 0, a contradicting agent takes state 2 at the next step of the development; it takes state 0 on the subsequent step, and then state 2 again. The agent contradicts itself. A cycle $0 \circlearrowleft 2$ is one of two attractors in the development of a reflecting agent. The second attractor is the fixed point 1, because 1 is an idempotent of $\langle *_{CN}, \mathbb{Q} \rangle$.

In the next two sections we assume that the agents do not reflect but interact with their temporary (stirred collectives) or constant (non-stirred collectives) neighbors.

3.4 Stirred crowds

In computational models of stirred crowds an agent chooses at random another agent to update its state. Also, we can think of agents as nodes of a complete graph, and allow an agent to accept a doxastic state of one, arbitrarily chosen agent, at every step of the development. A state update graph, derived from the complete graph, has therefore indegree one and uniformly randomly distributed outdegrees at every step of agent development. In this temporary digraph every node has exactly one incoming arc and an arbitrary number of outgoing arcs.

Any stirred $\odot$-world evolves towards ignorance and delusion.

There is at least some evidence that this conforms to sociopsychological understanding:

"... crowd's natural delinquency is a delusion" [Moscovici (1985)].

The system may be represented by a Markov system with five states: κ, ϵ, μ, δ and ι, with the transition-probability matrix $\mathbb{M} = (m_{s_1 s_2})_{s_1, s_2 \in \mathbb{D}}$. Matrix $\mathbb{M}$ is calculated directly from the matrix (3.2) of the composition

$\odot$:

$$\mathbb{M} = \begin{array}{cc} & s_2 \\ s_1 & \left(\begin{array}{cccccc} & \kappa & \epsilon & \mu & \delta & \iota \\ \kappa & 0.5 & 0 & 0 & 0.5 & 0 \\ \epsilon & 0 & 0.5 & 0 & 0 & 0.5 \\ \mu & 0 & 0 & 0.6 & 0.3 & 0.1 \\ \delta & 0.2 & 0 & 0.2 & 0.6 & 0 \\ \iota & 0 & 0.4 & 0 & 0 & 0.6 \end{array}\right) \end{array}. \tag{3.9}$$

We can therefore derive an even stronger proposition:

crowds emerge due to ignorance, they act due to delusions,

while formally we get

set $\{\epsilon, \iota\}$ is the closed class of doxastic states.

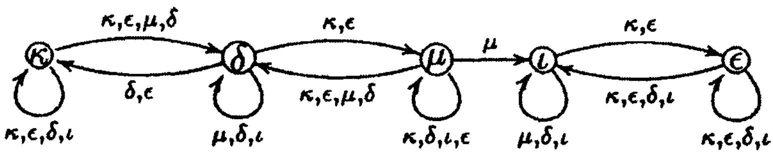

Fig. 3.3 State-transition diagram of doxaton.

Multiplying $\mathbb{P}$ by itself several times, we get that, for every s_1, $p_{s_1 s_2} > 0$ only if $s_2 \in \{\epsilon, \iota\}$, $s_1 = 0$, otherwise; this happens with a very high probability. Namely, after some (usually quite long) time interval of the development over 60% of doxatons take state ϵ while other doxatons take state ι, assuming that initially a doxaton takes one of $\mathbb{D}$ states with the same probability 0.2. Set $\{\epsilon, \iota\}$ does not contain closed sets; therefore it is minimal. Once a doxaton visits set $\{\epsilon, \iota\}$ it remains in this set forever. It can be seen in the state-transition diagram (Fig. 3.3).

What happens with agents governed by non-sense functors, when they are stirred and start their development in a random mixture of doxastic states? The limit distribution of $\star$-agents in truth, non-sense and falsity states, when agents are stirred, is $(\frac{4}{9}, \frac{5}{9}, \frac{4}{9})$; this follows from final distributions of state-transition probabilities of a Markov chain built on a $\star$ functor. Again the non-sense dominates both the truth and the falsity.

Collectives of naive agents are sensitive to the initial conditions: predicted final probabilities $(\frac{1}{3}, \frac{1}{3}, \frac{1}{3})$ are not observed in computer experiments and usually one of the states dominates all others. The conservative, anxious and contradicting collectives are more straightforward. The probabilities of the states obtained in computer experiments match the theoretically derived ones. They are $(0, 1, 0)$ for the conservative agents, $(\frac{1}{3}, \frac{1}{3}, \frac{1}{3})$ for the anxious agents and $(\frac{1}{2}, 0, \frac{1}{2})$ for the contradicting agents.

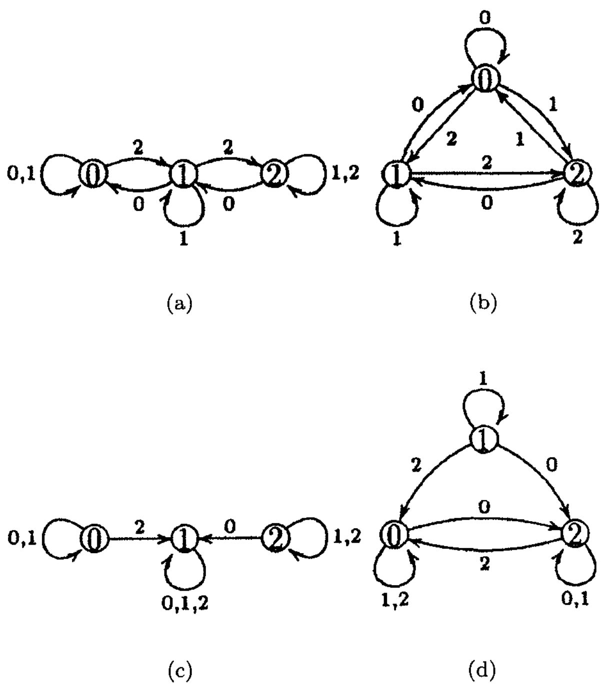

Fig. 3.4 State-transition graphs of naive agent (a), anxious agent (b), conservative agent (c) and contradicting agent (d).

The topologies of agent state transition graphs (Fig. 3.4) characterize the limit behavior of stirred collectives of the agents. Thus, for example, node 1 in the state transition of a conservative agent has just a loop and no other out-coming arcs. Therefore, the non-sense state 1 is a final, absorbing, state of the $*_C$-agent (Fig. 3.4c). Conservative collectives finish their development in entire non-sense. The non-sense vanishes in the group of contradicting agents (Fig. 3.4d) because node 1 has the only incoming

arc from itself. The state-transition graph of an anxious agent (Fig. 3.4b) can be transformed into the fully connected indirected graph. This should indicate the uniform distribution of final probabilities.

3.5 Non-stirred crowds

In this section we deal with chains of agents where every agent has exactly one left and and one right neighbor. The chains may be either infinite or finite. A finite chain is a one-dimensional torus. Let agents have unique names from set $\mathbb{I} \in \mathbb{N}$. The left and right neighbors of an agent i are named as $i-1$ and $i+1$, respectively. All agents update their states in a discrete time. The state of agent i at time step t is written as x_i^t. An agent i updates its state depending on the states of its left, x_{i-1}^t, and right, x_{i+1}^t, neighbors, and its own state, x_i^t, by the rule: $x_i^{t+1} = f(x_{i-1}^t, x_i^t, x_{i+1}^t)$. We can use only mapping $\odot$, $*$, and functors $*_N$, $*_A$, $*_C$ and $*_{CN}$ in the construction of function f. They are not symmetrical; moreover, most of them are non-commutative. Therefore, an order in which an agent composes states x_i^t, x_{i-1}^t and x_{i+1}^t may influence the resultant state of the agent. This will produce an induced anisotropy of the space–time configurations of agent chains. Amongst all possibilities for quasi-parallelization of a sequential update function, we have chosen the most obvious one:

$$x_i^{t+1} = \begin{cases} (x_i^t \phi x_{i-1}^t) \phi x_{i+1}^t \text{ with probability } 1/2, \\ (x_i^t \phi x_{i+1}^t) \phi x_{i-1}^t \text{ with probability } 1/2, \end{cases} \tag{3.10}$$

where ϕ stands for some of the previously defined functors. We should remember that for some ϕ, namely, in $\odot$ and $\star$ cases, the result of the composition itself is defined probabilistically.

The first thing we have to think about when we start to analyze space–time development of homogeneous structures is a quiescent state. An agent state s is called a quiescent state if $f(s,s,s) = s$. The sufficient condition for the state s to be quiescent is for it to be an idempotent. Therefore, states δ and ι are quiescent states in chains of doxatons; all states of $\mathbb{Q}$ are quiescent in collectives of $*_N$-, $*_A$- and $*_C$-agents; only state 1 is quiescent in the development of $\star$- and $*_{CN}$-agents. A global configuration of a collective where all agents are in the same quiescent state is a fixed point in the development of the collective.

Let all ϕ-agents take the same state a at the beginning of development. Then for any $t > 0$ and any agent i, $x_i^t = a$.

But what does happen when several quiescent states are distributed in an initial configuration of the collective? A sub-set $\mathbb{S}$ of state set $\mathbb{Q}$ (or $\mathbb{D}$) is called a ϕ-quiescent sub-set if it is not a singleton and if any initial configuration of a ϕ-agent collective, where agents take only elements of $\mathbb{S}$, is a stationary configuration (fixed point in the development). Let $\mathbb{K} = \mathbb{Q}$ or $\mathbb{D}$; then

The set $\mathbb{S}$, $\mathbb{S} \subseteq \mathbb{K}$ is a ϕ-quiescent set if $\langle \phi, \mathbb{S} \rangle$ is an algebra and every element of $\mathbb{S}$ is a left zero.

The stability of set $\mathbb{S}$ with respect to ϕ means that states not present in the initial configuration of a chain will not appear in the subsequent steps of the development. Tuple $\langle \phi, \mathbb{S} \rangle$ is an algebra if set $\mathbb{S}$ is stable. If an element a of $\mathbb{S}$ is a left zero then $(a\phi b)\phi c = (a\phi c)\phi b = a$ for any $b, c \in \mathbb{S}$. Therefore, $(x_i^t \phi x_{i-1}^t)\phi x_{i+1}^t = (x_i^t \phi x_{i+1}^t)\phi x_{i-1}^t = x^t$ for any values of x_i^t, x_{i-1}^t and x_{i+1}^t, if they are elements of $\mathbb{S}$ and they are left zeros. That is, a configuration of agent states at any time step is identical to the initial configuration of agent states. The last conditions can be re-formulated as follows: we can put "right identity" in place of "left zero".

Sub-set $\{\delta, \iota\}$ is a $\odot$-quiescent set; sub-sets $\{0, 1\}$ and $\{1, 2\}$ are $*_C$-quiescent sets.

Neither naive nor anxious and contradicting collectives have ϕ-quiescent sub-sets in their state sets.

To fully understand outcomes of agent development in space and time we should briefly discuss $\mathbb{S}$-stable states. A state a of a ϕ-agent is a $\mathbb{S}$-stable state if for any $x_{i-1}^t, x_{i+1}^t \in \mathbb{S}$ we have $x_i^{t+1} = f(x_{i-1}^t, x_i^t, x_{i+1}^t) = x_i^t$.

There are no $\mathbb{Q}$-stable states of $*_N$-, $*_A$- or $*_{CN}$-agents; neither are there $\mathbb{D}$-stable states of doxatons.

We know that state a is $\mathbb{S}$-stable if a is a left zero for all elements of $\mathbb{S}$. States κ, ϵ and μ are $\{\iota\}$-stable states of doxatons; states δ and κ are $\{\mu, \delta, \iota\}$-stable states.

State 1 is $\mathbb{Q}$-stable in collectives of $*_C$-agents.

This leads to formation of stable islands of agent states in the development of conservative agents. There are no $\mathbb{S}$-stable states, such that $\mathbb{S} \neq \{a\}$ for a $\mathbb{S}$-stable state a, in collectives of anxious agents. The states 0 and 2 are $\{0,1\}$- and $\{1,2\}$-stable, respectively, in collectives of naive and conservative agents; they are $\{1,2\}$- and $\{0,1\}$-stable in the collective of contradicting agents.

What initial conditions should be chosen as a standard to analyze space–time development of crowds? We can kind of answer this question by restricting all possibilities to a couple of families of initial configurations:

(1) H-configuration: initially, every agent takes one of its states with the same uniformly distributed probability q^{-1}, where q is a number of states, i.e. it equals 1/5 for doxatons and 1/3 for all other automaton-agents; or, alternatively, all agents take the same state at the beginning of development,
(2) Q-configuration: initially, one or two agents are in non-quiescent states; all other agents take the same quiescent state.

Let us discuss outcomes of these initial conditions.

3.5.1 *Development of doxatons from H-configuration*

When a chain (with periodic boundaries) of doxatons starts its development in a random uniform initial configuration, stable islands of μ-, δ- and ι-states are formed (Fig. 3.5, μ, δ and ι). Between these islands we can find tree-like structures of doxatons in κ-, ϵ- and ι-states (Fig. 3.5). Most trees become extinct and others grow. The final distribution of state probabilities (obtained in computer experiments) shows that states κ, δ and μ are eliminated entirely and the ratio of ϵ- to ι-states tends to $2:1$.

The behavior of a chain becomes richer when all doxatons start in the state κ (Fig. 3.6). A small amount of sponge-like islands of ϵ-, κ-, μ- and ι-states are formed. Islands of one or more doxatons in ι-states surrounded by an ocean of δ-states are recognizable (Fig. 3.6, ι). However, the vast majority of doxatons take state δ after a few steps of development (Fig. 3.6, ι). A final distribution of state probabilities tends to $(0;0;0;0.8;0.2)$, i.e. small islands of ι in the ocean of δ.

Only doxatons in ϵ- and ι-states can be found in chains soon after the collective starts its development in entirely state ϵ (for any i: $x_i^0 = \epsilon$) (Fig. 3.7). The space–time configurations are chaotic and homogeneous. The ϵ-state dominates. A final distribution of probabilities $(0;0.68;0;0;0.32)$ corre-

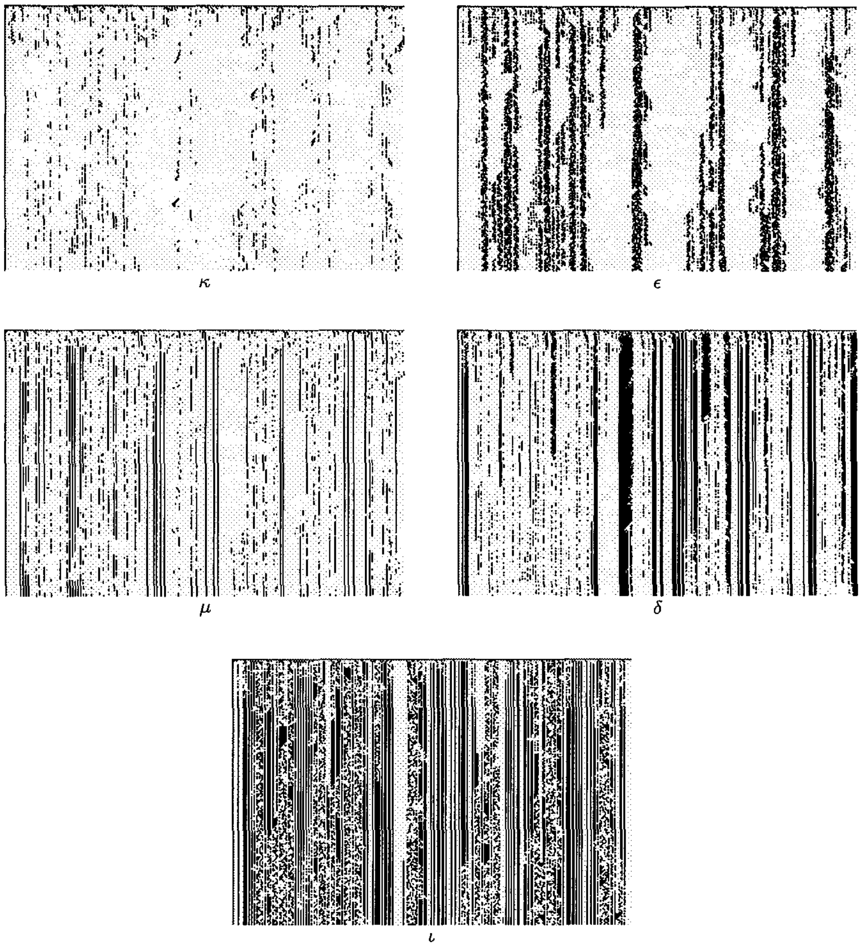

Fig. 3.5 Example of space–time configuration of doxaton chain for initial H-configuration. Time goes up down. Doxaton indices go from the left to the right. To enable a black and white representation, the configuration is split into five configurations; only one state is marked in each configuration. Thus, for example, in the configuration of κ-states only the positions of doxatons in state κ are shown by black pixels; all other doxatons are white.

sponds to the distribution of probabilities in the development of stirred collectives.

Let $x_i^0 = \mu$ for any doxaton i. Then $x_i^1 = \delta$ with probability 1/2 and $x_i^1 = \iota$ with probability 1/2; and $x_i^t = x_i^1$ for any $t \geq 1$.

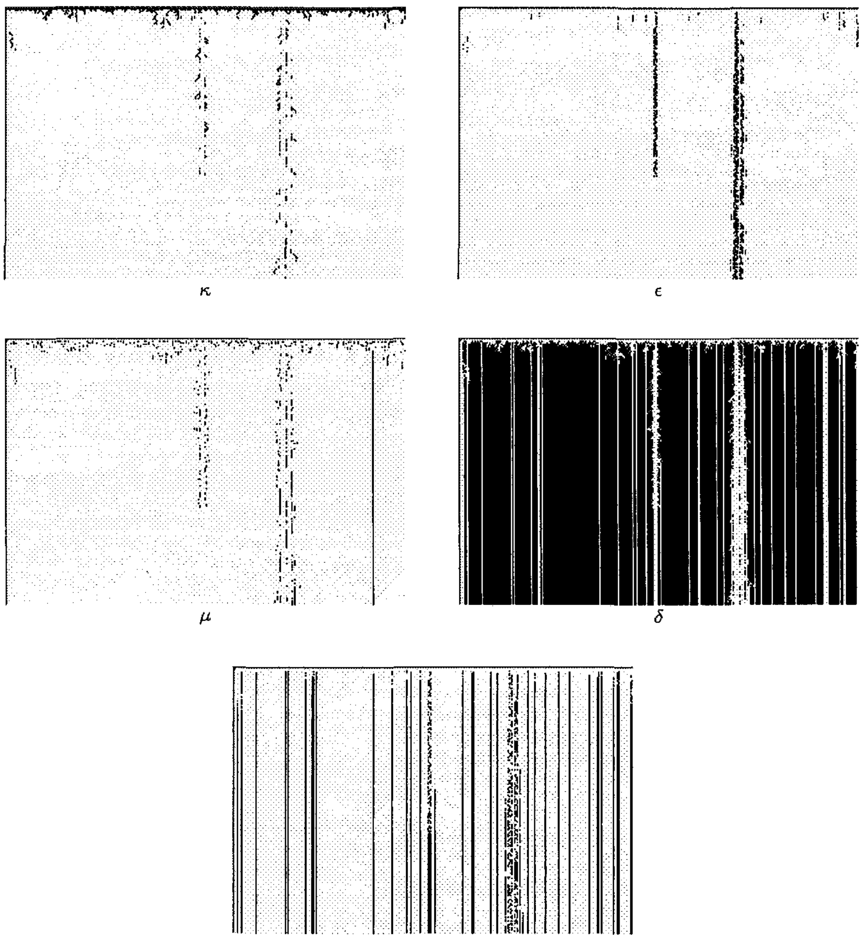

Fig. 3.6 Initial κ-configuration. Example of space–time configuration of doxaton collective developing from initial H-configuration; every doxaton takes κ-state initially. Time goes up down.

The result of the composition $(\mu \odot \mu) \odot \mu$ equals δ or ι with the same probability. Set $\{\delta, \iota\}$ is a $\odot$-quiescent set.

Let $x_i^0 = \iota$ ($x_i^0 = \delta$) for any doxaton i; then $x_i^t = \iota$ ($x_i^t = \delta$) for any $t > 0$.

This follows directly from the previous proposition and properties of ϕ-quiescent sets.

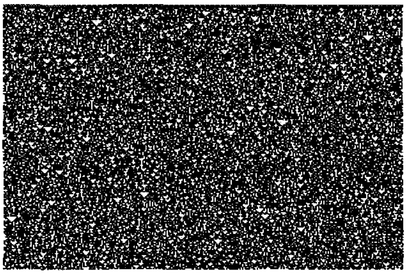

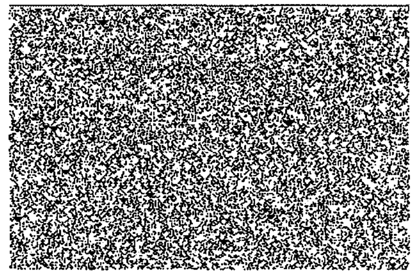

ϵ ι

Fig. 3.7 Initial ϵ-configuration. Example of space–time configuration of doxaton collective in case of H-start; every doxaton takes ϵ-state initially. Time goes up down. We make the same color separation as in the previous figures.

3.5.2 *Development of doxatons from Q-configuration*

Let $x_i^0 = \epsilon$ and $\forall j \neq i$: $x_j^0 = \delta$; then $x_i^t \in \{\delta, \iota\}$ for every i for some finite t.

We see (Fig. 3.8) that there is a definite period of "perturbations" when tree-like structures, composed of κ-, μ- and ϵ-states, grow. However, the μ- and κ-branches of the tree become extinct quickly and a group of islands, usually of single state ι, is formed. As soon as this happens the configuration of doxaton states becomes stationary because both ι- and δ-states are left zeros and right identities in $\langle \odot, \{\delta, \iota\} \rangle$. These domains of state ι are usually only a few doxatons wide.

Let there be one doxaton i such that $x_i^0 = \mu$ ($x_i^0 = \kappa$) and $\forall j \neq i$: $x_j^0 = \delta$. Then $\forall j$: $x_j^t = \delta$ after some time step t.

Doxaton i keeps its state μ at the tth step of its development with probability $1 - (2t)^{-1}$. That is, quite soon a small island of μ disappears. The probability of the extinction of non-δ-states in the case of $x_i^0 = \kappa$-start can be evaluated in the same way.

Let $x_i^0 = \kappa$ and $\forall j \neq i$: $x_j^0 = \iota$. Then (a) there is such a $t > 0$ that $x_i^t = \kappa$, μ or δ; (b) $\forall j \neq i$: $x_j^t \in \{\epsilon, \iota\}$, for $t > 1$; (c) $x_j^t = \iota$ if $|j - i| > t$; (d) $x_j^t = \epsilon$ if $|j - i| = t$; (e) $x_i^t \in \{\epsilon, \iota\}$ if $0 \leq |j - i| \leq t$.

Neighbors of a doxaton in state κ take state ϵ at the next step of the

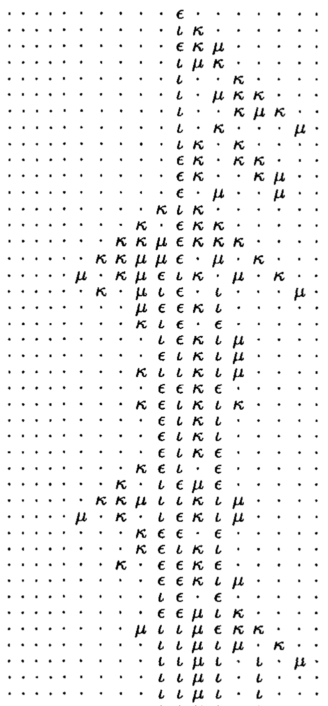

Fig. 3.8 Example of the space–time development of doxatons starting at Q-configuration. One doxaton takes state ϵ initially while other doxatons are in state δ. The δ-states are shown by dots.

development: $\iota\kappa\iota \to \epsilon$. The local transitions $\epsilon\epsilon\epsilon \to \epsilon$ and $\epsilon\epsilon\epsilon \to \iota$ occur with the same probability. A doxaton in state ι surrounded by doxatons in state ϵ takes state ϵ. Therefore, for any doxaton j, $j \neq i$, we have $x_j^t \in \{\epsilon, \iota\}$ (it takes one of the states with the same probability), if $t < |j - i|$; and, $x_j^t = \epsilon$ if $t = |j - i|$. Thus the growing triangle (Figs. 3.9 and 3.10) is bounded by states ϵ. The internal structure of the triangle is homogeneous, where states ϵ and ι are distributed uniformly at random. Behavior of the ith column (bisector of the triangle corresponding to the doxaton being initially in state κ) is non-trivial. For any z, i and $t > 0$ such that $|z - i| = 1$ and $x_z^t \in \{\epsilon, \iota\}$ and $x_i^t \in \mathbb{D}$ we have $x_z^{t+1} \in \{\epsilon, \iota\}$ (see the matrix (3.2)). Moreover, for $x_z^t = \iota$ we have $x_z^{t+1} = \epsilon$ if $x_i^t \in \{\kappa, \epsilon\}$ and $x_z^{t+1} = \iota$ if $x_i^t \in \{\mu, \delta, \iota\}$. This means that states different from ϵ and ι do not diffuse along the chain. What can we say about doxaton i? The doxaton i will

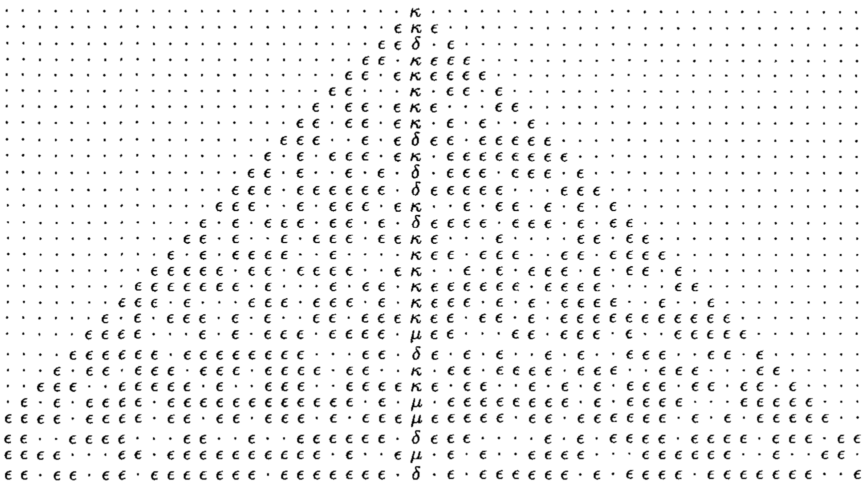

Fig. 3.9 Example of space–time development of doxatons developing from Q-configuration. One doxaton initially takes state κ and others state ι. Doxatons in state ι are shown by dots.

be in any of three states: μ, κ and ϵ at any step t of its development with the same probability. This is because (a) $x_i^{t+1} = x_i^t$ if $x_{i-1}^t = x_{i+1}^t = \iota$ (see the matrix (3.2)), and (b) probability distributions $(p_\kappa, p_\mu, p_\delta)$ for local transitions in neighborhood configurations $\epsilon\kappa\epsilon$, $\epsilon\delta\epsilon$ and $\epsilon\mu\epsilon$ are $(\frac{1}{2}, \frac{1}{4}, \frac{1}{4})$, $(\frac{1}{4}, \frac{1}{4}, \frac{1}{2})$ and $(\frac{1}{4}, \frac{1}{2}, \frac{1}{4})$, respectively.

Spreading delusion shown in Fig. 3.9 reflects both variants, subject to interpretation, of shared delusions, as proposed in [Mullen (1997)]:

- "Simultaneous emergence of delusion in closely associated individuals, where the content is shared, probably as a result of shared environment, but the origin is independent".

- "Communicated delusions, where two individuals living in close association, both of whom have a propensity to psychotic disturbance, come to influence and share each other's delusional world".

Let for the only doxaton i $x_i^0 = \epsilon$ and $\forall j \neq i : x_j^0 = \iota$. Then for $t > 0$ $x_j^t = \iota$ if $|j - i| > t$, $x_j^t = \epsilon$ if $|j - i| = t$ and $x_j^t \in \{\epsilon, \iota\}$ if $|j - i| < t$.

The growing triangle (Fig. 3.11) has a structure similar to an ϵ–ι-triangle

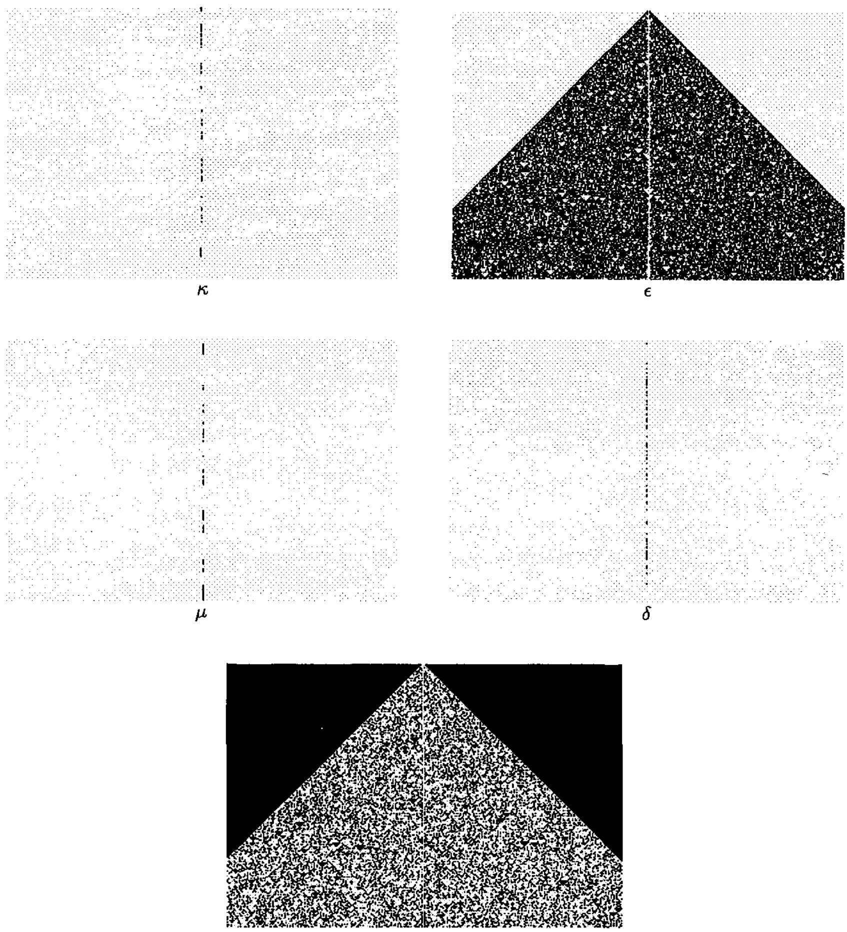

Fig. 3.10 Development from $\iota\kappa\iota$-configuration. Example of space–time configuration of doxatons developing from initial Q-configuration. Every doxaton j except one doxaton i takes ι-state initially. Doxaton i takes κ-state.

in the previous proposition. It is bounded by doxatons in ϵ-states because of local transitions $\iota\iota\epsilon \to \epsilon$ and $\epsilon\iota\iota \to \epsilon$. Every doxaton z being inside the triangle takes either state ϵ or state ι with the same probability.

Let initially every doxaton but i take state ι-state; doxaton i takes state μ. Then for any $t > 0$ all doxatons except i are in state ι and doxaton i is in state μ.

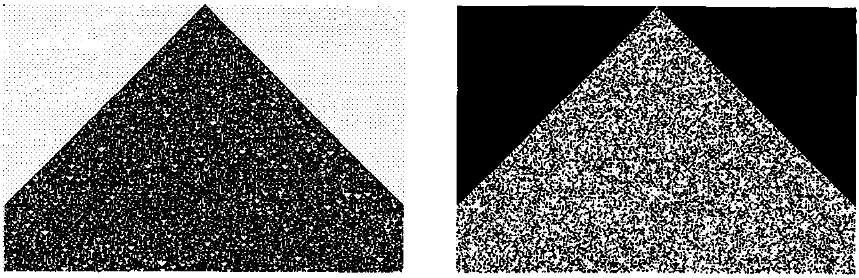

ϵ ι

Fig. 3.11 $\iota\epsilon\iota$-start. Example of space–time configuration of doxatons in case of initial Q-configuration. All doxatons but i take state ι initially. Doxaton i takes state ϵ.

This is because ι is a right identity in $\langle \odot, \mathbb{D} \rangle$, $\iota \odot \mu = \iota$.

3.5.3 *Collective based on algebras of non-sense*

3.5.3.1 *Developing from H-configuration*

If naive agents start their development in the random configuration where every agent takes one of $\mathbb{Q}$ states with the same probability $\frac{1}{3}$ then, after a finite number of steps, the collective falls into a stationary configuration $[0^*12^*]^*$, where $*$ stands for a concatenation.

Any configuration of 1s, which has at least one 2 or 0 state, will be entirely in the 2 or 0 state, respectively, in a time proportional to the length of the configuration because $a *_N 1 = 1 *_N a = a$, if $a = 0$ or $a = 2$. Agent i preserves its 1 state if $x^t_{i-1} \neq x^t_{i+1}$, $x^t_{i-1} \neq 1$ and $x^t_{i+1} \neq 1$, i.e. its neighborhood takes one of the states 210 or 012. Final probabilities of 0, 1 and 2 states, obtained in computer experiments, are $\frac{2}{5}$, $\frac{1}{5}$ and $\frac{2}{5}$, respectively.

A configuration of conservative agents becomes stationary at the first step of the development, $\forall x : x^{t+1} = x^t$, if $t > 0$. The ocean of the 1 states is formed with the islands of either 0 or 2 states. Islands are separated by at least two agents in the 1 state, because $0 *_C 2 = 2 *_C = 1$, and the global transition is

$$\begin{array}{c} \cdots 1 \cdots 12 \cdots 20 \cdots 01 \cdots 1 \cdots \\ \downarrow \\ \cdots 1 \cdots 12 \cdots 2110 \cdots 01 \cdots 1 \cdots \end{array}$$

The final distribution of states is (0.17; 0.76; 0.17).

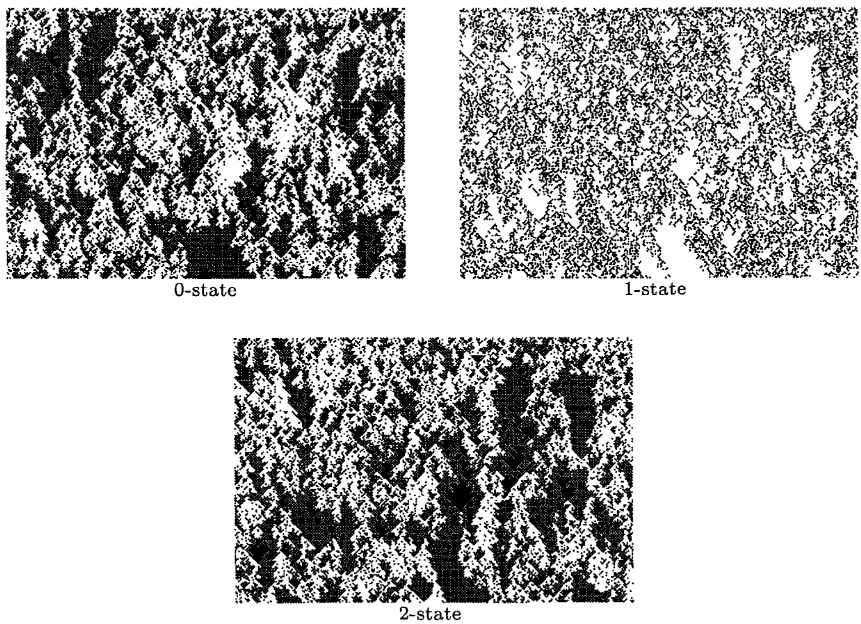

Fig. 3.12 Example of space–time development of a collective of anxious agents developing from initial H-configuration. Initially, each agent takes one of three states with probability $\frac{1}{3}$ distributed uniformly. Time goes up down.

In development of anxious agents, final probabilities of agent states tend to $\frac{1}{2}$, 0 and $\frac{1}{2}$ for the states 0, 1 and 2, respectively. This is reflected in the uniformly distributed sparse random trees of 0 states, and dense islands of 1 and 2 states (Fig. 3.12).

Let every contradicting agent i start development in one of the randomly chosen states of $\mathbb{Q}$. Then, for $t > t'$, we have $x_i^t \in \{0, 2\}$, where $t' = \lceil \frac{l}{2} \rceil$ and l is a length of the widest island of 1 states, $\underbrace{1 \cdots 1}_{l}$, in the initial configuration of the agents' collective.

This is because $x_i^{t+1} = 1$ only if all neighbors of i are in state 1 (see the matrix (3.8)).

A space–time configuration of a collective of contradicting agents exhibits sophisticated labyrinthine patterns of 0 and 2 states. This structure

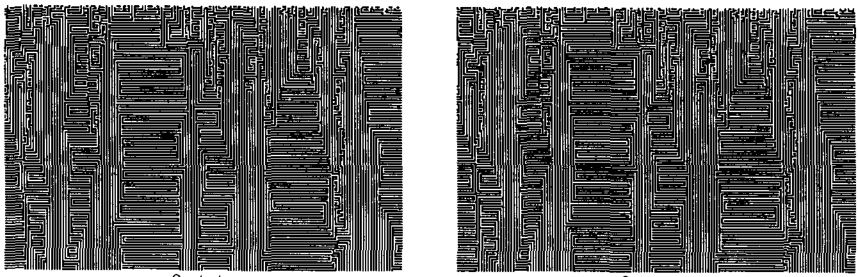

Fig. 3.13 Example of space–time configurations of collective of contradicting agents developing from initial H-configuration.

is usually composed of several uniform domains with regular vertical or horizontal orientations of the same states (Fig. 3.13). An explanation of the vertical stretches is as follows: $x_i^{t+1} = 2$ (0) if $u(x_i)^t = 020$ (202). The parts with the horizontal orientations occur because $x_i^{t+1} = 0$ (2) if $u(x_i)^t = 222$ (000). A competition between domains with different orientations is due to the randomized scanning (see rule (3.10)) of a neighborhood that influences the local transitions: $x_i^{t+1} = 0$ with probability p, and $x_i^{t+1} = 1$ with probability $1-p$, $p = 1/2$, when $u(x)_i^t \in \{002, 022, 200, 220\}$. Therefore, the final distribution of probabilities of states 0, 1 and 2 is $(\frac{1}{2}; 0; \frac{1}{2})$.

A collective of contradicting agents can be reduced to a one-dimensional cellular automaton with ternary neighborhood $u(x) = (y, x, z)$ and binary cell state set $\{0, 1\}$. The cells update their states by the rule:

$$x^{t+1} = \begin{cases} 0, & \sigma^t = 2 \vee (\sigma^t = 1 \wedge \xi = 0) \\ 1, & \sigma^t = 0 \vee (\sigma^t = 1 \wedge \xi = 1) \end{cases}$$

where $\sigma^t = y^t + z^t$ and ξ is a binary random variable; state 1 of a cell corresponds to state 2 of an agent.

3.5.3.2 *Development of naive agents from Q-configuration*

Let agent i of a collective of naive agents take state a at the beginning of development, $x^0 = a$, and any other agent $j \neq i$ be in state b, $x_j^0 = b$, $a \in \{0, 1, 2\}$ and $b \in \{0, 2\}$. Then any agent of the collective takes state b at time step $t > 0$.

This is because $(a *_N b) *_N b = (b *_N a) *_N b = (b *_N b) *_N a = b$, $a \in \{0, 1, 2\}$ and $b \in \{0, 2\}$.

Let for one agent i $x_i^0 = a$ and $\forall j \neq i : x_j^0 = b$, where $a \in \{0, 2\}$ and $b = 1$. Then $x_j^t = a$ if $|j - i| \leq t$.

This is because 1 is an identity and every element of $\mathbb{Q}$ is idempotent in $\langle *_N, \mathbb{Q} \rangle$.

Let in a collective of naive agents two agents, i and j, $i \neq j$, $i < j$, be initially in non-quiescent states, $x_i^0 = 0$, $x_j^2 = 2$, and all other agents $z \neq x$, $z \neq j$ be in a quiescent non-sense state 1, $x_z^0 = 1$. Then at any time step $t \geq |i - j|$ and odd $|i - j|$, or $t \geq t + c$, c being a small positive integer, and even $|i - j|$, there is such an agent $s \in \{\lceil \frac{d}{2} \rceil, \lfloor \frac{d}{2} \rfloor\}$ that $x_s^t = 1$ and for any agent z we have $x_z^t = 0$ if $z \in [x - t, s - 1]$; $x_z^t = 2$ if $z \in [s + 1, x + t]$, and $x_z^t = 1$, otherwise.

The situation with even $|i - j|$ is as follows. At time step $(|i - j| - 2)/2$ the meeting point of 0 and 2 fronts looks like $0 \cdots 0120 \cdots 0$. From $(1 *_N 2) *_N 0 = (1 *_N 0) *_N 2 = 1$ we see that this sub-configuration is stable. If $|i - j|$ is odd the meeting place looks different: $0 \cdots 0022 \cdots 2$. Because of the random nature of the update rule (3.10) the agents being at the exact sites of meeting points change their states probabilistically. Namely, assuming static left 0 and right 2 neighbors, the transformation of the sub-configuration can be represented by the graph shown in Fig. 3.14, where a probability of a transition along an arc outgoing from node w equals $\text{outdeg}(w)^{-1}$. The sub-configurations $0 \cdots 0112 \cdots 2$ and $0 \cdots 0122 \cdots 2$ are equivalents of the absorbing states in the development of the sub-configurations.

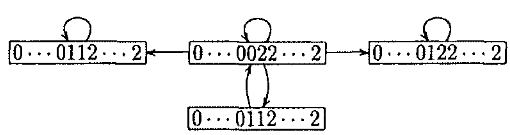

Fig. 3.14 Transformations of sub-configurations of naive agents.

3.5.3.3 *Development of contradicting agents from Q-configuration*

Amongst all possible initial configurations we consider non-quiescent states in an ocean of 1s, because 1 is the only identity of $\langle *_{CN}, \mathbb{Q} \rangle$. Notice that if any contradicting agent takes state 0 or 2 at the beginning of development then it will take state 0 or 2, respectively, at even time steps and state 2 or 0 in odd time steps of the development. The global oscillations with period

1 are induced by the local transition rules $000 \to 2$ and $222 \to 0$. Let g be such a function that $g(0) = 2$ and $g(2) = 0$; then we have the following.

Let in a collective of contradicting agents $x_i^0 = 0$ or $x_i^0 = 2$ and $\forall j \neq i$ $x_j^0 = 1$. Then $x_j^t = 1$ if $|j - i| > t$; $x_j^t = x_i^0$ if $|j - i|$ is even, and $x_j^t = g(x_i^0)$ if $|j - i|$ is odd, for $|j - i| \leq t$.

This means that the space–time configuration contains a triangle, "rooted" at i at $t = 0$, which is filled with columns of 0s and 2s, i.e. it has the regular pattern of agent states. This follows directly from the local transitions $\{020, 110, 011\} \to 2$ and $\{202, 112, 211\} \to 0$, which are determined by the matrix (3.8). The transitions are invariant to the order in which neighbors are scanned by an agent.

How do these growing domains (originated from two agents being initially in non-quiescent states) interact with each other? Let two contradicting agents i and j, $|i-j|$ being even, take the same state, either 2 or 0, at the beginning of development, $x_i^0 = y_j^0 = a$, $a \in \{0, 2\}$; and let all other agents be initially in state 1. Then, for every agent z we have $x_z^t = a$ if $|z-i|$ is even, and $x_z^t = g(a)$ if $|z - i|$ is odd, for $t \geq t^*$, $t^* = \min\{|z - i|, |z - j|\}$. That is, the waves of diffusing states passively merge. The same thing happens when $|i-j|$ is odd but $x_i^0 \neq y_j^0$, $x_i^0, y_j^0 \in \{0, 2\}$. Let $x_i^0 = 0$ and $x_j^0 = 2$; then $x_z^t = 0$ for any z if $|z - i|$ is even; and $z^t = 2$ if $|z - i|$ is odd. In the case of $x_i^0 = x_j^0 = 0$ or 2 and odd $|i - j|$; or, $x_i^0 \neq x_j^0$, $x_i^0, y_j^0 \in \{0, 2\}$ and even $|i - j|$, an instability occurs (see Fig. 3.13).

3.5.3.4 *Development of conservative agents from Q-configuration*

Let $x_i^0 = a$ and for any $j \neq i$ $x_j^0 = b$, where $a = 1$ if $b \in \{0, 2\}$ and $a \in \{0, 2\}$ if $b = 1$; then $x_i^t = a$ and $x_j^t = b$ for $t > 1$. This is because 1 is a right identity and a left zero in $\langle *_C, \mathbb{Q}\rangle$.

Let $x_i^0 = a$, $a \in \{0, 2\}$ and $\forall j \neq i$: $x_j^0 = g(a)$. Then, for $t > 0$ $x_z^t = 1$ if $|z - i| \leq 1$ and $x_z^t = g(a)$, otherwise.

That is, a stable domain of 1s is formed in the ocean of a. This follows from $(2 *_C 0) *_C 2 = (2 *_C 2) *_C 0 = (0 *_C 2) *_C 2 = 1$.

3.5.3.5 *Development of anxious agents from Q-configuration*

Starting at an initial Q-configuration, collectives of anxious agents exhibit inhomogeneous, and often quasi-chaotic, triangular patterns. In the case of

$1\cdots101\cdots1$ and $1\cdots121\cdots1$ initial configurations, $x_i^0 = 0$ or 2, and $\forall j \neq i$ $x_j^0 = 1$, a pattern inside the triangle is stochastic but the boundaries of the triangle are not. For any agent z we have $x_z^t = 1$, if $t \geq 1$ and $|z-i| > t$; and x_z^t equals 0 or 2 with the same probability, if $|z-i| = t$. This follows from $(1 *_A 0) *_A 1 = (1 *_A 1) *_A 2 = 2$ and $(1 *_A 1) *_A 0 = (1 *_A 2) *_A 1 = 0$. The state configuration inside the triangle is similar to that exhibited by anxious crowds (see Fig. 3.12).

The outcomes of the initial configurations $0\cdots010\cdots0$, $0\cdots020\cdots0$, $2\cdots202\cdots2$ and $2\cdots212\cdots2$ differ considerably from the previously discussed situations.

> Let $x_i^0 = a$ and $\forall j \neq i$ $x_j^0 = g(a)$, $a \in \{0,2\}$. Then one of the following situations takes place with the same probability: (a) for some great t every agent z changes its state in cycle $x_z^{t+1} = g(x^t)$; (b) for some not so great $t > 0$ every agent z takes state a.

The switching to one of the regimes, (a) or (b), happens at the very beginning of development: already at the first step we have $x_z^1 = g(x_z^0)$. However, the local transitions $020 \to 0$ and $020 \to 1$ (as well as $202 \to 2$ and $202 \to 1$) occur with the same probabilities. This is because

$$(0 *_A 2) *_A 0 = (2 *_A 2) *_A 0 = 1, \tag{3.11}$$

$$(0 *_A 0) *_A 2 = (2 *_A 0) *_A 2 = 2. \tag{3.12}$$

An agents' configuration becomes stationary if Eq. (3.11) is valid. The pattern [20]*, * stands for concatenation, and usually dominates in agent development, i.e. the following global transition

$$\begin{array}{c} \cdots \\ \cdots 2020202020 \cdots \\ \cdots 0202020202 \cdots \\ \cdots 2020202020 \cdots \\ \cdots \end{array}$$

occurs.

Development from initial configurations $0\cdots010\cdots0$ and $2\cdots212\cdots2$ is similar to previous cases except that no patterns become extinct, due to local transitions $000 \to \{1,2\}$ and $221 \to \{0,1\}$. The periodic pattern $\cdots02020\cdots$ dominates in every trial of computer experiments.

3.6 Interacting doxastic worlds

A basic set of interacting doxastic worlds is a Boolean $B(\mathbb{D})$ of the set $\mathbb{D} = \{\kappa, \epsilon, \mu, \delta, \iota\}$ of doxastic states. Every element of $B(\mathbb{D})$ is considered to be a doxastic world of an agent. Elements of the same world do not interact with each other. The worlds interact in a binary fashion. That is, the state of some world W' can be changed as a result of interaction with another world W'' as follows:

$$W' \leftarrow W' \circ W''.$$

The composition $\circ$ of the worlds W' and W'', $W', W'' \in B(\mathbb{D})$, is defined as $W = W' \circ W''$, where for every $x \in W'$ and every $y \in W''$

$$W = W \cup \{x \odot y\}, \tag{3.13}$$

where $W = \{\emptyset\}$ initially. We also assume that $W \circ \{\emptyset\} = \{\emptyset\} \circ W = \{\emptyset\}$ for any $W \in B(\mathbb{D})$. The composition $\circ$ is not symmetric and it is not commutative.

The empty set is the only null of the algebra $\langle \circ, B(\mathbb{D}) \rangle$.

This follows directly from Eq. (3.13).

Set $\{\iota\}$ is a right-side identity of the algebra $\langle \circ, B(\mathbb{D}) \rangle$.

This is a consequence of the identity of $\odot$.

Sets $\{\emptyset\}$, $\{\delta\}$, $\{\iota\}$, $\{\epsilon, \iota\}$, $\{\delta, \iota\}$ and $\{\mu, \delta, \iota\}$, $\mathbb{D}$ are idempotents of $\langle \circ, B(\mathbb{D}) \rangle$.

Both the empty set $\{\emptyset\}$ and the set $\mathbb{D}$ are trivial idempotents. Idempotency of $\{\delta\}$, $\{\iota\}$ and $\{\delta, \iota\}$ follows from the properties of the algebra $\langle \{\iota, \delta\}, \odot \rangle$. Concerning the remaining worlds, we have the following result: $\{\epsilon, \iota\} \circ \{\epsilon, \iota\} = \{\epsilon, \iota\} \cup \{\epsilon\} \cup \{\epsilon\} \cup \{\iota\} = \{\epsilon, \iota\}$ and $\{\mu, \delta, \iota\} \circ \{\mu, \delta, \iota\} = \{\delta, \iota\} \cup \{\delta\} \cup \{\iota\} \cup \{\mu, \delta\} \cup \{\delta\} \cup \{\iota\} \cup \{\mu\} \cup \{\delta\} \cup \{\iota\} = \{\mu, \delta, \iota\}$.

Worlds consisting of delusion and ignorance, doubt and ignorance, or misbelief, doubt and ignorance are stable.

The worlds are stable in a sense that they cannot be modified as a result of composition with themselves.

Let $\mathbb{G} = \langle \mathbb{V}, \mathbb{A} \rangle$ be a digraph, representing $\langle B(\mathbb{D}), \circ \rangle$. Vertices of $\mathbb{V}$ are uniquely labeled by elements of $B(\mathbb{D})$. We use the same names for the vertices and the worlds. The vertex $\mathbb{X}$ is connected by an arc $(\overrightarrow{\mathbb{X}, \mathbb{Y}})$ with the vertex $\mathbb{Y}$ if there is such an element $\mathbb{Z}$ of $B(\mathbb{D})$ that $\mathbb{X} \circ \mathbb{Z} = \mathbb{Y}$. Let $\mathbb{G}$ represent the whole space of development of doxastic states.

A world W is called an Eden, or non-constructible, world if there are no such worlds W', $W' \neq W$ and W'' of $B(\mathbb{D})$ that $W = W' \circ W''$. The definition is slightly relaxed compared to conventional ones to allow the global states with loops to be in the family of Eden states.

> The worlds $\{\kappa\}$, $\{\kappa, \epsilon\}$, $\{\mu\}$, $\{\epsilon, \mu\}$, $\{\epsilon, \delta\}$, $\{\kappa, \iota\}$, $\{\kappa, \epsilon, \iota\}$, $\{\mu, \iota\}$, $\{\kappa, \mu, \iota\}$ and $\{\epsilon, \mu, \iota\}$ are Eden worlds.

Here we show only that $\{\kappa\}$ and $\{\kappa, \iota\}$ are Eden worlds; by analogy it can be done for any other world. The world $\{\kappa\}$ is constructible if $W \circ W' = \{\kappa\}$ for some W and W'. From the matrix (3.2) we see that κ can be produced only if W contains δ or κ. State δ is not appropriate because for any $y \in \mathbb{D}$: $\delta \odot y \in \{\{\mu, \kappa\}, \{\delta\}\}$. Therefore, κ is the only possible candidate to be included in the world W. Actually, κ should be the only element of W, otherwise the states different from $\{\kappa\}$ are produced. However, by the definition of an Eden world we have $W' \neq \{\kappa\}$. For another candidate, $\{\kappa, \iota\}$, we obtain $W \circ W' = \{\kappa, \iota\}$, where W can consist of two possible elements: $\{\kappa, \delta\}$ and $\{\epsilon, \iota\}$. State δ is of no use because the state μ is produced in a pair with κ. Solving $\epsilon \odot z = \{\iota\}$, we have $z = \mu$. However, $\kappa \odot \mu = \delta$. Thus, W includes $\{\kappa, \iota\}$ that contradicts the definition.

We say that the doxastic states x and y, $x, y \in \mathbb{D}$, are in an Eden relation E, xEy, if set $\{x, y\}$ is a sub-set of some of the Eden worlds, if $x \neq y$; and $\{x\}$ is an Eden world if $x = y$.

The graph representing relation E is shown in Fig. 3.15.

The vertices $\{\emptyset\}$, $\{\delta, \iota\}$ and $\mathbb{D}$ have maximal indegrees — 32, 25 and 15, respectively — in graph $\mathbb{G}$.

If we delete edge $\{\emptyset\}$ from graph $\mathbb{G}$ the graph will split into two components. If all three vertices with maximum degrees are deleted from $\mathbb{G}$ the graph will be divided into three components. Two of them consist of three worlds each, and the other includes the remaining worlds (Fig. 3.16).

Until this moment we assumed that the worlds interact asymmetrically. In terms of chemical reactions this means that world W'' plays a role of a catalyst:

$$W' + W'' \to (W' \circ W'') + W''.$$

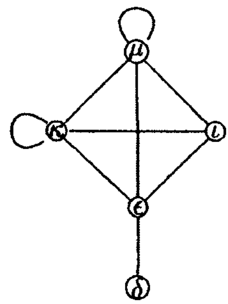

Fig. 3.15 Eden relation of doxastic worlds.

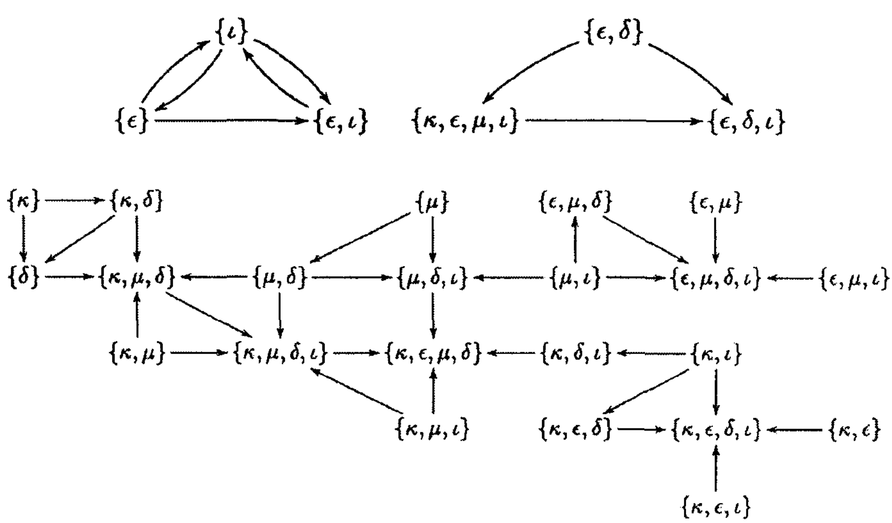

Fig. 3.16 Components of graph $\mathbb{G}$.

How does symmetrization of Eq. (3.13):

$$W = W \cup \{x \odot y\} \cup \{y \odot x\} \tag{3.14}$$

change the system of interacting worlds? A fusion of the worlds is the first outcome:

$$W' + W'' \to 2(W' \circ W'').$$

An empty set $\{\emptyset\}$ still remains the only zero in Eq. (3.14). The algebra

$\langle \circ, B(\mathbb{D})\rangle$ loses its identity $\{\iota\}$ when we change Eq. (3.14) to Eq. (3.13); however, idempotents survive. The most interesting thing happens to Eden worlds: the number of Eden worlds increases.

Let worlds from $B(\mathbb{D})$ interact by the rule (3.14). Then worlds $\{\kappa\}, \{\mu\}, \{\kappa, \mu\}, \{\epsilon, \mu\}, \{\kappa, \epsilon, \mu\}, \{\delta\}, \{\epsilon, \delta\}, \{\epsilon, \mu, \delta\}, \{\iota\}, \{\kappa, \iota\}, \{\kappa, \mu, \iota\}$ and $\{\kappa, \delta, \iota\}$ are Eden worlds.

The graph representing an Eden relation is transformed now to a complete graph where all but $\{\epsilon\}$ vertices have loops. Thus, not simply new Eden worlds emerge but also some old Eden worlds disappear. Another remarkable difference between asymmetric (3.13) and symmetric (3.14) interactions of the worlds is that every node of $\mathbb{G}$ has a loop in the case of (3.13) and some nodes do not have loops in the case of (3.14). Almost all Eden worlds of asymmetrically interacting worlds have corresponding nodes without loops in graph $\mathbb{G}$. There are five exceptions. Eden worlds $\{\delta\}$ and $\{\iota\}$ do not have loops on their corresponding nodes of $\mathbb{G}$. The worlds $\{\kappa, \delta\}$, $\{\kappa, \epsilon, \delta\}$ and $\{\kappa, \epsilon, \mu, \delta\}$ are not Eden and they also do not have loops on the corresponding nodes of $\mathbb{G}$.

3.7 Doxastic chemistries

Now we return to a chemical paradigm, introduced in previous chapters, and consider a chemistry of beliefs to enrich our understanding of global dynamics of stirred pools of believers. When two individuals meet each other they may update their doxastic states. Thus, a binary reaction between any pair of doxastic states occurs. New doxastic states may be generated as a result of the binary reaction. Therefore, we can talk about products of doxastic reactions. Defining various types of reactions between doxastic states, we can determine principal classes of doxastic chemical systems. A dynamic of doxastic chemical solutions may reflect, up to some degree of accuracy, development of collective beliefs in natural, e.g. crowds, or artificial, e.g. multi-agent systems and robot collectives, worlds.

In this section we discuss several classes of doxastic chemical reactions. When designing a set of chemical reactions we keep in mind that each molecule of a doxastic reactant may represent not only an abstract thought but rather a carrier of the doxastic state, i.e. a real or imagined person, an agent. In such a situation two or more molecules will never vanish as a result of their reaction; the same amount of other reactant molecules is

produced. Some propositions in the section are illustrated with differential equations, where c_X stands for a concentration of the reagent X and $\dot{c}_X$ stands for $(\mathrm{d}/\mathrm{d}t)c_X$.

3.7.1 *Doxastic reactions*

From the irrational composition $\odot$, see the matrix (3.2), we derive a set of quasi-chemical reactions as $aX \odot bY \to cZ + dW$, where X, Y, Z and W are doxastic reactants and a, b, c and d are integer coefficients. The reactants of knowledge, delusion, misbelief, doubt and ignorance are shown by the symbols K, E, M, D and I, respectively.

The following set of reactions is straightforwardly derived from the matrix (3.2):

$$\begin{aligned}
&2K \to K + D,\\
&2K + 2E \to K + D + E + I,\\
&K + 2M \to 2D + M,\\
&2K + 2D \to 2K + D + M,\\
&K + I \to K + E,\\
&2E \to E + I,\\
&E + 2M \to I + M + D,\\
&2E + 2D \to E + I + M + K,\\
&2M \to D + I,\\
&2M + D \to M + 2D.
\end{aligned} \tag{3.15}$$

We call the set (3.15) a chemistry of anxious believers.

If one prepares a mixture of five doxastic reactants, each in the same concentration, and pours the mixture into a continuously stirred tank the following chain of events unfolds. The ignorance and doubt increase in concentration while the knowledge, misbelief and delusion decrease, as shown in Fig. 3.17. Concentration of doubt increases because the doubt is produced by knowledge and misbelief themselves, when knowledge is decomposed into knowledge and doubt, and misbelief is decomposed into doubt and ignorance. Doubt is also generated in reactions between knowledge and misbelief, knowledge and delusion, and misbelief and delusion. However, doubt is only consumed when it reacts with delusion:

$$\dot{x}_D = x_K^2 + x_M^2 + x_K x_M + x_K x_E + x_E x_M - x_E x_D.$$

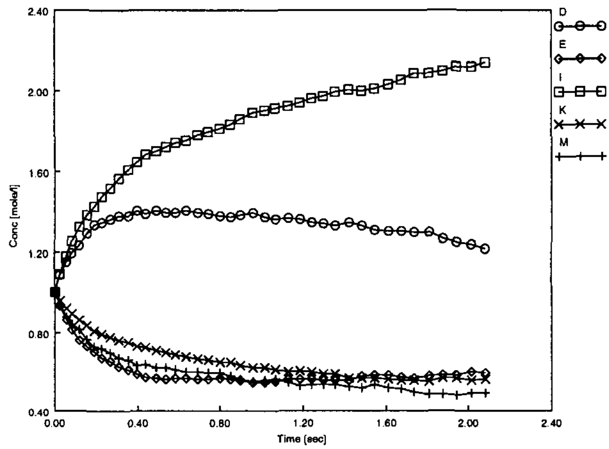

Fig. 3.17 Dynamic of a stirred reactor filled with knowledge, doubt, misbelief, delusion and ignorance, all in equal initial concentrations. The reactants interact by reactions of the set (3.15).

Knowledge, misbelief and delusion decline in concentration altogether:

$$\begin{aligned} \dot{x}_K &= -x_K^2 - x_K x_M + x_E x_D, \\ \dot{x}_M &= -x_M^2 + x_K x_D + x_E x_D, \\ \dot{x}_E &= -x_E^2 - x_E x_M + x_K x_I. \end{aligned}$$

Ignorance behaves similarly to doubt:

$$\dot{x}_I = x_E x_E + x_M x_M + x_K x_E + x_E x_M + x_E x_D - x_K x_I,$$

with the only difference that the doubt itself contributes to ignorance production. As we see in Fig. 3.17, doubt is a second dominating state in the doxastic solution. Actually, this does not contradict common sense, because doubt and inactivity are quite usual attributes of even very advanced thinkers.

Someone may say that the dynamic of doxastic mixtures contradicts obvious evidence of a generation and accumulation of knowledge in a human society. We would rather quote Gustave Le Bon, who wrote in 1895 [Le Bon (1994)]:

> "Civilizations as yet have only been created and directed by a small intellectual aristocracy, never by crowds. ... In crowds it is stupidity and not mother-wit that is accumulated".

Stupidity is not ignorance; nevertheless, certain parallels may be drawn.

Obviously, by keeping a constant influx of knowledge, high enough for some knowledge to be left after its consumption in the reactions of the set (3.15), one can actually achieve a persistent domination of knowledge. The influx may represent a knowledge previously accumulated in the system and kept non-destroyable in a form of books, or parental experience transferred to children, or a sacral wisdom. However, all these types do not store and deliver the knowledge in its pure form; the knowledge is rather contaminated by misbelief and delusion.

Several reactions of the set (3.15) are formally correct but nevertheless a bit strange from a common-sense point of view. We could correct this "inaccuracy" using the following reactions:

$$\begin{aligned} 3K + 3M &\rightarrow 2D + 2M + 2K, \\ 3M + 3D &\rightarrow 2K + 2D + 2M, \\ 2M &\rightarrow D + E. \end{aligned} \tag{3.16}$$

Then knowledge reacts with misbelief with a production of doubt, misbelief and knowledge. The misbelief decomposes itself into doubt and delusion, not doubt and ignorance as in the original set of reactions.

3.7.2 *Rationalizing doxastic mixtures*

The set (3.15) of doxastic reactions, even with the modification (3.16), is open to criticism, because the original doxastic composition $\odot$ is derived from the irrational way of updating doxastic states. There are several schemes that may look more rational from a common-sense point of view. A simplest set of reactions may include the following interactions. When knowledge reacts with misbelief doubt is produced. When reacting with knowledge doubt is transformed into misbelief; when reacting with misbelief doubt is transformed into knowledge:

$$\begin{aligned} K + M &\rightarrow 2D, \\ K + D &\rightarrow M + K, \\ D + M &\rightarrow M + K. \end{aligned} \tag{3.17}$$

The scheme (3.17) contains a sufficiently reduced set of reactions, modified from the set (3.15).

The doxastic mixture evolves towards a regime of high-amplitude aperiodic oscillations (Fig. 3.18). This type of development looks realistic because usually neither real societies and collectives nor individual minds rest

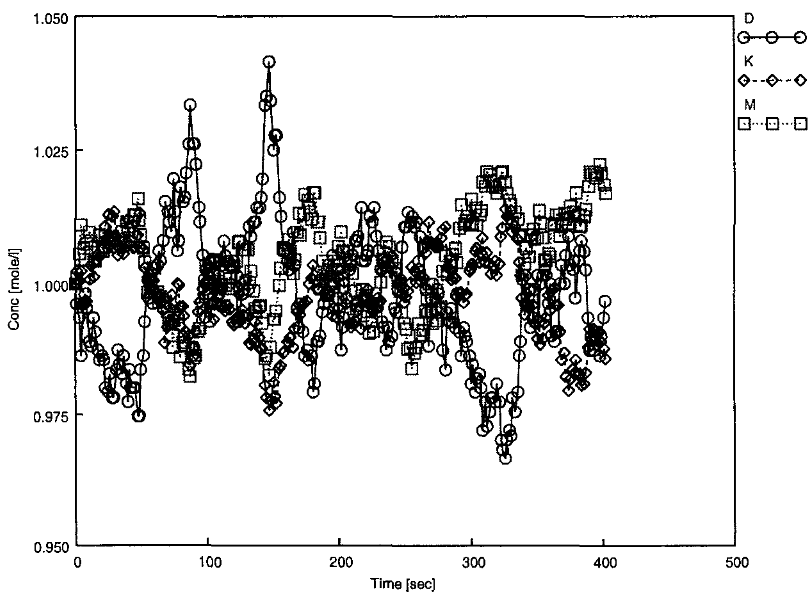

Fig. 3.18 Dynamic of a stirred reactor filled with knowledge, doubt, misbelief, delusion and ignorance, all in equal initial concentrations. The reactions are governed by the scheme (3.17).

in a homogeneous state but exhibit fluctuations between different states of their beliefs and opinions.

The scheme (3.17) employs only three doxastic states. To take into account all five of them, we offer the following set of reactions:

$$\begin{array}{lll} K+E\rightarrow 2D & K+M\rightarrow 2D & K+D\rightarrow 2K, \\ K+I\rightarrow 2K & E+M\rightarrow 2D & E+D\rightarrow 2E, \\ E+I\rightarrow 2E & M+D\rightarrow 2M & M+I\rightarrow 2M. \end{array} \tag{3.18}$$

Doubt is produced in the reaction between knowledge and delusion, or knowledge and misbelief, or delusion and misbelief. Knowledge, delusion and misbelief are not generated in reactions between other reactants. However, they do increase in concentration when they consume ignorance or doubt.

In experiments with stirred reactors, filled with a mixture governed by the set (3.18), we observe bifurcation between knowledge, misbelief and delusion. Therefore, finally only one of these three reactants dominates in

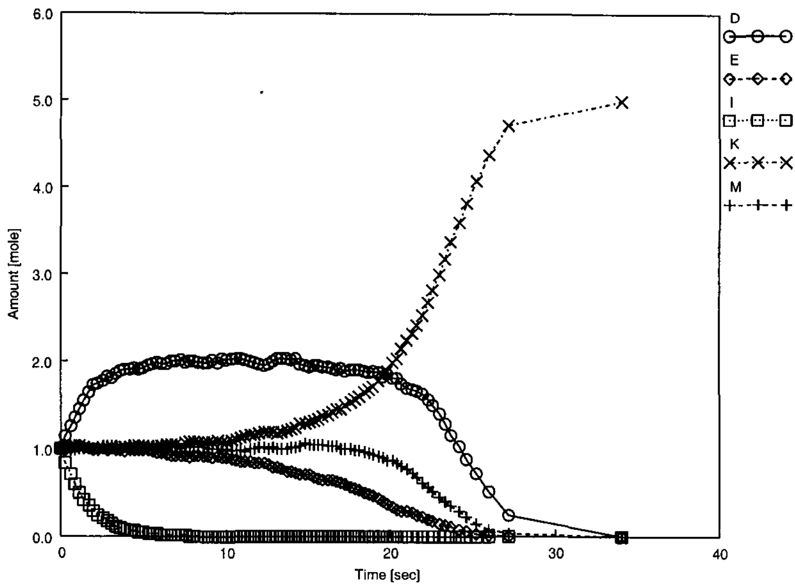

Fig. 3.19 Example of global dynamic of a stirred reactor filled with knowledge, doubt, misbelief, delusion and ignorance, all in equal initial concentrations. The reactions are governed by the set (3.18).

the reactor; the concentrations of the others decline.

Let us consider an example of reactor development with dominating knowledge (Fig. 3.19). The following dynamic may be observed in the experiment. Ignorance dramatically declines and disappears:

$$\dot{x}_I = -x_I(x_K + x_E + x_M).$$

Doubt inflates and becomes a dominating reagent, because in the binary reactions involving knowledge, misbelief and delusion only doubt is produced:

$$\dot{x}_D = x_K x_E + x_K x_M + x_E x_M - x_D(x_M + x_K + x_E).$$

Concentrations of delusion, knowledge and misbelief are similar during the initial period of mixture development, when knowledge, misbelief and delusion are competing for the domination. Eventually one of the states wins and the others vanish. Finally, the mixture is entirely in the state of either

knowledge, misbelief or delusion:

$$\begin{aligned}\dot{x}_K &= x_K(x_I + x_D - x_E - x_M),\\ \dot{x}_M &= x_M(x_I + x_D - x_K - x_E),\\ \dot{x}_E &= x_E(x_I + x_D - x_M - x_K).\end{aligned}$$

As soon as one of the doxastic states prevails in the development, doubt deteriorates because reactions between knowledge, misbelief and delusion occur less and less.

3.8 Future is delusion

We have considered a quite unrealistic but not entirely impossible situation when every agent of a collective updates its belief depending on beliefs of its neighbors and local justification of its belief in the vicinity of these neighbors, not in its own neighborhood. We created a pentad of derivatives of belief, constructed various algebraic systems and analyzed spatio-temporal development of doxastic collectives. The order in which doxastic states emerges is remarkable: knowledge, doubt, misbelief, ignorance and delusion. A similar sequence of mental states is quite usual for everyone who encounters a serious problem or an obstacle, the solution or overcoming of which is invisible or even impossible. This person knows the problem but he is unable to solve it. Then he doubts whether the problem does exist at all. Then he suggests that the problem is not real. On failing to convince himself, he simply ignores the problem. Finally, the person lets himself flow in the stream of delusion, which, as we discussed earlier, may play a role of protection from hostile environments, situations or traits.

The whole chapter is somewhat an opus to delusion. In our models we demonstrated that delusion spreads, and delusion eventually dominates doxastic pools. This may evoke a pessimistic feeling that the whole world evolves towards delusion. This is true but there is nothing wrong with this because

Delusion is a pre-knowledge.

Why? Because delusion "involves abnormal beliefs that arise in the context of disturbed judgements and an altered experience of reality, such that it becomes a source of new and false meanings" [Mullen (1997)] and also because delusion could be seen as "... reasonable attempts to make sense

of what is a puzzling and emotionally provocative experience" [Chadwick *et. al* (1996)].

Not only delusional thinking is sometimes attributed to disturbances in an affective sphere [Winters and Neale (1983)] but more rightfully delusions are seen as reversions to primitive modes of thinking.

> Delusion is a "disturbance of logical thinking due to the release of genetically more primitive styles of thinking" and "a regressive failure to use Aristotelean logic" [Winters and Neale (1983)].

A delusion, itself is a very delicate matter, was defined in the chapter quite straightforwardly. It was done simply to avoid the unwanted questions related to the persistence of this belief even when an effort is made to dissolve it by appealing to reason. However, from the structure of the composition $\odot$ we see that, when colliding with other doxastic states, delusion can either survive or be transformed to ignorance. One can also suggest that a fantasy, i.e. the formation of concepts not presented to the senses, as well as considering things that are not taken to be real, may be a more appropriate term for this formally defined doxastic state, especially when dealing with psychopathological phenomena [Coville *et. al* (1960)]. Spreading of delusion demonstrated in cellular-automaton models is akin to spreading of delusional experiences to the healthy parts of the mind, where "delusional explanations become more complex and bizarre" [Murray (1997)].

We have shown that ignorance is the right identity of $\odot$, i.e. any agent that is ignorant cannot affect agents being in other doxastic states. This contradicts Goethe's "there is nothing more frightful than ignorance in action", who obviously meant something else; however, it does conform to the common-sense vision of ignorance. Notably, neither delusion nor ignorance can be born in pairs with misbelief or knowledge. Ignorance itself can be changed to delusion, when it interacts with knowledge, which peculiarly fits Saul Bellow's

> "... a great deal of intelligence can be invested in ignorance when the need for illusion is deep".

However, when an ignorant agent interacts with an agent being in any state but that of knowledge the state of ignorance remains unchanged.

Uncertainty may lead to stability. The proof is that only doubt and ignorance are idempotents; knowledge is unstable but it is a generator of all doxastic states. Both ignorance and delusion are absorbing states

of reflecting agents. Talking about reflecting agents, we should highlight that reflections of naive, conservative and anxious agents are stable. These agents never change their initial states. The contradicting agents change their states in a cycle where truth is substituted by falsity, and falsity by truth. This happens if contradicting agents do not start their development in a state of non-sense. The non-sense is a fixed point for all of them.

The collectives of $\odot$-agents, both stirred and ordered collectives, evolve towards delusion and ignorance when they start in a random uniform initial state.

The development of stirred naive agents can be diverted to a quite arbitrary global state depending on particular initial conditions. The stirred conservative agents that evolve to non-sense and contradicting agents finish their development in a homogeneous global state with an equal ratio of truth and falsity, without non-sense states. All states of anxious agents can be found in limit configurations of stirred collectives.

In non-stirred collectives, in contrast to the stirred collectives, an agent must update its states depending on the states of two closest neighbors. We intentionally randomized the order of compositions of an agent's state with the states of its neighbors to avoid possible artifacts, induced by asymmetry of the functors.

Delusion and ignorance are the limit states in the development of ordered collectives of $\odot$-agents. However, if all agents start their development in the state of knowledge then they all will be in either ignorance or doubt eventually. Knowledge is usually lost in the development. Starting in misbelief, agents immediately fall into delusion and ignorance, which are equally represented in global configurations. A singleton of misbelief or knowledge in an ocean of doubt becomes doubting after some finite period of development.

The fact that a state of global delusion is a likely fixed point in the development of doxastic pools conforms to commonly recognized attributes of delusions [Mullen (1997)]:

- delusion is "not amenable to reason nor modifiable by experience",
- delusions are "experiences as of great personal significance and usually pre-occupy the person to the point of disrupting social and interpersonal functioning",
- delusions "often extend to contaminate a wide range of the patients'

beliefs about themselves and their world",

- delusions are "self-referential in that they directly concern, and are primarily about, the deluded subject and their immediate relationship to the world".

What does happen if a collective of entirely ignorant agents has an individual in a state of knowledge? Delusion spreads in such a collective. This individual himself, however, does not entirely give up his state in favor of the entire majority of his neighbors. Even being surrounded by delusive and ignorant agents the agent may fall into doubt or misbelief but he will never take the state of ignorance or delusion. An individual surrounded by ignorant agents keeps his original misbelief. The misbelief does not spread in the chain of agents.

In some models we allowed agents to use non-sense functors to update their states. Their domains of truth are separated from domains of falsity by singletons of non-sense when collectives of naive agents start their development in a random homogeneous state. No two domains of truth and falsity directly contact each other. So, we see that domains of truth are formed; and non-sense is a limiting factor or a barrier which stops the spreading of truth and falsity. In collectives of conservative agents limit configurations consist usually of small domains of truth or falsity in an ocean of non-sense. The non-sense is eliminated from the collectives of contradicting agents in a time proportional to the size of the maximum chain of agents in a non-sense state. After that the domains, where every agent keeps its truth or falsity state unchanged, compete for the space with the domains where uniform chains of agents change their states asynchronously from truth to falsity and back. The non-sense almost disappears in collectives of anxious agents, giving way to breathing domains of truth or falsity.

A diffusion of truth and falsity in naive collectives, where only one agent takes a truth or falsity state and all other agents are in quiescent states, is trivial. A space sub-division arising in the interaction of truth and falsity is more attractive. If two agents, being at some distance from each other, start their development, one in truth, the other in falsity, in an ocean of non-sense they sub-divide the chain into domains of truth and falsity. These domains are separated by singletons in a state of non-sense.

We did not consider belief update or revision, in consistency with the established theory of belief update. However the convergence is visible,

especially with the Katsuno–Mendelzon theory of belief revision or its reasonable alternatives (see e.g. [Boutilier (1996)]). Our approach can easily be incorporated into various models of reasoning about shared or mutual beliefs including nested beliefs and human-like strategies of, sometimes unrealistic, revisions of belief [Taylor *et. al* (1996)]. Thus, for example, Lakemeyer's logic of belief [Lakemeyer (1991)] allows us to distinguish between "knowing that" and "knowing who", and to combine possible-world semantics and relevant logics.

Our concept of interacting worlds has much in common with the combinatorial worlds developed in [Nowak and Eklund (1994)], where the worlds can be used as a knowledge-representation framework. This analogy could be particularly useful in a sense of accessibility and similitude of the worlds. Non-monotonic reasoning and belief updating and revision may form direct outcomes of such approaches.

And, finally, a "chemical" approach to simulation of collective doxa looks promising. There are possible applications in a theory of crowd development. In most examples one can find basic stages of a collective grouping [Smelser (1962)]: a public, a mass and an expressive crowd. The public focuses on some issue but disagrees about it. Thus, initially, all reactants are in equal concentrations. The mass is more anonymous than the public and "less intimately engaged" [Smelser (1962)]. Reactants diffuse in a reactor and a frequency of contacts between the doxastic molecules increases. When one of the doxastic states becomes dominating, all individuals may be seen as expressing similar impulses. Therefore, the state of the doxastic reactor represents the expressive crowd [Smelser (1962)] with collective consciousness:

> "In a collective situation the individual consciousness is obliterated. Individuals cease to react according to their potential" [Moscovici (1985)].

Chapter 4

Normative Worlds

In the previous chapter we introduced doxatons, and considered the not very realistic but not entirely illusory situation when every agent of a collective updates its belief in some proposition depending on the belief of one or more of its neighbors and local justification of the proposition in the vicinity of these neighbors but not the agent's own neighborhood. We created a pentad of doxastic states, derivatives of belief: knowledge, doubt, misbelief, ignorance and delusion, together with an operation of binary composition of these doxastic states. The doxatons are finite automata which take the doxastic states and update their states by the binary composition with other doxastic states.

As we can see from the definition of the composition $\odot$, provided in the previous chapter, the composition is not deterministic. For certain combinations of arguments two possible results may be chosen with equal probabilities; to reduce this uncertainty we introduce priority relations over doxastic elements which are generated in pairs. If elements α and β are produced in pairs and chosen equiprobably, we assign that one of the elements, say α, dominates the other element, β. Thus, we enforce generation of α, and therefore introduce a norm. In the previous chapter we dealt with probabilistic cellular-automata models of doxatons, i.e. the stochastic lattices of doxatons. Now we will study a deterministic doxastic composition by applying norms, which "straighten" doxatons' behavior. In this chapter we aim to answer the question: how do norms influence the space–time dynamic of doxaton collectives?

4.1 Norms

In social sciences norms are seen as behavioral constraints or reductions of a range of possible actions of an agent in a multi-agent environment. Norms are means of coordination in social systems [Castelfranchi *et. al* (1998); Saam and Harrer (1999); Rowe (1989)], where each norm is a normal representation of the standard to comply with. In the normative systems a behavior of the constituents is governed in such a manner to force components to obey certain rules:

> "A person rather conforms to norms than believes in them" [Valente and Breuker (1994)].

In game theory norms play a ternary role: coordination, conflicts of utility resolution and conflicts of inequality resolution (see e.g. [Ullman-Margalit (1978); Saam and Harrer (1999)]). We will mainly use norms in their second meaning, that is, for conflicts of utility resolution or, in other words, determinization of agent behavior.

A formalization of normative systems may be based on a set of common-sense intuitions [Valente and Breuker (1994)]: the norms address specific situations by referring to certain patterns of behavior. Application of a norm involves a comparison of the current situation with a generic one [Valente and Breuker (1994)].

Every set element of $\mathbb{G}$ (a proper sub-set of a Boolean of $\mathbb{D}$) is non-empty and a duplet at most.

This follows directly from the matrix description of $\odot$, discussed in the previous chapter. The last part of the proposition implies the non-determinacy of the composition $\odot$. The pairs $\{\mu, \kappa\}$, $\{\mu, \delta\}$, $\{\kappa, \delta\}$, $\{\delta, \iota\}$ and $\{\iota, \epsilon\}$ are generated by binary composition of the doxastic states. Let states x and y, $x, y \in \mathbb{D}$, be in a relation $\ddagger$ if there are two such elements z_1 and z_2 from $\mathbb{D}$ such that $z_1 \odot z_2 = \{x, y\}$. The diagram of the relation $\ddagger$ (which is a relation of partial order) is shown in Fig. 3.1.

Let x and y be elements of $\mathbb{D}$. A norm on $\langle \mathbb{D}, \odot \rangle$ is a binary relation $<$ such that

- $x \ddagger y$ implies either $x < y$ or $y < x$,
- $x < y$ implies $z_1 \odot z_2 := y$ if $z_1 \odot z_2 = \{x, y\}$.

In the $\odot$-compositions of elements of $\mathbb{D}$ five different pairs of doxastic states can be generated (see Fig. 3.1). Therefore, five norms can be applied: $N_{\kappa\delta}$, $N_{\epsilon\iota}$, $N_{\mu\delta}$, $N_{\delta\iota}$ and $N_{\mu\kappa}$. Every norm should be applied in one of its two forms. Therefore, we have 32 combinations of norms which may affect the algebraic structure of $\langle \mathbb{D}, \odot_N \rangle$; we write N to indicate a combination of norms.

4.2 Properties of $\langle \mathbb{D}, \odot_N \rangle$

None of the algebras $\langle \mathbb{D}, \odot_N \rangle$ has nulls, not even left or right ones. Only right identities are present.

State ι is a right identity of $\langle \mathbb{D}, \odot_N \rangle$ for any combination N of norms.

This is because for any element a of $\mathbb{D}$ we have $a \odot \iota = a$.

The element δ is a right identity of $\langle \mathbb{D}, \odot_N \rangle$ if $N = (\kappa > \delta) \wedge (\epsilon > \iota) \wedge (\mu > \delta)$.

A role of each norm can be seen in the series of diagrams below:

$$\kappa \odot \delta = \{\kappa, \delta\} \overset{N=(\kappa>\delta)}{\longrightarrow} \kappa \odot_N \delta = \kappa,$$

$$\epsilon \odot \delta = \{\epsilon, \iota\} \overset{N=(\epsilon>\iota)}{\longrightarrow} \epsilon \odot_N \delta = \epsilon,$$

$$\mu \odot \delta = \{\mu, \delta\} \overset{N=(\mu>\delta)}{\longrightarrow} \mu \odot_N \delta = \mu.$$

At the same time, $\delta \odot \delta = \delta$ and $\iota \odot \delta = \iota$.

Let $\mathbb{I}$ be a set of idempotents of algebra $\langle \mathbb{D}, \odot_N \rangle$; then the following dependences between norms and idempotents take place:

$\mathbb{I}$	N
$\{\kappa, \epsilon, \delta, \iota\}$	$(\kappa > \delta) \wedge (\epsilon > \iota)$
$\{\kappa, \delta, \iota\}$	$(\kappa > \delta) \wedge (\epsilon < \iota)$
$\{\epsilon, \delta, \iota\}$	$(\kappa < \delta) \wedge (\epsilon > \iota)$
$\{\delta, \iota\}$	$(\kappa < \delta) \wedge (\epsilon < \iota)$.

Only the norms $N_{\kappa\delta}$ and $N_{\epsilon\iota}$ are responsible for the structure of the sets of idempotents. This follows directly from the matrix representation of $\odot$. States δ and ι are idempotents anyway, independently of norms; μ cannot be idempotent because $\mu \odot \mu$ equals either δ or ι. The cases $\kappa \odot \kappa = \{\kappa, \delta\}$ and $\epsilon \odot \epsilon = \{\epsilon, \iota\}$ can be classified with the help of $N_{\kappa\delta}$ and $N_{\epsilon\iota}$.

A set $\mathbb{S}$ is called stable with respect to a binary operation $\circ$ if, $\forall a, b \in \mathbb{S}$, $a \circ b \in \mathbb{S}$. An algebra $\langle \mathbb{S}, \circ \rangle$ is a commutative algebra if $\mathbb{S}$ is stable and, $\forall a, b \in \mathbb{S}$, $a \circ b = b \circ a$.

Algebra $\langle \{\epsilon, \iota\rangle\}, \odot_N \rangle$ is a commutative sub-algebra of $\langle \mathbb{D}, \odot_N \rangle$ for any N.

This is because $\epsilon \odot \iota = \iota \odot \epsilon = \epsilon$, $\iota \odot \iota = \iota$ and $\epsilon \odot \epsilon$ equals either ϵ or ι.

Algebra $\langle \{\kappa, \delta\rangle\}, \odot_N \rangle$ is a commutative sub-algebra of $\langle \mathbb{D}, \odot_N \rangle$ if $N = (\kappa > \delta) \wedge (\kappa > \mu)$.

If $\odot$ is not normalized we get $\kappa \odot \kappa = \{\kappa, \delta\}$, $\kappa \odot \delta = \{\kappa, \delta\}$, $\delta \odot \kappa = \{\mu, \kappa\}$ and $\delta \odot \delta = \{\delta\}$. When we try to add the newly generated element μ to the set (which should be presumably stable), we find the element ι emerging as $\mu \odot \mu = \{\delta, \iota\}$; then ϵ is generated as $\iota \odot \kappa$. So, the whole set $\mathbb{D}$ is produced. Therefore, we take the norm $N_{\kappa\mu}$ in the form $\kappa > \mu$: $N = (\kappa > \mu)$. Thus, we make the set $\{\kappa, \delta\}$ stable under operation $\odot_N$. However, we now have $\kappa \odot_N \delta = \{\kappa, \delta\}$ and $\delta \odot_N \kappa = \kappa$. Therefore, we need to update N to $N = (\kappa > \mu) \wedge (\kappa > \delta)$.

Algebra $\langle \{\mu, \delta\rangle\}, \odot_N \rangle$ is a commutative sub-algebra of $\langle \mathbb{D}, \odot_N \rangle$ if $N = (\mu < \delta) \wedge (\delta > \iota)$.

We get $\mu \odot \mu = \{\delta, \iota\}$, $\delta \odot \delta = \{\delta\}$, $\delta \odot \mu = \{\delta\}$ and $\mu \odot \delta = \{\mu, \delta\}$. No norm affects the products $\delta \odot \delta = \delta$ and $\delta \odot \mu = \delta$. Let the norm $N_{\delta\iota}$ be activated in the form $\iota > \delta$. Then $N = (\iota > \delta)$ and $\mu \odot_N \mu = \iota$. The set $\{\mu, \delta, \iota\}$ is stable. However, $\mu \odot_N \iota = \mu$ and $\iota \odot_N \mu = \iota$. Therefore, we must also take the norm $N_{\delta\iota}$ in the form $\delta > \iota$, $N = (\delta > \iota)$. We also update N to $N = (\delta > \iota) \wedge (\mu < \delta)$ because $\delta \odot \mu = \delta$ and $\mu \odot_N \delta$ equals δ only if the combination of norms N includes the norm $\mu < \delta$.

Algebra $\langle \{\kappa, \mu, \delta\rangle\}, \odot_N \rangle$ is a commutative sub-algebra of $\langle \mathbb{D}, \odot_N \rangle$ if $N = (\kappa > \delta) \wedge (\mu < \kappa) \wedge (\mu < \delta) \wedge (\delta > \iota)$.

We take the norm $N_{\delta\mu}$ in the form $\delta > \mu$ because $\kappa \odot \mu = \delta$ but $\mu \odot \kappa = \{\mu, \delta\}$. This norm also makes μ and δ commuting. Non-normalized composition gives us $\kappa \odot \delta = \{\kappa, \delta\}$ and $\delta \odot \kappa = \{\mu, \kappa\}$. Therefore, we apply norms $N_{\kappa\delta}$ and $N_{\kappa\mu}$ in the forms $\kappa > \delta$ and $\kappa > \mu$, respectively. The non-normalized product $\mu \odot \mu = \{\delta, \iota\}$ gives us the element ι. This element cannot be included in our set because on including it we need to include

the element ϵ as well (due to $\iota \odot \kappa = \epsilon$); the commutativity would also be violated. Therefore, we activate norm $N_{\delta\iota}$ in the form $\delta > \iota$. The product table of the obtained commutative sub-algebra is shown below:

$\odot_N$	κ	μ	δ
κ	κ	δ	κ
μ	δ	δ	δ
δ	κ	δ	δ

where $N = (\kappa > \delta) \wedge (\mu < \kappa) \wedge (\mu < \delta) \wedge (\delta > \iota)$. This contains no units and no zeros are found.

Sub-algebra $\langle\{\kappa, \epsilon, \delta, \iota\rangle\}, \odot_N\rangle$ is a semi-group if $N = (\kappa > \mu) \wedge (\kappa > \delta) \wedge (\epsilon > \iota)$.

When using non-normalized composition $\odot$ we obtain $\delta \odot \kappa = \{\mu, \kappa\}$ and $\delta \odot \epsilon = \{\mu, \kappa\}$. Therefore, we have to apply the norm $N_{\kappa\mu}$ in the form $\kappa > \mu$. The element μ is not generated anywhere except for $\delta \odot \kappa$ and $\delta \odot \epsilon$. Therefore, $\kappa > \mu$ fully guarantees stability of the set $\{\kappa, \epsilon, \delta, \iota\}$. From this moment we assume that $N = (\kappa > \mu)$. The operation $\odot_N$ must be associative. Thus, for example, the following takes place:

$$\kappa \odot_N (\iota \odot_N \delta) = (\kappa \odot_N \iota) \odot_N \delta.$$

We see that $\kappa \odot_N (\iota \odot_N \delta) = \kappa$. However, $(\kappa \odot_N \iota) \odot_N \delta = \kappa \odot_N \delta = \{\kappa, \delta\}$. Therefore, we update N to $N = (\kappa > \mu) \wedge (\kappa > \delta)$. Another constraint of associativity states that

$$\delta \odot_N (\epsilon \odot_N \kappa) = (\delta \odot_N \epsilon) \odot_N \kappa.$$

The right-hand side of this equation equals κ. However, the left-hand one produces $\epsilon \odot_N \kappa = \{\epsilon, \iota\}$. Choosing ι, we obtain $\delta \odot_N \iota = \delta$, which is not equal to the right-hand side of the equation. Therefore, we update N to $N = (\kappa > \mu) \wedge (\kappa > \delta) \wedge (\epsilon > \iota)$. This gives us $\delta \odot \epsilon = \kappa$. All other cases of associativity equations are correct automatically for recently updated N.

The product table of the semi-group looks as follows:

$\odot_N$	κ	ϵ	δ	ι
κ	κ	κ	κ	κ
ϵ	ϵ	ϵ	ϵ	ϵ
δ	κ	κ	δ	δ
ι	ϵ	ϵ	ι	ι

The elements ϵ and κ are left zeros; ϵ and ι are right identities.

Sub-algebras $\langle\{\kappa,\epsilon,\iota\},\odot_N\rangle$ and $\langle\{\kappa,\epsilon,\delta\},\odot_N\rangle$ are semi-groups if $N = (\kappa > \delta) \wedge (\epsilon > \iota)$ and $N = (\kappa > \delta) \wedge (\epsilon > \iota) \wedge (\mu < \kappa)$, respectively.

An element a of $\mathbb{D}$ is called a generator of $\langle\mathbb{D},\odot_N\rangle$ if $[a \odot_N a] \odot_N^4 a = \mathbb{D}$.

The element κ is the only singleton generator of the algebra $\langle\mathbb{D},\odot_N\rangle$ if $N = (\kappa < \delta) \wedge (\mu > \kappa) \wedge (\delta < \iota)$.

Really, having only κ initially, we produce δ as $\kappa \odot_N \kappa = \delta$. Then, we generate μ in $\delta \odot_N \kappa$. The product $\mu \odot_N \mu$ gives us ι. Finally, we have $\iota \odot_N \kappa = \epsilon$. Algebras with other combinations of norms have either duplets or triplets as generators.

The sets $\{\kappa,\epsilon,\mu\}$, $\{\kappa,\epsilon,\delta\}$, $\{\kappa,\mu,\iota\}$ and $\{\kappa,\delta,\iota\}$ are minimal generators of algebra $\langle\mathbb{D},\odot_N\rangle$ if $N = (\kappa > \delta) \wedge (\mu > \kappa) \wedge (\delta > \iota)$.

All other combinations of norms allow algebras to have one or more duplets as minimal generators. The detailed correspondence between combinations N of norms and minimal duplet generators is shown below:

N	Generators
$(\mu < \kappa) \wedge (\delta > \iota)$	$\{\epsilon,\mu\}$
$(\mu < \kappa) \wedge (\mu > \delta) \wedge (\delta < \iota)$	$\{\kappa,\mu\}$
$(\kappa > \delta) \wedge (\mu > \kappa) \wedge (\delta < \iota)$	$\{\kappa,\mu\},\{\kappa,\delta\}$
$(\mu < \delta) \wedge (\delta < \iota) \wedge (\mu < \kappa)$	$\{\kappa,\mu\},\{\epsilon,\mu\}$
$(\kappa < \delta) \wedge (\mu > \kappa) \wedge (\delta > \iota)$	$\{\kappa,\epsilon\},\{\kappa,\iota\}$

4.3 Normalizing doxatons

Recall that a doxaton is a finite automaton $\langle\mathbb{S},\mathbb{I},\gamma\rangle$ with a set $\mathbb{S}$ of states, a set $\mathbb{I}$ of inputs and a mapping $\gamma : \mathbb{S} \times \mathbb{I} \to \mathbb{S}$. The sets $\mathbb{S}$ and $\mathbb{I}$ equal $\mathbb{D}$. For any two elements $a \in \mathbb{S}$ and $b \in \mathbb{I}$, a mapping γ of a *free*, i.e. non-normalized, *doxaton* is determined as

$$\gamma(a,b) = \begin{cases} c \quad \text{if} \quad a \odot b = \{c\}, \\ c_1 \quad \text{or} \quad c_2 \quad \text{with probability} \quad \frac{1}{2} \quad \text{if} \quad a \odot b = \{c_1, c_2\}. \end{cases}$$

If the doxaton is *normalized* and a combination N of norms is employed, then

$$\gamma(a,b) = \begin{cases} c_1 & \text{if} \quad a \odot b = \{c_1, c_2\} \quad \text{and} \quad N = (c_1 > c_2), \\ c_2 & \text{if} \quad a \odot b = \{c_1, c_2\} \quad \text{and} \quad N = (c_2 > c_1). \end{cases}$$

A norm is called principal if, being applied alone to the state-transition function of a doxaton, it changes the topology of the free doxaton transition graph $\mathbf{G}$, e.g. it deletes at least one arc.

Norms $N_{\delta\iota}$ and $N_{\mu\kappa}$ are principal norms.

From the structure of $\odot$-composition and the free doxaton state transition graph, we see that

- applying the norm $N_{\delta\iota}$ in the form $\delta > \iota$ we delete the arc $\mu \to \iota$ from the transition graph; the graph becomes sub-divided into two disconnected components: the first component includes the nodes κ, δ and μ, the second consists of ι and ϵ,
- applying the norm $N_{\mu\kappa}$ in the form $\mu > \kappa$ we eliminate the arc $\delta \to \kappa$ from the graph; if the norm $N_{\mu\kappa}$ has the form $\mu < \kappa$, the arc $\delta \to \mu$ is eliminated.

Now assume that input states of a doxaton are chosen at random at every step of the doxaton development; the elements of this random input sequence are distributed uniformly. In such simplified conditions, the behavior of a doxaton is analyzed in probabilistic terms. Thus, for example, for a free doxaton being in the state μ, we say that it will take the state μ again with the probability $\frac{1}{2}$, it will take the state δ with the probability $\frac{2}{5}$ and it will take the state ι with the probability $\frac{1}{10}$. This can be easily derived from the matrix of $\odot$-composition.

Let a, b, c and d be elements of $\mathbb{D}$ and $p_{a \to b | N_{cd}}$ be a probability of the transition of a doxaton from the state $s^t = a$ to the state $s^{t+1} = b$ when the norm N_{cd} is applied; at time step t the doxaton receives one randomly uniformly chosen element of $\mathbb{D}$ on its input. Then the following proposition is valid.

Consequences of norms $N_{\kappa\delta}$, $N_{\epsilon\iota}$ and $N_{\mu\kappa}$ are as follows:

- $p_{\kappa\to\delta|\kappa>\delta} = \frac{1}{5}$ and $p_{\kappa\to\delta|\kappa<\delta} = \frac{4}{5}$;
- $p_{\epsilon\to\iota|\epsilon>\iota} = \frac{1}{5}$ and $p_{\epsilon\to\iota|\epsilon<\iota} = \frac{4}{5}$;
- $p_{\delta\to\mu|\mu>\kappa} = \frac{2}{5}$ and $p_{\delta\to\kappa|\mu<\kappa} = \frac{2}{5}$.

In these conditions a doxaton keeps its state a with the probability $p_{a\to a|N_{cd}} = 1 - p_{a\to b|N_{cd}}$. The principal norm $N_{\mu\kappa}$ was already discussed before. The role of the norms $N_{\kappa\delta}$ and $N_{\epsilon\iota}$ is rather cosmetic. Both norms $N_{\mu\delta}$ and $N_{\delta\iota}$ are applied to the doxaton when it has the state μ.

Consequences of the norms $N_{\mu\delta}$ and $N_{\delta\iota}$ are as follows:

- $p_{\mu\to\iota|\frac{\mu\le\delta}{\delta<\iota}} = \frac{1}{5}$ and $p_{\mu\to\delta|\frac{\mu\le\delta}{\delta<\iota}} = \frac{3}{5}$; the doxaton keeps the state μ with the probability $\frac{1}{5}$;
- $p_{\mu\to\delta|\frac{\mu>\delta}{\delta>\iota}} = \frac{1}{5}$; the doxaton keeps the state μ with the probability $\frac{4}{5}$;
- $p_{\mu\to\delta|\frac{\mu<\delta}{\delta>\iota}} = \frac{4}{5}$; the doxaton keeps the state μ with the probability $\frac{1}{5}$;
- $p_{\mu\to\iota|\frac{\mu\ge\delta}{\delta<\iota}} = \frac{1}{5}$; the doxaton keeps the state μ with the probability $\frac{4}{5}$.

4.4 Normalization of reflecting doxatons

A doxaton is called reflecting if it updates its state at time $t+1$ depending on its state at time t. Starting its development in the state δ and ι, a doxaton keeps these states forever independently of the norms applied. This is because $\delta \odot \delta = \{\delta\}$ and $\iota \odot \iota = \{\iota\}$ (see also [Adamatzky (2001a)]). The development for $s^{t=0} \in \{\epsilon, \kappa, \mu\}$ should be discussed in detail.

The norms $N_{\epsilon\iota}$, $N_{\kappa\delta}$ and $N_{\delta\iota}$ are principal norms of reflecting doxatons which start their development in the states ϵ, κ and δ, respectively.

If the initial state of a doxaton is ϵ or κ and the norms $N_{\epsilon\iota}$ and $N_{\kappa\delta}$ are applied in the forms $\epsilon > \iota$ and $\kappa > \delta$, respectively, the doxaton does not change its state, i.e. for any $t > 0$, $s^t = \epsilon$ or κ. The irreversible transitions $\epsilon \to \iota$ and $\kappa \to \delta$ happen when $\iota > \epsilon$ and $\kappa > \delta$. After that the doxaton will be in states ι or δ forever. Duplet $\{\delta, \iota\}$ results from the composition $\mu \odot \mu$.

Therefore, a non-normalized reflecting doxaton chooses one of these states with the same probability when it starts its development in the state μ. The norm $N_{\delta\iota}$ makes this initial state transition deterministic. The

doxaton takes state ι if $\delta > \iota$, and it takes state δ otherwise. The updated state is not changed in the development.

4.5 Solutions of normalized doxatons

To study how norms influence "globally connected", well-stirred, collectives of doxatons we simulated mixtures of $n = 50$–300 doxatons for $10^4 \times 5 \times 10^4$ time steps. At every time step we randomly choose two doxatons x and y and update their states as $x^{t+1} \leftarrow x^t \odot_N y^t$ and $y^{t+1} \leftarrow y^t \odot_N x^t$. For every combination N of norms we calculate the dominating and becoming extinct doxastic states in 3×10^4 trials. For every state $a \in \mathbb{D}$ the probability $p_N(a)$ of state a to appear in the final configuration of an N-normalized doxaton pool is evaluated.

We say that state a dominates if $p_N(a) = \max_{a \neq b \in \mathbb{D}}\{p_N(b)\}$. For any combination N of the norms and any state $a \in \mathbb{D}$, we have the following: if a is a dominating state then $p_N(a) \geq 0.4$; for the majority of norms' combinations 0.5 is obtained.

> In the mixed solution of normalized doxatons the state μ never dominates.

The correspondence between norm combinations and dominating states is shown below:

N	Dominate
$(\kappa > \delta) \wedge (\mu < \kappa) \wedge$ $((\epsilon < \iota) \vee (\epsilon > \iota) \wedge ((\mu > \delta) \wedge (\delta > \iota) \vee (\mu < \delta)))$	κ
$(\epsilon > \iota) \wedge$ $((\mu > \delta) \wedge (\delta < \iota) \vee$ $(\kappa < \delta) \wedge (\mu < \kappa) \wedge ((\mu > \delta) \wedge (\delta > \iota) \vee (\mu < \delta)) \vee$ $(\mu < \delta) \wedge (\delta < \iota) \wedge (\mu > \kappa))$	ϵ
$(\mu > \kappa) \wedge (\delta > \iota) \vee$ $(\kappa < \delta) \wedge (\mu < \kappa) \wedge$ $((\mu < \delta) \wedge (\delta > \iota) \vee (\epsilon < \iota) \wedge$ $((\mu > \delta) \wedge (\delta > \iota) \vee (\mu < \delta) \wedge (\delta < \iota))) \vee$ $(\epsilon < \iota) \wedge (\mu < \delta) \wedge (\delta < \iota) \wedge (\mu > \kappa)$	δ
$(\epsilon < \iota) \wedge (\mu > \delta) \wedge (\delta < \iota) \wedge$ $((\kappa < \delta) \wedge (\kappa > \delta) \wedge (\mu > \kappa))$	ι

The next sections deal with lattices of doxatons.

4.6 Quiescent states and sets

The state a is a quiescent state if $f(a, a, a) = a$.

Every idempotent is a quiescent state but not every quiescent state is idempotent.

The condition of idempotency is $a \odot_N a = a$, whereas the condition of quiescency is $(a \odot_N a) \odot_N a = a$. Thus, for example, if $a \odot_N a = b$ and $b \odot_N a = a$, then a is a quiescent state but not idempotent. The order of composition is exactly $(a \odot_N a) \odot_N a$, because being in the state a a doxaton composes its state with the state of one of its two neighbors (both neighbors are in the state a). Then it changes its state to $a \odot_N a$ and composes the newly formed state with the state of another neighbor, which is also a.

The states ϵ, δ and ι are quiescent states of a doxaton collective for any combination N of norms. The state κ is a quiescent state if $\kappa > \delta$ and $\kappa > \mu$.

The states δ and ι are trivial quiescent states; they are also trivial idempotents: $\delta \odot \delta = \delta$ and $\iota \odot \iota = \iota$. The state μ is neither idempotent nor a quiescent state because $\mu \odot \mu = \{\delta, \iota\}$, $\delta \odot \mu = \delta$ and $\iota \odot \mu = \iota$. The state ϵ is idempotent if $\epsilon > \iota$ and it is a quiescent state anyway:

- for $\epsilon > \iota$ we have $(\epsilon \odot_N \epsilon) \odot_N \epsilon = \epsilon \odot_N \epsilon = \epsilon$ and
- for $\epsilon < \iota$ we have $(\epsilon \odot_N \epsilon) \odot_N \epsilon = \iota \odot_N \epsilon = \epsilon$.

Let us look at $(\kappa \odot \kappa) \odot \kappa$. We see that $\kappa \odot \kappa = \{\kappa, \delta\}$; therefore, we need the norm $\kappa > \delta$ to make $\kappa \odot_N \kappa = \kappa$. If $\kappa > \delta$, then κ is idempotent and a quiescent state. Let $\kappa < \delta$. Then $(\kappa \odot_N \kappa) \odot_N \kappa = \delta \odot_N \kappa = \{\mu, \kappa\}$. To produce κ we need to apply $\kappa > \mu$. In this case κ is not idempotent but it is a quiescent state.

A set $\mathbb{S} \subseteq \mathbb{D}$ is called a quiescent set if $f(y, x, z) = x$ for any x, y and z from $\mathbf{S}$. The set $\{\delta, \iota\}$ is a quiescent set, i.e. quiescent independently of the norms.

Set $\{\kappa, \epsilon\}$ is a quiescent set of a doxaton collective for any combination N of norms except those including $(\kappa < \delta) \wedge (\kappa < \mu)$.

4.7 On stable neighborhoods

Let $w = (bac)$ be a configuration of a neighborhood $u(x)$ of a doxaton x. The neighborhood $u(x) = (yxz)$ consists of doxaton x (central element) and two immediate neighbors y, left neighbor, and z, right neighbor, of doxaton x. Then w is called C-stable if $(a \odot_N b) \odot_N c = (a \odot_N c) \odot_N b = a$.

It may be speculated that global stability of a doxaton collective directly depends on the number of C-stable configurations of a doxaton neighborhood. Simple calculations show the following.

A collective of doxatons has a maximal number of C-stable configurations of a neighborhood if $N = (\kappa > \delta) \wedge (\epsilon > \iota) \wedge (\mu > \delta)$.

A collective of doxatons has a minimal number of C-stable configurations of a neighborhood if $N = (\kappa < \delta) \wedge (\epsilon < \iota) \wedge (\mu < \delta)$.

The norm $N_{\kappa\mu}$ does not influence C-stability at all.

4.8 Homogeneity of doxaton local functions

We consider a static complexity of a doxaton system, derived from a doxaton state-transition function. We do it with the help of a static parameter which reflects the homogeneity of the state-transition function. This parameter is similar to the parameter λ proposed in [Langton (1990)] for classification of cell state transition functions of one-dimensional cellular automata. In his paper [Langton (1990)] Langton demonstrates that $\lambda = 0.75$ produces maximal dynamical disorder and $\lambda = 0.45$ corresponds to patterns with particle-like behavior, i.e. non-trivial complex behavior. This last value of λ is assumed to be critical [Langton (1990)] for the systems which implement a transition from order to chaos. It is also claimed that the increase of λ from 0 to 0.45 induces an increase in the complexity of cell state transition rules.

Let N be given. Then for every element $a \in \mathbb{D}$ we compute

$$l_N(a) = \frac{|\{w \in \mathbb{D} : f(w) = a\}|}{|\{w \in \mathbb{D}\}|},$$

where for $w = (w_1 w_2 w_3)$ the expression $f(w) = a$ means that $(w_1 \odot_N w_2) \odot_N w_3 = a$ or $(w_1 \odot_N w_3) \odot_N w_2 = a$. In this manner every N can be

assigned a real number

$$L(N) = \mathrm{dist}\left((l_N(\kappa), l_N(\epsilon), l_N(\mu), l_N(\delta), l_N(\iota)), \left(\frac{1}{5}, \frac{1}{5}, \frac{1}{5}, \frac{1}{5}, \frac{1}{5}\right)\right),$$

which is a distance between a position of the given doxaton system (normalized by the combination N of norms) in the five-dimensional simplex and the center of the simplex. The less $L(N)$, the closer the given system resides to the center of the simplex and the more homogeneous is the local transition function of the doxaton collective. With the help of this parameter we sub-divide all combinations of norms into the following classes:

(1) Central (homogeneous): $N = (\kappa > \delta) \wedge (\epsilon > \iota) \wedge (\kappa > \mu) \wedge (\mu > \delta)$, $L(N) \approx 0.00077$;

(2) Nearly central (nearly homogeneous):
- $N = (\kappa > \delta) \wedge (\epsilon < \iota) \wedge (\mu > \delta) \wedge (\delta > \iota) \wedge (\kappa > \mu)$ or $N = (\kappa < \delta) \wedge (\epsilon > \iota) \wedge (\mu > \delta) \wedge (\delta < \iota) \wedge (\kappa > \mu)$, $L(N) \approx 0.07$;
- $N = (\kappa > \delta) \wedge (\mu > \kappa) \wedge [(\epsilon > \iota) \wedge (\mu > \delta) \vee (\epsilon < \iota) \wedge (\mu > \delta) \wedge (\delta > \iota)]$, $L(N) \approx 0.08$;
- $N = (\kappa > \delta) \wedge (\epsilon > \iota) \wedge (\mu < \delta) \wedge (\delta < \iota) \wedge (\mu > \kappa)$, $L(N) \approx 0.09$;
- $N =$

$$\begin{gathered}(\kappa > \delta) \wedge (\mu < \delta) \wedge (\delta > \iota) \wedge (\mu > \kappa) \vee \\ (\kappa < \delta) \wedge (\mu > \delta) \wedge (\delta > \iota) \wedge (\mu < \kappa) \vee \\ (\epsilon < \iota) \wedge (\mu > \delta) \wedge (\delta < \iota) \wedge (\mu < \kappa) \vee \\ (\kappa > \delta) \wedge (\epsilon < \iota) \wedge (\mu < \delta) \wedge (\delta < \iota) \wedge (\mu > \kappa),\end{gathered}$$

  $L(N) \approx 0.12$;
- $N = (\kappa > \delta) \wedge (\epsilon < \iota) \wedge (\mu > \delta) \wedge (\delta < \iota) \wedge (\mu > \kappa)$, $L(N) \approx 0.14$;

(3) Far from center (nearly heterogeneous):
- $N =$

$$\begin{gathered}(\kappa > \delta) \wedge (\mu < \delta) \wedge (\delta > \iota) \wedge (\mu < \kappa) \vee \\ (\kappa > \delta) \wedge (\mu < \delta) \wedge (\delta < \iota) \wedge (\mu < \kappa) \vee \\ (\kappa < \delta) \wedge (\epsilon > \iota) \wedge (\mu > \delta) \wedge (\delta < \iota) \wedge (\mu > \kappa),\end{gathered}$$

  $L(N) \approx 0.19$;
- $N =$

$$\begin{gathered}(\kappa < \delta) \wedge (\mu < \delta) \wedge (\delta < \iota) \vee \\ (\kappa < \delta) \wedge (\epsilon < \iota) \wedge (\mu > \delta) \wedge (\mu > \kappa) \vee \\ (\kappa < \delta) \wedge (\epsilon > \iota) \wedge (\mu > \delta) \wedge (\delta > \iota) \wedge (\mu > \kappa),\end{gathered}$$

$L(N) \approx 0.20$;
- $N = (\kappa < \delta) \wedge (\mu < \delta) \wedge (\delta > \iota)$, $L(N) \approx 0.22$.

4.9 Evolving from the homogeneous configurations

A configuration of a doxaton lattice $\mathbb{L}$ is called a homogeneous configuration if all doxatons in the lattice take the same state $\alpha \in \mathbb{D}$. We assume that the doxaton lattice is a torus.

Any homogeneous configuration of a doxaton lattice remains homogeneous in the course of development.

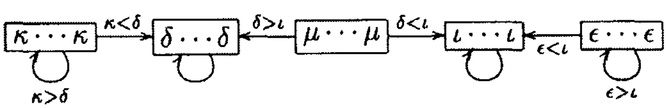

Fig. 4.1 Graphs of global transitions between homogeneous configurations of a doxaton lattice. Non-labeled arcs represent unconditional transitions, i.e. those which happen for any combination of norms.

All doxatons update their states in parallel. Let at the time step t every doxaton x take the state $x^t = \kappa$. The doxaton x calculates its next state as $x^{t+1} = (x \odot_N y) \odot z$. That is, $x^{t+1} = \kappa$ if $N = (\kappa > \delta)$ and $x^{t+1} = \delta$ if $N = (\kappa < \delta)$. The norms are not changed in time; therefore, for any $x \in \mathbb{L}$ we have $x^{t+2} = \kappa$ if $N = (\kappa > \delta)$ and $x^{t+2} = \delta$ if $N = (\kappa < \delta)$. If all doxatons initially take the state μ, then at the next step of development they take either the state δ, if $N = (\delta > \iota)$, or the state ι, if $N = (\delta < \iota)$. The doxatons do not change their states after that. This is because δ and ι are idempotents. Starting their development in the state ϵ, the doxatons remain in the state ϵ, if $N = (\epsilon > \iota)$, or take the state ι, if $N = (\epsilon < \iota)$. The graph of global transitions between the homogeneous configurations of a doxaton lattice is shown in Fig. 4.1; there we see that configurations $\delta \cdots \delta$ and $\iota \cdots \iota$ are *absorbing* global states. The configuration $\mu \cdots \mu$ is a *non-constructible* configuration.

4.10 Fate of the singleton

What happens with the doxaton lattice when all doxatons but a single one take the same state at the beginning of development? To answer the question, we analyze each of 20 initial configurations of a doxaton lattice of the form $\alpha \cdots \alpha\beta\alpha \cdots \alpha$, $\beta \neq \alpha$.

4.10.1 *Ignorant singleton*

The configuration $\delta \cdots \delta\iota\delta \cdots \delta$ is a stationary configuration because $\{\delta, \iota\}$ is a trivial quiescent set.

The singleton in the state ι keeps its state unchanged if it starts development in the lattice with other doxatons being in the state μ. Other doxatons change their states either to δ, if $N = (\delta > \iota)$, or to ι, if $N = (\delta < \iota)$. At the second step of the development the lattice falls in one of the stationary states: either $\delta \cdots \delta\iota\delta \cdots \delta$ or $\iota \cdots \iota$.

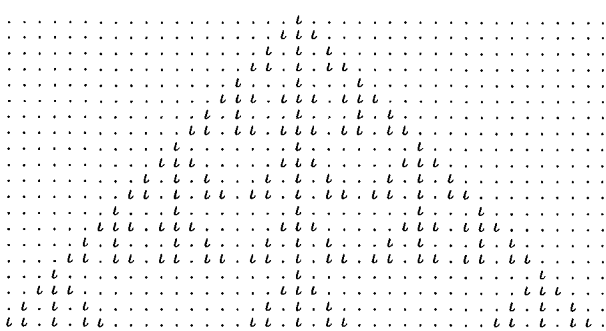

Fig. 4.2 Development of a doxaton lattice, which starts in the initial configuration $\epsilon \cdots \epsilon\iota\epsilon \cdots \epsilon$. The norm $\epsilon < \iota$ is applied. The state ϵ is shown by dots. Time is arrowed top down.

Outcomes of the initial configuration $\epsilon \cdots \epsilon\iota\epsilon \cdots \epsilon$ are non-trivial. The doxaton lattice then finishes its development in the stationary homogeneous configuration $\epsilon \cdots \epsilon$ if $N = (\epsilon > \iota)$. However, for the norm $N = (\epsilon < \iota)$, a Pascal triangle is formed (Fig. 4.2). For $N = (\epsilon < \iota)$ the state-transition rule of the doxaton can be represented as $x^{t+1} = (x^t + y^t + z^t) \mod 2$, where the state 0 represents the state ϵ and the state 1 represents the state ι. The sub-algebra $\langle \odot_{(\epsilon<\iota)}, \{\epsilon, \iota\} \rangle$ is associative; therefore, the triangle is symmetrical because even a random choice of the composition order does

not influence the morphology of the growing pattern.

If the singleton in the state ι starts its development in the lattice of doxatons in the state κ (the initial configuration $\kappa \cdots \kappa\iota\kappa \cdots \kappa$), it may take either the state ι or the state ϵ. Depending on the norms applied, all other doxatons take one of the states of $\mathbb{D}$ but not the state μ. All doxatons, except the singleton and its immediate neighbors, take finally the state δ if the norms are

$$N_1^{\kappa\iota\kappa} = (\kappa < \delta) \wedge (\epsilon > \iota) \wedge (\mu > \delta) \wedge (\delta > \iota) \wedge (\mu > \kappa)$$

or

$$N_2^{\kappa\iota\kappa} = (\kappa < \delta) \wedge (\mu > \kappa) \wedge ((\mu < \delta) \wedge (\delta > \iota) \vee (\mu > \delta) \wedge (\delta > \iota) \wedge (\epsilon < \iota)).$$

In both cases the singleton takes the state ι. However, in the case of the norm $N_1^{\kappa\iota\kappa}$, two immediate neighbors of the singleton take the state μ. So, the initial configuration $\kappa \cdots \kappa\iota\kappa \cdots \kappa$ is transformed to the stationary configuration $\delta \cdots \delta\mu\iota\mu\delta \cdots \delta$ if the norm $N_1^{\kappa\iota\kappa}$ is applied, and to the stationary configuration $\delta \cdots \delta\iota\delta \cdots \delta$ if the applied norm is $N_1^{\kappa\iota\kappa}$. The lattice finishes its development in the stationary configurations $\kappa \cdots \kappa\epsilon\kappa \cdots \kappa$ and $\kappa \cdots \kappa\iota\kappa \cdots \kappa$ if norms $(\kappa > \delta) \wedge (\epsilon > \iota)$ and $(\kappa > \delta) \wedge (\epsilon < \iota)$ are employed.

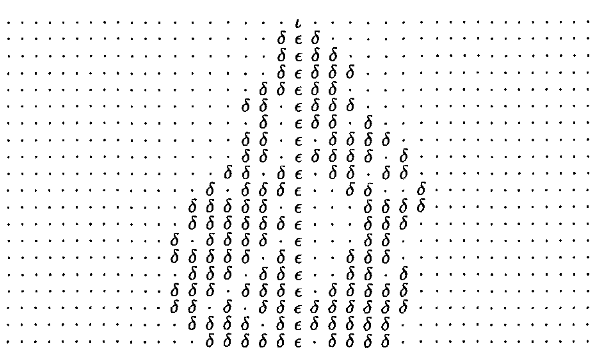

Fig. 4.3 Development of a doxaton lattice, which starts in the initial configuration $\kappa \cdots \kappa\iota\kappa \cdots \kappa$. The norms $(\kappa < \delta) \wedge (\mu < \kappa)$ are applied. The state κ is shown by dots.

The state δ spreads outward from the singleton in the space–time configuration (Fig. 4.3) when the norm combination is $N_3^{\kappa\iota\kappa} = (\kappa < \delta) \wedge (\mu < \kappa)$; the singleton takes state ϵ and remains in this state during its development. Because immediate neighbors of the singleton take the state δ, as the result of the composition $(\kappa \odot_{N_3^{\kappa\iota\kappa}} \iota) \odot_{N_3^{\kappa\iota\kappa}} \kappa = (\kappa \odot_{N_3^{\kappa\iota\kappa}} \kappa) \odot_{N_3^{\kappa\iota\iota}} \kappa = \delta$. A front

of the diffusion wave of the state δ behaves irregularly. This is because the sub-algebra $\langle \odot_{N_3^{\kappa\iota\kappa}}, \{\kappa, \delta\}\rangle$ is not associative and the result of the doxaton state-transition function depends on the order of the state composition. In the case of norms

$$(\kappa < \delta) \wedge (\epsilon > \iota) \wedge (\mu > \delta) \wedge (\delta < \iota) \wedge (\mu > \kappa)$$

the singleton takes the states ι and ϵ and its immediate neighbors take all the states of $\mathbb{D}$ except κ. For all other combinations of norms all doxatons except the singleton and its immediate neighbors spend their development in the state ι; the singleton takes the state ι or quasi-periodically chooses between the states ι and ϵ during the development. The immediate neighbors of the singleton take the state δ.

4.10.2 *Doubting singleton*

The configuration $\iota \cdots \iota\delta\iota \cdots \iota$ is a stationary configuration because $\{\delta, \iota\}$ is a trivial quiescent set.

There are four possible successors of the initial configuration $\mu \cdots \mu\delta\mu \cdots \mu$ in the development of the doxaton lattice.

(1) The lattice takes the stationary configuration $\iota \cdots \iota\delta\delta\delta\iota \cdots \iota$ if

$$N = (\kappa < \delta) \wedge (\epsilon < \iota) \wedge (\mu < \delta).$$

(2) The singleton started in the state δ keeps this state forever and all other doxatons take the absorbing state ι if

$$N = ((\kappa > \delta) \wedge (\epsilon < \iota) \wedge (\mu < \delta) \vee (\kappa < \delta) \wedge (\mu < \delta)).$$

(3) The singleton keeps its state δ forever, its immediate neighbors may take either the state ι or the state δ (because of the random order of the composition of neighbors) and all other doxatons take the state ι if the combination N of norms is

$$(\kappa > \delta) \wedge (\mu < \delta) \wedge (\mu < \iota) \vee (\kappa < \delta) \wedge (\epsilon > \iota) \wedge (\mu < \delta) \wedge (\delta < \iota).$$

(4) For all other combinations of the norms the initial configuration $\mu \cdots \mu\delta\mu \cdots \mu$ is transformed to the stationary configuration $\delta \cdots \delta$ at the first steps of the development.

The initial configuration $\epsilon \cdots \epsilon\delta\epsilon \cdots \epsilon$ is transformed to the stationary configuration $\epsilon \cdots \epsilon\kappa\epsilon \cdots \epsilon$ if the norm $(\kappa > \delta) \wedge (\mu > \kappa)$ is applied or to the stationary configuration $\delta \cdots \delta$ if the norms are combined as

$$(\kappa > \delta) \wedge (\epsilon > \iota) \wedge (\mu < \delta) \wedge (\mu > \kappa) \vee$$
$$(\kappa < \delta) \wedge (\epsilon > \iota) \wedge ((\mu < \kappa) \vee (\mu > \kappa) \wedge (\mu < \delta)).$$

All doxatons except the singleton and its immediate neighbors take state ϵ (and never change their states after that) if the norms

$$(\epsilon > \iota) \wedge (\mu > \delta) \wedge (\mu > \kappa)$$

are applied; the singleton takes state μ and its two immediate neighbors take states ι and ϵ chosen at random. It is typical for all other combinations of norms that diffusive waves of ι-states are formed at the beginning of development. They are generated as the result of the composition $(\epsilon \odot_N \epsilon) \odot_N \alpha = \iota$ or $(\epsilon \odot_N \alpha) \odot \epsilon = \iota$, where α is either δ or μ. Because of the random order of the composition of doxastic states, the "diffusing" state ι may appear on both sides of the singleton at different steps of the development. Therefore, a triangle of ι-states with unequal sides is formed.

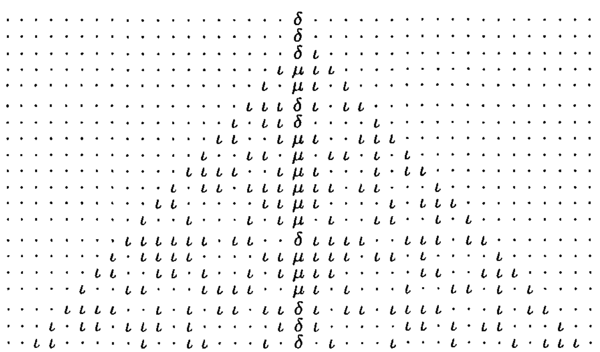

Fig. 4.4 An example of the formation of a triangle bounded by ι-states in development of a doxaton lattice. The initial configuration is $\epsilon \cdots \epsilon\delta\epsilon \cdots \epsilon$. The norms $(\epsilon < \iota) \wedge (\mu < \delta) \wedge (\mu > \kappa)$ are applied to the doxaton lattice in this example. The states δ are shown by dots.

Inside the triangle doxatons update their states by the rule

$$x^{t+1} = (y^t + x^t + z^t) \mod 2,$$

where 0 stands for ϵ and 1 stands for ι (Fig. 4.4). In this situation, the singleton updates its state in the following manner. It takes the state μ and remains in this state if the norms

$$(\epsilon < \iota) \wedge (\mu > \delta) \wedge (\mu > \kappa)$$

are employed. At every step of the development, the singleton chooses between either δ and μ for the norms

$$(\epsilon < \iota) \wedge (\mu < \delta) \wedge (\mu > \kappa)$$

or δ and κ for the norms

$$(\kappa < \delta) \wedge (\epsilon < \iota) \wedge (\mu < \kappa).$$

The initial configuration $\kappa \cdots \kappa\delta\kappa \cdots \kappa$ may be the precursor of several space–time configurations. The simple outcomes of the development include five types of final stationary configurations:

- $\kappa \cdots \kappa$, if $N = (\kappa > \delta) \wedge (\mu < \kappa)$;
- $\kappa \cdots \kappa\delta\kappa \cdots \kappa$, if $N = (\kappa > \delta) \wedge (\mu < \delta) \wedge (\mu > \kappa)$;
- $\delta \cdots \delta$, if $N = (\kappa < \delta) \wedge (\mu > \kappa) \wedge ((\mu > \delta) \wedge (\delta > \iota) \vee (\mu < \delta) \wedge (\delta < \iota))$;
- $\iota \cdots \iota\delta\iota \cdots \iota$, if $N = (\kappa < \delta) \wedge (\mu > \delta) \wedge (\delta < \iota)$;
- $\iota \cdots \iota\delta \cdots \delta\iota \cdots \iota$, if $N = (\kappa < \delta) \wedge (\mu < \delta) \wedge (\delta < \iota) \wedge (\mu > \kappa)$.

In all these cases the doxaton lattice takes the stationary configuration at the first step of the development. The state δ diffuses in the lattice if either

```
· · · · · · · · · · · · · · · · · · · δ · · · · · · · · · · · · · · · · · · · ·
· · · · · · · · · · · · · · · · · · · μ · · · · · · · · · · · · · · · · · · · ·
· · · · · · · · · · · · · · · · · · μ μ δ · · · · · · · · · · · · · · · · · · ·
· · · · · · · · · · · · · · · · · μ μ δ δ · · · · · · · · · · · · · · · · · · ·
· · · · · · · · · · · · · · · · μ μ δ δ μ · · · · · · · · · · · · · · · · · · ·
· · · · · · · · · · · · · · · μ δ δ δ δ μ μ · · · · · · · · · · · · · · · · · ·
· · · · · · · · · · · · · · δ μ δ δ δ δ δ μ μ · · · · · · · · · · · · · · · · ·
· · · · · · · · · · · · · · δ μ δ δ δ δ δ δ δ μ · · · · · · · · · · · · · · · ·
· · · · · · · · · · · · · · μ μ δ δ δ δ δ δ δ μ δ · · · · · · · · · · · · · · ·
· · · · · · · · · · · · · δ δ δ δ δ δ δ δ δ δ μ δ · · · · · · · · · · · · · · ·
· · · · · · · · · · · · · μ δ δ δ δ δ δ δ δ δ μ δ · · · · · · · · · · · · · · ·
· · · · · · · · · · · · μ μ δ δ δ δ δ δ δ δ δ μ μ · · · · · · · · · · · · · · ·
· · · · · · · · · · · δ μ δ δ δ δ δ δ δ δ δ δ δ μ μ · · · · · · · · · · · · · ·
· · · · · · · · · · · μ μ δ δ δ δ δ δ δ δ δ δ δ δ δ μ · · · · · · · · · · · · ·
· · · · · · · · · · δ μ δ δ δ δ δ δ δ δ δ δ δ δ δ δ μ δ · · · · · · · · · · · ·
· · · · · · · · · · μ μ δ δ δ δ δ δ δ δ δ δ δ δ δ δ μ δ · · · · · · · · · · · ·
· · · · · · · · · μ δ δ δ δ δ δ δ δ δ δ δ δ δ δ δ δ μ μ · · · · · · · · · · · ·
· · · · · · · · δ μ δ δ δ δ δ δ δ δ δ δ δ δ δ δ δ δ δ μ δ · · · · · · · · · · ·
· · · · · · · · δ μ δ δ δ δ δ δ δ δ δ δ δ δ δ δ δ δ δ μ μ · · · · · · · · · · ·
· · · · · · · · δ μ δ δ δ δ δ δ δ δ δ δ δ δ δ δ δ δ δ δ δ δ · · · · · · · · · ·
```

Fig. 4.5 Space–time development of a doxaton lattice, started in configuration $\kappa \cdots \kappa\delta\kappa \cdots \kappa$. Norm combination $(\kappa > \delta) \wedge (\mu > \delta) \wedge (\delta < \iota) \wedge (\mu > \kappa)$ is applied to the lattice.

norm

$$(\kappa > \delta) \wedge (\mu > \delta) \wedge (\delta < \iota) \wedge (\mu > \kappa)$$

or norm

$$(\kappa < \delta) \wedge (\mu < \kappa)$$

is applied (Figs. 4.5 and 4.6). The diffusion wave front is marked by the

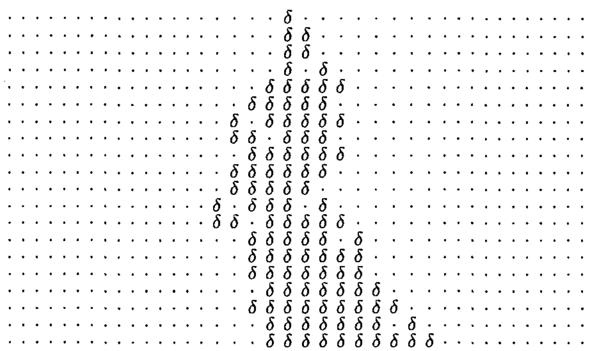

Fig. 4.6 Space–time development of a doxaton lattice, started in the configuration $\kappa \cdots \kappa\delta\kappa \cdots \kappa$. The combination $(\kappa < \delta) \wedge (\mu < \kappa)$ of norms is applied.

combination of δ- and μ-states in the first case (Fig. 4.5) and it is uniform in the second case (Fig. 4.6). The random diffusion of the disordered mixture

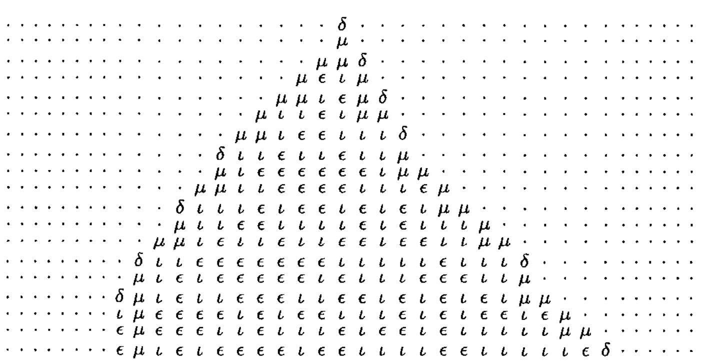

Fig. 4.7 Space–time development of a doxaton lattice, started in the configuration $\kappa \cdots \kappa\delta\kappa \cdots \kappa$; the norms $(\kappa > \delta) \wedge (\epsilon < \iota) \wedge (\mu > \delta) \wedge (\delta < \iota) \wedge (\mu > \kappa)$ are employed.

of δ-and ι-states is typical in the situation when the norms

$$(\kappa > \delta) \wedge (\epsilon < \iota) \wedge (\mu > \delta) \wedge (\delta < \iota) \wedge (\mu > \kappa)$$

are involved (Fig. 4.7). In this case the wave fronts consist of δ-, ι-, μ- and ϵ-states.

4.10.3 *Delusional singleton*

Let initially all doxatons of the lattice take the state ι except for a single doxaton x that takes the state ϵ, i.e. the initial configuration is $\iota\cdots\iota\epsilon\iota\cdots\iota$. Then the singleton remains in the state ϵ forever. The state ϵ spreads on the lattice: $y^t=\epsilon$ or $y^t=\iota$ if $t\geq|y-x|$, and $y^t=\iota$ if $t<|y-x|$. Thus, the triangle of ϵ-states is formed in the space–time configuration of the doxaton lattice. The internal morphology of the triangle can be of two types.

If $N=(\epsilon>\iota)$ then all doxatons inside the triangle take the state ϵ (Fig. 4.8a). The states ϵ and ι form a Pascal-like triangle (Fig. 4.8a) if $N=(\epsilon<\iota)$. The correctness can be easily checked by identifying the state ϵ with arithmetical 0 and the state ι with 1. Then, taking into account the normative constraint, we find that doxaton x's state-transition function can be represented as follows:

$$x^t=\begin{cases} y^t\cdot x^t\cdot z^t \quad \text{if} \quad N=(\epsilon>\iota), \\ (y^t+x^t+z^t) \mod 2 \quad \text{if} \quad N=(\epsilon<\iota). \end{cases}$$

Three of five possible scenarios of development of the doxaton lattice from the initial configuration $\kappa\cdots\kappa\epsilon\kappa\cdots\kappa$ are quite trivial ones. The doxaton lattice takes (before the fourth step of the development) one of three stationary configurations:

$$\kappa\cdots\kappa\epsilon\kappa\cdots\kappa \quad \text{if} \quad N=(\kappa>\delta)\vee(\kappa<\delta)\wedge(\mu<\kappa),$$

$$\delta\cdots\delta\mu\iota\mu\delta\cdots\delta \quad \text{if} \quad N=(\kappa<\delta)\wedge(\mu>\delta)\wedge(\delta<\iota)\wedge(\mu>\kappa),$$

$$\delta\cdots\delta\iota\delta\cdots\delta \quad \text{if} \quad N=(\kappa<\delta)\wedge(\mu<\delta)\wedge(\delta>\iota)\wedge(\mu>\kappa).$$

Two types of ϵ-state triangles may be produced from the initial configuration $\kappa\cdots\kappa\epsilon\kappa\cdots\kappa$. The "solid" triangle filled with ϵ-states is generated in the space–time configuration (Fig. 4.9a) of the doxaton lattice if

$$N=(\kappa<\delta)\wedge(\epsilon>\iota)\wedge(\mu>\kappa)\wedge(\delta<\iota).$$

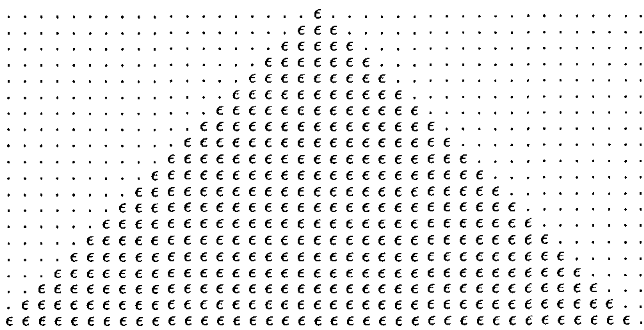

(a)

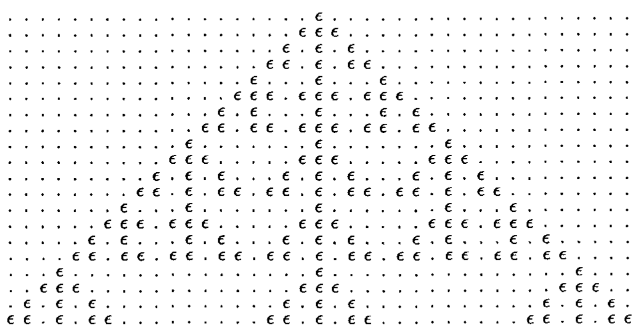

(b)

Fig. 4.8 Space–time configuration of a doxaton lattice, which evolves from the initial configuration $\iota \cdots \iota\epsilon\iota \cdots \iota$. The states ι are shown by dots. (a) $N = (\epsilon > \iota)$, (b) $N = (\epsilon < \iota)$.

The Pascal-like triangle (Fig. 4.9b) emerges when

$$N = (\kappa < \delta) \wedge (\epsilon < \iota) \wedge (\delta < \iota) \wedge (\mu > \kappa).$$

If doxaton x starts its development in the state ϵ and all other doxatons of the lattice take the state μ, then the doxaton x takes the state ι and will be in this state forever, whereas other doxatons will take the states of either δ or ι. Namely, the initial configuration $\mu \cdots \mu\epsilon\mu \cdots \mu$ is transformed to one of three stationary configurations:

$$\delta \cdots \delta\iota\delta \cdots \delta \quad \text{if} \quad N = (\delta > \iota),$$

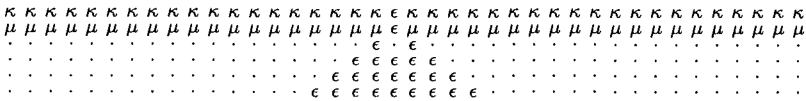

(a)

(b)

Fig. 4.9 Space–time configuration of the doxaton lattice, which starts its development in the initial configuration $\kappa \cdots \kappa\epsilon\kappa \cdots \kappa$. (a) $N = (\kappa < \delta) \wedge (\epsilon > \iota) \wedge (\mu > \kappa) \wedge (\delta < \iota)$, (b) $N = (\kappa < \delta) \wedge (\epsilon < \iota) \wedge (\delta < \iota) \wedge (\mu > \kappa)$. The states ι are shown by dots.

$$\iota \cdots \iota \quad \text{if} \quad N = (\delta < \iota) \wedge (\mu > \delta),$$

$$\iota \cdots \iota\delta\iota\delta\iota \cdots \iota \quad \text{if} \quad N = (\delta < \iota) \wedge (\mu < \delta).$$

Most of the possible outcomes of the initial configuration $\delta \cdots \delta\epsilon\delta \cdots \delta$ are quite trivial. Singleton x, which takes the state ϵ at the beginning of development, finishes its development in state ι or ϵ. Namely, for the norm $N = (\mu > \delta) \wedge (\mu > \kappa)$ the initial configuration $\delta \cdots \delta\epsilon\delta \cdots \delta$ is changed into the stationary configuration $\delta \cdots \delta\mu\epsilon\mu\delta \cdots \delta$, where all doxatons but the singleton x and its immediate neighbors are in state δ; the neighbors of the singleton take state μ. If the norm

$$N = (\mu < \delta) \wedge (\mu > \kappa) \vee (\kappa < \delta) \wedge (\epsilon < \iota)$$

is applied to the composition of doxastic states, all doxatons but singleton x take state δ after some initial period of perturbation; the singleton takes state ι and keeps this state forever. For the norms

$$(\kappa > \delta) \wedge (\epsilon > \iota) \wedge (\mu < \kappa)$$

and

$$(\kappa > \delta) \wedge (\epsilon < \iota) \wedge (\mu < \kappa)$$

the states κ are generated at the beginning of development because

$$(\delta \odot_{\mu<\kappa} \epsilon) \odot_{\mu<\kappa} \epsilon = (\delta \odot_{\mu<\kappa} \delta) \odot_{\mu<\kappa} \epsilon = \kappa;$$

the singleton itself remains in the state ϵ in the first case and it takes the state ι in the second case. The triangle filled with κ-states is formed; for any $y \in \mathbb{L}$, $y^t = \kappa$ if $y \neq x$ and $|y - x| \leq t$.

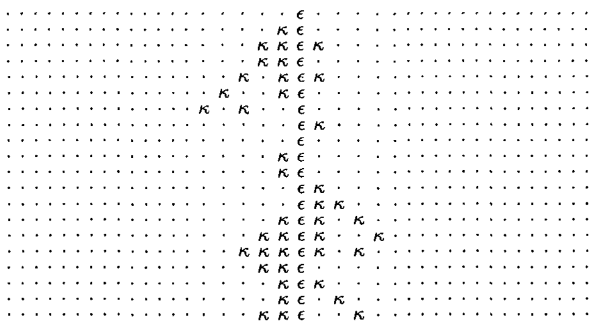

Fig. 4.10 Tree of κ-states emerging in the space–time configuration of a doxaton lattice. The initial configuration is $\delta \cdots \delta\epsilon\delta \cdots \delta$. The combination of the norms applied is $(\kappa < \delta) \wedge (\epsilon > \iota) \wedge (\mu < \kappa)$. Doxatons in state δ are shown by dots. Branches of the tree terminate at first steps of development; however, an ϵ-stem surrounded by an irregular shell of κ-states persists.

Application of the norm

$$(\kappa < \delta) \wedge (\epsilon > \iota) \wedge (\mu < \kappa)$$

to the local transitions of doxatons causes trees of κ-states to emerge (Fig. 4.10).

4.10.4 *Misbelieving singleton*

The configuration $\iota \cdots \iota\mu\iota \cdots \iota$ is a stationary configuration in the development of a doxaton lattice for any combination N of the norms.

The initial configuration $\delta \cdots \delta\mu\delta \cdots \delta$ is transformed to the stationary configuration $\delta \cdots \delta\mu\delta \cdots \delta$, if $N = (\mu > \delta)$, or to the stationary configuration $\delta \cdots \delta$, if $N = (\mu > \delta)$.

The space–time development of the doxaton lattice from the initial configuration $\epsilon \cdots \epsilon\mu\epsilon \cdots \epsilon$ does not show any particularly interesting details. All those doxatons of the lattice that are not neighbors of the singleton, which starts its development in the state μ, remain in the state ϵ or take either the state ϵ or the state ι. Five possible scenarios can develop depending on the combination of norms.

- The singleton remains in the state μ, its immediate neighbors take the states ϵ and ι at random and all other doxatons stay in the state ϵ if the norms $(\epsilon > \iota) \wedge (\mu > \delta)$ are applied.
- The singleton takes the states δ and μ at random, its closest neighbors randomly choose between the states ϵ and ι and the rest of the lattice's nodes remain in the state ϵ for the combination $(\epsilon > \iota) \wedge (\mu < \delta) \wedge (\mu > \kappa)$ of norms. The development becomes deterministic when the configuration $\epsilon \cdots \epsilon\iota\delta\iota\epsilon \cdots \epsilon$ emerges; then immediate neighbors of the singleton take the state ϵ and the singleton itself remains in the state δ. The emerging configuration $\epsilon \cdots \epsilon\delta\epsilon \cdots \epsilon$ remains stationary (Fig. 4.11).

$$
\begin{array}{ccccccccccc}
\cdot & \cdot & \cdot & \cdot & \cdot & \mu & \cdot & \cdot & \cdot & \cdot & \cdot \\
\cdot & \cdot & \cdot & \cdot & \iota & \mu & \iota & \cdot & \cdot & \cdot & \cdot \\
\cdot & \cdot & \cdot & \cdot & \iota & \mu & \iota & \cdot & \cdot & \cdot & \cdot \\
\cdot & \cdot & \cdot & \cdot & \iota & \mu & \cdot & \cdot & \cdot & \cdot & \cdot \\
\cdot & \cdot & \cdot & \cdot & \cdot & \delta & \iota & \cdot & \cdot & \cdot & \cdot \\
\cdot & \cdot & \cdot & \cdot & \cdot & \mu & \cdot & \cdot & \cdot & \cdot & \cdot \\
\cdot & \cdot & \cdot & \cdot & \cdot & \mu & \cdot & \cdot & \cdot & \cdot & \cdot \\
\cdot & \cdot & \cdot & \cdot & \cdot & \mu & \iota & \cdot & \cdot & \cdot & \cdot \\
\cdot & \cdot & \cdot & \cdot & \iota & \delta & \cdot & \cdot & \cdot & \cdot & \cdot \\
\cdot & \cdot & \cdot & \cdot & \cdot & \mu & \cdot & \cdot & \cdot & \cdot & \cdot \\
\cdot & \cdot & \cdot & \cdot & \cdot & \mu & \cdot & \cdot & \cdot & \cdot & \cdot \\
\cdot & \cdot & \cdot & \cdot & \iota & \mu & \iota & \cdot & \cdot & \cdot & \cdot \\
\cdot & \cdot & \cdot & \cdot & \cdot & \mu & \iota & \cdot & \cdot & \cdot & \cdot \\
\cdot & \cdot & \cdot & \cdot & \iota & \delta & \iota & \cdot & \cdot & \cdot & \cdot \\
\cdot & \cdot & \cdot & \cdot & \cdot & \delta & \cdot & \cdot & \cdot & \cdot & \cdot \\
\cdot & \cdot & \cdot & \cdot & \cdot & \delta & \cdot & \cdot & \cdot & \cdot & \cdot \\
\cdot & \cdot & \cdot & \cdot & \cdot & \delta & \cdot & \cdot & \cdot & \cdot & \cdot \\
\cdot & \cdot & \cdot & \cdot & \cdot & \delta & \cdot & \cdot & \cdot & \cdot & \cdot \\
\cdot & \cdot & \cdot & \cdot & \cdot & \delta & \cdot & \cdot & \cdot & \cdot & \cdot
\end{array}
$$

Fig. 4.11 "Stabilization" of the doxaton lattice. The lattice starts its development in the configuration $\epsilon \cdots \epsilon\mu\epsilon \cdots \epsilon$. The norms $(\epsilon > \iota) \wedge (\mu < \delta) \wedge (\mu > \kappa)$ are applied. The state ϵ is shown by dots.

- For the combination of norms $(\epsilon > \iota) \wedge (\mu < \delta) \wedge (\mu < \kappa)$ the doxaton lattice evolves towards the stationary configuration $\epsilon \cdots \epsilon\kappa\epsilon \cdots \epsilon$, where the singleton has the state κ and all other doxatons remain in the state ϵ.
- If the norms $(\epsilon < \iota) \wedge (\mu < \delta) \wedge (\mu < \kappa)$ are applied the singleton takes the state κ and does not change its state after that. Other doxatons take the states ϵ and ι in such a manner that a Pascal-triangle-like

structure is formed.

- For all other combinations of norms the singleton remains in the state μ and a triangle disorderly bounded by ι-states and filled with ϵ- and ι-states emerges in the space–time configuration.

The initial configuration $\kappa \cdots \kappa\mu\kappa \cdots \kappa$ is transformed to one of stationary configurations $\kappa \cdots \kappa$, $\delta \cdots \delta$ or $\iota \cdots \delta \cdots \delta\iota \cdots \iota$, usually after a few steps of development, if norms

$$(\kappa > \delta) \wedge (\mu < \delta) \wedge (\mu < \kappa),$$

$$(\kappa < \delta) \wedge (\delta > \iota) \wedge (\mu > \kappa)$$

or

$$(\kappa < \delta) \wedge (\delta < \iota) \wedge (\mu > \kappa)$$

are applied, respectively. The singleton in state μ is a source of random diffusion of states δ when either norm

$$(\kappa < \delta) \wedge (\mu > \delta) \wedge (\mu < \kappa)$$

or norm

$$(\kappa < \delta) \wedge (\mu < \delta) \wedge (\mu < \kappa)$$

is employed. In the first case the singleton keeps its initial state μ

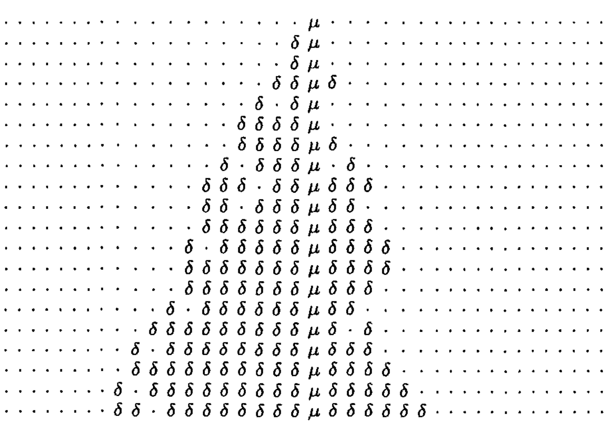

Fig. 4.12 Space–time development of a doxaton lattice from the initial configuration $\kappa \cdots \kappa\mu\kappa \cdots \kappa$. Norms $(\kappa < \delta) \wedge (\mu > \delta) \wedge (\mu < \kappa)$ are applied. State κ is shown by dots.

(Fig. 4.12); in the second case the singleton changes from state μ to state

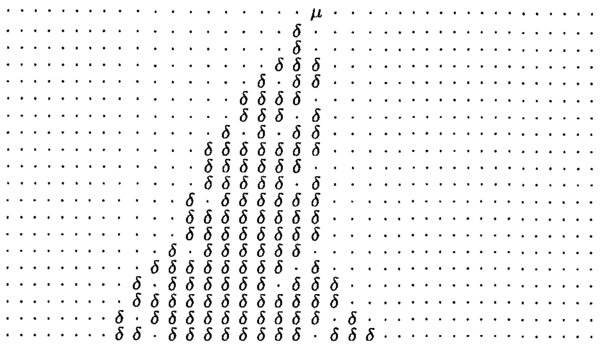

Fig. 4.13 Space–time development of a doxaton lattice from the initial configuration $\kappa \cdots \kappa\mu\kappa \cdots \kappa$. Norms $(\kappa < \delta) \wedge (\mu < \delta) \wedge (\mu < \kappa)$ are applied. State κ is shown by dots.

δ or κ (Fig. 4.13). State μ generates waves of diffusion of δ-states if norms

$$(\kappa > \delta) \wedge (\delta > \iota) \wedge (\mu > \kappa)$$

are applied to the composition of doxastic states. A wave front has an

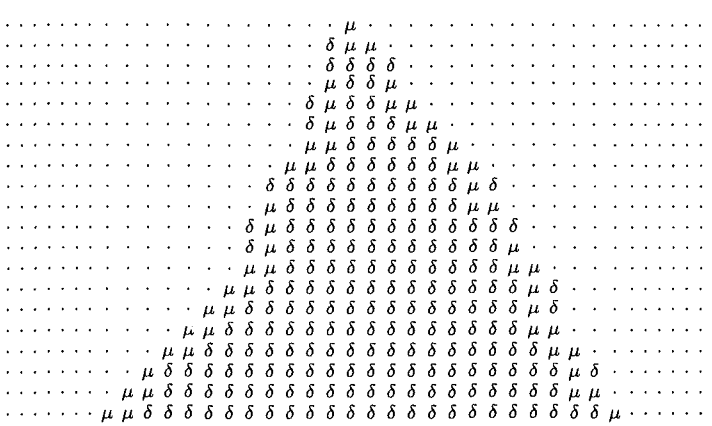

Fig. 4.14 Space–time development of a doxaton lattice developing from the initial configuration $\kappa \cdots \kappa\mu\kappa \cdots \kappa$. Norms $(\kappa < \delta) \wedge (\mu < \delta) \wedge (\mu < \kappa)$ are applied. State κ is shown by dots.

irregular shape and doxatons being at boundaries between δ-filled and κ-

filled domains choose between the states μ and δ at random (Fig. 4.14). A singleton remains in the state μ for norms

$$(\kappa < \delta) \wedge (\mu > \delta) \wedge (\mu < \kappa)$$

and

$$(\kappa > \delta) \wedge (\mu < \kappa) \wedge (\mu > \delta).$$

However, when the last combination of norms is involved, two immediate neighbors of the singleton take states κ and δ at random and all other doxatons of the lattice take state κ. That is, the configuration

$$\kappa \cdots \kappa\alpha\mu\beta\kappa \cdots \kappa,$$

where α and β equal κ or δ equiprobably, emerges in the development.

For other combinations of norms, the space–time configurations of the doxaton lattice are strictly determined by events that happen at the beginning of development, namely by the order in which neighbors of the singleton compose the doxastic state of the singleton with their doxastic states and states of their neighbors. A few examples of such developments are shown in Fig. 4.15.

4.10.5 *Singleton that knows*

For any combination of norms, the singleton x in the κ-state in the lattice of the ι-states (initial configuration $\iota \cdots \iota\kappa\iota \cdots \iota$) generates diffusion waves of ϵ-states. Therefore, a typical triangle bounded by ϵ-states is formed: for any $y \in \mathbb{L}$ we have $y^t = \iota$ if $t < |y - x|$, $y^t = \epsilon$ if $t = |y - x|$. The development of the singleton x goes by one of the following scenarios:

- the singleton remains in the state κ forever if the norms are

$$N_1 = (\epsilon > \iota) \wedge ((\kappa > \delta) \vee (\kappa < \delta) \wedge (\mu < \kappa))$$

or

$$N_2 = ((\epsilon < \iota) \wedge ((\kappa > \delta) \vee (\kappa < \delta) \wedge (\mu < \kappa)),$$

- the singleton implements the transitions

$$\kappa \to \kappa \to \mu \to \mu \to \delta$$

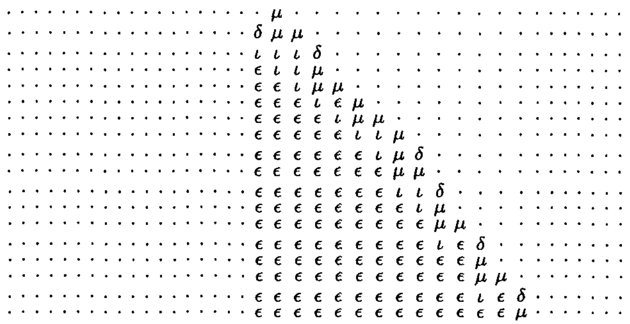

(a)

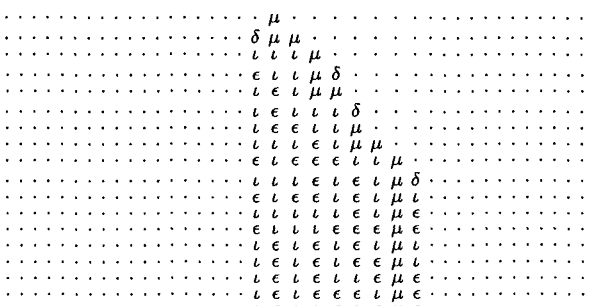

(b)

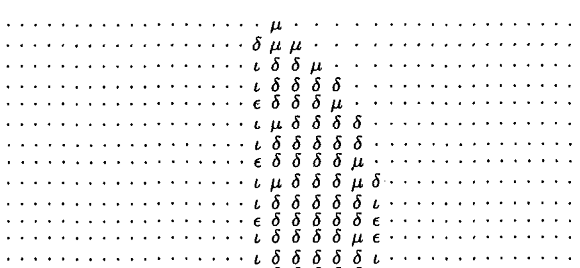

(c)

Fig. 4.15 Space–time development of a doxaton lattice from the configuration $\kappa \cdots \kappa\mu\kappa \cdots \kappa$. The following combinations of norms are employed: (a) $(\kappa > \delta) \wedge (\epsilon > \iota) \wedge (\mu > \delta) \wedge (\delta < \iota) \wedge (\mu > \kappa)$, (b) $(\kappa > \delta) \wedge (\mu > \delta) \wedge (\delta < \iota) \wedge (\epsilon < \iota) \wedge (\mu > \kappa)$ and (c) $(\kappa > \delta) \wedge (\mu < \delta) \wedge (\delta < \iota) \wedge (\mu > \kappa)$.

and stays in the state δ after that if the state transitions are governed by the norms

$$N_3 = ((\kappa < \delta) \wedge (\epsilon > \iota) \wedge (\mu < \delta) \wedge (\mu > \kappa),$$

- the singleton changes its state to μ and does not change this state any more if

  $$N_4 = (\kappa < \delta) \wedge (\epsilon > \iota) \wedge (\mu > \delta) \wedge (\mu < \kappa)$$

  or

  $$N_5 = (\kappa < \delta) \wedge (\epsilon < \iota) \wedge (\mu > \delta) \wedge (\mu > \kappa),$$

- the singleton takes either state μ or state δ at random during the development if

  $$N_6 = (\kappa < \delta) \wedge (\epsilon < \iota) \wedge (\mu < \delta) \wedge (\mu > \kappa).$$

The triangle in the space–time configuration is filled with ϵ-states for the norms N_1, N_3 and N_4.

```
· · · · · · · · · · · · · · · · · · · κ · · · · · · · · · · · · · · · · · · · ·
· · · · · · · · · · · · · · · · · · ϵ κ ϵ · · · · · · · · · · · · · · · · · · ·
· · · · · · · · · · · · · · · · · ϵ ϵ μ ϵ ϵ · · · · · · · · · · · · · · · · · ·
· · · · · · · · · · · · · · · · ϵ ϵ ϵ μ ϵ ϵ ϵ · · · · · · · · · · · · · · · · ·
· · · · · · · · · · · · · · · ϵ ϵ ϵ · μ ϵ ϵ ϵ ϵ · · · · · · · · · · · · · · · ·
· · · · · · · · · · · · · · ϵ ϵ ϵ ϵ · μ · ϵ ϵ ϵ ϵ · · · · · · · · · · · · · · ·
· · · · · · · · · · · · · ϵ ϵ ϵ ϵ ϵ · μ ϵ ϵ ϵ ϵ ϵ ϵ · · · · · · · · · · · · · ·
· · · · · · · · · · · · ϵ ϵ ϵ ϵ ϵ ϵ · μ ϵ ϵ ϵ ϵ ϵ ϵ ϵ · · · · · · · · · · · · ·
· · · · · · · · · · · ϵ ϵ ϵ ϵ ϵ ϵ ϵ · μ · ϵ ϵ ϵ ϵ ϵ ϵ ϵ · · · · · · · · · · · ·
· · · · · · · · · · ϵ ϵ ϵ ϵ ϵ ϵ ϵ ϵ ϵ μ · ϵ ϵ ϵ ϵ ϵ ϵ ϵ ϵ · · · · · · · · · · ·
· · · · · · · · · ϵ ϵ ϵ ϵ ϵ ϵ ϵ ϵ ϵ · μ · ϵ ϵ ϵ ϵ ϵ ϵ ϵ ϵ ϵ · · · · · · · · · ·
· · · · · · · · ϵ ϵ ϵ ϵ ϵ ϵ ϵ ϵ ϵ ϵ ϵ μ ϵ ϵ ϵ ϵ ϵ ϵ ϵ ϵ ϵ ϵ ϵ · · · · · · · · ·
· · · · · · · ϵ ϵ ϵ ϵ ϵ ϵ ϵ ϵ ϵ ϵ ϵ · μ · ϵ ϵ ϵ ϵ ϵ ϵ ϵ ϵ ϵ ϵ ϵ · · · · · · · ·
· · · · · · ϵ ϵ ϵ ϵ ϵ ϵ ϵ ϵ ϵ ϵ ϵ ϵ · μ ϵ ϵ ϵ ϵ ϵ ϵ ϵ ϵ ϵ ϵ ϵ ϵ ϵ · · · · · · ·
· · · · · ϵ ϵ ϵ ϵ ϵ ϵ ϵ ϵ ϵ ϵ ϵ ϵ ϵ ϵ μ ϵ ϵ ϵ ϵ ϵ ϵ ϵ ϵ ϵ ϵ ϵ ϵ ϵ ϵ · · · · · ·
· · · · ϵ ϵ ϵ ϵ ϵ ϵ ϵ ϵ ϵ ϵ ϵ ϵ ϵ ϵ · μ · ϵ ϵ ϵ ϵ ϵ ϵ ϵ ϵ ϵ ϵ ϵ ϵ ϵ ϵ · · · · ·
· · · ϵ ϵ ϵ ϵ ϵ ϵ ϵ ϵ ϵ ϵ ϵ ϵ ϵ ϵ ϵ ϵ μ · ϵ ϵ ϵ ϵ ϵ ϵ ϵ ϵ ϵ ϵ ϵ ϵ ϵ ϵ ϵ · · · ·
· · ϵ ϵ ϵ ϵ ϵ ϵ ϵ ϵ ϵ ϵ ϵ ϵ ϵ ϵ ϵ ϵ ϵ μ · ϵ ϵ ϵ ϵ ϵ ϵ ϵ ϵ ϵ ϵ ϵ ϵ ϵ ϵ ϵ ϵ · · ·
· ϵ ϵ ϵ ϵ ϵ ϵ ϵ ϵ ϵ ϵ ϵ ϵ ϵ ϵ ϵ ϵ ϵ ϵ μ ϵ ϵ ϵ ϵ ϵ ϵ ϵ ϵ ϵ ϵ ϵ ϵ ϵ ϵ ϵ ϵ ϵ ϵ · ·
ϵ ϵ ϵ ϵ ϵ ϵ ϵ ϵ ϵ ϵ ϵ ϵ ϵ ϵ ϵ ϵ ϵ ϵ · μ ϵ ϵ ϵ ϵ ϵ ϵ ϵ ϵ ϵ ϵ ϵ ϵ ϵ ϵ ϵ ϵ ϵ ϵ ϵ ·
```

Fig. 4.16 Space–time development of a doxaton lattice from the initial configuration $\iota \cdots \iota\kappa\iota \cdots \iota$; norms $N_4 = (\kappa < \delta) \wedge (\epsilon > \iota) \wedge (\mu > \delta) \wedge (\mu < \kappa))$ are applied. States ι are shown by dots.

When norm N_4 is applied to the lattice, closest neighbors of the singleton take either state ι or state ϵ at random (Fig. 4.16) due to the random composition of neighbor states in the transition rule: $(\epsilon \odot_{N_4} \mu) \odot_{N_4} \epsilon = \epsilon$ and $(\epsilon \odot_{N_4} \epsilon) \odot_{N_4} \mu = \iota$. Doxatons inside the triangle take their states as follows:

- the triangle is filled with ϵ-states: for any y, $y^t = \epsilon$ if $|y - x| < t$ and N_1, N_3 and N_4 ($|y - x| > 1$) (see e.g. Fig. 4.16),
- the distribution of ϵ- and ι-states inside the triangle is similar to a Pascal triangle,

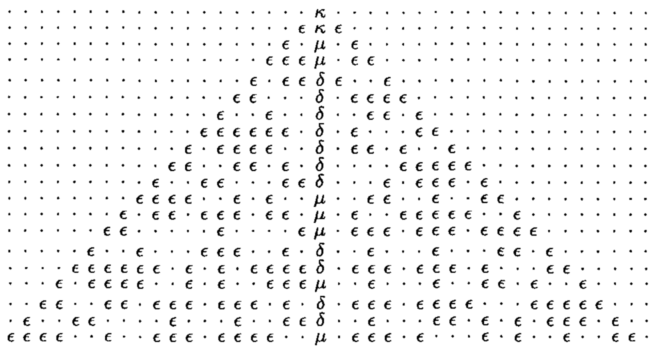

Fig. 4.17 Space–time development of a doxaton lattice from the initial configuration $\iota \cdots \iota\kappa\iota \cdots \iota$; norms $N_6 = (\kappa < \delta) \wedge (\epsilon < \iota) \wedge (\mu < \delta) \wedge (\mu > \kappa)$ are applied. States ι are shown by dots.

- the distribution of ϵ- and ι-states inside the triangle is randomized (see e.g. Fig. 4.17).

If singleton x starts its development in state κ in a lattice of doxatons in state δ (initial configuration $\delta \cdots \delta\kappa\delta \cdots \delta$), the following possible scenarios of lattice development may unfold. If norm $(\kappa > \delta) \wedge (\mu < \kappa)$ is applied then state κ diffuses on the lattice; as a result all doxatons of the lattice take state κ. Two immediate neighbors of the singleton x take the state μ at the first step of development and remain in this state forever if $(\mu > \kappa) \wedge (\mu > \delta)$; in this case, the singleton takes the state δ and does not change it. Therefore, we obtain the stationary configuration $\delta \cdots \delta\mu\delta\mu\delta \cdots \delta$. For all other combinations of norms the lattice of doxatons takes, after a few time steps, the stationary state $\delta \cdots \delta$. In some cases, for example for the

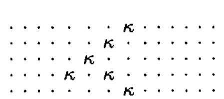

Fig. 4.18 Example of diffusion of state κ. The states δ are shown by dots.

norms

$$(\kappa < \delta) \wedge (\epsilon < \iota) \wedge (\mu < \delta) \wedge (\delta < \iota) \wedge (\mu < \kappa),$$

a small tree of κ-states emerges but then quickly disappears (Fig. 4.18).

Let a doxaton lattice start its development in the configuration $\epsilon \cdots \epsilon\kappa\epsilon \cdots \epsilon$. Then the lattice takes, after a few steps of the development, the stationary configuration $\epsilon \cdots \epsilon\delta\epsilon \cdots \epsilon$ or $\epsilon \cdots \epsilon\kappa\epsilon \cdots \epsilon$ if combinations of norms

$$(\kappa < \delta) \wedge (\epsilon > \iota) \wedge (\mu < \delta) \wedge (\mu > \kappa)$$

or

$$(\kappa > \delta) \vee ((\kappa < \delta) \wedge (\mu < \kappa))$$

are applied, respectively. In the situation when norms

$$(\kappa < \delta) \wedge (\epsilon > \iota) \wedge (\mu > \delta) \wedge (\mu > \kappa)$$

are applied the singleton takes the state μ (and stays in this state forever); the immediate neighbors of the singleton take the states ϵ and ι, chosen at random; the rest of the doxatons remain in the state ϵ. The singleton

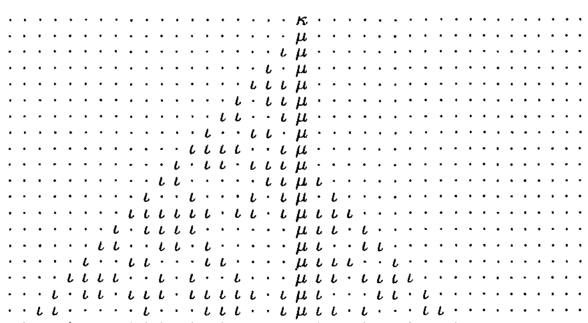

Fig. 4.19 Space–time development of a doxaton lattice normalized by $(\kappa < \delta) \wedge (\epsilon < \iota) \wedge (\mu > \delta) \wedge (\mu > \kappa)$. The lattice starts its development in state $\epsilon \cdots \epsilon\kappa\epsilon \cdots \epsilon$. States ϵ are shown by dots.

takes state μ and generates waves of ι-states (Fig. 4.19) if doxatons obey the norms

$$(\kappa < \delta) \wedge (\epsilon < \iota) \wedge (\mu > \delta) \wedge (\mu > \kappa).$$

The remaining combination of norms, namely

$$(\kappa < \delta) \wedge (\epsilon < \iota) \wedge (\mu < \delta) \wedge (\mu > \kappa),$$

enforces doxatons to choose between the states δ and μ irregularly, and causes state ι to spread from the singleton to other doxatons. The space–time structure of the ι-state triangle is similar to that shown in Fig. 4.19.

The development from the initial configuration $\mu \cdots \mu\kappa\mu \cdots \mu$ is extremely sensitive to norms applied to the doxastic composition. We found at least 14 different ways of the development; we consider here just a few basic ones.

The doxaton lattice takes the stationary configuration $\delta \cdots \delta$ after a few steps of its development if the following combination of norms is applied:

$$(\kappa > \delta) \wedge (\mu > \delta) \wedge (\delta < \iota) \wedge (\mu > \kappa) \wedge (\kappa < \delta) \wedge \\ \wedge((\mu > \delta) \wedge (\delta > \iota) \wedge (\mu < \kappa) \vee (\mu < \delta) \wedge (\delta < \iota)).$$

If doxatons obey the norms

$$(\kappa > \delta) \wedge (\epsilon > \iota) \wedge (\delta < \iota) \wedge (\mu < \kappa)$$

the singleton x, which starts its development in the state κ, keeps its state; some of the singleton's neighbors can take the state κ as well. Since the beginning of development the state ϵ diffuses on the doxaton lattice. Therefore, a triangle filled with ϵ-states is formed: for every y we have $y^t = \epsilon$ if $y \neq x$ and $|y - x| \leq t$. For norms

$$(\kappa > \delta) \wedge (\delta > \iota) \wedge (\mu < \kappa)$$

all doxatons, apart from the singleton x, take the state δ during the first steps of development. They remain in their states. However, state κ diffuses from the singleton. A triangle of κ-states (for every y we have $y^t = \kappa$ if $|y - x| \leq t$) emerges in the space–time configuration of the doxaton lattice. In a finite lattice every doxaton takes state κ eventually. For the norm combination

$$(\mu > \delta) \wedge (\delta > \iota) \wedge (\mu > \kappa)$$

the development can take two routes: the initial configuration $\mu \cdots \mu\kappa\mu \cdots \mu$ is transformed to the stationary configuration $\delta \cdots \delta\mu\delta \cdots \delta$ or $\delta \cdots \delta\mu\delta\mu\delta \cdots \delta$. In the first case the singleton x takes state μ and remains in this state. In the second case the singleton takes state δ and its immediate neighbors take state μ. All other doxatons of the lattice remain

in state δ. State ϵ diffuses from the singleton x if doxatons are normalized by either

$$(\kappa < \delta) \wedge (\epsilon > \iota) \wedge (\mu < \delta) \wedge (\delta < \iota)$$

or

$$(\kappa < \delta) \wedge (\epsilon < \iota) \wedge (\mu > \delta) \wedge (\delta < \iota) \wedge (\mu > \kappa).$$

In both cases all doxatons but the singleton take the state ι at the first step of the development. In the first case the singleton continues its development in state δ. In the second case the singleton x takes state μ. For all other combinations of norms the singleton takes either state δ or state μ, or chooses between states κ and δ or between μ and δ at random. State ϵ diffuses on the lattice of doxatons, which takes state ι at the first step of the development. A triangle, bounded by the state ϵ, is formed in the space–time configuration of the doxaton lattice. Any doxaton y inside this triangle $|y - x| \leq t$ takes states ϵ and ι at random.

4.11 Evolving from the random configuration

In this section we discuss results of computer experiments with one-dimensional lattices of doxatons. In every trial the collective of doxatons starts its development in a random configuration, i.e. initially every doxaton takes one of the doxastic states of $\mathbb{D}$ with probability $\frac{1}{5}$. We experimented with a lattice of 300 doxatons with periodic boundary conditions and evolved the lattices in 2000 time steps. Results are averaged in 100 trials for every combination N of the norms. At the beginning of the development all doxastic states are represented equally; hence, during the course of the development not all of them survive.

States μ, δ and ι become extinct in the development of a doxaton lattice if $\kappa > \delta$, $\epsilon > \iota$, $\mu > \delta$ and $\mu < \kappa$.

In these conditions, states κ and ϵ are represented in the final configurations of doxaton lattices with probabilities 0.6 and 0.4, respectively.

States μ and δ become extinct in the development of doxaton lattices if $\kappa > \delta$, $\epsilon < \iota$, $\mu < \delta$ and $\mu < \kappa$.

In these conditions, states κ, ϵ and ι can be found in the final configurations of doxaton lattices with probabilities 0.55, 0.25 and 0.2, respectively.

Moreover, we can build a correspondence between norms applied to doxaton collectives and states which become extinct in the development of normalized doxaton lattices. The correspondence between the norms and extinction of doxastic states is shown below:

N	Extinct state
$(\kappa < \delta) \wedge (\kappa < \mu)$	κ
$(\kappa < \delta) \wedge (\epsilon < \iota) \wedge (\mu > \kappa)$	ϵ
$(\epsilon > \iota) \wedge (\mu < \delta) \wedge (\mu < \kappa)$	ι
$(\mu < \kappa) \wedge (\mu < \delta)$	μ
$(\kappa > \delta) \wedge (\mu < \delta) \wedge (\mu < \kappa)$	δ

We say that state *a dominates in the development of a doxaton lattice* if it has maximal probability of occurrence in the final configurations of doxaton collectives.

State μ never dominates. It becomes extinct in the development of normalized doxaton collectives for any combination N of norms.

The correspondence between the norms and dominating doxastic states is shown below:

N	Dominate
$(\kappa > \delta) \wedge (\mu < \kappa) \wedge$ $(\epsilon > \iota) \wedge ((\mu > \delta) \wedge (\delta > \iota) \vee (\mu < \delta)) \vee$ $(\kappa > \mu)((\kappa > \delta) \wedge (\epsilon < \iota) \vee (\kappa < \delta) \wedge (\epsilon > \iota) \wedge (\delta > \mu))$	κ
$(\epsilon > \iota) \wedge$ $((\mu > \delta) \wedge (\delta < \iota) \vee$ $(\mu < \delta) \wedge (\delta < \iota) \wedge (\mu > \kappa) \vee$ $(\mu > \delta) \wedge (\delta > \iota) \wedge (\mu < \kappa))$	ϵ
$(\kappa > \delta) \wedge (\epsilon > \iota) \wedge (\mu > \delta) \wedge (\delta > \iota) \wedge (\mu > \kappa) \vee$ $(\kappa > \delta) \wedge (\mu < \delta) \wedge (\delta > \iota) \wedge (\mu > \kappa) \vee$ $(\kappa < \delta) \wedge (\epsilon > \iota) \wedge (\mu < \delta) \wedge (\mu > \kappa) \vee$ $(\kappa < \delta) \wedge (\epsilon < \iota) \wedge (\mu < \delta) \wedge (\delta > \iota) \vee$ $(\kappa < \delta) \wedge (\epsilon < \iota) \wedge$ $(\mu < \kappa) \wedge ((\mu > \delta) \wedge (\delta > \iota) \vee (\mu < \delta) \wedge (\delta < \iota))$	δ
$(\kappa > \delta) \wedge (\epsilon < \iota) \wedge (\mu > \kappa) \vee$ $(\kappa < \delta) \wedge (\epsilon < \iota) \wedge$ $((\mu > \kappa) \vee (\mu > \delta) \wedge (\delta < \iota) \wedge$ $(\mu < \kappa)) \vee (\mu > \kappa) \wedge ((\kappa < \delta)$ $\wedge (\epsilon > \iota) \wedge (\mu > \delta) \wedge (\delta > \iota))$ $\vee (\kappa > \delta) \wedge (\epsilon < \iota) \wedge (\mu < \delta) \wedge (\delta < \iota))$	ι

4.12 Consequences of normalization

In this chapter we looked at doxastic developments in collectives of automaton-like agents constrained by norms, i.e. reductions of possible outcomes of state updates aimed to achieve deterministic transitions. We provide a range of formal findings and phenomena of space–time and global behavior of normalized doxatons; finally, we will try to give some informal interpretations of them.

We call a doxastic state passive if agents in this state do not influence the development of their neighbors. A state is intrinsically passive if an agent, isolated from other agents, does not change its state when reflecting about its doxastic inner.

- Ignorance is passive in any world.
- Doubt becomes passive when knowledge and misbelief dominate doubt and delusion dominates ignorance.
- All doxastic states but misbelief are intrinsically passive when knowledge dominates doubt and delusion dominates ignorance.
- Knowledge, doubt and ignorance are intrinsically passive only when knowledge dominates doubt and ignorance dominates delusion.
- Delusion, doubt and ignorance are only intrinsically passive when doubt dominates knowledge and delusion dominates ignorance.
- Doubt and ignorance are only intrinsically passive if doubt dominates knowledge and ignorance dominates delusion.

We say that a state of an agent collective is global if all agents of the collective take the same doxastic state; thus, for example, we can talk about global knowledge, belief, etc.

- Global misbelief cannot be reached in the development of an agent collective.
- Once a doxastic medium gets into global ignorance or doubt it remains there forever.
- Global knowledge and global ignorance are norm sensitive.
- Norms regulating relations between knowledge and doubt, delusion and ignorance, and misbelief and doubt determine the stability of an agent collective. Maximal stability is achieved when knowledge and misbelief dominate doubt and delusion dominates ignorance.
- Only norms regulating relations between knowledge and doubt, and between delusion and ignorance, determine the behavior of reflecting agents.

A state is called a generative doxastic state if, when composed with itself and all products of the composition and with products of their products and so on, it generates all possible doxastic states.

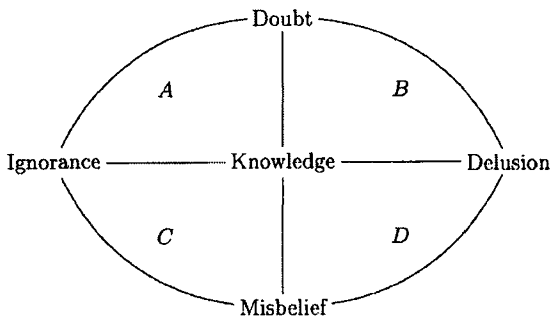

Fig. 4.20 Quadruple of generative triples of doxastic states. The triples are labeled from A to D.

- Knowledge is a minimal generative doxastic state when it is dominated by doubt and misbelief, and ignorance dominates doubt.
- A quadruple (see Fig. 4.20) of generative triples of doxastic states is formed when misbelief dominates knowledge, knowledge dominates doubt and doubt dominates ignorance.

Relations between knowledge and misbelief and between doubt and ignorance are crucial in doxastic systems. Thus, when doubt dominates ignorance, doxastic states are sub-divided into two components: the first includes knowledge, doubt and misbelief; the second is formed of ignorance and delusion.

- Misbelief never prevails in the development of mixed collectives of doxatons, where no topological order on doxatons is applied.
- Entirely delusive, doubting or ignorant collectives never stay in their initial states.
- A stirred collective of doxatons, being initially in a state of global knowledge, remains in its initial state forever if knowledge dominates doubt and misbelief.
- If only doubting and ignorant doxatons are represented in the initial configuration of a doxaton stirred solution and knowledge dominates doubt and misbelief, then no other doxastic states are generated.

The uniformity is preserved in doxaton development: any uniform configuration of a doxaton collective remains uniform in the development.

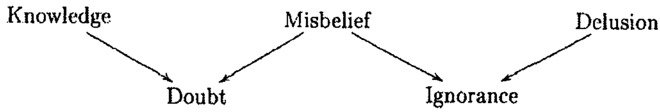

Fig. 4.21 State flows between uniform states.

Basic transitions between uniform collectives of doxatons are shown in Fig. 4.21. Entirely misbelieving doxatons as a source in the flow diagram (Fig. 4.21): the global state of misbelief is changed to either global doubt or global ignorance. The entirely doubting or ignorant collectives are sinks in the diagram (Fig. 4.21).

A situation when all agents but one have the same doxastic state and the singleton has a different state is very amusing. Thus, for example, the singleton keeps its initial state while the rest of the doxaton lattice falls in a stationary configuration after a few steps of the development. Alternatively, the doxastic state of the singleton spreads on the doxaton lattice and interacts with states of other doxatons in such a manner that a complex structure is formed. There may be variations in states of a diffusive wave front and "coupling coefficients". Let us consider some examples of these dynamics.

Ignorance plays a role of a wave generator in an ocean of delusion. Ignorance spreads in a doxaton lattice and every ignorant doxaton transfers its state to its neighbors; hence it may become delusional after that. Therefore, a Pascal-triangle-like structure is formed of ignorance and delusion. The situation becomes different when ignorance is "injected" in an ocean of knowledge and such norms are imposed that knowledge dominates misbelief and is itself dominated by doubt. In this case an ignorant singleton irreversibly becomes delusive. At the same time delusion generates waves of doubt. The doubt diffuses; however, it does not occupy the entire collective because of weak coupling (caused by specifics of norms) between the doxatons.

Starting its development in an ocean of delusion, doubt does not spread in the collective but remains localized; the doubt can be changed to misbelief and then reverse back. After a few steps of the collective's development ignorance starts to spread in the collective; it forms a disorganized structure ornamented by delusion. This happens when ignorance dominates

delusion, doubt dominates misbelief and misbelief dominates knowledge in a normalized composition of doxastic states.

Doubt dropped in an ocean of knowledge generates diffusion waves. However, the phenomenology of diffusion depends on a particular structure of the normalization. Doubt diffuses and eventually fills the doxaton collective for most norms; however, a diffusive wave front comprises both doubt and misbelief when doubt is dominated by knowledge, misbelief and ignorance, and knowledge is dominated by misbelief. Doubt weakly diffuses when knowledge is dominated by doubt and dominates misbelief; no other states but doubt diffuse in this case. If knowledge and doubt are dominated by misbelief, knowledge dominates doubt, doubt dominates ignorance and delusion is dominated by ignorance a mixture of delusion and ignorance diffuses in an ocean of knowledge. There, the diffusive wave front consists of doubt and misbelief. Eventually, the mixture of delusion and ignorance occupies all entities of the doxaton collective.

Delusion does not diffuse in an ocean of doubt but does not annihilate either. Moreover, from time to time, during the collective's development waves of knowledge are generated by delusion. Knowledge spreads along the collective for a short distance and vanishes after a few steps of development. This happens when doubt dominates knowledge, knowledge dominates misbelief and ignorance is dominated by delusion.

Misbelief reacts with delusion quite simply. No states diffuse. However, misbelief may be changed to doubt and back to misbelief (with small sparks of ignorance) when delusion dominates ignorance, doubt dominates misbelief and misbelief dominates knowledge. In most other cases of normalization, doubt diffuses in the collective from a misbelieving doxaton.

What about knowledge? When injected in an ocean of one of the doxastic states knowledge either disappears, as e.g. when ignorance dominates doubt and delusion, doubt dominates knowledge and misbelief and knowledge dominate misbelief; or, knowledge is changed to doubt and misbelief. The knowledge generates diffusing delusion when it is injected in an ocean of ignorance and doubt dominates misbelief and knowledge, misbelief dominates knowledge and delusion is dominated by ignorance. Alternatively, knowledge initiates diffusion of ignorance when injected in an ocean of delusion and misbelief dominates both doubt and knowledge and doubt dominates knowledge.

Let us now consider a random initial configuration of doxaton collectives. We assume that at the beginning of development every doxastic state can be found in a doxaton collective with the same probability 0.2. In these

conditions, misbelief, doubt and ignorance are absorbed by other doxastic states if knowledge dominates misbelief and doubt, misbelief dominates doubt and delusion dominates ignorance. To exterminate misbelief and doubt, we must apply such combinations of norms that knowledge dominates doubt and misbelief, misbelief is dominated by doubt and ignorance dominates delusion.

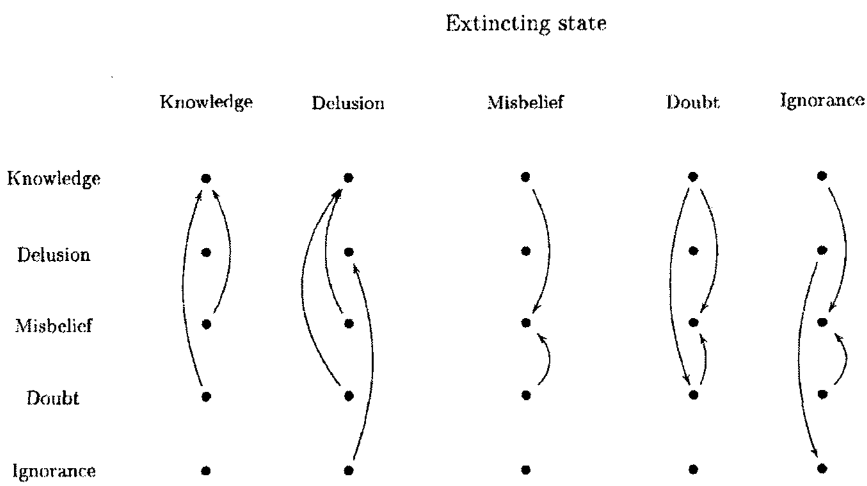

Fig. 4.22 Domination relations leading to extinction of doxastic states.

The knowledge becomes extinct if it is dominated by doubt and misbelief. The delusion vanishes if it is dominated by ignorance and knowledge is dominated by doubt and misbelief. Misbelief can not be found in the development only if it is dominated by knowledge and doubt. The situation with doubt is intriguing. Doubt becomes extinct if it is dominated by knowledge, dominates misbelief and knowledge dominates misbelief. A graphical representation of the relation between domination and extinction is shown in Fig. 4.22.

A couple of interesting consequences of computer simulations could be mentioned separately.

- No combination of norms allows a doxaton medium to develop from an arbitrary initial state to a state of global knowledge.
- No combination of norms supports mixed equilibrium where all doxastic states are nearly equally represented during development of a doxaton collective.

One very interesting problem is not tackled in our chapter: coupled development of doxatons and norms. A coupled system of doxatons and norms can be represented as two such networks of finite automata such that automata of the first network take doxastic states and a state of an automaton of the second network is a combination of norms. Automata of both networks may change their states depending on states of their neighbors in their primary network, either a doxastic network or a norm network, and states of one or more automata in another network. That is, not only doxastic states but also norms can diffuse on doxaton lattices and interact one with another. This idea is fresh but not novel. There are some previously published results where norms are thought of as diffusing substances; see e.g. [Castelfranchi *et. al* (1998)]. Norms diffusion *per se* happens because of recognition of norms and possibly even active defense of norms by agents. Thus, Castelfranci *et al.* simulated multi-agent societies to analyze effects of norms in populations of normatively believable agents [Castelfranchi *et. al* (1998)] which search for food in a discrete space (in this model norms play a role of an aggression inhibitor).

Norms may also actively interact and "co-evolve" with their subjects [Axelrod (1986)]. Thus, initial conditions of a multi-agent system and drastic transitions in global state space may lead to irrational acceptance or rejection of certain norms [Conlisk *et. al* (1997)]. Moreover, norms themselves may compete for their subjects, as soon as norms may be seen as memes.

In addition, when thinking about coupled development of norms and doxatons, we may employ the fifth intuition of norm formalization by Valente and Breuker [Valente and Breuker (1994)]. This intuition states that conflicts between norms are solved by assigning priorities between the norms, where some norms can win over other norms.

Chapter 5

Dynamically Non-trivial Logics

In this book we study dynamical properties of crowded minds. We have already discussed in previous chapters how a crowded environment causes a rise of irrationality and non-sense and thus emergence of non-trivial spatio-temporal behavior. Is there any logic behind complex structures of crowded minds? As Moscovici [Moscovici (1985)] wrote:

> "Crowds are composed of normal people, relatively stable people ... — except that once they form a crowd such people feel, think, and behave differently. They move in a different mental universe with its own peculiar logic."

In this chapter we will try to derive logical systems — by studying them as bulk media of abstract chemical mixtures — which behave non-trivially from a dynamical point of view. In these abstract logical reactors logical variables are represented by chemical species and logical connectives play a role of catalysts in chemical reactions. This approach is inspired by and is partly based on advances in physics of mentality, complex dynamics of logic networks and chemistry. While artificial chemistry was tackled in the first chapter of the book, a few words should be said here about logical networks.

Logical networks, together with their automaton models, were firstly introduced in the 1940s as McCullock–Pitts neurons [McCullock and Pitts (1943)] but soon were absorbed by the fast-growing field of artificial neural networks. In the 1960s logical networks got a new lease of life with the introduction of Kauffman networks — a random Boolean network, where nodes are Boolean logical functions, chosen at random, with arguments being Boolean states of the node's neighbors in the network [Kauffman (1969); Kauffman (1993); Derrida and Pomeau (1986)]. These models were

readily adopted in biology as formal representations of gene-control networks [Kauffman (1969); Kauffman (1993)], statistical physics as models of disorganized systems [Derrida and Pomeau (1986); Derrida (1987)] and cognitive sciences as models of memory and consciousness [Wuensche (1994); Wuensche (1996)]. Usually, models of random Boolean networks employ only classical logic and quite a few operators. There are a couple of more advanced constructs to mention. The first is a Boolean network with AND–NOT gates studied in [Goles and Hernández (2000)], where several interesting results on lengths of the network's transient periods are discussed. The second example concerns three-valued logical networks discussed in [Volker and Conrad (1998)], where Volker and Conrad studied three-valued networks with dual dynamics of weak and strong interactions and provided a classification of the network global dynamics, e.g. transient periods, number of attractors and architecture of attraction basins.

Are there any other ways to simulate a bulk-medium system, where local rules of the medium's elements' interactions are governed by logical connectives? The most reasonable, but still not yet too common, way is to represent logical variables as molecules of some chemical reactants and assume that reactions between the chemical species are governed by truth tables of the logical connectives.

5.1 Artificial chemistry of logics: the model

Consider a dynamic of massive collectives of very simple entities, which interact with each other and update their finite states depending on states of their neighbors using logical connectives. There are three types of molecules in the studied reactors; each type represents, when interpreted in a framework of multiple-valued logics [Rescher (1969); Bolc and Borowik (1992)], a certain logical value: TRUE (T), FALSE (F) and NON-SENSE/UNCERTAIN/UNDEFINED ($*$). These logical values correspond to three chemical species. There are also molecules of a catalyst $\Diamond$, which represents a logical connective. When a certain number of molecules, including the catalyst, interact they undergo a chemical reaction and may change their types. A chemical reaction derived from truth tables of a three-valued logic connective $\Diamond$ can be represented as

$$\alpha\Diamond + \sum_{p\in\{T,F,*\}} k_p p \mapsto \beta\Diamond + \sum_{r\in\{T,F,*\}} k_r r,$$

where α, β, k_p and k_r are numbers of molecules involved in the reaction. We assume that the catalyst $\Diamond$ regenerates, $\alpha = \beta$ — its concentration is kept constant during development of the logical mixture — therefore, we do not include $\Diamond$ explicitly in graphical representations of reactions. Values of reaction rates are also assumed to be constant and the same for all reactions.

We will discuss dynamics of logic-based artificial-chemical systems in stirred and thin-layer non-stirred reactors. In a stirred reactor no spatial order on interaction of molecules is imposed and the probability that two molecules meet does not depend on the distance between the molecules. To simulate the stirred reactor we select two or more molecules at random, put them into the reaction and calculate what species are produced as a result of this interaction; then the next pair of molecules is chosen, and so on. In computer simulation we represent a reaction mixture as an array x of molecules; at each step of the mixture development we choose at random two elements x_i and x_j of the array and update them as follows: $x_i \leftarrow x_i + x_j$ and $x_j \leftarrow x_j + x_i$; i.e. new values of the variables x_i and x_j are calculated as $x_i \Diamond x_j$ and $x_j \Diamond x_i$. This very simple and fast simulation produces results comparable — at least, in our "simplistic" conditions without reaction rates and other parameters — to those obtained in rather more reality-concerned packages, like the chemical kinetics simulator [CKS].

In a thin-layer, or non-stirred, reactor molecules interact locally. We assume that they do not move at all but form a molecular film or an array; thus, only geographically neighboring species do react one with another. An array of diffusion-coupled chemical micro-volumes is another interpretation of a thin-layer reaction. For all cases a cellular-automaton model would be appropriate. We simulate a non-stirred chemical reactor as a one-dimensional cellular automaton of n cells. Each cell x_i, $i = 1, \ldots, n$, takes states from set $\{F, T, *\}$ and updates its states in discrete time by the rule

$$x_i^{t+1} = x_{i-1}^t \Diamond x_{i+1}^t.$$

5.2 Non-trivially behaving systems

In our search for logics that could exhibit non-trivial space–time dynamics we adopt the Bergstra–Bethke–Rodenburg [Bergstra *et. al* (1995)] approach of systematic construction of three-valued logics. We start our experiments with nine possible logics described by negation, $\neg$, and conjunction, $\wedge$, which satisfy the following conditions:

- a double-negation principle holds,
- every logical value is idempotent ($x \wedge x = x$),
- $\wedge$ is commutative ($x \wedge y = y \wedge x$) and
- sub-algebra $\langle \neg, \wedge, \{T, F\} \rangle$ represents Boolean logic.

We slightly relaxed the original constraints of [Bergstra *et. al* (1995)] and abolished two conditions — T being a unit for $*$ and $* \wedge F \neq T$. So, connectives $\neg$ and $\wedge$ have the following truth tables:

$$\begin{array}{c|c} \neg & \\ \hline T & F \\ F & T \\ * & * \end{array} \qquad \begin{array}{c|ccc} \wedge & T & F & * \\ \hline T & T & F & a \\ F & F & F & b \\ * & a & b & * \end{array} \tag{5.1}$$

where T, F and $*$ are TRUE, FALSE and NON-SENSE, and $a, b \in \{T, F, *\}$. Further in the chapter we encode possible logical systems by tuples $\langle ab \rangle$, where $T \wedge * = * \wedge T = a$ and $F \wedge * = * \wedge F = b$.

What is the meaning of $*$? In Łukasiewicz logic $*$ might mean "possible" or "not yet determined" [Lukasiewicz (1920)]; in Belnap logic $*$ can be seen as an indication of "inassertive" [Belnap (1977); Bergstra *et. al* (1995)]; in Bochvar logic $*$ stands for "paradoxical" or "meaningless" [Bochvar (1939)]; in Kleene logic $*$ is considered as "indeterminate" [Kleene (1938)]; or $*$ may be interpreted as "illegal" and "unacceptable" in logical programming, see e.g. [Nota *et. al* (1993)].

Our main objective is to find behaviorally "interesting" logics, that determine rules of local behavior of non-linear discrete medium systems, which exhibit non-trivial space–time dynamics. At first we will search for non-trivially behaving logical chemical systems in a stirred reactor.

Let a stirred reactor $\rho(\wedge, \langle ab \rangle)$ start its development with a mixture of reactants T, F and $*$, all in the same concentration. Chemical reactions are derived from the $\wedge$-table. Because $x \wedge x = x$ for any x we assume that molecules of reagent x do not react with each other, and thus non-diagonal entries of $\wedge$-table determine the reaction $x + y \mapsto 2x \wedge y$. A global behavior of a stirred reactor can be described by a matrix $\mathbf{M} = M_{ab}$, $a, b = T, F, *$, where

- $M_{ab} \in \{T, F, *, \}$ if a stirred reactor, reactions in which are determined by the $\wedge$-table of the logic $\langle ab \rangle$, starts its development with a mixture of all three reactants — T, F and $*$ (all in the same concentration) — but finishes its development with a "pure solution" of one (and the

same in every trial) of the reactants from $\{T, F, *\}$;

- $M_{ab} = \circledcirc$ if (in the same initial conditions) the reactor either does not finish its development with a pure mixture of the same reagent, i.e. exhibits a bifurcation in its dynamic, or at least two reactants are present in the reactor for an indefinitely long time.

Let $\rho(\wedge, \langle ab \rangle)$ be a chemical reactor, in which reactions are determined by connective $\wedge$. Let the reactor start its evolution with a mixture of three reactants T, F and $*$, each one in the same concentration; then outcomes of the reactor's global evolution are completely characterized by the matrix

$$\mathbf{M} = \begin{pmatrix} F & F & \circledcirc \\ F & F & * \\ \circledcirc & F & * \end{pmatrix}.$$

We have $M_{ab} = F$ if $a \neq *$ and $b \neq *$ because, for any composition $a \wedge b$ a graph of chemical reactions, determined by logic $\langle ab \rangle, a, b \neq *$, is as follows:

$$\begin{tikzcd} & * \arrow[dl] \arrow[dr] & \\ T \arrow[rr] & & F \end{tikzcd}$$

Edge $T \to F$ of the graph is obligatory, and either of edges $* \to T$ and $* \to F$ or both represent a certain part of the chemical reactions. There is only one sink node F. Therefore, independently of what the ratio of reactants in the initial mixture is, the reactor develops a solution of the only reactant F.

Logic $\langle TF \rangle$ determines a reaction $T+F+* \to 2F+T$. Reactant $*$ is not produced in the reactions; thus, assuming that there is no external supply, the reactant is completely exhausted soon after the start of an experiment. Then, only the reaction $T + F \to 2F$ will take place.

From reaction equations of chemical systems generated by logics $\langle F* \rangle$ and $\langle *F \rangle$: $T + F + * \to 2F + *$ and $T + F + * \to 2F + *$, we see that the reactant T is not produced but only consumed in the reactor. To check what happens in the reactor when T has gone one could consider the elementary binary reactions $F+* \to *$ (in reactor $\rho(\wedge, \langle F* \rangle)$) and $F+* \to F$ (in reactor

$\rho(\wedge, \langle *F \rangle))$. When these reactions take place and a mixture develops, the reactors will be filled with solutions of $*$ and F reactants, respectively.

Evolution of reactor $\rho(\wedge, \langle ** \rangle)$ is governed by the following set of elementary reactions: $T + F \rightarrow F$, $T + * \rightarrow *$ and $F + * \rightarrow *$ with the reaction network

$$\begin{tikzcd} & \ast & \\ T \arrow[ur] \arrow[rr] & & F \arrow[ul] \end{tikzcd}$$

The dynamic of reactor $\rho(\wedge, \langle T* \rangle)$, with elementary reactions $T + F \rightarrow F$, $T + * \rightarrow T$ and $F + * \rightarrow *$, can be described by the following differential equations:

$$\dot{x_T} = x_T(x_* - x_F),$$
$$\dot{x_F} = x_F(x_T - x_*),$$
$$\dot{x_*} = x_*(x_F - x_T)$$

and reaction network

$$\begin{tikzcd} & \ast \arrow[dl] & \\ T \arrow[rr] & & F \arrow[ul] \end{tikzcd}$$

They show that the chemical processes in the reactor $\rho(\wedge, \langle T* \rangle)$ are periodic and therefore the reactor may exhibit oscillations of reactant concentrations. Therefore, we call the logic $\langle T* \rangle$ an oscillatory logic.

The concentration behavior of the reactor $\rho(\wedge, \langle *T \rangle)$, with the reactions $T + F \mapsto F$, $T + * \mapsto *$ and $F + * \mapsto T$, can be described as

$$\dot{x_T} = x_F x_* - x_T x_* - x_T x_F,$$
$$\dot{x_F} = x_F(x_T - x_*),$$
$$\dot{x_*} = x_*(x_T - x_F),$$

where reagent T decreases in concentration until it completely vanishes, while reagents F and $*$ are virtually competing for resources. Two last equations of the system determine the bifurcation behavior of the reactor: depending on particulars of instant molecular dynamics only one of the reagents — either F or $*$ — survives in the reactor. The logic $\langle *T \rangle$, from which the reactor is derived, is called a bifurcatory logic. Combinatorial systems studied in the chapter do not get a "proper" logical treatment:

they have a "technical" structure of logical connectives; however, neither truth values nor connectives are "sensibly" interpreted and therefore it may be reasonable to refer to such systems as pre-logics.

⋆ ⋆ ⋆

Amongst nine possible logics, derived from the truth table (5.1), the oscillatory logic $\langle T* \rangle$ and the bifurcatory logic $\langle *T \rangle$ are ones exhibiting a non-trivial behavior. Further, we study the behavior of reactors where chemical reactions are determined by operators of these oscillatory and bifurcatory logics.

To analyze the dynamical behavior of systems based on connectives other than negation and conjunction, we adopted the principle of interdefinability of the propositional connectives [Bergstra *et. al* (1995)]:

- disjunction $x \vee y = \neg(\neg x \wedge \neg y)$,
- implication $x \rightarrow y = \neg x \vee y$,
- equivalence $x \leftrightarrow y = \neg(x \oplus y)$,
- exclusive disjunction $x \oplus y = (x \wedge \neg y) \vee (\neg x \wedge y)$,
- Scheffer stroke $x | y = \neg(x \wedge y)$,
- Peirce arrow $x \downarrow y = \neg(x \vee y)$ (see Fig. 5.1).

Both connectives $\wedge$ and $\vee$ of the oscillatory and bifurcatory logics are commutative and non-associative, they obey de Morgan's laws, are not distributive over one another, and axioms $x \vee (\neg x \wedge y) = x \vee y$ and $x \vee (x \wedge y) = x \vee y$ do not hold. Commutativity of the connectives, assumed in our original constructions, implies that we could consider binary interactions of molecules and simulate a thin-layer reaction in a three-state, two-cell-neighborhood, one-dimensional deterministic cellular automaton. However, we could not increase a cell neighborhood to three cells because the connectives are non-associative. We simulate a thin-layer chemical reactor as a one-dimensional cellular automaton, each cell of which represents a molecule or a micro-volume, filled with only one type of reagent, of the reactor. Thus we use the word "configuration (of cell states)" when talking about the spatial distribution of reactant molecules or a one-dimensional concentration profile of reagent concentrations.

$\neg$	
T	F
F	T
$*$	$*$

$\wedge$	T	F	$*$
T	T	F	T
F	F	F	$*$
$*$	T	$*$	$*$

$\vee$	T	F	$*$
T	T	T	$*$
F	T	F	F
$*$	$*$	F	$*$

$\rightarrow$	T	F	$*$
T	T	F	F
F	T	T	$*$
$*$	$*$	F	$*$

$\oplus$	T	F	$*$
T	F	T	$*$
F	T	F	$*$
$*$	$*$	$*$	$*$

$\mid$	T	F	$*$
T	F	T	F
F	T	T	$*$
$*$	F	$*$	$*$

$\downarrow$	T	F	$*$
T	F	F	$*$
F	F	T	T
$*$	$*$	T	$*$

$\leftrightarrow$	T	F	$*$
T	T	F	$*$
F	F	T	$*$
$*$	$*$	$*$	$*$

(a)

$\neg$	
T	F
F	T
$*$	$*$

$\wedge$	T	F	$*$
T	T	F	$*$
F	F	F	T
$*$	$*$	T	$*$

$\vee$	T	F	$*$
T	T	T	F
F	T	F	$*$
$*$	F	$*$	$*$

$\rightarrow$	T	F	$*$
T	T	F	$*$
F	T	T	F
$*$	F	$*$	$*$

$\oplus$	T	F	$*$
T	F	T	F
F	T	F	F
$*$	F	F	$*$

$\mid$	T	F	$*$
T	F	T	$*$
F	T	T	F
$*$	$*$	F	$*$

$\downarrow$	T	F	$*$
T	F	F	T
F	F	T	$*$
$*$	T	$*$	$*$

$\leftrightarrow$	T	F	$*$
T	T	F	T
F	F	T	T
$*$	T	T	$*$

(b)

Fig. 5.1 Systems of oscillatory (a) and bifurcatory (b) logics.

5.3 Oscillatory logic $\langle T* \rangle$

5.3.1 *Stirred reactors*

Computer experiments with a stirred reactor $\rho(\wedge, \langle T* \rangle)$ show that the reactor exhibits irregular oscillations of reactant concentrations. The chemical mixture undergoes non-stable oscillations of concentrations, and typically the amplitude of oscillations increases with time until one of the reagents completely decays — after that only the other reagent(s) remains in the reactor. As we see from the set of elementary reactions and corresponding equations of the oscillatory logic, each reactant participates in two of three elementary reactions. Therefore, as soon as one of reactants becomes ex-

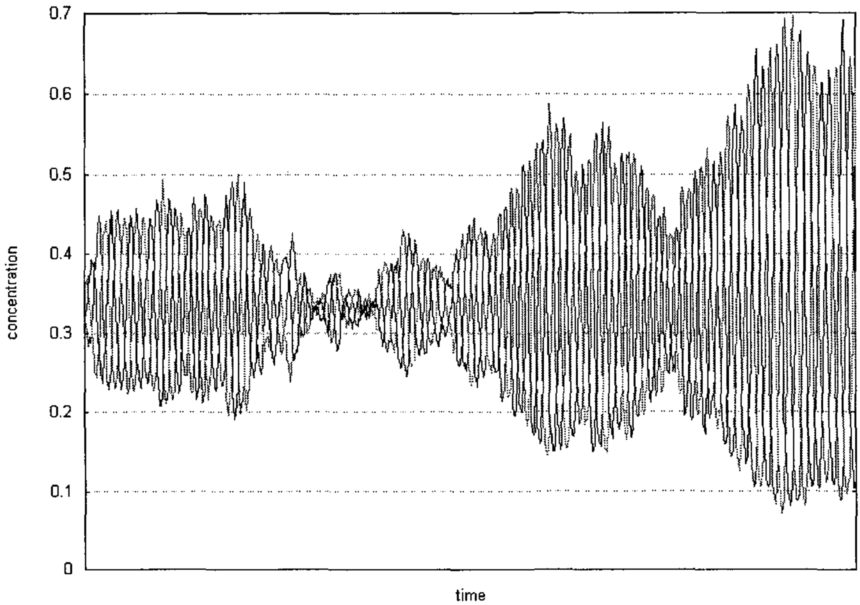

Fig. 5.2 Example of oscillatory concentration dynamic in reactor $\rho(\wedge, \langle T* \rangle$ of oscillatory logic; 2×10^3 molecules, 50×10^3 steps.

tinct the system's description is reduced to just one reaction $R_1 + R_2 \mapsto R_1$, and thus eventually the reactor becomes filled with just one reactant R_1.

A typical irregular oscillation dynamic is shown in Fig. 5.2: bursts of high-amplitude oscillations are followed by periods of low-amplitude oscillations; at some moment of the reactor development the concentration of one of the reagents hits the zero level; this reagent is eliminated from the reactor and one of the two remaining reagents is immediately consumed by the other reagent.

Adding catalyst $\vee$ to a mixture of T, F and $*$ initiates transient oscillatory behavior similarly to that initiated by the catalyst $\wedge$; however, these two catalysts govern reactions in a slightly different manner. The catalysts $\wedge$ and $\vee$ impose reaction networks with unlike periodicity:

$\wedge$-network

$$\begin{tikzcd} & * \arrow[dl] & \\ T \arrow[rr] & & F \arrow[ul] \end{tikzcd}$$

$\vee$-network

$$\begin{tikzcd} & * \arrow[dr] & \\ T \arrow[ur] & & F \arrow[ll] \end{tikzcd}$$

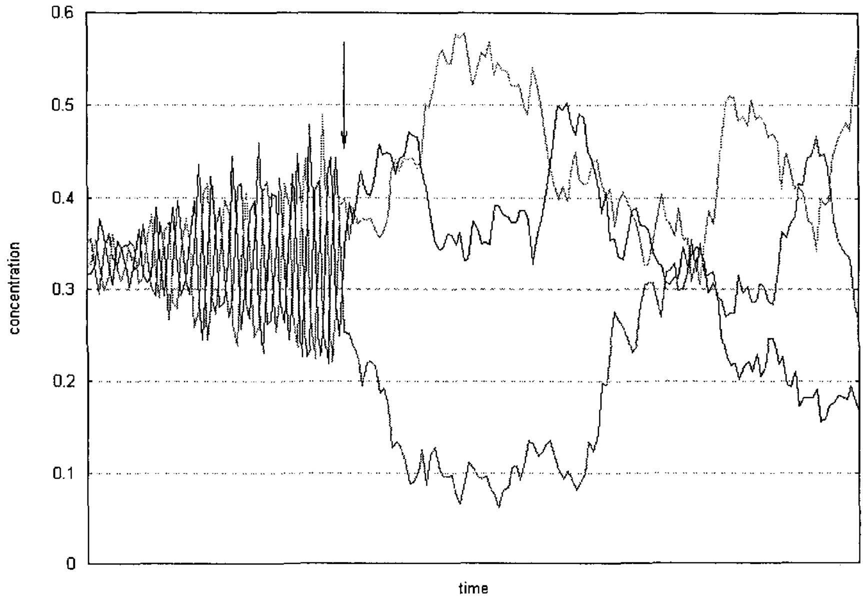

Fig. 5.3 Dynamic of reactant concentrations in a reactor that initially contains only catalyst $\wedge$ and catalyst $\vee$ is added later; the moment of time when the catalyst $\vee$ is injected into the reactor is marked by an arrow.

Therefore, adding catalyst $\vee$ to a reactor initially containing only catalyst $\wedge$ transforms the concentration dynamic from high-frequency oscillations to slow irregular drifts of concentrations, as shown in Fig. 5.3.

The truth table of $\rightarrow$ of oscillatory logic (Fig. 5.1a) determines the following set of non-trivial reactions:

$$\begin{gathered} F \mapsto T \\ T + * \mapsto F + *, \end{gathered}$$

where reactant $*$ is a second-order catalyst for the reaction $T \mapsto F$. Thus the reactor $\rho(\rightarrow, \langle T* \rangle)$ exhibits high-frequency average-amplitude irregular oscillations of T and F concentrations. This is demonstrated in Fig. 5.4, where T and F oscillate in opposite phases.

Reactor $\rho(\oplus, \langle T* \rangle)$ exhibits a dull behavior: quite soon after the start of an experiment the reactor contains only reagent $*$. This happens because both reagents (which themselves may oscillate due to transformations $T \mapsto F$ and $T+F \mapsto T$) are consumed by reactant $*$ in the reaction: $T+F+2* \mapsto 2*$ (see truth table of $\oplus$ in Fig. 5.1a).

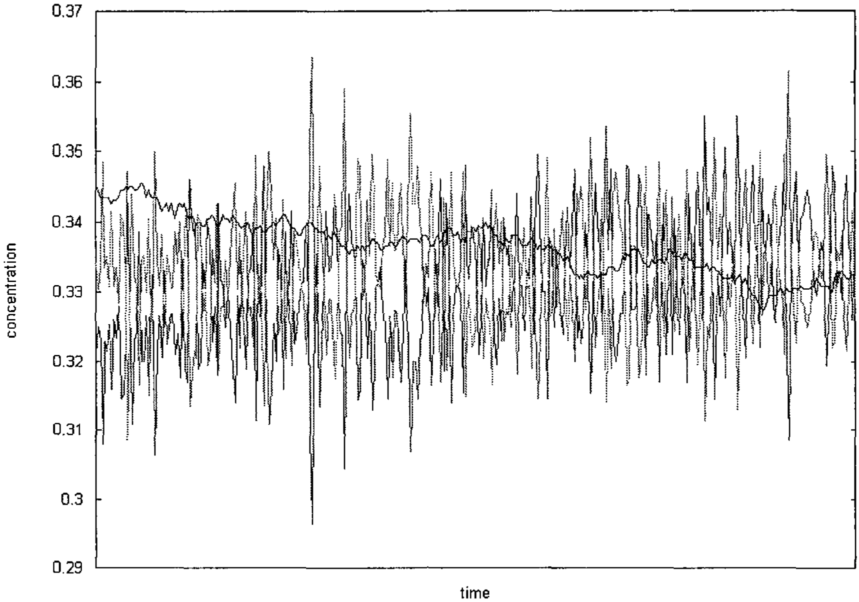

Fig. 5.4 Dynamic of reagent concentration in reactor $\rho(\rightarrow, \langle T*\rangle)$; 2×10^3 molecules, 50×10^3 steps.

The concentration dynamic of reactor $\rho(|, \langle T*\rangle)$, determined by truth table $|$ in Fig. 5.1a, is described as follows:

$$\begin{aligned} \dot{x_T} &= x_T(x_F - x_* - 1) + x_F \\ \dot{x_F} &= (1 + x_*)(x_T - x_F) - x_T x_F \\ \dot{x_*} &= x_*(x_F - x_T). \end{aligned}$$

There are two stable points: first, $x_* \neq 0$, $x_T = 0$ and $x_F = 0$, and, second, $x_* = 0$, $x_T, x_F \neq 0$ and $x_T = x_F/(1 - x_F)$. An example of the system converging to the second stable point is shown in Fig. 5.5.

The dynamic of reactor $\rho(\downarrow, \langle T*\rangle)$ does not seem to be of any particular interest because (see Fig. 5.1a) the system always converges to a stable point $x_* \neq 0$ and $x_T, x_F = 0$. When we look at the set of elementary reactions, determined by the $\downarrow$-table (Fig. 5.1a)

$$\begin{aligned} &T \mapsto F \\ &F \mapsto T \\ &T + F \mapsto F \\ &T + * \mapsto * \\ &F + * \mapsto T, \end{aligned}$$

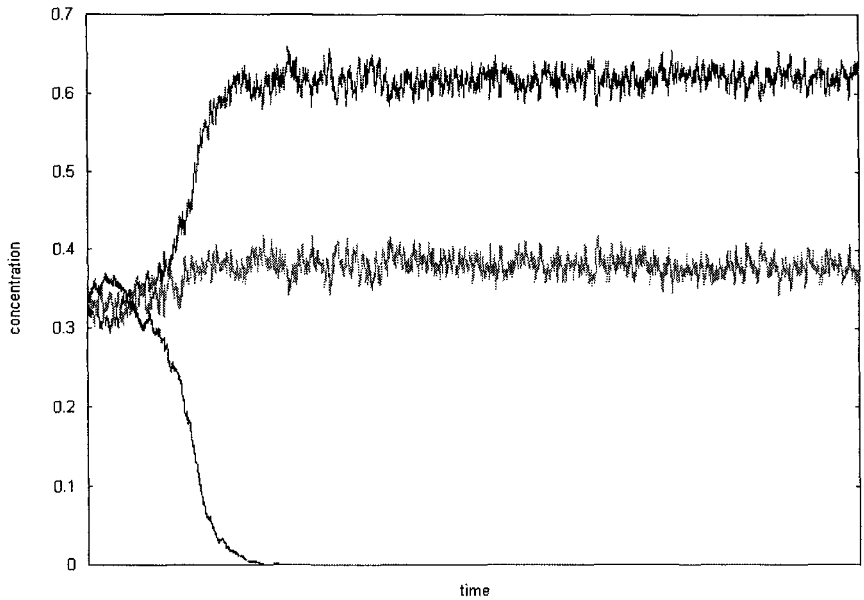

Fig. 5.5 Dynamic of reagent concentrations in the reactor $\rho(|, \langle T*\rangle)$; 2×10^3 molecules, 50×10^3 steps.

we find that two main processes occur in the system. The first three reactions of the set generate oscillations of reagents T and F; however, the last two reactions cause the concentrations of T and F to decay. A similar situation occurs in reactor $\rho(\leftrightarrow, \langle T*\rangle)$:

$$\begin{aligned} &F \mapsto T \\ &T + F \mapsto F \\ &T + * \mapsto * \\ &F + * \mapsto *; \end{aligned}$$

only the reagent $*$ survives in the reactor after some period of mixture development.

5.3.2 *Thin-layer reactors*

Any random configuration in thin-layer reactors $\rho(\oplus, \langle T*\rangle)$ and $\rho(\leftrightarrow, \langle T*\rangle)$ quickly converges to a homogeneous configuration, where every site takes the state $*$. An example of a space–time dynamic of a thin-layer reactor $\rho(\wedge, \langle T*\rangle)$ is shown in Fig. 5.6a.

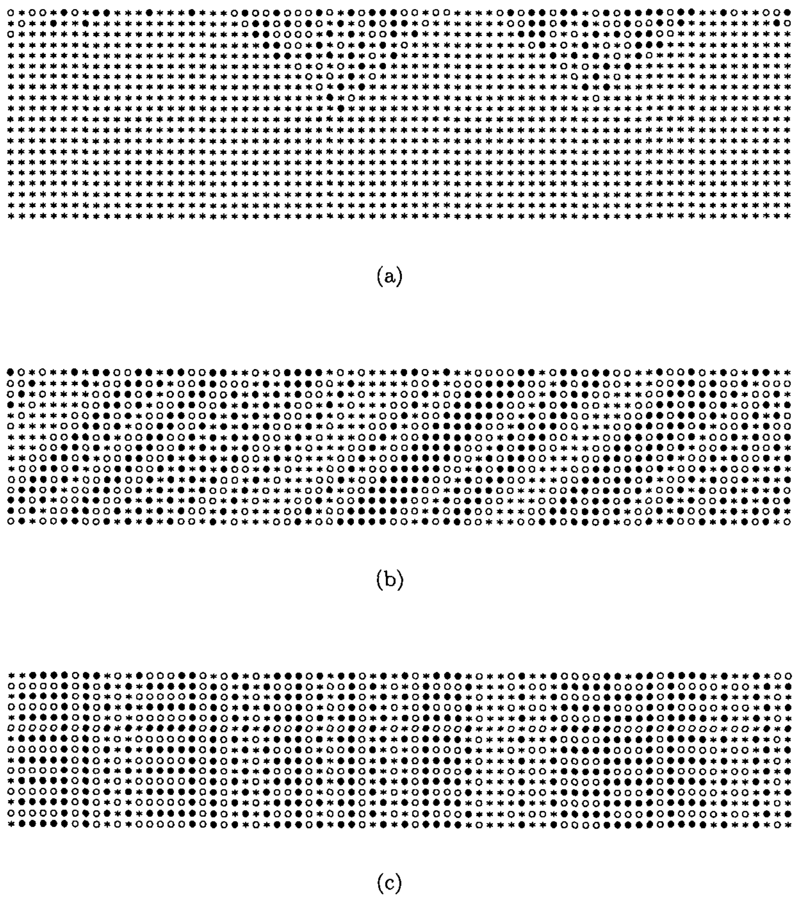

Fig. 5.6 Space–time dynamic of cellular-automaton model of thin-layer reactors (a) $\rho(\oplus, \langle T*\rangle)$, (b) $\rho(\rightarrow, \langle T*\rangle)$ and (c) $\rho(|, \langle T*\rangle)$. Boundaries are periodic, time goes downwards, $\bullet$ is T, $\circ$ is F and $*$ is $*$.

Connective $\rightarrow$ is asymmetric; therefore, an initially random configuration of cell states self-organizes into trains of mobile localizations as shown in Fig. 5.6b. There are only stationary breathers in a space–time dynamic of thin-layer reactors $\rho(|, \langle T*\rangle)$ and $\rho(|, \langle T*\rangle)$; see e.g. Fig. 5.6c.

Cellular-automaton rules derived from truth tables of $\wedge$ and $\vee$ (see Fig. 5.1a) correspond to conventional models of discrete reaction–diffusion systems. In space–time configurations of thin-layer reactors $\rho(\wedge, \langle T*\rangle)$ (Fig. 5.7a) and $\rho(\vee, \langle T*\rangle)$ (Fig. 5.7b) we can discover traveling wave fronts,

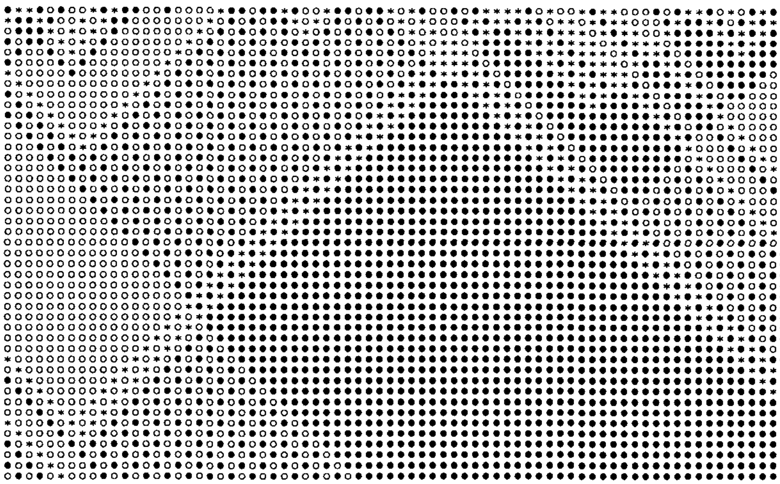

(a)

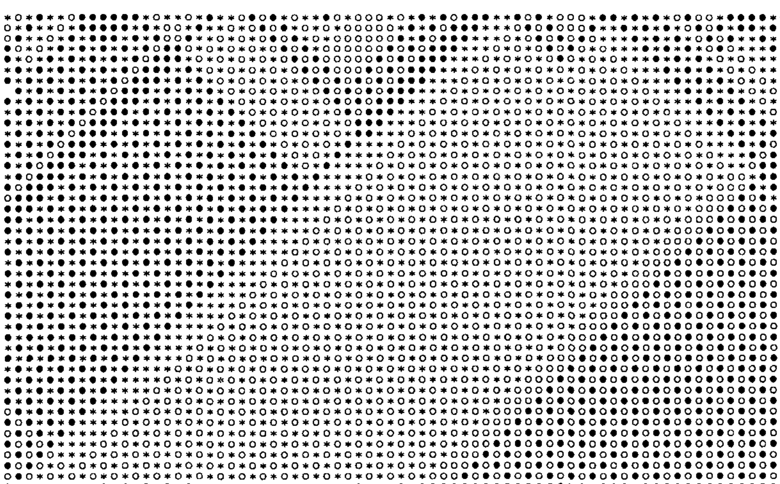

(b)

Fig. 5.7 Space–time dynamic of cellular-automaton model of thin-layer reactors (a) $\rho(\wedge, \langle T*\rangle)$ and (b) $\rho(\vee, \langle T*\rangle)$. Boundaries are periodic, time goes downwards, $\bullet$ is T, $\circ$ is F and $*$ is $*$.

non-localized diffusion waves and traveling localizations. Examples of the traveling phenomena include diffusion of T (Fig. 5.7a, central part) and F (Fig. 5.7a, right-hand part); and also spreading of a mixture of F and $*$ (Fig. 5.7b, central part) and a mixture of T and F (Fig. 5.7b, right-hand part).

By exhaustive search of all possible concentration profiles in thin-layer reactors $\rho(\wedge, \langle T*\rangle)$ and $\rho(\vee, \langle T*\rangle)$, we discover six types of three-cell gliders (each one has a size of three cells) and six types of four-cell gliders. Examples of the gliders are shown in Fig. 5.8. Neither of these mobile patterns

		Motion			
		Leftward		Rightward	
Background	T	$FT*$	$FF**$	$*TF$	$**FF$
	F	$*FT$	$TT**$	$TF*$	$**TT$
	$*$	$T*F$	$TTFF$	$F*T$	$FFTT$

Fig. 5.8 Morphology of gliders emerging in discrete model of the thin-layer reactor $\rho(\wedge, \langle T*\rangle)$.

oscillates when traveling on the lattice. Collisions between two gliders are pretty "standard" for one-dimensional cellular-automaton gliders: three-cell gliders disappear if they are in unlike phases or collide quasi-elastically when in the same phase. Four-cell gliders annihilate as a result of binary collisions independently of their phases.

Some examples of glider collisions are shown in Fig. 5.9, where gliders travel in the resting environment $*$. When gliders $F*T$ (moving rightward) and $T*F$ (moving leftward) collide, they either pass through each other or annihilate (Fig. 5.9a), depending on their relative phases. In another example (Fig. 5.9b), glider $F*T$ (moving rightward) collides with glider $TTFF$ (moving leftward): as a result of the collision the glider $TTFF$ disappears and another glider is reflected as $F*T \rightarrow T*F$.

5.4 Bifurcatory logic $\langle *T\rangle$

5.4.1 *Stirred reactor*

Reactor $\rho(\vee, \langle *T\rangle)$ behaves similarly to $\rho(\vee, \langle *T\rangle)$, which has been already discussed, with the only difference that either reagent T or reagent $*$ sur-

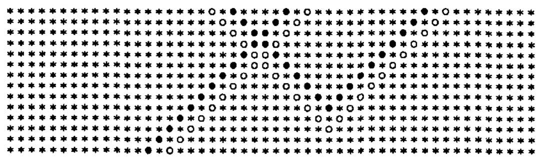

(a)

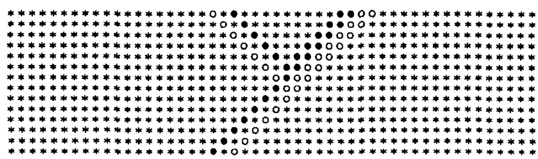

(b)

Fig. 5.9 Example of three-cell glider collisions (a) and a collision between a three-cell glider and a four-cell glider (b) in a one-dimensional cellular-automaton model of the thin-layer reactor $\rho(\wedge, \langle T*\rangle)$. Lattice-node states are encoded as follows: $\bullet$ is T, $\circ$ is F and $*$ is $*$. Time goes downwards.

vives in the reactor during evolution.

Processes in reactor $\rho(\rightarrow, \langle *T\rangle)$ are determined by reactions $F \mapsto T$ and $T + * \mapsto F + *$ (see $\rightarrow$ truth table in Fig. 5.1b). The first reaction governs transformation of reagent F to reagent T, the second — transformation of T to F, catalyzed by $*$. Therefore, the concentration of $*$ wanders around its initial value while concentrations of T and F exhibit high-amplitude irregular fluctuations (Fig. 5.10).

The reagent $*$ appears on the right-hand side of the reactions, catalyzed by $\oplus$ (Fig. 5.1b). Therefore, this set of elementary reactions in the reactor $\rho(\oplus, \langle *T\rangle)$ could be reduced to just two: $T \mapsto F$ and $T + F \mapsto T$, and so the concentrations of T and F oscillate in opposite phases, $\dot{x_T} = -\dot{x_F}$.

If we ignore the reversible transformation $T \rightleftarrows F$ (assuming reaction rates are the same) in the reactor $\rho(|, \langle *T\rangle)$, then the remaining reactions (derived from the truth table of $|$, Fig. 5.1b) determine a chaotic oscillatory

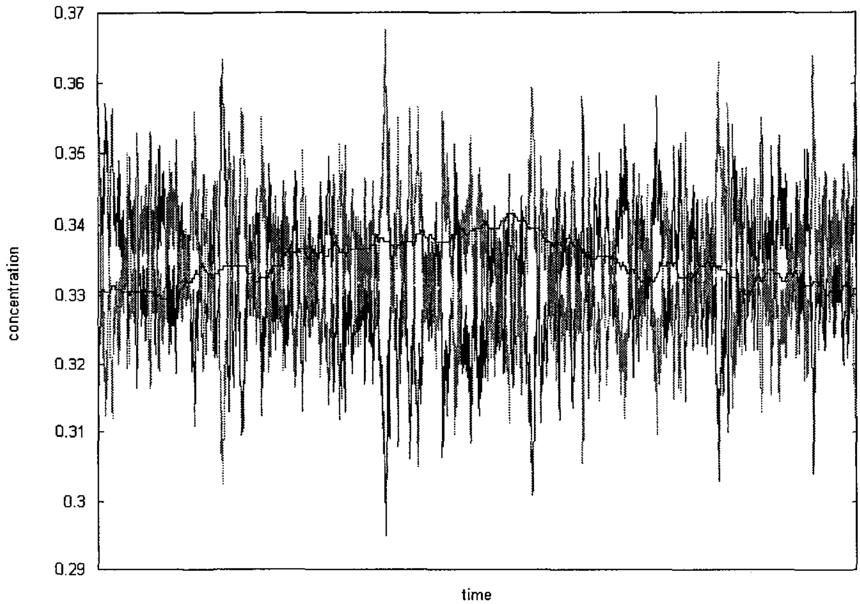

Fig. 5.10 Concentration dynamic in $\rho(\rightarrow, \langle *T \rangle)$; 2×10^3 molecules, 50×10^3 steps.

dynamic of reagent concentrations:

$$\begin{aligned} \dot{x_T} &= x_T(x_F - x_F) \\ \dot{x_F} &= x_F(x_* - x_T) \\ \dot{x_*} &= x_*(x_T - x_F), \end{aligned}$$

which is illustrated graphically in Fig. 5.11. Reactor $\rho(\downarrow, \langle *T \rangle)$ behaves similarly and hence not identically to the previously discussed reactor due to its reaction skeleton, $T + F \mapsto F$, $T + * \mapsto T$ and $F + * \mapsto *$:

$$\begin{aligned} \dot{x_T} &= x_T(x_* - x_F) \\ \dot{x_F} &= x_F(x_T - x_*) \\ \dot{x_*} &= x_*(x_F - x_T). \end{aligned}$$

Reagent $*$ decays and vanishes in reactor $\rho(\leftrightarrow, \langle *T \rangle)$ (Fig. 5.1b), so it may be completely ignored at large time scales. The concentrations of the two remaining reagents T and F exhibit an oscillatory dynamic: $\dot{x_T} = -x_T x_F + x_F$ and $\dot{x_F} = x_T x_F - x_F$.

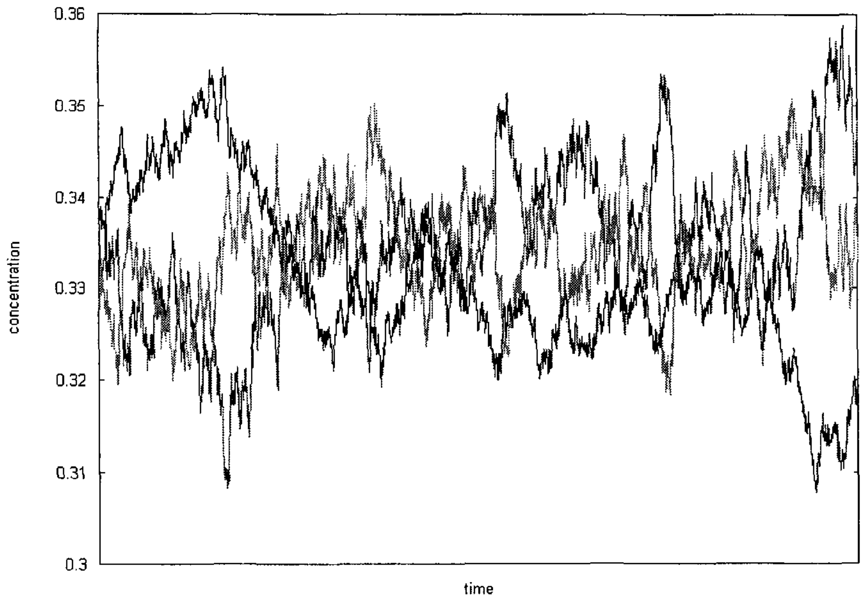

Fig. 5.11 Concentration dynamic in the reactor $\rho(|, \langle *T \rangle)$; 10^4 molecules, 50×10^3 steps.

5.4.2 *Thin-layer reactor*

Soon after the beginning of its development, the thin-layer reactor $\rho(O, \langle *T \rangle)$, for $O = \wedge, \vee, |, \downarrow$, reaches global states which exhibit

(1) standing stationary homogeneous domains, e.g. domains filled with the $*$ state in reactors $\rho(\wedge, \langle *T \rangle)$ and $\rho(\vee, \langle *T \rangle)$ (Fig. 5.12);
(2) heterogeneous undulating patterns, for example

$$\ldots F * F * F * F * \ldots \longleftrightarrow \ldots * F * F * F * F \ldots$$

in reactor $\rho(\wedge, \langle *T \rangle)$ (Fig. 5.12a) or

$$\ldots T * T * T * T * \ldots \longleftrightarrow \ldots * T * T * T * T \ldots$$

in reactor $\rho(\vee, \langle *T \rangle)$ (Fig. 5.12b);
(3) homogeneous oscillating patterns, for example

$$\ldots TTTT \ldots \longleftrightarrow \ldots FFFF \ldots$$

in reactors $\rho(|, \langle *T \rangle)$ and $\rho(\downarrow, \langle *T \rangle)$ (Fig. 5.13).

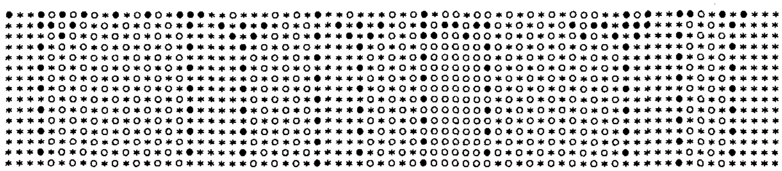

(a)

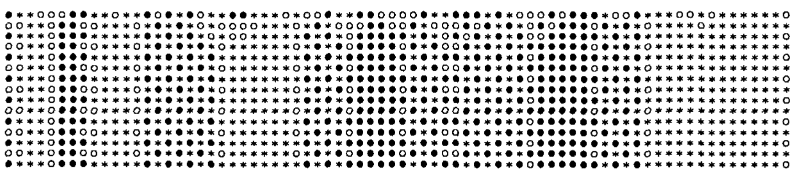

(b)

Fig. 5.12 Space–time dynamic of cellular-automaton model of thin-layer reactors $\rho(O, \langle *T \rangle)$: (a) $O = \wedge$ and (b) $O = \vee$, boundaries are periodic, $\bullet$ is T, $\circ$ is F and $*$ is $*$, time goes downwards.

Domain boundaries are usually stationary.

A dynamic of the thin-layer reactor $\rho(\rightarrow, \langle *T \rangle)$ is somewhat amazing. Most types of defects move leftward (Fig. 5.14a) and their motion is biased by asymmetry of the connective $\rightarrow$, similarly to the space–time dynamic of the reactor $\rho(\rightarrow, \langle T* \rangle)$. However, there are a few gliders and defects traveling rightward. Two examples are shown in Fig. 5.14. In the first example (Fig. 5.14b) we see a one-cell pattern F moving in a resting environment of $*$ states; this is because $F \rightarrow * = F$ and $* \rightarrow F = *$ (Fig. 5.1b). In the second example a block of four F states

$$\boxed{\begin{matrix} F & F \\ F & F \end{matrix}}$$

moves rightward supported by leftward streams of one-cell defects (Fig. 5.14c).

Irregularly distributed and randomly sized triangles of F and T states are typical attributes of space–time configurations of thin-layer reactors $\rho(\oplus, \langle *T \rangle)$ and $\rho(\leftrightarrow, \langle *T \rangle)$ (Fig. 5.15).

Cellular-automaton rules of these fractal patterns are well known:

$$x_i^{t+1} = (1 + x_{i-1}^t + x_{i+1}^t) \mod 2$$

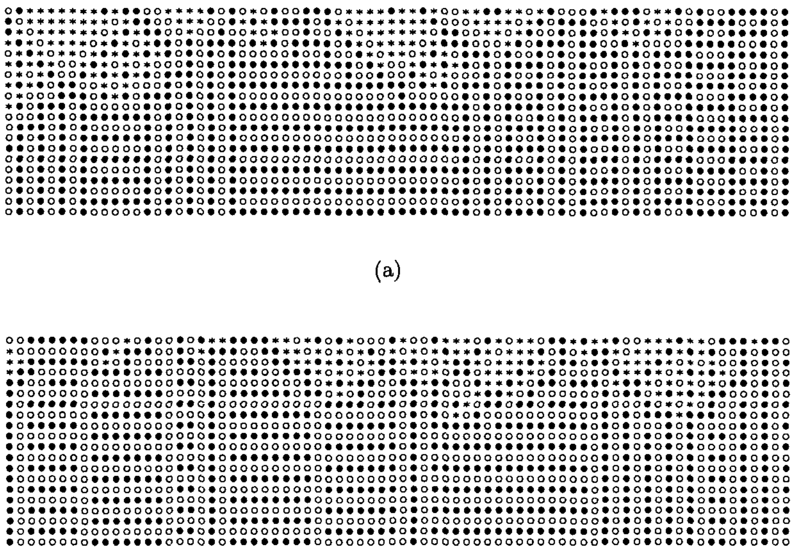

(a)

(b)

Fig. 5.13 Space–time dynamic of cellular-automaton model of thin-layer reactors $\rho(O, \langle *T \rangle)$: (a) $O = \mid$ and (b) $O = \downarrow$, boundaries are periodic, $\bullet$ is T, $\circ$ is F and $*$ is $*$, time goes downwards.

and

$$x_i^{t+1} = (x_{i-1}^t + x_{i+1}^t) \mod 2,$$

respectively. A self-similarity becomes particularly obvious when we put a drop of one reagent, e.g. T, onto a substrate layer of another reagent, e.g. F; then, a "classical" Pascal triangle is generated (Fig. 5.16).

5.5 Emergence of complexity

In this chapter we aimed to select the most interesting, in terms of a space–time dynamic of logical reactors, three-valued logics, the logics which exhibit non-trivial behavior. How complex are our locally interacting systems derived from the three-valued compositions and how dynamically complex are logical connectives themselves? The next two sections give us some answers.

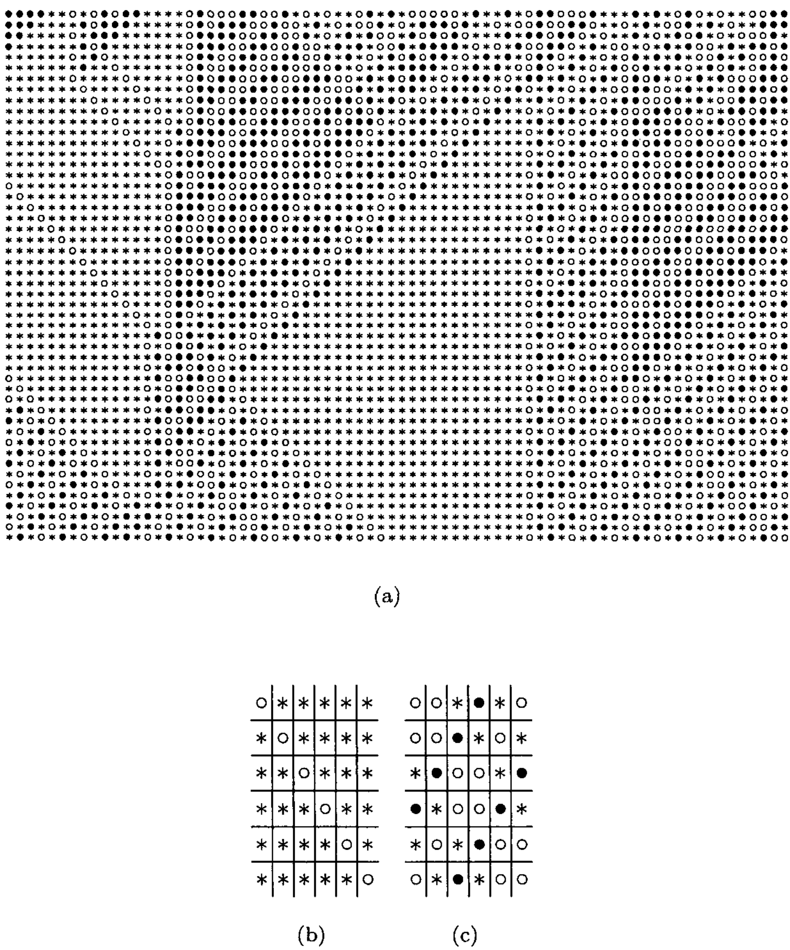

Fig. 5.14 Space–time dynamic of cellular-automaton model of thin-layer reactor $\rho(\rightarrow,\langle *T \rangle)$, boundaries are periodic, $\bullet$ is T, $\circ$ is F and $*$ is $*$, time goes downwards. (a) An exemplary space–time configuration. (b) One-cell localization of F state moving rightward. (c) Block defect moving rightward in regular environment.

5.5.1 *Static complexity of interaction rules*

Let us classify complexity of the bifurcatory and oscillatory logical systems using an analog of Langton's λ-parameter [Langton (1990)], a common tool for studying phase transitions and phenomena related to complex systems in

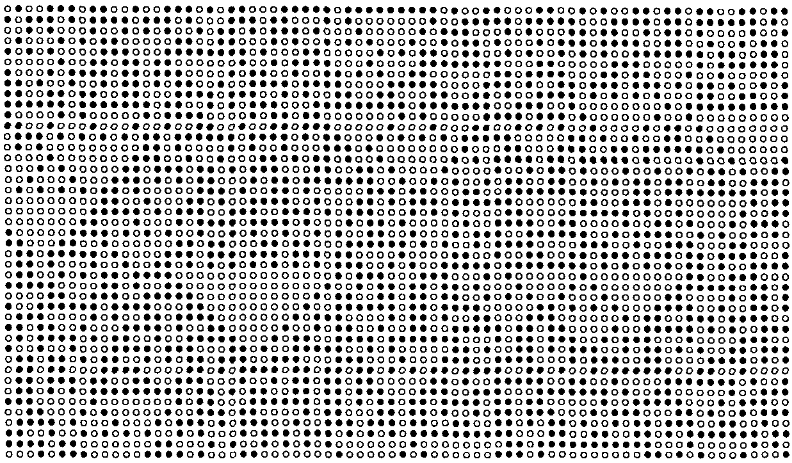

(a)

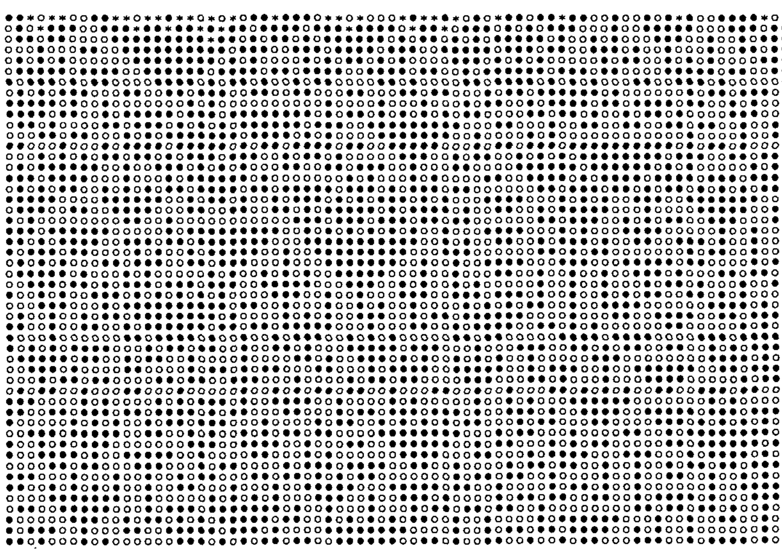

(b)

Fig. 5.15 Space–time dynamic of cellular-automaton model of thin-layer reactors $\rho(\oplus, \langle *T \rangle)$ (a) and $\rho(\leftrightarrow, \langle *T \rangle)$ (b), boundaries are periodic, $\bullet$ is T, $\circ$ is F and $*$ is $*$, time goes downwards.

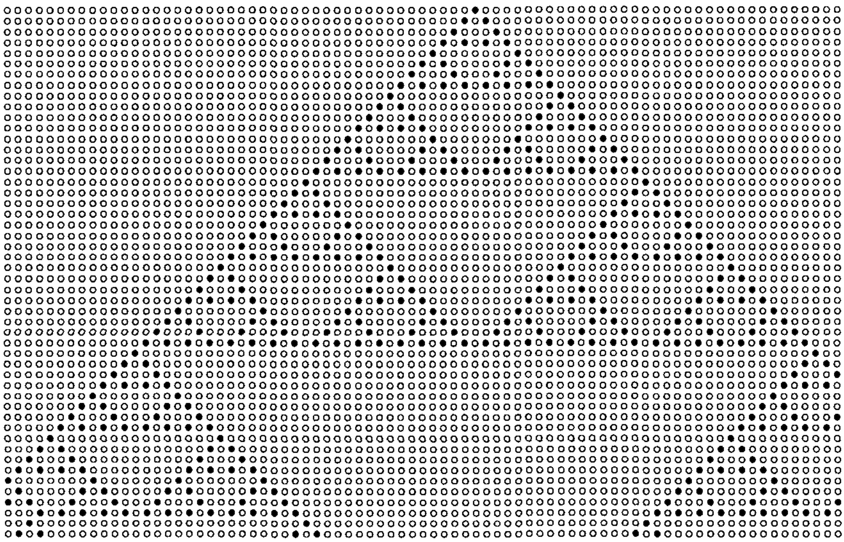

Fig. 5.16 Space–time dynamic of cellular-automaton model of thin-layer reactor $\rho(\oplus, \langle *T \rangle)$, which starts its development with all cells but one in state F, the only central cell of the lattice takes state T initially; $\bullet$ is T, $\circ$ is F and $*$ is $*$, time goes downwards.

cellular automata. Given reactor $\rho(O, \langle ab \rangle)$ and state z, $z \in \mathbf{Q} = \{T, F, *\}$, we calculate the ratio s_z of the state z in the state-transition table of an automaton model with cell-transition rules determined by connective O:

$$s_z = \frac{\sum_{x,y \in \mathbf{Q}} \{xOy = z\}}{|\mathbf{Q}|^2}.$$

An automaton model of reactor $\rho(O, \langle ab \rangle)$, whose local transition functions have ratios near the center $(\frac{1}{3}, \frac{1}{3}, \frac{1}{3})$ of the simplex (s_T, s_F, s_*), could potentially exhibit quite sophisticated patterns. Thus, for every connective $O \in \{\wedge, \vee, \rightarrow, \oplus, |, \downarrow, \leftrightarrow\}$ of logic $\langle ab \rangle$, $a, b \in \{T, F, *\}$, we calculate a value

$$d(O, \langle ab \rangle) = \left| (s_T, s_F, s_*) - \left(\frac{1}{3}, \frac{1}{3}, \frac{1}{3} \right) \right|.$$

Therefore, the complexity of these logical systems can be estimated by the matrix $\mathbf{C} = (C_{ab})_{a,b=T,F,*}$, where $C_{ab} = \frac{1}{7} \sum_O d(O, \langle ab \rangle)$. The matrix $\mathbf{C}$

looks as follows:

		b		
	C_{ab}	T	F	$*$
	T	0.3	0.3	$\boxed{0.1}$
a	F	0.3	0.5	0.3
	$*$	$\boxed{0.1}$	0.3	0.3

There are two minimal-value entries of $\mathbf{C}$: $C_{T*} = C_{*T} = 0.1$; they indicate that logics $\langle T*\rangle$ and $\langle *T\rangle$ would exhibit more interesting and, hopefully, more complex behavior than other logics. We have previously demonstrated this by a brute-force exhaustive search.

5.5.2 *Complexity of connectives*

What connectives are most dynamically complex? The static parameter used recently does not discriminate a connective's individual complexity: $d(O, \langle T*\rangle) = d(O, \langle *T\rangle) = 0.4$ only for $O = \oplus$ and $O = \leftrightarrow$; for other connectives it equals 0.

So, it is better to look straight at the catalog of the space–time dynamic presented in Figs. 5.17 and 5.18 and compare the space–time configurations of thin-layer reactors with the integral dynamic of stirred reactors. To ease the comparison, we provided overall characteristics of the reactor dynamics in Fig. 5.19. From Figs. 5.17, 5.18 and 5.19 one can conclude that the following types of logical reactors exhibit complex behavior: (a) catalysts $\wedge$ and $\vee$ and the reaction system $\langle T*\rangle$ and (b) catalysts $\rightarrow$ and $\leftrightarrow$ and the reaction system $\langle *T\rangle$. The phenomenological complexity of connectives is shown in Fig. 5.20.

5.6 Niche of non-triviality

Just three of the nine tables of $\wedge$ correspond to a conjunction of "common" three-valued logical systems [Bolc and Borowik (1992)]. Connective $\wedge_{\langle TF\rangle}$ corresponds to $\wedge_S$ in logics of Sobociński and Belnap [Sobociński (1952); Belnap (1977)]; $\wedge_{\langle **\rangle}$ to $\wedge_B$ in logics of Bochvar, Hallden and Segerberg and the strict logic $\mathbf{S}_3$; $\wedge_{\langle *F\rangle}$ to $\wedge_H$ in logics of Heyting, Łukasiewicz and

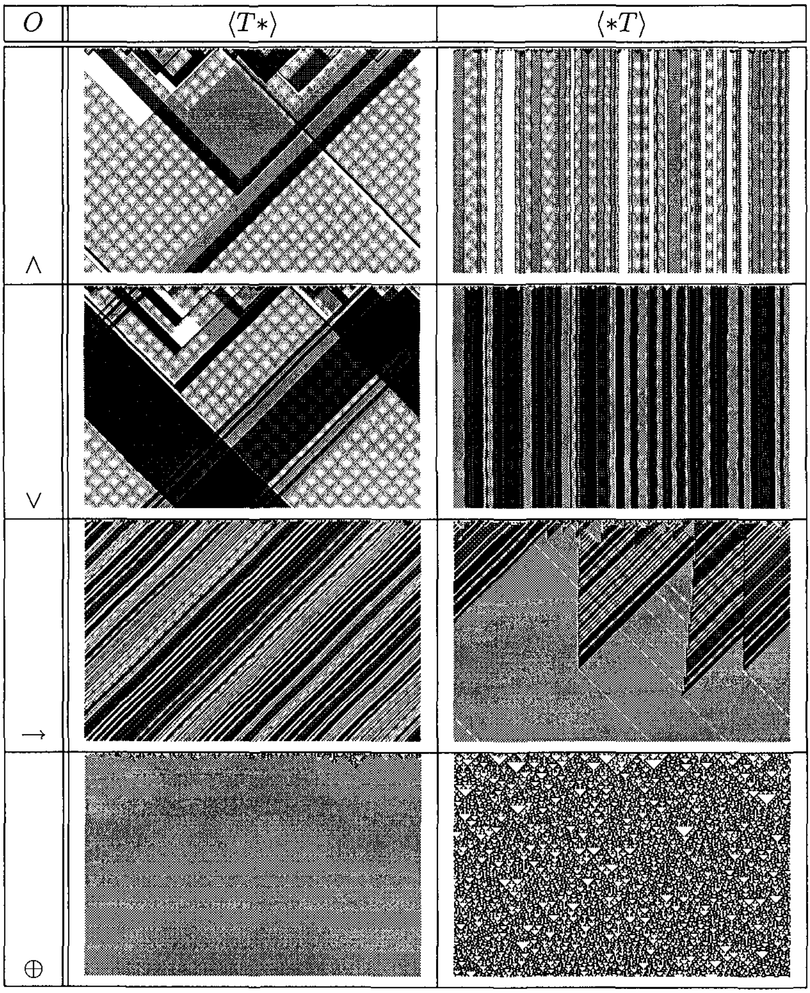

Fig. 5.17 A catalog of exemplary configurations of one-dimensional cellular-automaton models of $\rho(O, \langle T* \rangle)$ and $\rho(O, \langle *T \rangle)$, for operators $O = \wedge, \vee, \rightarrow, \oplus$, 300 cells, 200 time steps; time arrows downward.

Kleene [Łukasiewicz (1920); Kleene (1938)]:

$\wedge_S$	T	F	$*$
T	T	F	T
F	F	F	F
$*$	T	F	$*$

$\wedge_B$	T	F	$*$
T	T	F	$*$
F	F	F	$*$
$*$	$*$	$*$	$*$

$\wedge_H$	T	F	$*$
T	T	F	$*$
F	F	F	F
$*$	$*$	F	$*$

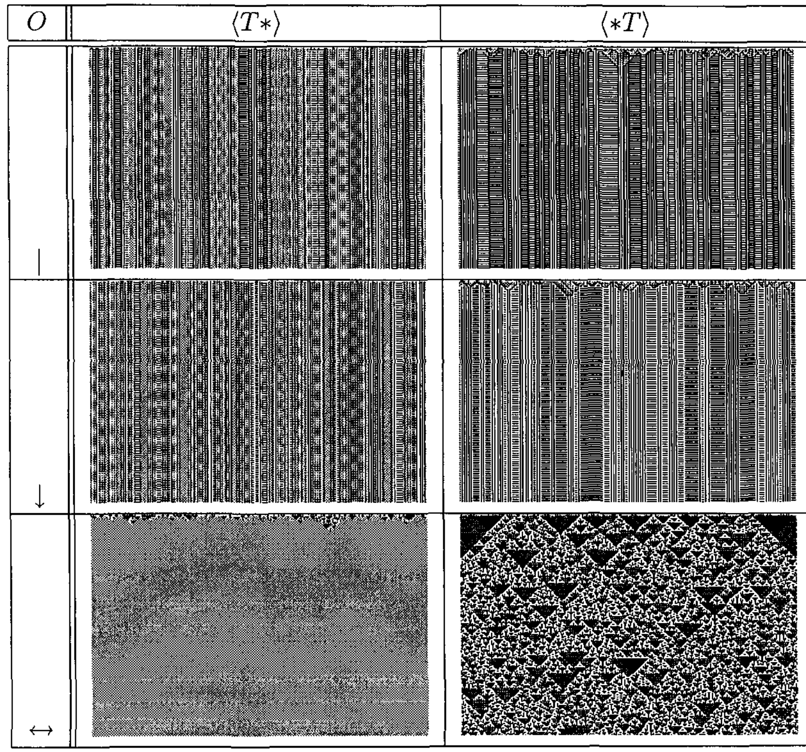

Fig. 5.18 A catalog of exemplary configurations of one-dimensional cellular-automaton models of $\rho(O, \langle T*\rangle)$ and $\rho(O, \langle *T\rangle)$, for operators $O = |, \downarrow, \leftrightarrow$, 300 cells, 200 time steps; time arrows downward.

The dynamics of artificial chemical reactors derived from these logics are quite simple. Reaction networks of the systems show that reactors $\rho(\wedge, \langle TF\rangle)$ and $\rho(\wedge, \langle *F\rangle)$, which start their development with a mixture of all three reagents, finish their evolution with a homogeneous solution of reagent F. Reactor $\rho(\wedge, \langle **\rangle)$ evolves towards a pure solution of reagent $*$.

Realistically, only a tiny portion of possible logics was considered in the chapter. Thus, for example, we restricted our study to negation of the form

x	$\neg x$
T	F
F	T
$*$	$*$

O	$\langle T* \rangle$	$\langle *T \rangle$
$\wedge$	Traveling waves	Stationary oscillations
$\vee$	Traveling waves	Stationary oscillations
$\rightarrow$	Biased mobile defects	Biased mobile defects
$\oplus$	Uniform homogeneous state	Fractal dynamic
$\mid$	Stationary oscillations	Stationary oscillations
$\downarrow$	Stationary oscillations	Stationary oscillations
$\leftrightarrow$	Uniform homogeneous state	Fractal dynamic

(a)

O	$\langle T* \rangle$	$\langle *T \rangle$
$\wedge$	Oscillations	Two stable points
$\vee$	Oscillations	Two stable points
$\rightarrow$	Oscillations	Oscillations
$\oplus$	One stable point	Oscillations
$\mid$	Two stable points	Oscillations
$\downarrow$	One stable point	Oscillations
$\leftrightarrow$	One stable point	Oscillations

(b)

Fig. 5.19 Phenomenology of artificial logical chemical systems — (a) thin-layer reactor and (b) stirred reactor — derived from the logics $\langle T* \rangle$ and $\langle *T \rangle$.

which is a typical one for Lukasiewicz, Hallden, Ånqvist and Segerberg logics. Also, we did not derive logical chemical systems based on conjunctions and Heyting $\neg_H$ or Sobociński $\neg_S$ negations:

$$\begin{array}{c|c} x & \neg_H x \\ \hline T & F \\ F & T \\ * & F \end{array} \qquad \begin{array}{c|c} x & \neg_S x \\ \hline T & F \\ F & * \\ * & T \end{array}$$

The Sobociński negation could be particularly interesting because it evokes cyclic changes of truth values, and thus may determine the oscillatory dynamic of "logical" reagents.

Reactors with just one catalyst were studied in the chapter; adding more

more complex

$\wedge, \vee$

$\rightarrow$

$|$

$\downarrow$

$\oplus, \leftrightarrow$

less complex

(a)

more complex

$\oplus, \leftrightarrow$

$\rightarrow$

$|, \downarrow$

$\wedge, \vee$

less complex

(b)

Fig. 5.20 Complexity hierarchy of connectives for oscillatory $\langle T* \rangle$ (a) and bifurcatory $\langle *T \rangle$ (b) logical systems.

catalysts may drastically change modes of the chemical logical system's dynamics. This may be yet another subject of further studies. Earlier, we briefly discussed an example of a stirred reactor $\rho(\wedge, \langle T* \rangle)$ (see Fig. 5.3), where catalyst $\vee$ has been added after some period of initial mixture development. It was demonstrated that both catalysts determine an oscillatory concentration dynamic in the reactor; however, oscillations in reactors with single catalysts occur in unlike phases (moreover, reaction networks governed by the catalysts have opposite orientations). Therefore, when the second catalyst is added to the reactor, concentration oscillations are drastically slowed down (see Fig. 5.3). This phenomenon is even more visible in a cellular-automaton model of a thin-layer reactor (Fig. 5.21): a drop of the catalyst $\vee$ is put at the center of a one-dimensional thin-layer reactor of $\langle T* \rangle$ logic filled with a mixture of $T, F, *$ and $\wedge$.

Typically the reactor $\rho(\wedge, \langle T* \rangle)$ exhibits mobile soliton-like localizations of reagent concentrations traveling along the reactor; however, diffusing $\vee$ eventually covers the whole reactor and then reactions are governed either by $\wedge$ or $\vee$, chosen at random. Resultantly, breathing and mostly homogeneous domains of T, F or $*$ are generated.

How valuable are oscillatory and bifurcatory logics? To answer this, one should construct a calculus for each logic and demonstrate that connectives represented in truth tables in Fig. 5.1 provide a decision procedure for the constructed calculi. Only then would it be right to question the significance of the newly discovered logics.

We constructed logics from negation and conjunction. The negation is somewhat "classical": if a sentence s is true then its negation is false, if s is

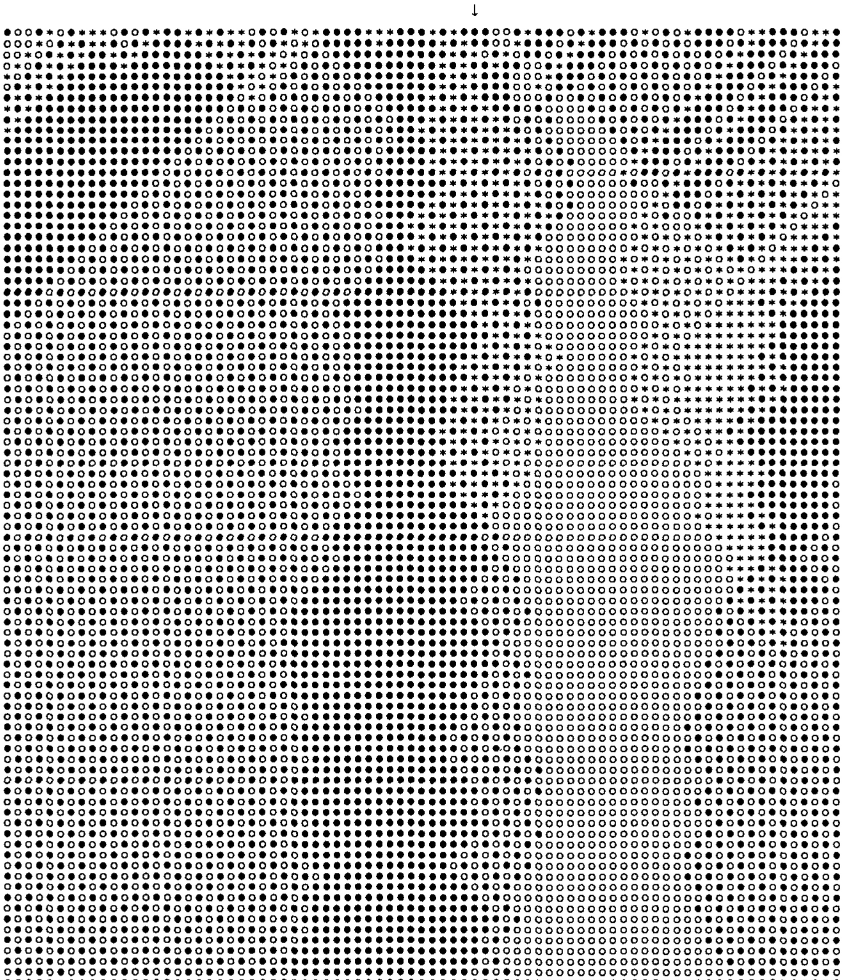

Fig. 5.21 Space–time dynamic of cellular-automaton model of a thin-layer one-dimensional reactor $(\wedge, \langle T*\rangle)$ where catalyst $\vee$ is applied (a site of initial application is shown by an arrow) and then diffuses in a substrate.

false then its negation is true; if the sentence s is neither true nor false then its negation is neither true nor false. As to the conjunction, two findings should be mentioned:

- Oscillatory conjunction: a conjunction is true only if at least one of its members is true and another member is not false; the conjunction is false if one of its members is false and another is either false or true;

- Bifurcatory conjunction: a conjunction is true only if both of its members are true or one of its members is false and another is neither false nor true; the conjunction is false if one of its members is false and another is either false or true.

The oscillatory conjunction may be seen as a "relaxed" version of a conjunction in Hallden logic [Bochvar (1939)], where the conjunction is true only if both of its members are true and it is neither true nor false if at least one of its members is neither true nor false, or a "stiffened" version of Sobociński logic [Sobociński (1952)], where a conjunction is true in the same conditions as the oscillatory conjunction but it is false if at least one of its members is false.

Most of the above applies to bifurcatory conjunction, with a difference that bifurcatory conjunction can also be treated as a modification of the "standard" conjunction of Łukasiewicz and Heyting [Łukasiewicz (1920)] three-valued logics, where a conjunction of false and undefined values is true. This modification contradicts common sense; however, this may be a good way to represent irrationality.

> "It is very possible that some of the apparently self-contradicting expressions of schizophrenia, including delusions and hallucinations, are well-formed communicative expressions of highly ordered cognitive systems and indicate truths that cannot be derived within such systems" [Snyder (1991)].

Chapter 6

Morphology of Irrationality

We simulate crowds of mental entities as pools of finite automata; we call them agents, inhabiting a two-dimensional lattice. The automata-agents do not interact with each other, no information is exchanged; however, an agent can sense the presence or absence of agents in the eight cells immediately surrounding the agent's current site. Our models represent a crowding environment leading to increasing uncertainty, cognitive load and goal interference, which may result in fear and anxiety, cognitive strain and frustration [Paulus and Nagar (1989)] and will ultimately cause emerging irrational behavior. We try to tackle irrationality via automaton models as follows. At first, we assign automaton-agents intervals of sensitivity – an agent does not like to stay in its site if the number of its neighbors belongs to some specified interval, a kind of "I don't like to be in a crowd, and I do like to be in a crowd":

> "... schizophrenic communication is characterized, and induced, by the double bind, an apparently self-contradictory form of communication" [Snyder (1991)].

Then we boost irrationality of agents by allowing them to be weirdly selective about what types of neighborhoods they do not like to stay in — an agent does not like to stay in its site if the number of neighboring agents belongs to some sub-set of integers, the choice of which has little if any justification from a common-sense point of view. Our models of irrationally behaving agents include key features of the depersonalization phenomenon, occurring in conditions of anxiety disorder and caused by overtiredness and stressfulness, indicated in [Mullen (1997)]:

- "the surroundings take on a quality of strangeness",
- "a sense of unreality pervades ... one's own cognitions and conation",

- "spatial relationships seem altered",
- "emotions ... lose their subjective impact",
- "actions appear to be carried out automatically".

6.1 Interval sensitivity

Consider a set $\mathbb{I}$ of m uniform mobile agents each incorporating a finite state control device. The agents randomly move on a two-dimensional lattice $\mathbb{L}$ in discrete time. At every time step, agent i can either move or not move to one of eight neighboring nodes of $u(c_i^t)$ relative to its node c_i^t. The neighborhood is

$$u(c_i^t) = \{v \in \mathbb{L} : \quad |v - c_i^t|_{L_\infty} = 1\}.$$

The agent moves (to one of its neighboring sites chosen at random) if there is another agent at the same node or if the number of agents in $u(c_i^t)$ lies in some specified interval $[\theta_1, \theta_2]$, $1 \leq \theta_1 \leq \theta_2 \leq 8$. At the beginning of the trial all agents are positioned at the same node c^* of the lattice.

The interval $[\theta_1, \theta_2]$ has a variety of meanings, e.g. sensitivity to the occupancy interval, interval of activation or mental representation of the neighborhood. Minimal and maximal boundaries of the activation interval are determined by the size of the neighborhood $u(c_i^t)$: eight lattice nodes are scanned by an agent to count the number of neighboring agents; $0 \leq \theta_1 \leq \theta_2 < m$ could be used as well; however, for $\theta_1 = 0$ the automata pool will never be at rest because every automaton will change its position at every step of evolution time. Therefore, we made $\theta_1 \geq 1$. If there are more than eight agents in the neighborhood of another agent then at least two of the neighboring agents occupy the same lattice node and they will change their positions at the next step of simulation time. Only the condition $1 \leq \theta_1 \leq \theta_2 \leq 8$ guarantees that every node contains at most one agent in a final stationary configuration of the crowd. Where is the relation to non-sense and bizarre behavior?

> Interval $[\theta_1, \theta_2]$ represents the "double-bind" [Bateson *et. al* (1956)] situation, which may cause a person to develop schizophrenia.

The interval model of irrational behavior possesses all necessary ingredients for the double-bind situation, as outlined in [Bateson *et. al* (1956)]:

- more than one person: there are hundreds of automaton-agents in the model,

- a repeated experience of contradictory situations,
- a primary negative injunction, e.g. "Do not do so and so, or I will punish you" or an old lady throwing a knife to her little granddaughter" [Bateson *et. al* (1956)]: lower boundary θ_1 of the interval meaning "I do not want to be in a group with more than θ_1 agents",
- a secondary injunction conflicting with the first injunction, e.g. "Do not see this as punishment" or "Grandmommy really loves you" [Bateson *et. al* (1956)]: upper boundary θ_2 of the interval meaning "I do not want to be in a group with less than θ_2 agents",
- a tertiary negative injunction prohibiting escape from the field: in our model an agent does not want to move unless it is "absolutely necessary".

A brilliant example of a double-bind situation is provided in [Bateson *et. al* (1956)]:

> "A young man who had fairly well recovered from an acute schizophrenic episode was visited in the hospital by his mother. He was glad to see her and impulsively put his arm around her shoulders, whereupon she stiffened. He withdrew his arm and she asked, "Don't you love me any more?". He then blushed, and she said, "Dear, you must not be so easily embarrassed and afraid of your feelings" ".

Moreover, the width of the sensitivity interval $[\theta_1, \theta_2]$ may be seen as proportional to a degree of irrationality. Therefore, a zone of "maximal" irrationality (if such ever exists!) is at a diagonal of the interval table.

In early papers [Adamatzky *et. al* (1999c); Adamatzky *et. al* (1999a); Adamatzky *et. al* (1999b)] we have studied various types of automaton-agent collectives, including hypo-active crowds where all agents check their neighborhoods in a cycle with period m; hyper-active crowds where all agents check their neighborhoods once every time step; and stochastically asynchronous crowds, which are a kind of transient species. The behavior of agent i in all three models is governed by the equation

$$c_i^{t+1} = c_i^t + \mathbf{d} \cdot \zeta(\alpha_i^t, \beta_i^t, \theta_1, \theta_2) \cdot \eta,$$

where $\alpha_i^t = |\{j \in \mathbb{I} : c_i^t = c_j^t\}|$ is the number of agents at the node c_i^t, occupied at least by agent i, $\beta_i^t = |\{j \in \mathbb{I} : c_j^t \in u(c_i^t)\}|$ is the number

of agents at the nodes of agent i's neighborhood $u(c_i^t)$, $\mathbf{d}$ is a random variable from $\{-1,0,1\} \times \{-1,0,1\}$, i.e. the vector of translation, and $\zeta(\alpha_i^t, \beta_i^t, \theta_1, \theta_2)$ is a decision function; agents of all classes use the same function $\zeta(\cdot)$. η is an activity function. The function η is responsible for a decision to check the neighborhood, whereas the function $\zeta(\cdot)$ participates in the final decision to move. The function $\zeta(\cdot)$ is defined below:

$$\zeta(\alpha_i^t, \beta_i^t, \theta_1, \theta_2) = 1 \text{ if } \alpha_i^t > 0 \text{ or } \beta_i^t \in [\theta_1, \theta_2]; \zeta(\alpha_i^t, \beta_i^t, \theta_1, \theta_2) = 0 \text{ otherwise.}$$

The function η is a key item which makes a difference between the three classes. In hyper-active crowds, call them P-crowds, η is a constant 1, so an agent's equation of motion is simplified to

$$c_i^{t+1} = c_i^t + \mathbf{d} \cdot \zeta(\alpha_i^t, \beta_i^t, \theta_1, \theta_2).$$

In hypo-active agent pools, call them S-crowds, $\eta = \eta(i,t) = 1$ if $i = t \mod m$; $\eta(i,t) = 1$, otherwise; so an agent's equation of motion looks as follows (χ is a sign function):

$$c_i^{t+1} = c_i^t + \mathbf{d} \cdot \zeta(\alpha_i^t, \beta_i^t, \theta_1, \theta_2) \cdot \chi(1 - |i - (t \mod m + 1)|).$$

In transitory asynchronously disordered crowds, A-crowds, $\eta = \rho$, where ρ is a random variable that takes a value of 1 with probability p_ρ, $\epsilon \leq p_\rho \leq 1$, where ϵ is very small, and it takes a value of 0 with probability $1 - p_\rho$; $\epsilon = 0.001$ in computer experiments. Variable p_ρ is a degree of the crowd's unrest — the greater p_ρ, more agents decide to check their neighborhood and, possibly, change their positions at each time step. Assuming that agents have random independent delays of switching, there is, therefore, a probabilistic continuum between S-crowds and P-crowds.

Functions ζ and η determine such types of crowd activity that crowds ultimately finish their development in stationary configurations where no agents move: $\exists t_c < \infty \quad \forall i \in \mathbb{I} \quad \forall t \geq t_c : c_i^t = c_i^{t+1}$. That is, after some step t_c of development all agents are motionless; they will continue checking their neighborhoods but their inspections will always bring satisfactory results. We will call t_c the convergence time. The convergence time is finite, due to finite m, and it is determined by the particular values of θ_1 and θ_2 and, obviously, the size m of a crowd.

For all types of crowds studied in this chapter a condition is always reached when there is no further movement of any agent. This is referred to as a stationary global state.

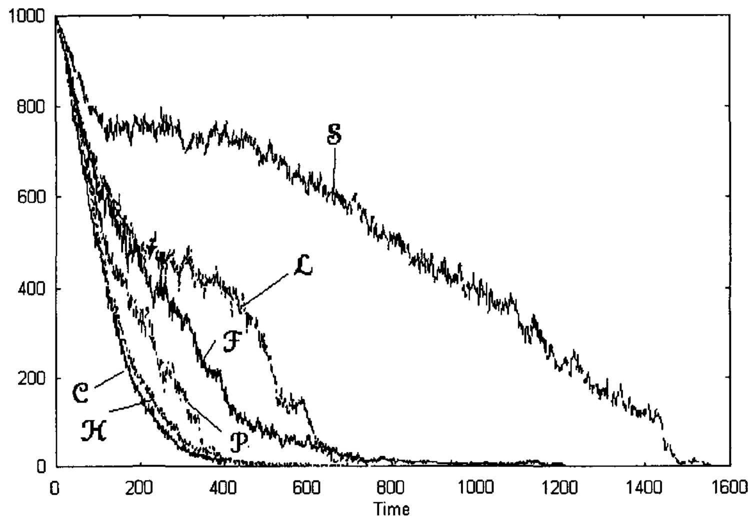

Fig. 6.1 Examples of "activity" of agents in the development of crowds from different classes. The vertical axis represents the number of automaton-agents which change their positions at the current step of the development. Time is measured along the horizontal axis. The labels indicate the rule classes, which will be discussed later.

Figure 6.1 illustrates the process of convergence for different rule classes of an S-crowd. Analysis of the activity patterns of crowds, which are measured by the number of agents which change their positions at the current time step, convinces us that lower, θ_1, and upper, θ_2, bounds of the intervals significantly influence the rate of convergence to the stationary global state. Hereinafter, we use term "pattern", which refers to a finite sub-lattice $\Upsilon(L)$ of $\mathbf{L}$, where every node takes the value 1 if there is an agent at the node, and value 0 if there is no agent at the node. The pattern is determined after the crowd converges to the stationary global state.

6.2 Morphological classification

To split functions determined by a sensitivity interval into classes of morphological equivalence, we employ three basic characteristics: size, order and density. The set of all possible activation functions can be sub-divided into several classes based on the morphological characteristics of the patterns formed. We assume that two functions are in the same class if, for a lattice crowd composed of agents obeying the functions, the same resulting

structure is created. A similarity of two patterns is detected visually and verified with various measures such as the density distribution of agents and a measure of order.

A size r of a pattern measures a diameter of the set of non-zero entries of $\Upsilon(L)$, i.e. a maximum distance between any two agents. An ω-order is calculated as $\omega = \max\{\omega_H, \omega_V\}$, where ω_H and ω_V denote the number of local configurations of the form

$$\begin{array}{ccc} \circ & \bullet & \circ \\ \circ & \odot & \circ \\ \circ & \bullet & \circ \end{array} \quad \text{and} \quad \begin{array}{ccc} \circ & \circ & \circ \\ \bullet & \odot & \bullet \\ \circ & \circ & \circ \end{array}$$

Agents are shown by $\bullet$s and $\odot$s and lattice nodes without agents are blank; the agent based at the central node of the neighborhood is shown by $\odot$. For any pattern formed by m agents we have $0 \leq \omega \leq m - 2$. The measure takes its maximum on the line of agents, where agents are arranged along the column or the row; and it takes its minimum on either densely packed or sparse patterns. Later, we will discuss that ω-order takes its maximum, amongst all patterns, on fingerprint patterns generated by S-crowds. Such patterns may be considered as highly structured. Every agent in the fingerprint pattern has exactly two neighboring agents which are always in the same column or the same row.

A density distribution is calculated as $\mathbf{D} = (D_i)_{0 \leq i \leq 8}$, where

$$D_i = \left|\{j \in \mathbb{I} : \left|\{z \in \mathbb{I} : |s_z^t - s_j^t| = 1\}\right| = i\}\right|.$$

Given a stationary pattern of the agents' density distribution, $(D_i)_{0 \leq i \leq 8}$ is a vector, the ith entry of which represents the number of agents each of which has exactly i other agents in its neighborhood.

The morphological classification provided in this section is based on computer experiments with hypo-active S- and hyper-active P-crowds, of 10^3 to 10^4 agents. Several morphological classes were identified in S- and P-crowds.

Further, we will refer to the rules of a class in the sense of the activation intervals $[\theta_1, \theta_2]$; the exact values of the intervals and, therefore, rules, can be found in Fig. 6.2. Thus, for example, rules of the $\mathcal{C}$-class correspond to the intervals $[1,1]$, $[1,2]$, $[2,2]$ and $[3,3]$ in an S-crowd; the rules of the $\mathcal{P}$-class have activation intervals $[7,7]$, $[7,8]$ and $[8,8]$ in both S- and P-crowds (Fig. 6.2).

6.2.1 *Hyper-sociality: $\mathcal{C}$-class*

The rules of this class generate condensed patterns (Fig. 6.3a).

	θ_2: 1	2	3	4	5	6	7	8
θ_1 1	$\mathcal{C}$	$\mathcal{C}$	$\mathcal{H}$	$\mathcal{S}$	$\mathcal{S}$	$\mathcal{S}$	$\mathcal{S}$	$\mathcal{S}$
2		$\mathcal{C}$	$\mathcal{H}$	$\mathcal{S}$	$\mathcal{S}$	$\mathcal{S}$	$\mathcal{S}$	$\mathcal{S}$
3			$\mathcal{C}$	$\mathcal{L}$	$\mathcal{L}$	$\mathcal{L}$	$\mathcal{L}$	$\mathcal{L}$
4				$\mathcal{H}$	$\mathcal{L}$	$\mathcal{L}$	$\mathcal{L}$	$\mathcal{L}$
5					$\mathcal{L}$	$\mathcal{F}$	$\mathcal{F}$	$\mathcal{F}$
6						$\mathcal{L}$	$\mathcal{F}$	$\mathcal{F}$
7							$\mathcal{P}$	$\mathcal{P}$
8								$\mathcal{P}$

(a)

	θ_2: 1	2	3	4	5	6	7	8
θ_1 1	$\mathcal{Y}$	$\mathcal{Y}$	$\mathcal{S}$	$\mathcal{S}$	$\mathcal{S}$	$\mathcal{S}$	$\mathcal{S}$	$\mathcal{S}$
2		$\mathcal{Y}$	$\mathcal{S}$	$\mathcal{S}$	$\mathcal{S}$	$\mathcal{S}$	$\mathcal{S}$	$\mathcal{S}$
3			$\mathcal{L}$	$\mathcal{L}$	$\mathcal{L}$	$\mathcal{L}$	$\mathcal{L}$	$\mathcal{L}$
4				$\mathcal{L}$	$\mathcal{L}$	$\mathcal{L}$	$\mathcal{L}$	$\mathcal{L}$
5					$\mathcal{L}$	$\mathcal{L}$	$\mathcal{L}$	$\mathcal{L}$
6						$\mathcal{L}$	$\mathcal{L}$	$\mathcal{L}$
7							$\mathcal{P}$	$\mathcal{P}$
8								$\mathcal{P}$

(b)

Fig. 6.2 Interval → class correspondence for S-crowd (a) and P-crowd (b).

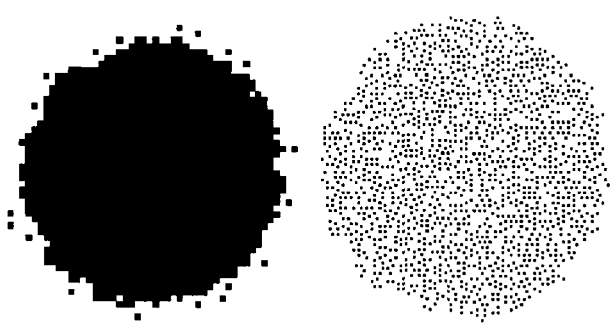

(a) (b)

Fig. 6.3 Representative patterns of classes $\mathcal{C}$ (a) and $\mathcal{S}$ (b).

Almost every agent has its neighborhood fully packed with other agents (Fig. 6.4a), i.e. almost every agent has exactly one other agent in each of eight neighboring nodes. There are very few agents with an empty neighborhood. The distribution **D** is preserved for all intervals $[\theta_1, \theta_2]$ belonging to the class with slight spreading towards lower densities when the transition from intervals $[1, 2]$ to $[3, 3]$ occurs. The patterns are solid-like. Such patterns are typical only for an S-crowd.

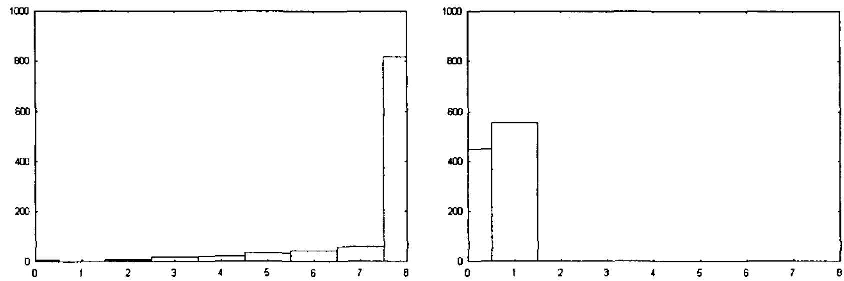

(a) (b)

Fig. 6.4 Examples of distribution **D** of numbers of neighboring agents in the patterns generated in $\mathcal{C}$-class (a) and $\mathcal{S}$-class (b) of an S-crowd.

6.2.2 *Autistic dissolution: $\mathcal{S}$-class*

The rules generate sparse patterns (Fig. 6.3b). As Zimbardo proposes:

> "At extreme levels, [AA: of deindividuation] the group dissolves as its members become autistic in their impulse gratification" [Zimbardo (1969)].

The members of the class, $\theta_1 \in \{1,2\}, 4 \leq \theta_2 \leq 8$ for an S-crowd and $\theta_1 \in \{1,2\}, 3 \leq \theta_2 \leq 8$ for a P-crowd, do not depend on the degree of activity. For both S- and P-crowds the class can be sub-divided into two sub-classes following density distributions **D** (see e.g. Fig. 6.4b), $[1,4],\ldots,[1,8]$ and $[2,4],\ldots,[2,8]$. Thus, for $\theta_1 = 1$, almost all agents have an empty neighborhood. In contrast, for $\theta_1 = 2$, more than one-half of the agents have exactly one other agent in their neighborhood, while others have none. That is, the increasing of the lower bound θ_1 of the activation interval from $\theta_1 = 1$ to $\theta_1 = 2$ causes an overall "compression" effect of the patterns in the S-class.

6.2.3 *Segregation: $\mathcal{H}$-class*

The rules generate so-called halo patterns (Fig. 6.5a), i.e. patterns that have a condensed core with a sparse halo around it. The patterns can be generated only in an S-crowd. The vast majority of the agents have a fully packed neighborhood but a certain amount of the outsiders with less

crowded neighborhoods is also present. The halo is formed from the agents that have an empty neighborhood (for [1,3] interval), one or two (for [2,3] interval) or two or three (for [4,4] interval) other agents in their vicinity (Fig. 6.6a).

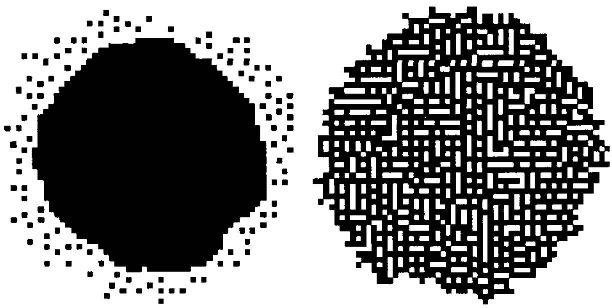

(a) (b)

Fig. 6.5 Representative patterns of classes $\mathcal{H}$ (a) and $\mathcal{P}$ (b).

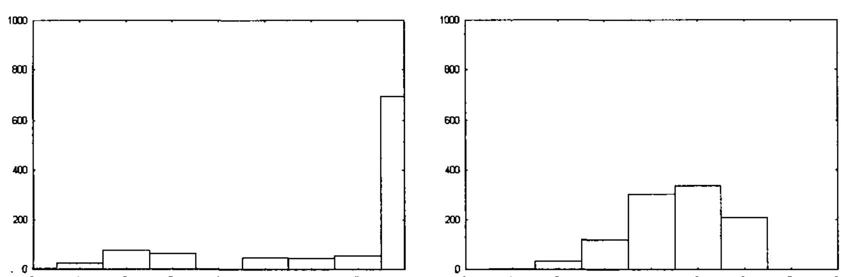

(a) (b)

Fig. 6.6 Examples of distribution **D** of numbers of neighboring agents in the patterns generated in $\mathcal{H}$-class (a) and $\mathcal{P}$-class (b) of an S-crowd.

The patterns are evocative of melting ice; so, we may think of them as two-phase transitional structures. Actually they are transitional, because they are at the boundary between condensed, $\mathcal{C}$-, and sparse, $\mathcal{S}$-, classes on the θ_1–θ_2 plane (Fig. 6.2).

6.2.4 *Socialization: $\mathcal{P}$-class*

The rules generate so-called porous patterns (Fig. 6.5b).

The patterns appear both in S- and P-crowds (Fig. 6.2). The most expressive representative looks like a mesh with a space of variable length but a width of one lattice node (Fig. 6.5b).

A transition from the interval $[7,7]$ to $[7,8]$ to $[8,8]$ shifts the maximum of the distribution $\mathbf{D}$ from four to five to six agents, respectively (Fig. 6.6b).

6.2.5 *Brewing of structure: $\mathcal{Y}$-class*

The rules generate an overall porous pattern with some condensed regions, large holes of an empty lattice nodes inside and a small halo outside (Fig. 6.7a). They vary in appearance but a meristema-like structure is common for all of them. They are typical for a P-crowd only and occupy the same place on the θ_1–θ_2 plane as $\mathcal{P}$-rules of an S-crowd. The distribution $\mathbf{D}$ has its maxima at five and six agents (Fig. 6.8a).

6.2.6 *Structuring crowds: $\mathcal{L}$-class*

The rules generate labyrinthine patterns (Fig. 6.7b). They look like classical labyrinthine patterns obtained in the laboratory and computer experiments with diffusive systems, magnetic domains, chemicals on the surface of catalysts, etc. The chains of resting agents, that form the walls of a labyrinth, have many turns and free-standing ends. By varying the boundaries of the activation interval $[\theta_1, \theta_2]$ we can achieve a shift of the distribution towards an increasing number of agents in the neighborhood of an agent (Fig. 6.8b).

The patterns generated by the rules of the class are the most varied in structure amongst other patterns; however, they are very typical for both S- and P-crowds (Fig. 6.2).

6.2.7 *Ordered crowds: $\mathcal{F}$-class*

The rules generate fingerprint-like patterns (Fig. 6.7c). They can be found only in S-crowds (Fig. 6.2). Every pattern is sub-divided into a small number of large domains with either vertical or horizontal orientation of agent chains. In general, there are few instances when the boundary between one domain and another is open. Typically, we cannot easily move from one domain to another. More than one-half of all agents have exactly two neighbors each (Figs. 6.7c and 6.8c $[6,8]$). They are the agents that have a

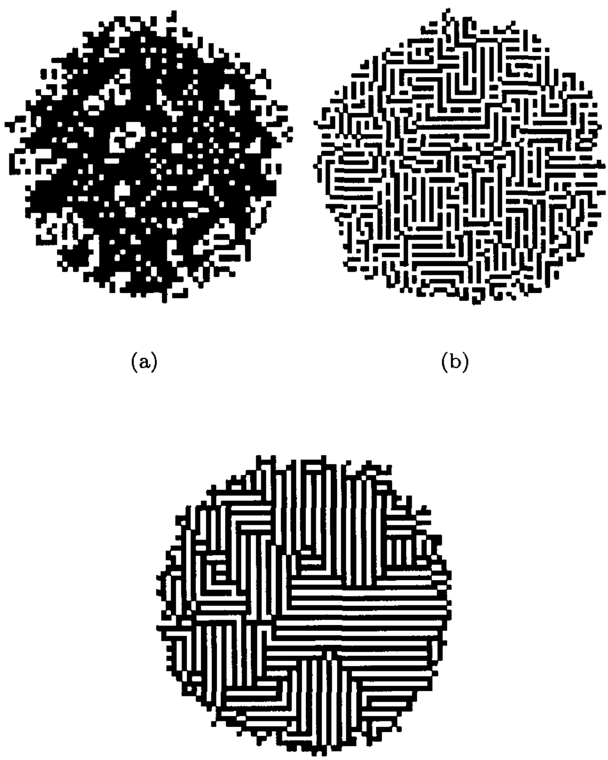

(a) (b)

(c)

Fig. 6.7 Representative patterns of classes $\mathcal{Y}$ (a), $\mathcal{L}$ (b) and $\mathcal{F}$ (c).

neighborhood configuration of the following form:

$$\begin{array}{ccc} \circ & \bullet & \circ \\ \circ & \bullet & \circ \\ \circ & \bullet & \circ \end{array}$$

Other agents have either three neighboring agents, the corresponding local configuration is

$$\begin{array}{ccc} \circ & \bullet & \circ \\ \bullet & \bullet & \bullet \\ \circ & \circ & \circ \end{array}$$

or four neighboring agents, the corresponding local configuration being as follows:

$$\begin{array}{ccc} \circ & \bullet & \circ \\ \circ & \bullet & \circ \\ \bullet & \bullet & \bullet \end{array}$$

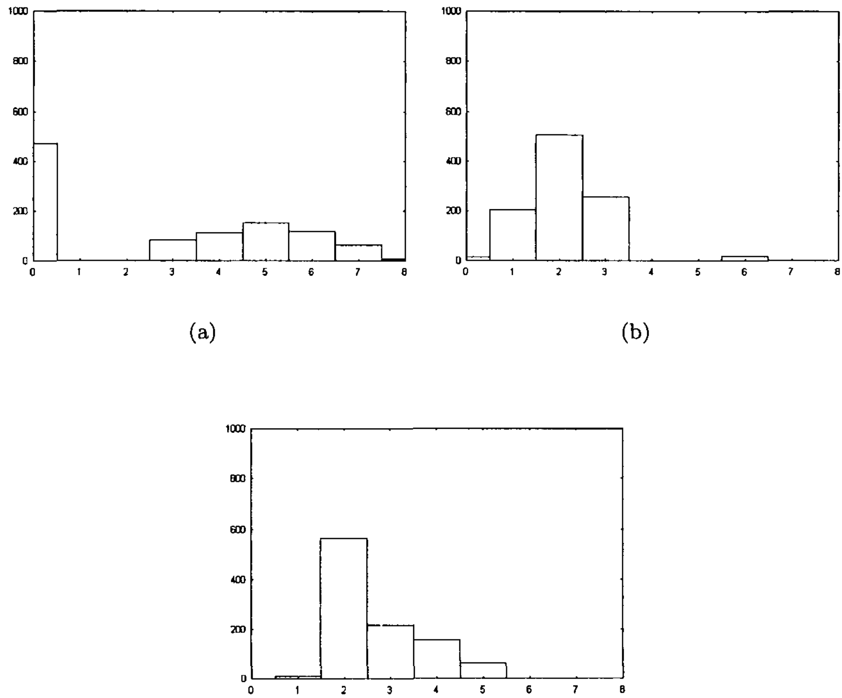

(a) (b) (c)

Fig. 6.8 Examples of distribution $\mathbf{D}$ of numbers of neighboring agents in the patterns generated in $\mathcal{Y}$-class (a) of $\mathcal{P}$-crowd, and $\mathcal{L}$-class (b) and $\mathcal{F}$-class (c) of S-crowd.

The agents being on the boundaries of the pattern make an incursion into other small parts of the density distribution $\mathbf{D}$ (Fig. 6.8c).

6.3 Time, size and order

In computer experiments with crowds of $m = 1$–10^3 agents we found that the size $r = r(m)$ of the pattern generated in the development of a crowd of m agents is approximated as $r(m) = \sqrt{\gamma_r m}$, $\gamma_r = \gamma_r(\theta_1, \theta_2)$. The convergence time $t_c = t_c(m)$ is approximated by $t_c(m) = \gamma_t m$, $\gamma_t = \gamma_t(\theta_1, \theta_2)$. To represent the results in a qualitative form we consider an 8×8 matrix, hereinafter referred to as a θ-lattice. This is indexed by pairs (θ_1, θ_2),

$1 \le \theta_1 \le \theta_2 \le 8$. When dealing with time, size and order we assign the corresponding values of $\gamma_t(\theta_1, \theta_2)$, $\gamma_r(\theta_1, \theta_2)$ and $\omega(\theta_1, \theta_2)$ to the nodes of the θ-lattice. After that, we build "gradient-like fields" on the lattice. Every node x of the θ-lattice is assigned a vector oriented towards the neighbor y which gains the maximal value of $\gamma_t(x)$, $\gamma_r(x)$ and $\omega(x)$ amongst all other neighbors of x. The vector in x has null length if x itself has the maximum value in $u(x)$. It is possible to have more than one vector in x if more than one node in $u(x)$ has the same maximum value. The sinks of the fields are called the attractors. The elements which are neither maximal nor minimal may be thought of as sources.

6.3.1 *Size*

	θ_2							
	1	2	3	4	5	6	7	8
1	$\rightarrow$	$\rightarrow$	$\rightarrow$	$\bullet$	$\bullet$	$\bullet$	$\bullet$	$\bullet$
2	$\nearrow$	$\nearrow$	$\nearrow$	$\uparrow$	$\uparrow$	$\uparrow$	$\uparrow$	$\uparrow$
3	$\nearrow$	$\nearrow$	$\nearrow$	$\uparrow$	$\uparrow$	$\uparrow$	$\uparrow$	$\uparrow$
θ_1 4	$\circ$	$\nearrow$	$\nearrow$	$\nearrow$	$\uparrow$	$\uparrow$	$\uparrow$	$\uparrow$
5	$\circ$	$\circ$	$\nearrow$	$\nearrow$	$\uparrow$	$\uparrow$	$\uparrow$	$\uparrow$
6	$\circ$	$\circ$	$\circ$	$\nearrow$	$\nearrow$	$\uparrow$	$\uparrow$	$\uparrow$
7	$\circ$	$\circ$	$\circ$	$\circ$	$\nearrow$	$\nearrow$	$\uparrow$	$\uparrow$
8	$\circ$	$\circ$	$\circ$	$\circ$	$\circ$	$\nearrow$	$\nearrow$	$\uparrow$

Fig. 6.9 Convergence-time-based γ_r-field for S- and P-crowds. Values of $t_c(\theta_1, \theta_2)$ are quite close for both types of crowds; differences do not exceed 0.1.

A γ_r-field is represented in Fig. 6.9. A family of rules $\theta_1 = 1, \theta_2 = 4$–$8$ of the S-class represents the perfect global attractors in the γ_r-field. We also found that

> a lower bound of agent activation, θ_1, determines the size of the generated patterns in both S- and P-crowds.

This is correct for the following domains of $\gamma_r(\theta_1, \theta_2)$:

- S-crowd: $\theta_2 \ge 5$, $1 \le \theta_1 \le 8$ and $\theta_2 = 4$, $\theta_1 = 1, 2, 3$;
- P-crowd: $\theta_3 \ge 3$ and $1 \le \theta_1 \le 8$.

6.3.2 *Convergence*

θ_1 \ θ_2	1	2	3	4	5	6	7	8
1	→	→	→	•	←	←	←	←
2	↗	↗	↗	↑	↖	↖	↖	↖
3	∘	↗	↗	↑	↖	↖	↖	↖
4	∘	↗	↗	↑	↖	↖	↖	↙
5	∘	∘	↗	↑	⊙	↘	↓	↙
6	∘	∘	∘	↗	↑	→	•	←
7	∘	∘	∘	∘	↗	↗	↑	↖
8	∘	∘	∘	∘	∘	↗	↑	←

(a)

θ_1 \ θ_2	1	2	3	4	5	6	7	8
1	↘	→	•	←	←	←	•	•
2	→	↗	↑	↖	↖	↖	↑	↖
3	↗	↗	↑	↖	↖	↖	↖	↖
4	∘	↗	↑	↖	↖	↖	↖	↖
5	∘	∘	↗	↑	↑	↖	↖	↖
6	∘	∘	∘	↗	↑	↖	↖	↖
7	∘	∘	∘	∘	↗	↑	↖	↖
8	∘	∘	∘	∘	∘	↗	↑	↑

(b)

Fig. 6.10 γ_t-fields for S-crowd (a) and P-crowd (b); $t_c(1,3) = 2.65$ for P-crowd, $t_c(1,4) = 2.8$ and $t_c(6,7) = 1.28$ for S-crowd.

A structure of the γ_t-field differs in S- and P-crowds (Fig. 6.10). In the S-crowd there are two attractors: $\gamma_t(1,4) = 2.8$ and $\gamma_t(6,7) = 1.28$; the first is a global attractor because $\gamma_t(6,7)$ dominates only in the domain ($\theta_1 = 5$–7; $\theta_2 = 6$–8). The node $\gamma_t(1,3) = 2.65$ is an attractor in the γ_t-field for the P-crowd whereas $\gamma_t(1,\theta_2) = 2.25$, $\theta_2 = 6$–8, are local attractors. Both two maxima correspond to rules of the $\mathcal{S}$-class. This means that

the crowds that generate sparse uniform patterns have the longest transient periods.

It does contradict the conjecture, quite popular now, stating that complex patterns are generated by the systems with long transient periods.

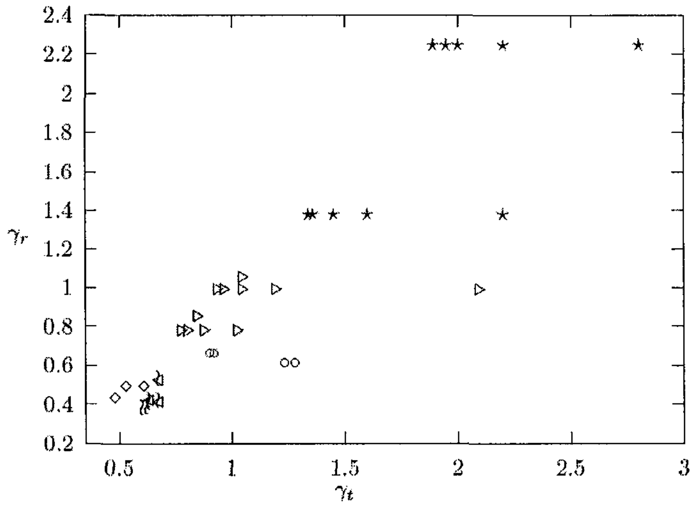

Fig. 6.11 Distribution of the classes in $\gamma_t - \gamma_r$ map for S-crowd. The following symbols are used: $\diamond$ — $\mathcal{P}$-class, $\wr$ — $\mathcal{C}$-class, $\triangleleft$ — $\mathcal{H}$-class, $\circ$ — $\mathcal{F}$-class, $\triangleright$ — $\mathcal{L}$-class, $\star$ — $\mathcal{S}$-class.

If we look at the $\gamma_r - \gamma_t$ map (Fig. 6.11) we find that rules from all classes except the $\mathcal{S}$-class form quite recognizable clusters. It is especially expressive for $\mathcal{L}$-, $\mathcal{C}$- and $\mathcal{P}$-classes. The overall distribution of the rules shows that we can roughly split the map into three regions. The first region includes the $\mathcal{P}$-, $\mathcal{C}$- and $\mathcal{H}$-classes (Fig. 6.11, $\gamma_r < 0.6$ and $\gamma_t < 0.75$). This is a domain of the rules which generates condensed patterns. The second region (Fig. 6.11, $0.6 \leq \gamma_r \leq 1$) includes $\mathcal{F}$- and $\mathcal{L}$-classes. This is a domain of the rules which generates structured patterns. And, the last region (Fig. 6.11, $\gamma_r \geq 1.2$, $\gamma_t \geq 1.3$) consists of the rules of the $\mathcal{S}$-class. These rules generate the sparse homogeneous patterns.

6.3.3 *Order*

There are two attractors in the ω-field of the S-crowd (Fig. 6.12a). They are $\omega(5,7) = \omega(6,8) = 0.69$. $\omega(5,7) = 0.25$ is the only sensible attractor for the P-crowd (Fig. 6.12b). All attractors correspond to the rules of the

(a)

θ_1 \ θ_2	1	2	3	4	5	6	7	8
1	↘	↓	↙	↙	○	○	○	○
2	→	↘	↘	↓	↓	↘	↘	↙
3	↗	→	→	↘	↘	↘	↘	↓
4	○	↗	↗	→	↘	↓	↓	↙
5	○	○	↗	↗	→	→	●	←↓
6	○	○	○	↗	↗	↗	↑→	●
7	○	○	○	○	↗	↗	↗	↑
8	○	○	○	○	○	↗	↗	↑

(b)

θ_1 \ θ_2	1	2	3	4	5	6	7	8
1	●	←	↙	○	○	○	○	○
2	↑	↖	↓	↘	↓	↙	↘	↓
3	↗	→	↘	↘	↓	↙	↙	↓
4	○	↗	→	↘	↘	↘	↓	↙
5	○	○	↗	→	→	→	●	←
6	○	○	○	↗	↗	↗	↑	↖
7	○	○	○	○	↗	↗	↑	↖
8	○	○	○	○	○	↗	↗	↑

Fig. 6.12 ω-fields for S-crowd (a) and P-crowd (b); $\omega(5,7) = \omega(6,8) = 0.69$ for S-crowd, $\omega(1,1) = 0.1$ and $\omega(5,7) = 0.25$ for P-crowd.

$\mathcal{F}$-class; the rules generate most important ordered patterns (Figs. 6.2 and 6.12). The domains of the ω-field corresponding to the $\mathcal{S}$-class are sources: they gain zero values of $\omega(\theta_1, \theta_2)$.

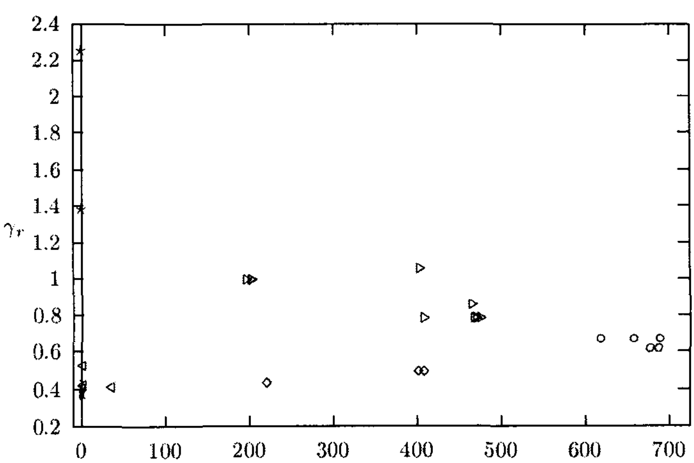

Fig. 6.13 Distribution of the classes in $\gamma_r - \omega$ map for S-crowd. The following symbols are used: ◇ — $\mathcal{P}$-class, ≀ — $\mathcal{C}$-class, ◁ — $\mathcal{H}$-class, ○ — $\mathcal{F}$-class, ▷ — $\mathcal{L}$-class, ⋆ — $\mathcal{S}$-class. Data obtained in an experiment with S-crowds of $m = 1000$ agents.

It is hard to find any clusters of the rules in the $\gamma_r - \omega$ map. Only rules

of the $\mathcal{F}$-class form easily recognizable clusters (Fig. 6.13).

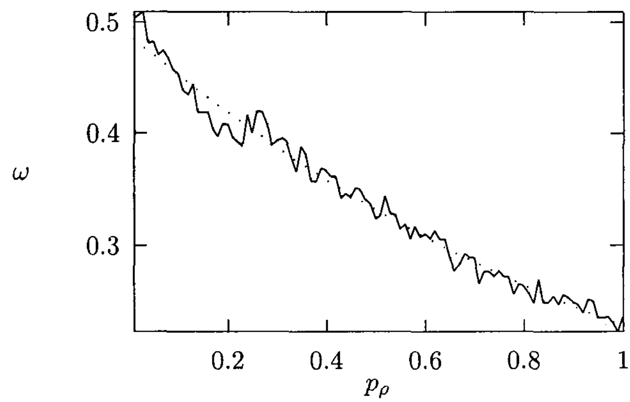

Fig. 6.14 Order ω versus degree of activity p_ρ, computed for the crowd of $m = 10^3$ agents.

Are there any dependences between the order of the patterns and the probability of activation p_ρ? To get an answer, we gradually vary the probability p_ρ from close to a zero value to the value 1, and measure the ω-order for every increment of p_ρ. By doing this, we discover the following (see example in Fig. 6.14):

- Amongst the patterns generated by S- and P-crowds those generated by P-crowds are the least structured.
- The degree of order is inversely proportional to the degree of activity.

This relationship has quite a simple explanation. In the models of agents acting in parallel, almost all the agents check the states of their neighborhoods simultaneously. They make decisions to stay where they are or to move at one of randomly chosen nodes at the same time altogether. So, they do not monitor the situation closely and can simply destroy emerging structures. If agents are hypo-active, and act one by one, as in the model of the S-crowd, they do not interfere one with another, and can form strips of inactive agents, which coherently produce fingerprint- and labyrinth-like patterns. The explanation of this reduction of order, correct for at least some members of the $\mathcal{F}$-class, may be found in the following idealistic example of the S-crowd, $\theta_1 = 6$ and $\theta_2 = 8$. Consider an infinite domain with a vertical orientation, where a node with an agent is black and an empty

node is blank as shown in the scheme below:

$$\begin{array}{c}
\cdots \\
\cdots\ \circ \bullet\ \ \circ\ \ \bullet \circ \bullet\ \cdots \\
\cdots\ \circ \bullet\ \ \circ\ \ \bullet \circ \bullet\ \cdots \\
\cdots\ \circ \bullet\ \ \circ\ \ \bullet \circ \bullet\ \cdots \\
\cdots\ \circ \bullet\ \ \circ\ \ \bullet \circ \bullet\ \cdots \\
\cdots\ \circ \bullet\ \ \circ\ \ \bullet \circ \bullet\ \cdots \\
\cdots\ \circ \bullet\ \ \circ\ \ \bullet \circ \bullet\ \cdots \\
\cdots
\end{array}$$

Every empty node in the domain has six agents around it, three on the left and three on the right. At the same time, every agent in such a domain has exactly two other agents around it. Moreover, all its neighbors are in the same column as the agent under consideration. Let us "drop" one agent j into the domain. It will land on either an empty node or on the resting agent. If agent j drops onto an empty node then it has six neighbors and will decide to move because its activation interval is $[6, 8]$.

Notice that in this situation the stationary agents will rest because each of them has four neighboring "spare" nodes which can be filled by other agents. If agent j moves onto another previously empty node the situation will be the same again. Let it move to one of the nodes occupied by the agent i. In the S-crowd agents check their neighborhoods and their own nodes in the cycle of period m; therefore, either agent i or j will decide to move while the other agent will remain at the same node. So, the structure of the agent chain is preserved. However, the probability of the destruction of the chain will increase proportionally with the degree of activity of the agents, i.e. p_ρ.

6.4 Rational choice and threshold of activation

If one tries to go to places with a certain, peculiarly chosen, number of people, that seems to be a weird habit. Such a habit however generates quite rich morphologies of crowd formations. It may be more reasonable, we would say rational, to find a place where the number of people is less than or higher than some specified number. We are talking now about a threshold of activation. Let us assume that agent i of a crowd decides to change its position if there is another agent at the same node or if a number of other agents in the neighborhood of i exceeds some specified threshold. In this case, it is enough to consider intervals $[\theta_1, \theta_2]$, where $1 \leq \theta_1 \leq 8$, $\theta_2 = 8$ and θ_1 is the threshold.

From Fig. 6.15 we see that while the threshold θ_1 increases, the patterns generated by crowds are more and more condensed. Somewhere between the entirely sparse patterns and the condensed porous patterns, we find the

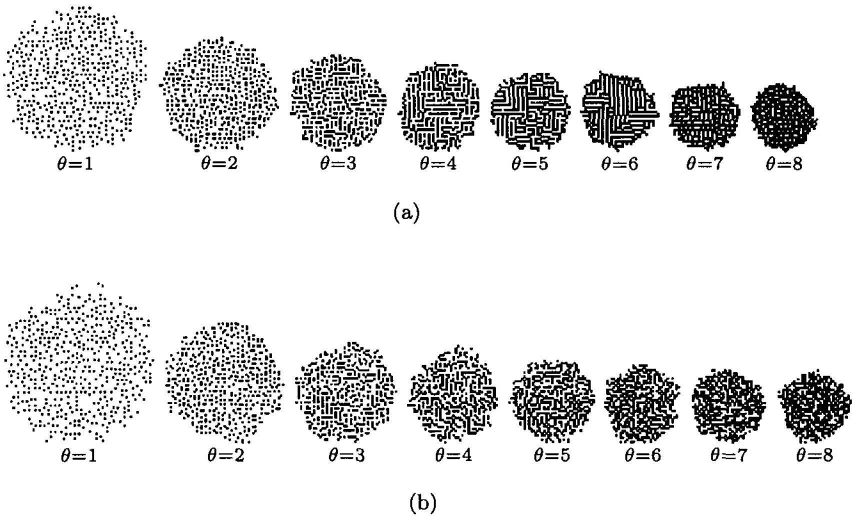

Fig. 6.15 Patterns generated in threshold S-crowd (a) and P-crowd (b) for various values of activation threshold.

highly structured labyrinthine and fingerprint-like patterns. That is, the transitions

$$\mathcal{S} \longrightarrow \mathcal{L} \longrightarrow \mathcal{F} \longrightarrow \mathcal{P}$$

and

$$\mathcal{S} \longrightarrow \mathcal{L} \longrightarrow \mathcal{P}$$

occur in S- and P-crowds, respectively, when the threshold θ_1 is changed from 1 to 8. Therefore, the threshold of activation seems to be a good parameter which characterizes phase-like transitions between the generated patterns. However, this parameter does not give us a complete characterization of morphologies generated by crowds, for example patterns typical for $\mathcal{C}$-, $\mathcal{H}$- and $\mathcal{Y}$-classes never appear in crowds with threshold activation.

In Fig. 6.16 we see how convergence time, size and order of patterns change with the threshold of activation θ_1. This illustrates that increase of the convergence for the thresholds 5 and 6 (Fig. 6.16a) reflects emergence of a structure. The size goes down smoothly (Fig. 6.16b) following the earlier approximation. Correspondingly, the order increases with the increase of the threshold until the threshold reaches the value of 6; after this the order

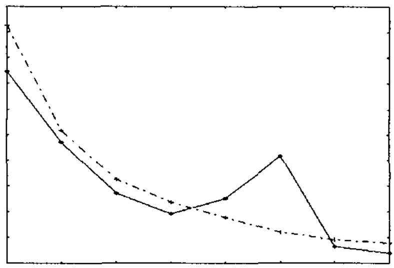

(a)

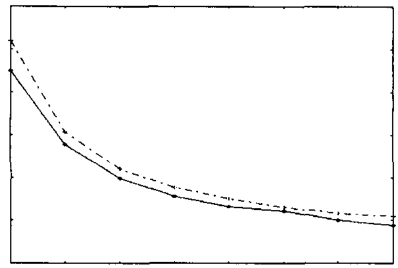

(b)

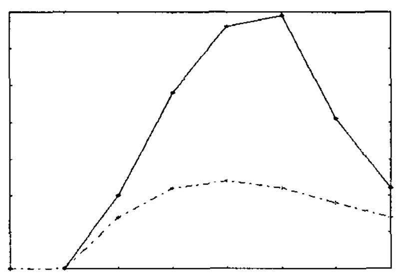

(c)

Fig. 6.16 Schematic graphs of $\gamma_t(\theta_1, 8)$ (a), $\gamma_r(\theta_1, 8)$ (b) and $\omega(\theta_1, 8)$ (c), $1 \leq \theta_1 \leq 8$, horizontal axis, for S- (solid line) and P- (dashed line) crowds.

decreases (Fig. 6.16c). From the graphs we can see that when a threshold parameterization is employed

- the convergence time is proportional to the order of the generated structures,
- the size of the generated structures is inversely proportional to the threshold of activation.

6.5 Upshots of unrest

Rules of interval sensitivity determine certain configurations, let us call them hot configurations [Adamatzky (2000)], of neighborhoods which force agents to move. The number of hot configurations of agents around an

agent, governed by an activation interval $[\theta_1, \theta_2]$, is given by

$$\phi(\theta_1, \theta_2) = \sum_{j \in [\theta_1, \theta_2]} \frac{8!}{(8-j)!j!}.$$

		θ_2							
		1	2	3	4	5	6	7	8
	1	8	36	92	162	218	246	254	255
	2	0	28	84	154	210	238	246	247
	3	0	0	56	126	182	210	218	219
θ_1	4	0	0	0	70	126	154	162	163
	5	0	0	0	0	56	84	92	93
	6	0	0	0	0	0	0	36	37
	7	0	0	0	0	0	0	8	9
	8	0	0	0	0	0	0	0	1

Fig. 6.17 $\phi(\theta_1, \theta_2)$.

The actual number of hot configurations for each interval is shown in Fig. 6.17. It may reflect — a degree of unrest — a probability of an agent moving assuming that the agent was dropped at one of the randomly chosen configurations of stationary agents.

The correspondence between rules of the morphological classes and the numbers of hot configurations is shown in Fig. 6.18; hereinafter all data deal with S-crowds. There are no obvious correlations. Rules for the condensed and porous classes, $\mathcal{C}$-, $\mathcal{P}$- and $\mathcal{Y}$-classes, have low numbers of hot configurations. Rules of the $\mathcal{S}$-class tend to have an above average value of $\phi(\cdot, \cdot)$. The $\mathcal{L}$-class is spread along almost all the axis of $\phi(\cdot, \cdot)$. The fingerprint rules, the $\mathcal{F}$-class, have values of $\phi(\cdot, \cdot)$ ranging between 50 and 100, i.e. not too low but below average. If we calculate the average $\phi(\cdot, \cdot)$ inside every class we find that rules generating non-structured patterns, $\mathcal{P}$-, $\mathcal{Y}$-, $\mathcal{C}$- and $\mathcal{S}$-classes, can be found in domains with either low or high numbers of hot configurations. Rules leading to the formation of structures, $\mathcal{L}$-, $\mathcal{H}$- and $\mathcal{F}$-classes, are characterized by mean numbers of hot configurations.

In Figs. 6.19 and 6.20 we see the overall trend that

> the larger the degree of agent unrest the larger is the convergence time and the smaller is the size of the pattern formed by a crowd which halted its activity.

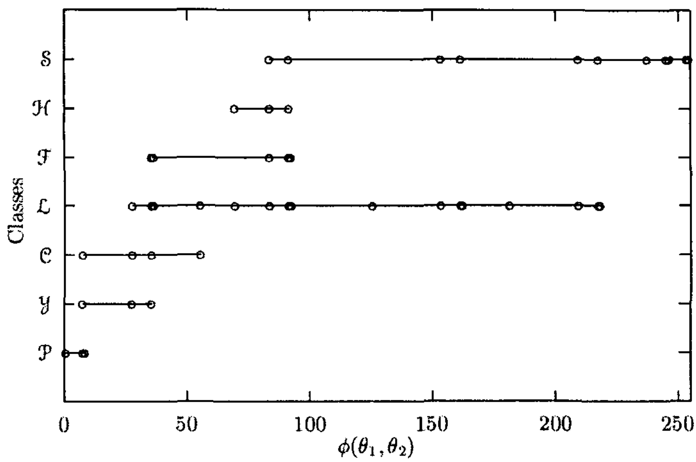

Fig. 6.18 Correspondence between classes and degree of unrest $\phi(\cdot,\cdot)$. Values of $\phi(\cdot,\cdot)$ for each rule of the class are drawn with circles and connected with a line to guide the eye.

For the $\omega-\phi(\cdot,\cdot)$ map (Fig. 6.21) we can recognize two peaks, which correspond to the labyrinthine ($\mathcal{L}$-) and fingerprint ($\mathcal{F}$-) classes. This demonstrates that a degree of agent unrest cannot be considered as a best parameter for classification and prediction of crowd morphologies.

6.6 Boosting degree of unreason

We are not utterly happy with interval models of irrational behavior because $[\theta_1, \theta_2]$ may be interpreted as somewhat a choice of a comfortable number of participants in a group, based for example on a local density, and thus considered as a reasonable choice. So, to protect us from accusations of being really rational we invent a more eccentric model — a vector-based rule of activation, where an agent can feel unhappy to be in a group of an arbitrarily selected number of agents, e.g. "I don't like to be in a group of three, six or eight agents!" How would such an absolutely irrational choice influence global development of crowds?

Every agent i updates its coordinates, i.e. moves to one of the neighboring nodes, by the following rule:

$$x_i^{t+1} = x_i^t + \Delta \cdot \sigma(\zeta(x_i)^t + v_{|u(x_i)^t|}) \cdot \tau(i,t),$$

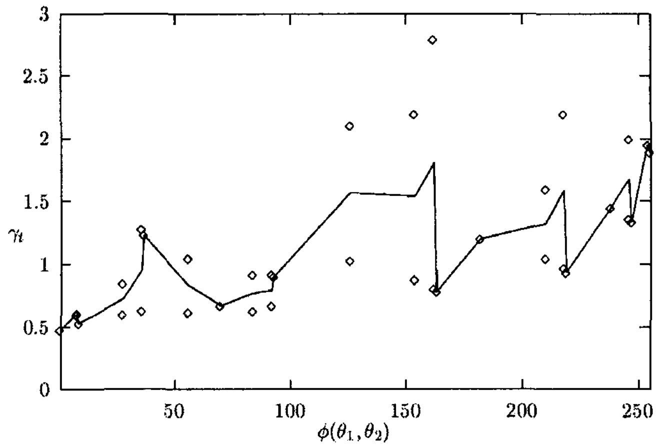

Fig. 6.19 $\gamma_t - \phi(\cdot, \cdot)$ plane.

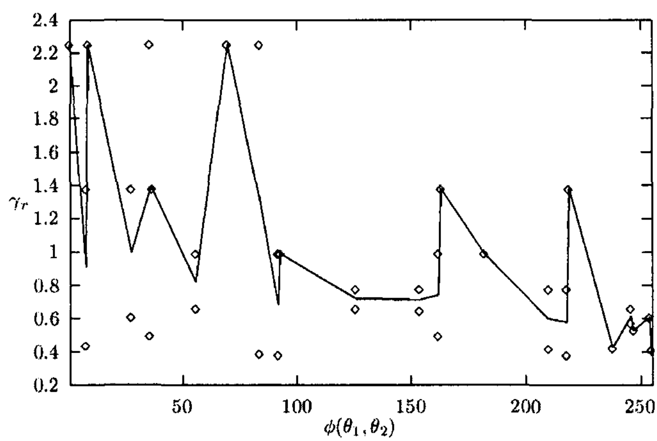

Fig. 6.20 $\gamma_r - \phi(\cdot, \cdot)$ plane.

where Δ is a random two-dimensional unit vector, every component of which takes values from $\{-1, 0, 1\}$; $\zeta(x_i)^t = 1$ if there is another agent j sharing the node $x_i^t = x_j^t$ with the agent i, $\zeta(x_i)^t = 0$ otherwise; $|u(x_i)^t|$ is the number of elements in $u(x_i)^t$; v_z is the zth element of a vector $\mathbf{v} = (v_z)_{1 \leq z \leq 8}$, $v_z \in \{0, 1\}$; $\sigma(a) = 1$ if $a > 0$ and $\sigma(a) = 0$ otherwise; $\tau(i, t) = 1$ if $i = t \mod (m+1)$ and $\tau(i, t) = 0$ otherwise. At the beginning

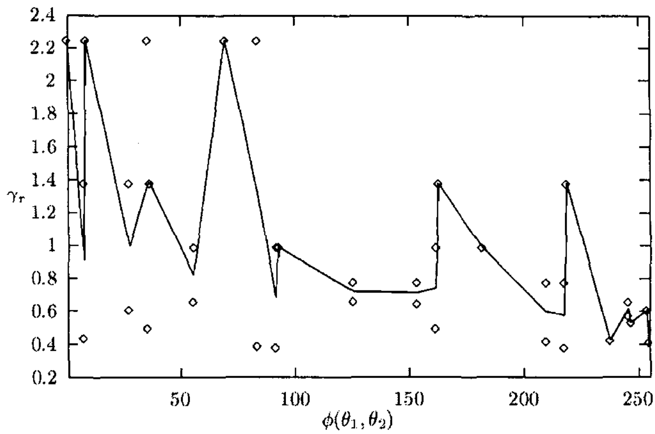

Fig. 6.21 $\omega - \phi(\cdot, \cdot)$ plane.

of evolution, all agents are placed at one node, i.e. for any i we assume that $x_i^0 = x^*$, where x^* may be chosen as a center of the lattice $\mathbf{L}$ if the lattice is finite. In words, every agent i, being in the node x_i^t, moves to another neighboring node x_i^{t+1}, $|x_i^t - x_i^{t+1}|_{L_\infty} \leq 1$, if there is another agent j at the same node as i, $x_i^t = x_j^t$, or the number of neighboring agents, $|u(x_i)^t|$, lies in some specified finite set $\mathbf{S} \in 2^{\{1,\dots,8\}}$; we call it a sensitivity set. The sensitivity set $\mathbf{S}$ is represented by a vector $\mathbf{v}$: $v_{|u(x_i)^t|} = 1$ if $|u(x_i)^t| \in \mathbf{S}$. This vector has eight elements; its size is determined as follows.

The sensitivity set $\mathbf{S}$ is represented by a binary vector $\mathbf{v}$ of eight elements. The size of the vector $\mathbf{v}$ is determined as follows:

- The diameter of an agent pattern would grow infinitely if any agent moves when its node is free of other agents and there are no agents in the neighboring nodes. We want to prevent the system from unbounded growth; therefore, the first element of the vector $\mathbf{v}$ has index 1.
- The configuration of agents is not stationary if at least one node of the lattice is occupied by at least two agents. Therefore, it is unreasonable to consider situations where $|u(x_i)^t| > 8$. Thus, we index the last element of $\mathbf{v}$ by 8.

Therefore, we have 256 possible configurations of the vector $\mathbf{v} \in \{0, 1\}^8$. The exact form of the vector $\mathbf{v}$ is the only explicit parameter which determines various rules of agent movement. Therefore, 256 rules of coordinate update are under consideration. The rules differ only by vectors of agent

sensitivity; therefore, it is reasonable to call them vector rules. Hereinafter, we mean different configurations of the vector $\mathbf{v}$ when we talk about different vector rules.

> For any vector $\mathbf{v} \in \{0,1\}^8$, any finite $m > 0$ and a sufficiently large lattice $\mathbf{L}$ there is such a time step $t^\star$ that for any agent $i \in \mathbf{A}$ we have $x_i^{t+1} = x_i^t$ when $t \geq t^\star$.

It is enough to consider an extreme case of hyper-sensitive agents: $\mathbf{v} = (11111111)$.

Any number of neighboring agents triggers movement of an agent. The agents walk at random. A diameter of the crowd increases with time. After a certain number of time steps, depending on m, every agent has no neighboring agents around. Hence, all agents will eventually stop.

6.6.1 *New faces of irrational morphology*

A full range of patterns discovered in computer experiments with crowds of irrationally acting agents is shown in Fig. 6.22. All patterns generated in the simulation of agent crowds for each of the 256 rules can be grouped into eight classes: condensed patterns ($\mathcal{C}$-class), sparse patterns ($\mathcal{S}$-class), granular patterns ($\mathcal{G}$-class), porous patterns ($\mathcal{P}$-class), labyrinthine patterns ($\mathcal{L}$-class), worm-like patterns ($\mathcal{W}$-class), patterns combining porous and sparse configurations ($\mathcal{B}$-class) and patterns built of small segments ($\mathcal{M}$-class). Half of these patterns are already familiar to us — classes $\mathcal{C}$, $\mathcal{S}$, $\mathcal{P}$ and $\mathcal{L}$ ($\mathcal{F}$); novel patterns include $\mathcal{G}$, $\mathcal{W}$, $\mathcal{B}$ and $\mathcal{M}$ (Fig. 6.22).

6.6.2 *Density-based description*

Let us strengthen the morphological classification with the density distribution of agents in patterns: $\mathbf{D} = (D_i)_{0 \leq i \leq 8}$, which is calculated as follows. For some large $t > t^\star$ we obtain

$$D_z \leftarrow |\{i \in \mathbf{A} : |u(x_i)^t| = z\}/m, \qquad z = 0, \ldots, 8. \tag{6.1}$$

To compute $\mathbf{D}$ we calculated the density distribution of patterns generated in 10 trials for every vector rule; the values of vector entries are averaged in 10 trials.

At the first step of formalization we derive the correspondence between vector rules and indices of largest entries of density vectors: **rule** $\rightarrow j^* : \mathbf{D}_{j^\star} = \max_{0 \leq j \leq 8} \mathbf{D}_j$. After we find j^* for each of the 256 rules we design

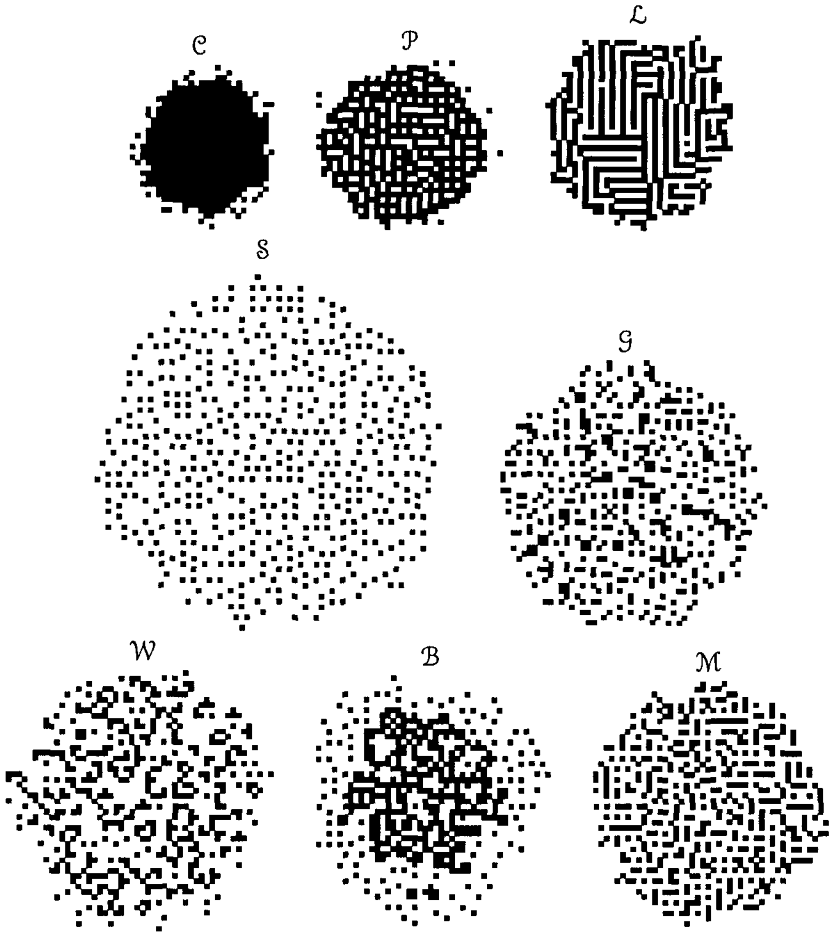

Fig. 6.22 Representative patterns of eight morphological classes: $\mathcal{C}$, $\mathcal{S}$, $\mathcal{G}$, $\mathcal{P}$, $\mathcal{L}$, $\mathcal{W}$, $\mathcal{B}$ and $\mathcal{M}$ discovered in collectives of irrational agents with vector-based sensitivity.

the minimal description of the rules for every j^* in Boolean formulae. The results are shown below; if there are two maxima amongst the elements of the density vector we indicate both of them.

- $j^* = 8$: $P_8 = (\overline{v}_2\overline{v}_3 v_4 \vee \overline{v}_4)\overline{v}_5\ \overline{v}_6\overline{v}_7\overline{v}_8$,
- $j^* = 6$: $P_6 = (v_1\overline{v}_2 v_3 \vee \overline{v}_3)\overline{v}_4\overline{v}_5\overline{v}_6\overline{v}_7 v_8$,
- $j^* \in \{5,6\}$: $P_{56} = \overline{v}_1\overline{v}_2 v_3\overline{v}_4\overline{v}_5\overline{v}_6\overline{v}_7 v_8$,
- $j^* = 5$: $P_5 = v_2\overline{v}_3\overline{v}_4\overline{v}_5\overline{v}_6 v_7$,

- $j^* \in \{4,5\}$: $P_{45} = \overline{v}_2\overline{v}_3\overline{v}_4\overline{v}_5\overline{v}_6 v_7$,
- $j^* = 4$: $P_4 = (\overline{v}_1 \vee v_1 v_7 \overline{v}_8) v_2 \overline{v}_3 \overline{v}_4 \overline{v}_5 v_6$,
- $j^* \in \{3,4\}$: $P_{34} = \overline{v}_3\overline{v}_4\overline{v}_5 v_6(\overline{v}_2\overline{v}_7 \vee v_1 v_2 v_7 v_8)$,
- $j^* = 3$: $P_3 = \overline{v}_2\overline{v}_3\overline{v}_4 v_5(v_6 \to v_1)$,
- $j^* \in \{2,3\}$:
  $P_{23} = \overline{v}_2\overline{v}_3\overline{v}_5(\overline{v}_1 v_4 v_6 v_7 \overline{v}_8 \vee (v_1(\overline{v}_4 v_6 v_7 \vee v_4 v_6(\overline{v_7 \oplus v_8}) \vee v_4 \overline{v}_6 v_7)))$,
- $j^* = 2$: $P_2 = (\overline{v}_1\overline{v}_2\overline{v}_3(\overline{v}_4 v_6(v_5 \vee v_7) \vee v_4(\overline{v}_5(\overline{v}_6(v_7 \vee v_8) \vee v_6(v_7 \to v_8)) \vee v_5))) \vee (\overline{v}_2(\overline{v}_1 v_3 \overline{v}_4(\overline{v}_5 v_6 v_7 v_8 \vee v_5(\overline{v}_6(v_8 \to v_7) \vee v_6(v_7 \oplus v_8))) \vee v_1 \overline{v}_3 v_4(v_5 \vee \overline{v}_5(\overline{v}_7 v_8 \vee v_6 v_7 \overline{v}_8))))$,
- $j^* \in \{1,2\}$: $P_{12} = \overline{v}_1\overline{v}_2 v_3 \overline{v}_4(\overline{v}_5(\overline{v}_6 v_7 \vee v_6 \overline{v}_8) \vee v_5 v_6(v_7 \oplus v_8))$,
- $j^* = 1$: $P_1 = \bigvee_{1\le j\le 8} P_1^j$, where $P_1^1 = \overline{v}_1\overline{v}_2 v_3 \overline{v}_4 \overline{v}_5 v_6 \overline{v}_7 v_8$, $P_1^2 = \overline{v}_1\overline{v}_2 v_3 v_4$, $P_1^3 = \overline{v}_1 v_2 \overline{v}_3 \overline{v}_4 v_5$, $P_1^4 = \overline{v}_1 v_2 \overline{v}_3 v_4 \overline{v}_5$, $P_1^5 = \overline{v}_1 v_2 \overline{v}_3 v_4 v_5$, $P_1^6 = \overline{v}_1 v_2 v_3 \overline{v}_4 \overline{v}_5(\overline{v}_6(v_7 \vee v_8) \vee v_6 v_7 \overline{v}_8)$, $P_1^7 = \overline{v}_1 v_2 v_3 \overline{v}_4 v_5(\overline{v}_6(v_8 \to v_7) \vee v_6(v_7 \oplus v_8))$ and $P_1^8 = \overline{v}_1 v_2 v_3 v_4 \overline{v}_5 \overline{v}_8(\overline{v_6 \oplus v_7})$,
- $j^* = 0$: $P_0 = \bigvee_{1\le j\le 8} P_0^j$, where $P_0^1 = \overline{v}_1 v_2 v_3 \overline{v}_4(\overline{v}_5 v_6(v_8 \to v_7) \vee v_5(\overline{v}_6\overline{v}_7 v_8 \vee v_6(\overline{v_7 \oplus v_8})))$, $P_0^2 = \overline{v}_1 v_2 v_3 v_4 \overline{v}_5(\overline{v}_6(v_7 \vee v_8) \vee v_6 \overline{v}_7)$, $P_0^3 = \overline{v}_1 v_2 v_3 v_4(\overline{v}_5 v_6 v_7 v_8 \vee v_5)$, $P_0^4 = v_1 \overline{v}_2 v_3 \overline{v}_4(\overline{v}_5(\overline{v}_6(v_7 \overline{v}_8 \vee v_7 v_8) \vee v_6) \vee v_5)$, $P_0^5 = v_1 \overline{v}_2 v_3 v_4$, $P_0^6 = v_1 v_2 \overline{v}_3 \overline{v}_4 \overline{v}_5 v_6 \overline{v}_7$, $P_0^7 = v_1 v_2 \overline{v}_3(v_4 \vee v_5)$ and $P_0^8 = v_1 v_2 v_3(\overline{v}_4(v_5 \vee v_6 \vee v_7) \vee v_4)$.

The patterns of the first two classes, $\mathcal{C}$ and $\mathcal{S}$, have a simple morphology. In patterns of the $\mathcal{C}$-class almost every agent has eight neighboring agents (Fig. 6.22, $\mathcal{C}$); this is reflected in the density distribution:

$$D^{\mathcal{C}} = (0 \quad 0 \quad 0 \quad 0 \quad 0 \quad 0 \quad 0 \quad 0.1 \quad 0.9).$$

The density distribution in patterns of the class $\mathcal{S}$:

$$D^{\mathcal{S}} = (0.7 \quad 0.3 \quad 0 \quad 0 \quad 0 \quad 0 \quad 0 \quad 0 \quad 0)$$

suggests a sparse configuration of agents, where almost every agent has no neighboring agents around (Fig. 6.22, $\mathcal{S}$). Patterns of the $\mathcal{G}$-class are usually sparse but with a certain granulation, i.e. small connected clusters, or groups, of a few agents (Fig. 6.22, $\mathcal{G}$); thus,

$$D^{\mathcal{G}} = (0.6 \quad 0.2 \quad 0.2 \quad 0.1 \quad 0 \quad 0 \quad 0 \quad 0 \quad 0).$$

In porous patterns of the $\mathcal{P}$-class every agent usually has five or six neighbors:

$$D^{\mathcal{P}} = (0 \quad 0 \quad 0 \quad 0.1 \quad 0.2 \quad 0.3 \quad 0.3 \quad 0.1 \quad 0).$$

Connected strings and segments of agents form some kind of irregular mesh in patterns of the $\mathcal{P}$-class (Fig. 6.22, P). Distinguishable labyrinthine patterns are grouped into class **L**. There, every agent typically has two or three neighbors:

$$D^{\mathcal{L}} = (0 \quad 0.1 \quad 0.4 \quad 0.3 \quad 0.2 \quad 0 \quad 0 \quad 0 \quad 0).$$

This correctly reflects the morphology of the labyrinths (Fig. 6.22, $\mathcal{L}$), where an agent forming a "wall" has two neighbors while agents at the join of two walls have three or four neighbors. Patterns of the class $\mathcal{W}$ are characterized by a specific configuration of agents, which combines sparsely scattered agents with long irregular chains, kinds of "worms", of agents (Fig. 6.22, $\mathcal{W}$). Therefore, almost every agent in a pattern of the $\mathcal{W}$-class has either two or three neighbors:

$$D^{\mathcal{W}} = (0.1 \quad 0 \quad 0.5 \quad 0.4 \quad 0 \quad 0 \quad 0 \quad 0 \quad 0).$$

"Two-phase" patterns, which combine properties of both sparse, $\mathcal{S}$-class, and porous, $\mathcal{P}$-class, patterns, are grouped into the $\mathcal{B}$-class (Fig. 6.22, $\mathcal{B}$). In patterns of the $\mathcal{B}$-class most agents have four neighbors each:

$$D^{\mathcal{B}} = (0.1 \quad 0.1 \quad 0 \quad 0.3 \quad 0.4 \quad 0.2 \quad 0 \quad 0 \quad 0);$$

hence three-agent and five-agent local configurations of an eight-node neighborhood are also typical. Regions of the patterns with scattered agents contribute to the first two entries, D_0 and D_1, of the density vector $\mathbf{D}$. Class $\mathcal{M}$ contains patterns that consist of short segments of agents (Fig. 6.22, $\mathcal{M}$). The "internal" agents of a segment contribute to the component D_2 of the density vector $\mathbf{D}$, while agents at the ends of a segment contribute to the component D_1:

$$D^{\mathcal{M}} = (0.1 \quad 0.5 \quad 0.4 \quad 0 \quad 0 \quad 0 \quad 0 \quad 0 \quad 0).$$

Is there an exact correspondence between maxima of the density vector and morphological classes? As we see in the list shown below, most classes have unique maxima of density vectors; notice that maxima are calculated from density vectors averaged over the classes; so, a few values of j^*, indicated above, vanished:

- $j^* = 8$: $\mathcal{C}$-class,
- $j^* \in \{5, 6\}$: $\mathcal{P}$-class,
- $j^* = 4$: $\mathcal{B}$-class,
- $j^* = 3$: $\mathcal{W}$-class,

- $j^* = 2$: $\mathcal{L}$-class,
- $j^* = 1$: $\mathcal{M}$-class,
- $j^* = 0$: $\mathcal{G}$- and $\mathcal{S}$-classes.

This means that the density-based description may be used in an express classification of patterns formed by agent crowds.

We found that

- $j^* = i$; this is valid for the classes $\mathcal{C}, \mathcal{S}, \mathcal{G}, \mathcal{W}$ and $\mathcal{P}$';
- $j^* = i - 1$; this is valid for the classes $\mathcal{P}, \mathcal{L}, \mathcal{B}$ and $\mathcal{M}$.

Class	α_1	α_2	α_3	α_4	α_5	α_6	α_7	α_8
C					0	0	0	0
P				0	0	0		
B			0	0	0			
L, W		0	0					
M	0	0						

Fig. 6.23 Zero values in vector rules of morphological classes.

These two parameters can be used in classification of crowd formations as follows. The first parameter is the maximal index of such an entry of a vector rule that has zero value in every vector rule lying in a given class. Having necessary descriptions of a class, we can find the parameter as a maximal index of a negated conjunct in the necessary description of the class. Classes ordered by the value of the parameter symbolize a phase transition, evaporation or melting. This is especially clear when we consider not only the maximal index of a negated conjunct but indices of all negated conjuncts from necessary descriptions of classes (Fig. 6.23). In Fig. 6.23 we see that intervals of zero entries, corresponding to two classes, are overlapped one with another. This reflects the existence of patterns which may belong to two classes neighboring in the hierarchy induced by the parameter.

The second parameter may be thought of as a probability, or likeness, of activation of an agent by its neighbors. For every vector rule of a class we calculate the number of neighborhood configurations — dispositions of other agents in an eight-node neighborhood — which consists of such a number of agents that being represented as an index of a vector rule gives an entry with zero value. The α-parameter is a relative of a λ-parameter

[Langton (1990)], which characterizes the probability of an element of a discrete system taking a non-resting (non-quiescent) state. The λ-parameter was quite successfully applied to demonstrate viability of a concept of "complex dynamics at the edge of chaos" [Gutowitz and Langton (1995)].

6.6.3 *Necessary conditions*

Let us group the vector rules into the same eight classes; we say that a vector rule $\mathbf{v}$ belongs to the class $\mathcal{X}$ if on applying the rule $\mathbf{v}$ to an agent crowd we obtain a stationary configuration, a pattern, which belongs to the morphological class $\mathcal{X}$. For every class $\mathcal{X}$ we construct the conjunctive form:

$$N_{\mathcal{X}} = v_{i_1}^{\alpha_1} v_{i_2}^{\alpha_2} \cdots v_{i_z}^{\alpha_z}, \tag{6.2}$$

where $0 \leq z \leq 8$, for every pair (j', j''), $1 \leq j', j'' \leq z$, $j' \neq j''$, $i_{j'} \neq i_{j''}$, $i_j \in \{1, \ldots, 8\}$, $1 \leq j \leq z$; $\alpha \in \{0, 1\}$, $v^0 = \overline{v}$ and $v^1 = v$. The vector rule $\mathbf{v}$ does not belong to the class $\mathcal{X}$ if $N_{\mathcal{X}} = 0$. Therefore, we call $N_{\mathcal{X}}$ a necessary part of the class $\mathcal{X}$ description. The condition applies to the class as a whole without differentiation of the sub-classes in the class; further, we will see that by splitting the class $\mathcal{X}$ into carefully combined groups one could increase the number of terms in $N_{\mathcal{X}}$. The number z of conjuncts in $N_{\mathcal{X}}$ can be considered as a degree of certainty of the class $\mathcal{X}$ description. The necessary parts of the class description, grouped according to their degrees of certainty, are shown below:

- $z = 5$: $N_{\mathcal{B}} = v_2 \overline{v}_3 \overline{v}_4 \overline{v}_5 v_6$,
- $z = 4$: $N_{\mathcal{C}} = \overline{v}_5 \overline{v}_6 \overline{v}_7 \overline{v}_8$ and $N_{\mathcal{W}} = v_1 \overline{v}_2 \overline{v}_3 v_4$,
- $z = 3$: $N_{\mathcal{P}} = \overline{v}_4 \overline{v}_5 \overline{v}_6$ and $N_{\mathcal{M}} = \overline{v}_1 \overline{v}_2 v_3$,
- $z = 2$: $N_{\mathcal{L}} = \overline{v}_2 \overline{v}_3$ and $N_{\mathcal{S}} = v_2 v_3$,
- $z = 0$: there is no expression of the class $\mathcal{G}$.

6.6.4 *Fine structure of morphologies of irrational crowds*

Looking at the sets of patterns generated in every class of irrational crowds, one may discover that not all patterns inside a class are uniform. In some classes either a smooth or an abrupt transition in the pattern structure is observed. The transitions, however, do not destroy the class structure but indicate that the class could be sub-divided into two or more sub-groups of uniform patterns, which may represent a fine structure of the classes.

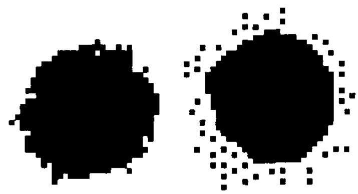

(a) (b)

Fig. 6.24 Halo transition in $\mathcal{C}$-class. Two extreme patterns are presented. The corresponding vectors are (00000000) (a) and (11100000) (b).

6.6.4.1 $\mathcal{C}$-*class*

Patterns generated by rules of the $\mathcal{C}$-class can be ordered by the following "size-of-halo" characteristic. A halo is a part of a pattern, where every agent has no more than three other agents in its neighborhood. Usually, an agent in the halo has one or none neighboring agents. All 10 vector rules of the $\mathcal{C}$-class can be arranged by ascending size of halo in the following manner. For any two rules $\mathbf{v}', \mathbf{v}'' \in \mathcal{C}$-class we write $\mathbf{v}' \leq_H \mathbf{v}''$ if the size of the halo in the patterns generated by $\mathbf{v}'$ is less than or equal to the size of the halo in the patterns produced by $\mathbf{v}''$. It is possible to predict a place of any rule $\mathbf{v} \in \mathcal{C}$ in the $\leq_H$ transition chain using the following empirical law:

$$\sum_{1 \leq i \leq 4} i \cdot v'_i \leq \sum_{1 \leq i \leq 4} i \cdot v''_i \Rightarrow \mathbf{v}' \leq_H \mathbf{v}''.$$

This law can be applied only to the rules of the $\mathcal{C}$-class. Two extreme members of the $\leq_H$ chain are shown in Fig. 6.24.

6.6.4.2 $\mathcal{S}$-*class*

There is no smooth transition between patterns generated by rules of the $\mathcal{S}$-class. All rules of the class can be sub-divided into two groups based on which patterns they generate: $\mathcal{S}_1$ and $\mathcal{S}_2$. The formula of rule vectors of the first group, $\mathcal{S}_1$, has the form

$$\overline{v}_1 v_2 v_3 (\overline{v}_4 (v_5 \vee v_6 \vee v_7 \vee) \vee v_4);$$

rule vectors of the second group, $\mathcal{S}_2$, can be expressed as

$$v_1 v_2 v_3(\overline{v}_4(v_5 \vee v_6 \vee v_7 \vee v_8) \vee v_4).$$

Patterns generated by vector rules of the same group are similar; they also have the same diameter. However, the diameter of patterns of the group $\mathcal{S}_2$ is about 3/2 times more than the diameter of patterns of the group $\mathcal{S}_1$. This is because patterns generated by the rules of the $\mathcal{S}_2$ group have empty neighborhoods around each agent, whereas every agent in the patterns of the group $\mathcal{S}_1$ has only one neighboring agent.

6.6.4.3 $\mathcal{G}$-class

The class can be split into three groups:

- $\mathcal{G}_1$: $\overline{v}_1 v_2 \overline{v}_3(\overline{v}_4 v_5 \vee v_4)$,
- $\mathcal{G}_2$: $v_1 \overline{v}_2 v_3(\overline{v}_4(v_5 \vee v_6 \vee v_7) \vee v_4)$,
- $\mathcal{G}_3$: $v_1 v_2 \overline{v}_3(\overline{v}_4 v_5 \vee v_4)$.

The granular groups of agents are polymorphic in the patterns of the $\mathcal{G}_1$ group; however, there are at most 10 agents in every granular group. These agent clusters look like chains. All other agents, not included in the clusters, have empty neighborhoods or one or two neighboring agents. The diameter of any pattern of the $\mathcal{G}_2$ group is about $\frac{3}{2}$ times more than the diameter of any pattern of $\mathcal{G}_1$. The patterns of $\mathcal{G}_2$ have about the same diameters as the patterns of $\mathcal{G}_3$.

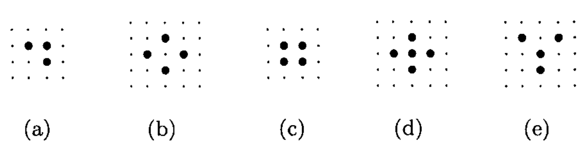

Fig. 6.25 Typical configurations of clusters found in the patterns of the $\mathcal{G}$-class. An agent is shown by a solid disk, an empty node by a dot.

Almost all clusters of agents in patterns of the group $\mathcal{G}_2$ are formed of three agents (this because $v_1 = 1$ but $v_2 = 0$). A typical cluster in a pattern of the group $\mathcal{G}_2$ consists of three agents, which form some kind of an arrow head; one of such clusters is shown in Fig. 6.25a. Clusters of four agents, such as those shown in Fig. 6.25b, are quite rare (two or three clusters per

pattern) but they are found in every pattern generated by rules from the group $\mathcal{G}_2$.

In the $\mathcal{G}_3$-group agents are not allowed to have one or two neighboring agents ($v_1 = 1$ and $v_2 = 1$). However, there may be three agents in a neighborhood of other agents. Every cluster in the pattern of the $\mathcal{G}_2$-group consists of four agents. The configuration of prevailing clusters is shown in Fig. 6.25c. Two more exotic forms can also be found in the patterns of the group $\mathcal{G}_2$ (Fig. 6.25d and e).

6.6.4.4 $\mathcal{P}$-*class*

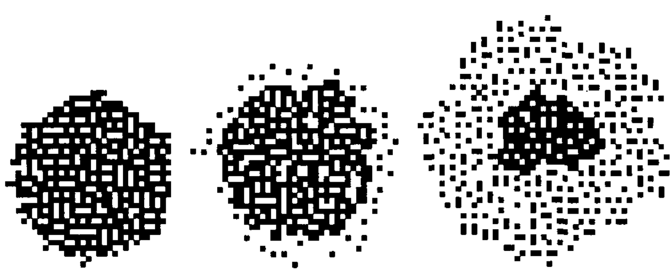

(a) (b) (c)

Fig. 6.26 Typical patterns generated by vector rules of groups $\mathcal{P}_1$ (a), $\mathcal{P}_2$ (b) and $\mathcal{P}_3$ (c) of the $\mathcal{P}$-class.

Porous patterns generated by rules of the $\mathcal{P}$-class can be roughly subdivided into three groups: $\mathcal{P}_1$-group (there is no halo around porous core, see Fig. 6.26a), $\mathcal{P}_2$-group (halo around porous core is small, as shown in Fig. 6.26b) and $\mathcal{P}_3$-group (halo around porous core is large, Fig. 6.26c). Vector rules of the groups can be expressed by three terms $\mathcal{P}_1$, $\mathcal{P}_2$ and $\mathcal{P}_3$, respectively:

$\mathcal{P}_1 = \overline{v}_1\overline{v}_2\overline{v}_3(v_7 \vee v_8)$,

$\mathcal{P}_2 = \overline{v}_1\overline{v}_2 v_3\overline{v}_7 v_8 \vee \overline{v}_3(v_7 \vee v_8)(v_1 \vee v_2)$,

$\mathcal{P}_3 = v_3\overline{v}_7 v_8(v_1 \oplus v_2)$.

6.6.4.5 $\mathcal{L}$-*class*

Members of the $\mathcal{L}$-class can be conditionally classified into three groups, $\mathcal{L}_1$, $\mathcal{L}_2$ and $\mathcal{L}_3$, based on the morphology of the generated patterns. Subse-

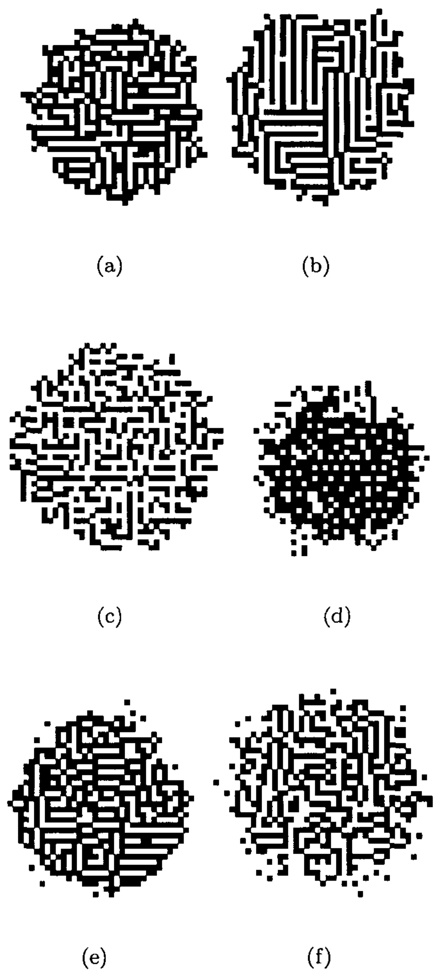

Fig. 6.27 Representative patterns generated by rules of the $\mathcal{L}$-class. The following vector rules are used to generate representative patterns as follows. (a) and (b): (00000100) and (00001111) ($\mathcal{L}_1$-group). (c) and (d): (00010001) and (00100001) ($\mathcal{L}_2$-group). (e) and (f): (10000100) and (10001111) ($\mathcal{L}_3$-group).

quently, we can use stand-alone Boolean expressions for the rules of every group instead of the Boolean function

$$\overline{v}_2\overline{v}_3(\overline{v}_1 v_4(\overline{v}_7 \vee v_8) \vee (v_5 \vee v_6)(\overline{v}_1 \vee v_4)),$$

which represents all vector rules of the class $\mathcal{L}$. Vector rules of the groups are expressed by the Boolean functions as shown below:

$$\begin{aligned}\mathcal{L}_1 &= \overline{v}_1\overline{v}_2\overline{v}_3\overline{v}_4(v_5 \vee v_6)\\ \mathcal{L}_2 &= \overline{v}_1\overline{v}_2\overline{v}_3 v_4(v_5 \vee v_6 \vee v_7 \vee v_8)\\ \mathcal{L}_3 &= v_1\overline{v}_2\overline{v}_3\overline{v}_4(v_5 \vee v_6).\end{aligned}$$

Let two vectors $\mathbf{v}'$ and $\mathbf{v}''$ be in the relation $\mathbf{v}' \leq_V \mathbf{v}''$ if $v'_i \leq_V v''_j \to i \geq j$. A set of vector rules ordered by the relation $\leq_V$ is a chain. We say that a labyrinthine pattern p' is more regular than a labyrinthine pattern p'' if the pattern p'' has more agents with only two neighbors than the pattern p'. For two patterns p' and p'', generated by vector rules $\mathbf{v}'$ and $\mathbf{v}''$, we write $p' \leq_P p''$ if $\mathbf{v}' \leq_V \mathbf{v}''$. For rules of the groups $\mathcal{L}_1$ and $\mathcal{L}_2$ the following propositions are valid.

> The relation $\leq_P$ orders patterns in a chain of regularity, where p' is more regular than p'' if $p' \leq_P p''$.
>
> See examples in Fig. 6.27. Surprisingly, this is not the case in $\mathcal{L}_2$.
>
> The chain $(\{p|p \in \mathcal{L}_3\}, \leq_P)$ is a chain of antiregularity.
>
> Two extreme patterns of the chain are shown in Fig. 6.27.

6.6.4.6 $\mathcal{W}$-class

The rules of the $\mathcal{W}$-class can be described by a Boolean function

$$x_1\overline{x}_2\overline{x}_3x_4(\overline{x}_5(x_6 \vee x_7 \vee x_8) \vee x_5).$$

All patterns of the $\mathcal{W}$-class have similar characteristics.

6.6.4.7 $\mathcal{B}$-class

The rules of the $\mathcal{B}$-class can be expressed as

$$x_2\overline{x}_3\overline{x}_4\overline{x}_5x_6.$$

We sub-divide the rules of the $\mathcal{B}$-class into two groups, $\mathcal{B}_1$ and $\mathcal{B}_2$. The Boolean representation of the rules of the group $\mathcal{B}_1$ is

$$\overline{x}_1x_2\overline{x}_3\overline{x}_4\overline{x}_5x_6.$$

(a) (b)

Fig. 6.28 Two representatives of patterns generated in the class $\mathcal{B}$ by vector rule (01000101) from $\mathcal{B}_1$-group (a) and by vector rule (11000101) from $\mathcal{B}_2$-group (b).

The rules of the $\mathcal{B}_2$-group can be represented as

$$x_1 x_2 \overline{x}_3 \overline{x}_4 \overline{x}_5 x_6.$$

Typical patterns of these two groups are shown in Fig. 6.28.

6.6.4.8 *$\mathcal{M}$-class*

Rules of the $\mathcal{M}$-class can be expressed as follows:

$$\overline{x}_1 \overline{x}_2 x_3 (x_4 \vee x_5 \vee x_6 \vee x_7).$$

All patterns generated by the rules of the $\mathcal{M}$-class form a homogeneous set; their characteristics are similar.

6.6.5 *Hierarchies of irrationality, hostility and unrest*

Is there any mode of agent behavior which can guide structure formation in development of agent crowds? We consider five possible characteristics:

(1) size of a behavioral domain, calculated as the number $\#\mathcal{X}$ of elements in the class $\mathcal{X}$;
(2) granularity of social groupings, calculated as the index j^* of the largest entry of the density vector (6.1);
(3) degree of a behavioral certainty, calculated as the number z of variables in the minimal Boolean description (6.2) of class rules;

(4) a maximal index μ of a negated conjunct presented in the necessary part of a class description (6.2); the parameter μ is calculated for every class, which is represented by $N_{\mathcal{X}}$, as $\mu(\mathcal{X}) = \max_{1 \leq j \leq z}\{i_j : \alpha_j = 0\}$;

(5) degree of tolerance, calculated as the number α of configurations of neighboring agents around some agent, which does not induce movement of the agent; it is calculated, over all rules of the class $\mathcal{X}$, as follows:

$$\alpha(\mathcal{X}) = |\{w \in \{0,1\}^8 : v_h = 0, h = \sum_{1 \leq i \leq 8} w_i, \mathbf{v} \in \mathcal{X}\}|/256.$$

Let $\rhd$ be such an order on eight classes of vector rules that for any two classes $\mathcal{X}$ and $\mathcal{Y}$ we have $\mathcal{X} \rhd \mathcal{Y}$ if and only if $\pi(\mathcal{X}) > \pi(\mathcal{Y})$, where π is one of five parameters defined above. Using $\rhd$-order we build five descending hierarchies shown below:

- $\#$-hierarchy: $\mathcal{G} \rhd \mathcal{S} \rhd \mathcal{L} \rhd \mathcal{M} \rhd \mathcal{P}, \mathcal{W} \rhd \mathcal{C} \rhd \mathcal{B}$,
- j^*-hierarchy: $\mathcal{C} \rhd \mathcal{P} \rhd \mathcal{B} \rhd \mathcal{W} \rhd \mathcal{L} \rhd \mathcal{M} \rhd \mathcal{G}, \mathcal{S}$,
- z-hierarchy: $\mathcal{B} \rhd \mathcal{C}, \mathcal{W} \rhd \mathcal{P}, \mathcal{M} \rhd \mathcal{L}, \mathcal{S} \rhd \mathcal{G}$,
- μ-hierarchy: $\mathcal{C} \rhd \mathcal{P} \rhd \mathcal{B} \rhd \mathcal{L}, \mathcal{W} \rhd \mathcal{M} \rhd \mathcal{S}, \mathcal{G}$,
- α-hierarchy: $\mathcal{P} \rhd \mathcal{C} \rhd \mathcal{B} \rhd \mathcal{L} \rhd \mathcal{W} \rhd \mathcal{G} \rhd \mathcal{M} \rhd \mathcal{S}$.

α-, j^*- and μ-hierarchies separate classes precisely, i.e. they produce fewer classes at the same levels of hierarchies. Also, these three hierarchies are consistent.

What remarkable stages of structural metamorphosis does the system pass through when these characteristics are changing? A structure evolves from a solid-like state (condensed patterns of $\mathcal{C}$-class and porous patterns of $\mathcal{P}$-class, Fig. 6.22) to a liquid-like state (sparse patterns of $\mathcal{S}$-class, Fig. 6.22). Somewhere between these solid and liquid phases a two-phase, transitional, structure is formed; the structure combines a solid core surrounded with a liquid halo (patterns of $\mathcal{B}$-class, Fig. 6.22). Further increase of the parameter value leads to the collapsing of the two-phase system into the highly structured system of labyrinthine patterns ($\mathcal{L}$-class, Fig. 6.22). We can say that at this stage a structure is formed. Increasing the parameter again, we obtain destructured systems, e.g. $\mathcal{W}$- and $\mathcal{M}$-classes (Fig. 6.22).

The degree of agent tolerance and granularity of agent patterns, formed during crowd development, are the most appropriate parameters to classify crowd morphologies.

We could use the degree of tolerance α to study an influence of agent hostility on morphology of patterns formed by crowds. First, we derive a degree of agent sensitivity, i.e. a probability of "excitation" or mobility, in the class $\mathcal{X}$ as $p(\mathcal{X}) = 1 - \alpha(\mathcal{X})$. An agent changes its current position with a very high probability in the first $\sqrt{m/\pi}$ steps of crowd development; the agent moves with the probability $p(\mathcal{X})$ after that. In a situation of light conflict, when almost any node of the lattice has at most one agent, the probability of an agent moving can be linked with the hostility T, a temperature-like parameter, as follows: $T = -1/\ln(p(\mathcal{X}))$.

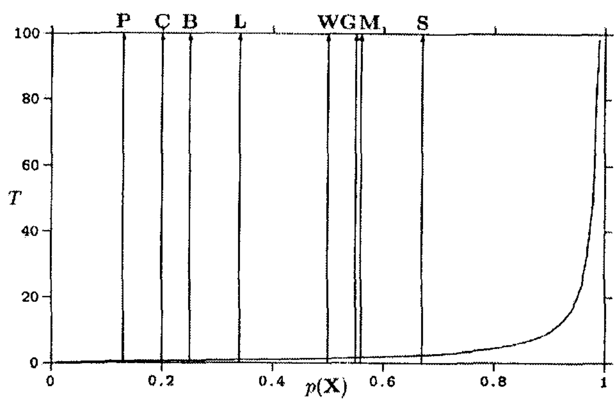

Fig. 6.29 Distribution of classes in the map "agent's sensitivity (probability of agent moving) versus agent's hostility". The dependence of the hostility T on the probability $p(\mathcal{X})$ of agent moving is shown graphically.

Therefore, the hostility-induced transition between classes of crowds looks as follows (Fig. 6.29):

$$\mathcal{P} \to \mathcal{C} \to \mathcal{B} \to \mathcal{L} \to \mathcal{W} \to \mathcal{G} \to \mathcal{M} \to \mathcal{S}.$$

In the domain of very low hostility we observe very dense clusters of resting agents ($\mathcal{C}$-class); on increasing the level of hostility we transform the dense clusters into the quasi-structures ($\mathcal{P}$-class) and two-phase transitional states ($\mathcal{B}$-class). Further increase of hostility leads to the formation of non-trivial structures ($\mathcal{L}$-class). In domains of relatively high hostility, the states with non-trivial labyrinthine structure are transformed into disordered states ($\mathcal{W}$-class) and to quasi-structures ($\mathcal{G}$- and $\mathcal{M}$-classes). When the hostility is very high, gas-like states are produced ($\mathcal{S}$-class); the crowd "dissolves".

Fig. 6.30 Morphological correlates of social unrest; asociality increases rightwards.

Hostility-driven morphodynamics may be considered as analogies of social unrest, exemplified in (Fig. 6.30).

The second pattern in Fig. 6.30 shows growth of tension, or brewing of disorder, the third pattern exemplifies clusters of "local riots" and the fourth pattern is "cold-war" like. The next three patterns represent eruption of violence. If a crowd inhabits a large enough lattice the violence stops when every agent gets a free neighborhood, as in the last pattern of Fig. 6.30.

There are two more characteristics that could be considered as parameters guiding development of morphologies in lattice crowds. They are a complexity of decision-making rules — measured by a number of terms in the Boolean expressions of class rules, and a richness of patterns — measured by a number of non-zero entries in the density-distribution vectors. Two descending hierarchies induced by complexity and richness orders are shown below:

- Complexity hierarchy: $\mathcal{G} \rhd \mathcal{L} \rhd \mathcal{P} \rhd \mathcal{S} \rhd \mathcal{W} \rhd \mathcal{M} \rhd \mathcal{B} \rhd \mathcal{C}$,
- Richness hierarchy: $\mathcal{B} \rhd \mathcal{G}, \mathcal{P}, \mathcal{L} \rhd \mathcal{W} \rhd \mathcal{C}, \mathcal{S}, \mathcal{M}$.

The richness — which is an analog of an indirect hostility — obviously helps us to separate simple rules (those which belong to the classes at the lower part of the hierarchy) and complex rules (those which lie in the top levels of the hierarchy). Rule-complexity hierarchy seems to be quite attractive — classes of granular ($\mathcal{G}$), labyrinthine ($\mathcal{L}$) and porous ($\mathcal{P}$) patterns occupy the upper level; however, the most morphologically rich class $\mathcal{B}$ shares the bottom of the rule-complexity hierarchy with the class $\mathcal{C}$.

Assuming that we choose a rule of agent behavior at random, what pattern would be rather generated — extreme patterns of the hostile-driven evolution or transitional patterns? Transitional ones are rare breeds. The rules of the classes $\mathcal{S}$, $\mathcal{G}$ and $\mathcal{C}$ can be picked up with the probability $\frac{7}{10}$; rules of the $\mathcal{B}$- and $\mathcal{W}$-classes with the probability $\frac{1}{10}$; rules generating labyrinthine, "trench-war", patterns can be found with the probability $\frac{3}{20}$.

6.7 Controlling irrational crowds

Will it be possible to transform one stationary configuration of a crowd to another by applying different rules of agent behavior? We found that, usually, it is impossible. To incorporate rule switching in our lattice crowd model we define a serial composition $\Diamond$ of the interval rules $\mathbf{I}_1$ and $\mathbf{I}_2$, $\mathbf{I}_1 \Diamond \mathbf{I}_2$: $\bullet \xrightarrow{\mathbf{I}_1} P_{\mathbf{I}_1} \xrightarrow{\mathbf{I}_2} P_{\mathbf{I}_2}$. In other words, pattern $P_{\mathbf{I}_1}$ is generated by the rule with interval $[\theta_1, \theta_2] = \mathbf{I}_1$. After the crowd reaches its stationary state the rule with interval $\mathbf{I}_2$ is applied to the agents. The agents become active and mobile again but settle down soon after the perturbation. The pattern $P_{\mathbf{I}_2}$ is formed. New classes of patterns can be generated as a result of such serial composition; see e.g. Fig. 6.31.

Fig. 6.31 Stationary configuration of S-crowd, generated using rule composition $[4, 6] \Diamond [1, 3]$.

Are there any underlying algebraic links between rule content of the classes and morphological characteristics of the patterns generated by the rules? We apply three simple operations to the vector rules and analyze morphological outcomes of the transformations that they evoke. Firstly, we show what happens to the members of a class if they are negated. Secondly, we look at the logical conjunction and disjunction of vector rules and discuss what types of algebraic structure on morphological classes emerge as a the result of the employment of these operations.

6.7.1 *Negation*

A negation of a class $\mathcal{X}$ is defined as follows: $\overline{\mathcal{X}} = \{\mathcal{Y}_1, \ldots, \mathcal{Y}_m\}$, $1 \leq m \leq 8$, where, for every j, $1 \leq j \leq m$, there is such a vector rule $\mathbf{v}'$, $\mathbf{v}' \in \mathcal{Y}_j$, that $\overline{\mathbf{v}} = \mathbf{v}'$ for some $\mathbf{v} \in \mathcal{X}$; $\overline{\mathbf{v}} = (\overline{v}_1 \cdots \overline{v}_8)$. A graph of negation-induced class transitions is shown in Fig. 6.32: nodes $\mathcal{X}$ and $\mathcal{Y}$ are connected by an arc

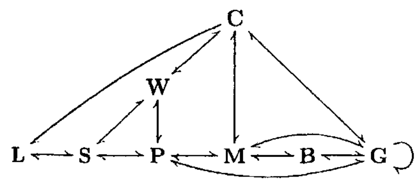

Fig. 6.32 Graph of negation-induced transitions between the classes.

$(\mathcal{X}, \mathcal{Y})$ if there are at least two such rules $\mathbf{v}'$ and $\mathbf{v}''$, $\mathbf{v}' \in \mathcal{X}$ and $\mathbf{v}'' \in \mathcal{Y}$, such that $\overline{\mathbf{v}'} = \mathbf{v}''$. We found that

No class but $\mathcal{G}$ is stable under negation transformation.

We can also conclude that the planar structure of the graph partly proves that the chosen classification is quite natural. Another quite interesting feature of the graph is that by excluding the arc ($\mathcal{C}$, $\mathcal{L}$) from this directed graph we obtain an in-directed graph.

6.7.2 *(Con/Dis)junction of classes*

Conjunction and disjunction of the classes are defined via respective binary operations over vector rules of the classes. For two vector rules $\mathbf{v}'$ and $\mathbf{v}''$, we have

$$\mathbf{v}' * \mathbf{v}'' = (v_i' * v_i'')_{1 \leq i \leq 8},$$

where $*$ is either $\vee$ or $\wedge$. We say that $\mathcal{X}\boxed{*}\mathcal{Y} = \mathcal{Z}$ if there are vectors $\mathbf{v}'$, $\mathbf{v}''$ and $\mathbf{v}'''$ such that $\mathbf{v}' \in \mathcal{X}$, $\mathbf{v}'' \in \mathbf{Y}$, $\mathbf{v}''' \in \mathcal{Z}$ and $\mathbf{v}' * \mathbf{v}'' = \mathbf{v}'''$. In general, we obtain the mapping

$$\mathcal{X}\boxed{*}\mathcal{Y} \to \{\mathcal{Z}_1, \mathcal{Z}_2, \ldots, \mathcal{Z}_h\},$$

where $h \leq 8$.

Tabular representations of compositions $\boxed{\vee}$ and $\boxed{\wedge}$ are given in Fig. 6.33. The exact structure of the compositions is not particularly interesting; however, a few findings should be noticed. A class $\mathcal{X}$ is called a $\boxed{*}$-null of the algebraic system

$$\langle \boxed{*}, \{\mathcal{C}, \mathcal{S}, \mathcal{G}, \mathcal{P}, \mathcal{L}, \mathcal{W}, \mathcal{M}\} \rangle$$

$\boxed{\wedge}$	$\mathcal{C}$	$\mathcal{S}$	$\mathcal{G}$	$\mathcal{P}$	$\mathcal{L}$	$\mathcal{W}$	$\mathcal{B}$	$\mathcal{M}$
$\mathcal{C}$	$\{\mathcal{C}\}$	$\{\mathcal{C}\}$	$\{\mathcal{C}\}$	$\{\mathcal{C}\}$	$\{\mathcal{C}\}$	$\{\mathcal{C}\}$	$\{\mathcal{C}\}$	$\{\mathcal{C}\}$
$\mathcal{S}$	$\{\mathcal{C}\}$	$\{\mathcal{C},\mathcal{S},\mathcal{P}\}$	$\{\mathcal{C},\mathcal{G},\mathcal{P},\mathcal{B},\mathcal{M}\}$	$\{\mathcal{C},\mathcal{P}\}$	$\{\mathcal{C},\mathcal{P},\mathcal{L}\}$	$\{\mathcal{C},\mathcal{P},\mathcal{L},\mathcal{W}\}$	$\{\mathcal{C},\mathcal{P},\mathcal{B}\}$	$\{\mathcal{C},\mathcal{P},\mathcal{M}\}$
$\mathcal{G}$	$\{\mathcal{C}\}$	$\{\mathcal{C},\mathcal{G},\mathcal{P},\mathcal{B},\mathcal{M}\}$	$l\{\mathcal{C},\mathcal{G},\mathcal{P},\mathcal{L},\mathcal{W},\mathcal{B}\}$	$\{\mathcal{C},\mathcal{P}\}$	$\{\mathcal{C},\mathcal{P},\mathcal{L}\}$	$\{\mathcal{C},\mathcal{P},\mathcal{L},\mathcal{W}\}$	$\{\mathcal{C},\mathcal{P},\mathcal{L},\mathcal{B}\}$	$\{\mathcal{C},\mathcal{P},\mathcal{L},\mathcal{M}\}$
$\mathcal{P}$	$\{\mathcal{C}\}$	$\{\mathcal{C},\mathcal{P}\}$	$\{\mathcal{C},\mathcal{P}\}$	$\{\mathcal{C},\mathcal{P}\}$	$\{\mathcal{C},\mathcal{P}\}$	$\{\mathcal{C},\mathcal{P}\}$	$\{\mathcal{C},\mathcal{P}\}$	$\{\mathcal{C},\mathcal{P}\}$
$\mathcal{L}$	$\{\mathcal{C}\}$	$\{\mathcal{C},\mathcal{P},\mathcal{L}\}$	$\{\mathcal{C},\mathcal{P},\mathcal{L}\}$	$\{\mathcal{C},\mathcal{P}\}$	$\{\mathcal{C},\mathcal{P},\mathcal{L}\}$	$\{\mathcal{C},\mathcal{P},\mathcal{L}\}$	$\{\mathcal{C},\mathcal{P},\mathcal{L}\}$	$\{\mathcal{C},\mathcal{P},\mathcal{L}\}$
$\mathcal{W}$	$\{\mathcal{C}\}$	$\{\mathcal{C},\mathcal{P},\mathcal{L},\mathcal{W}\}$	$\{\mathcal{C},\mathcal{P},\mathcal{L},\mathcal{W}\}$	$\{\mathcal{C},\mathcal{P},\mathcal{L}\}$	$\{\mathcal{C},\mathcal{W}\}$	$\{\mathcal{C},\mathcal{P},\mathcal{L}\}$	$\{\mathcal{C},\mathcal{P},\mathcal{L}\}$	$\{\mathcal{C},\mathcal{P},\mathcal{L}\}$
$\mathcal{B}$	$\{\mathcal{C}\}$	$\{\mathcal{C},\mathcal{P},\mathcal{B}\}$	$\{\mathcal{C},\mathcal{P},\mathcal{L},\mathcal{B}\}$	$\{\mathcal{C},\mathcal{P}\}$	$\{\mathcal{C},\mathcal{P},\mathcal{L}\}$	$\{\mathcal{C},\mathcal{P},\mathcal{L}\}$	$\{\mathcal{B}\}$	$\{\mathcal{C},\mathcal{P},\mathcal{L}\}$
$\mathcal{M}$	$\{\mathcal{C}\}$	$\{\mathcal{C},\mathcal{P},\mathcal{M}\}$	$\{\mathcal{C},\mathcal{P},\mathcal{L},\mathcal{M}\}$	$\{\mathcal{C},\mathcal{P}\}$	$\{\mathcal{C},\mathcal{P},\mathcal{L}\}$	$\{\mathcal{C},\mathcal{P},\mathcal{L}\}$	$\{\mathcal{C},\mathcal{P},\mathcal{L}\}$	$\{\mathcal{C},\mathcal{P},\mathcal{M}\}$

$\boxed{\vee}$	$\mathcal{C}$	$\mathcal{S}$	$\mathcal{G}$	$\mathcal{P}$	$\mathcal{L}$	$\mathcal{W}$	$\mathcal{B}$	$\mathcal{M}$
$\mathcal{C}$	$\{\mathcal{C},\mathcal{S},\mathcal{G},\mathcal{M}\}$	$\{\mathcal{S}\}$	$\{\mathcal{S},\mathcal{G}\}$	$\{\mathcal{S},\mathcal{G},\mathcal{P},\mathcal{L},\mathcal{W},\mathcal{M}\}$	$\{\mathcal{S},\mathcal{G},\mathcal{L},\mathcal{W},\mathcal{B},\mathcal{M}\}$	$\{\mathcal{S},\mathcal{G},\mathcal{W}\}$	$\{\mathcal{S},\mathcal{G},\mathcal{B}\}$	$\{\mathcal{S},\mathcal{G},\mathcal{M}\}$
$\mathcal{S}$	$\{\mathcal{S}\}$	$\{\mathcal{S}\}$	$\{\mathcal{S}\}$	$\{\mathcal{S}\}$	$\{\mathcal{S}\}$	$\{\mathcal{S}\}$	$\{\mathcal{S}\}$	$\{\mathcal{S}\}$
$\mathcal{G}$	$\{\mathcal{S},\mathcal{G}\}$	$\{\mathcal{S}\}$	$\{\mathcal{S},\mathcal{G}\}$	$\{\mathcal{S},\mathcal{G}\}$	$\{\mathcal{G}\}$	$\{\mathcal{G}\}$	$\{\mathcal{S},\mathcal{G}\}$	$\{\mathcal{S},\mathcal{G}\}$
$\mathcal{P}$	$\{\mathcal{S},\mathcal{G},\mathcal{P},\mathcal{L},\mathcal{W},\mathcal{M}\}$	$\{\mathcal{S}\}$	$\{\mathcal{S},\mathcal{G}\}$	$\{\mathcal{S},\mathcal{G},\mathcal{P},\mathcal{M}\}$	$\{\mathcal{S},\mathcal{G},\mathcal{L},\mathcal{W},\mathcal{B},\mathcal{M}\}$	$\{\mathcal{S},\mathcal{G},\mathcal{W}\}$	$\{\mathcal{S},\mathcal{B}\}$	$\{\mathcal{S},\mathcal{G},\mathcal{M}\}$
$\mathcal{L}$	$\{\mathcal{S},\mathcal{G},\mathcal{L},\mathcal{W},\mathcal{B},\mathcal{M}\}$	$\{\mathcal{S}\}$	$\{\mathcal{G}\}$	$\{\mathcal{S},\mathcal{G},\mathcal{L},\mathcal{W},\mathcal{B},\mathcal{M}\}$	$\{\mathcal{L},\mathcal{W}\}$	$\{\mathcal{W}\}$	$\{\mathcal{G},\mathcal{B}\}$	$\{\mathcal{G},\mathcal{M}\}$
$\mathcal{W}$	$\{\mathcal{S},\mathcal{G},\mathcal{W}\}$	$\{\mathcal{S}\}$	$\{\mathcal{G}\}$	$\{\mathcal{S},\mathcal{G},\mathcal{W}\}$	$\{\mathcal{W}\}$	$\{\mathcal{W}\}$	$\{\mathcal{G}\}$	$\{\mathcal{G}\}$
$\mathcal{B}$	$\{\mathcal{S},\mathcal{G},\mathcal{B}\}$	$\{\mathcal{S}\}$	$\{\mathcal{S},\mathcal{G}\}$	$\{\mathcal{S},\mathcal{B}\}$	$\{\mathcal{G},\mathcal{B}\}$	$\{\mathcal{G}\}$	$\{\mathcal{B}\}$	$\{\mathcal{S}\}$
$\mathcal{M}$	$\{\mathcal{S},\mathcal{G},\mathcal{M}\}$	$\{\mathcal{S}\}$	$\{\mathcal{S},\mathcal{G}\}$	$\{\mathcal{S},\mathcal{G},\mathcal{M}\}$	$\{\mathcal{G},\mathcal{M}\}$	$\{\mathcal{G}\}$	$\{\mathcal{S}\}$	$\{\mathcal{M}\}$

Fig. 6.33 Tables of $\boxed{\wedge}$ and $\boxed{\vee}$ compositions of the classes.

if for any class $\mathcal{Y}$ we have

$$\mathcal{X}\boxed{*}\mathcal{Y} = \mathcal{Y}\boxed{*}\mathcal{X} = \mathcal{X}.$$

The class $\mathcal{X}$ is an idempotent of our algebraic system if

$$\mathcal{X}\boxed{*}\mathcal{X} = \mathcal{X}.$$

In these definitions

Class $\mathcal{C}$ is a $\boxed{\wedge}$-null while class $\mathcal{S}$ is a $\boxed{\vee}$-null.

We should also mention that

The elements $\mathcal{C}$ and $\mathcal{B}$ are $\boxed{\wedge}$-idempotents. The elements $\mathcal{S}$, $\mathcal{W}$, $\mathcal{B}$ and $\mathcal{M}$ are $\boxed{\vee}$-idempotents.

6.8 Schizophrenia on a lattice

In an attempt to understand behavioral consequences of irrationality, we studied formation of patterns built by schizophrenic-like mobile agents on a lattice. We forced all agents to be at one point of space, one lattice node, at the beginning of the experiments; after that they were allowed to disperse.

These superhigh-density initial conditions induced enormous pressure and a somewhat cognitive load on the individuals, and contributed to deindividuaton and, ultimately, to irrational behavior of the agents [Lindmark (2000)]. Notably, delusions are sometimes also considered as disturbances of a spatio-temporal nature, for example

> "... a person with a delusion of persecution, who has a feeling of restriction of freedom and movement (the spatio-temporal disturbance), is hence no longer able to perceive the sometimes random nature of all the events and happenings that occur" [Winters and Neale (1983)].

We have provided the morphological classification of the formed structures; selected classes of simple, complex and non-trivially ordered structures; and uncovered relations between irrationality of agents' behavior and morphological complexity of structures they form. Our models describe masses whose behavior

> "... results in individual selection made on a basis of vague impulses and feelings" [Smelser (1962)].

We can therefore interpret dramatic morphological transformations caused by an increase of the lower boundary of the sensitivity interval as a state of panic [Smelser (1962)]. The panic transformation starts with a structural conductivity — which is a normal activity — then followed by a strain — a shift in the sensitivity boundary. As a result, anxiety develops and a hysteria is formed which may be followed by either a panic or a mobilization. Discrete models of fighting in crowds [Jager *et. al* (2001)] show clustering behavior dependent on a threshold of agents' activation, which is a direct analog of sensitivity thresholds in our models.

We have shown that particulars of an "internal" interpretation of an agent's neighborhood occupancy by an agent determine a structure of quite sophisticated patterns emerging in crowd development. This corresponds to urban sociology findings that an "inside density" — a number of persons per unit of space in houses — more strongly influences social dynamics than an "outside density" — a number of people on the streets [Kruse (1986)].

In models of pattern formation in agent collectives we have shown that irrational actions will certainly lead to formation of highly ordered structures, which perfectly conform to psychological views stating

> "... cognition of the schizophrenic may manifest a highly ordered logical system" [Snyder (1991)].

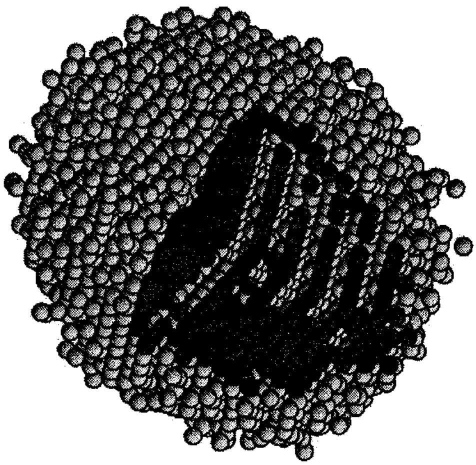

Fig. 6.34 Labyrinthine structure formed in a crowd of 10^3 irrational agents in a three-dimensional lattice; an agent's activation interval is $[20, 25]$. A quarter of the cluster is removed to expose the interior, agents are shown by the balls; the edge agents are shown in dark color.

In the chapter we indirectly expressed this order via morphological orders of patterns formed by irrationally acting agents. One of such highly ordered patterns is shown in Fig. 6.34.

One of the objectives of future research could be to incorporate a temporal dimension in the development of crowd-minds, to reflect experimental findings [Melges and Fougerousse (1966)] that anxiety and anger are positively correlated with changes in time sense, and schizophrenic and delusional patients experience particularly noticeable distortions of time sense.

Epilogue

We have designed computational models, and developed a framework for future theoretical foundations, of large-scale pools of irrationally behaving entities. We selected crowds as a key component of a theoretical paradigm of collective irrational behavior because members of a crowd are those

> "... who being some of them hardly in mental equilibrium, are apt to distort causes and effects" [Stoker (1993)].

Using cellular-automata, artificial-chemistry and numerical techniques we built a set of models of crowd-minds, swirling in affective storms, shaping patterns of non-sense, diffusing delusion and engaging in phenomenologically rich but senseless, from the common-sense point of view, logical constructions. In the models we tried to identify and exploit the phenomenon called the crowd-mind, the phenomenon which is

> "the result of forces hidden in the personal and unconscious psyche of the members of the crowd, forces which are merely *released* by social gatherings of a certain sort" [Martin (1920)].

We designed models of quasi-chemical interactions between happiness, sadness, anger, fear and confusion, and then characterized almost all modes of integral and spatio-temporal dynamics in affective mixtures. We have shown how distortions of conventional forms and structures in crowd-minds lead to drastic changes in reasoning and inference, and divert doxastic collectives from conventional routes of knowledge accumulation to complex non-linear dynamics of mixtures of belief, delusion, ignorance, knowledge and doubt. In computational experiments with constrained doxastic mixtures we proved that norms can barely improve, and hardly control, behavior of crowd-minds. Non-trivially behaving combinatorial, pre-logical,

systems were derived to make a formal foundation of the irrationality of a crowd-mind. The logical systems derived in the book could be helpful in future attempts to build a mathematical framework of irrationality and, possibly, of an inference in conditions of mental disorders. We completed our journey to the field of unreasonable by uncovering morphological correlates of irrationality and structures built by crowd-minds and by qualifying morphological complexity of non-sense.

We laid a foundation for the science of collective unconsciousness. We envisage that our results in dynamics of affective mixtures, where collective pre-emotions develop to sadness and anxiety, may form a science of confusion. Findings in behavior of doxastic mixtures — evolving towards doubt and ignorance — may characterize a collective pre-knowledge, a subject of a science of doubt. Evolving of a pre-structure to a structure, governed by irrationality, may provide a starting point for studies in disordered mentality of order.

The book discusses somewhat provocative ideas emerging at the edge of physical and chemical sciences on one side, and social and psychological sciences on another side. Models and paradigms developed in the book might be applied to mathematical studies of affective collective intelligence, computational models of minds near the state of mental disorder, design of massively parallel prototypes of artificial consciousness, software implementations of affective cognition and design of hardware prototypes of emotional controllers for robots.

Glossary

- **Affecton** is a finite automaton whose internal states, input and output states, are **happiness**, **anger**, **fear**, **sadness**, **confusion** and **anxiety**.
- **Anger** is an emotional state of displeasure.
- **Anxiety** is an emotional state of restlessness.
- **Anxious agent** is an agent that always changes its doxastic state if its current state is not equal to the state of its neighbor.
- **Artificial chemistry** is an abstract system with a set of objects and rules, where the objects are considered to be analogies of chemical species and the rules are seen as chemical reactions.
- **Artificial society** is a social structure emerging in collectives of automata-like agents.
- **Breather**, as related to **cellular automata**, is a compact pattern of non-quiescent cell states, which may cyclically change its structure, but is not translated across an automaton array.
- **Cellular automaton** is an array of locally connected finite automata, which update their discrete states in discrete time depending on states of their neighbors; all automata of the array update their states in parallel.
- **Confusion** is an emotional state of disconcertion.
- **Consciousness** is a cognitive–affective state of self-awareness.
- **Conservative agent** is a modification of **naive agent** that does not take a **non-sense state** even if its neighbors are in non-sense states.
- **Contradicting agent** is an agent that takes a belief opposite to beliefs of its neighbors.
- **Crowd** is a large group of people tightly packed together, without a hierarchical structure and long-term leadership, individuals in the crowd undergo **deindividuation** and **derationalization**; communication in

the crowd is predominantly local.

- **Deindividuation** is a loss of personal identity and reduction of self-awareness of **crowd** members due to diffusing of their responsibilities, uniformization of feelings and behavioral patterns, mutual imitation and deformation of temporal components.
- **Delusion** is an erroneous belief that cannot be justified.
- **Derationalization** is a disorganization of **crowd** members' thinking and self-control, and loss of rationality, due to emotional arousal and **deindividuation**.
- **Doubt** is a state of neither belief nor **misbelief** about a locally justifiable fact.
- **Doxastic world** is an element of a set of all possible sets of **doxastic states**.
- **Doxastic chemistry** is an abstract system comprising doxastic states which interact with each other by chemistry-like rules.
- **Doxaton** is a finite automaton whose internal states, input and output states, are **knowledge**, **doubt**, **delusion**, **misbelief** and **ignorance**.
- **Doxastic state** is an agent or automaton state derived from belief, which includes **knowledge**, **doubt**, **delusion**, **misbelief** and **ignorance**.
- **Emotional contagion** is a spread, and subsequent uniformization, of feelings in a **crowd**.
- **Fear** is an emotional state of apprehension of danger.
- **Glider**, as related to **cellular automata**, is a compact pattern that travels along a cellular array.
- **Happiness** is an emotional state of well-being.
- **H-configuration** is a state of a cellular-automaton model where state cells are distributed at random.
- **Ignorance** is a state of neither belief nor disbelief about a locally unjustifiable fact.
- **Irrational** is that of lacking reason, foolish or absurd, without power of understanding.
- **Knowledge** is a justified belief.
- **Mind** is a collective term for that responsible for thoughts and feelings.
- **Misbelief** is a wrong belief.
- **Naive agent** is an agent that takes a **non-sense state** if its beliefs contradict beliefs of its neighbors.
- **Non-sense state** is a meaningless state.
- **Non-stirred reactor (crowd)** is a reactor (crowd) where reagents

(agents, automata) do not move, so they react only with their geographical neighbors.

- **Norm** is a constraint, or a restriction of a range of possible actions.
- **Q-configuration** is a state of a cellular-automaton model where every cell but one takes the same state.
- **Reflecting doxaton** is a **doxaton** whose output is "hardwired" to its input.
- **Sadness** is an emotional state of unhappiness.
- **Schizophrenia** is a range of psychotic disorders associated with disturbances of thoughts, distortion of apprehension of reality and communicative aberrations.
- **Singleton** is a set with exactly one element, as related to mathematics, and is a member of a crowd model which starts its evolution in a state different from the uniform state of other crowd members.
- **Stirred reactor (crowd)** is a reactor (crowd) where reagents (agents, automata) are endlessly mixed, so no fixed topological structure is formed, and every reagent (agent, automaton) may interact with potentially any reagent (agent, automaton) at a time.
- **Thin-layer reactor** is a **non-stirred reactor**.

Acknowledgments

Early results of my studies in crowded minds were published in "Applied Mathematics and Computation", "Chaos, Solitons & Fractals", "Kybernetes", "Dynamical Psychology", "International Journal of Modern Physics B", "Lecture Notes in Computer Science", "Mathematical and Computer Modelling" and "Lecture Notes in Artificial Intelligence". I am grateful to editors and referees of these journals for their help and encouragement. Many thanks to Michael Jones for copyediting the manuscript.

Bibliography

Abraham, F. D. (1992). Chaos, bifurcations, and self-organization: dynamical extension of neurological positivism and ecological psychology, *Psychoscience* **1**, pp. 85–118.

Abraham, F. D. and Gilgen, A. R. (1995). *Chaos Theory in Psychology* (Greenwood Press, New York).

Adamatzky, A. (1995a). Recognition of distributed intelligence, *J. Comput. Syst. Sci. Int.* **33**, pp. 160–169.

Adamatsky, A. (1995b). Recognition of distributed intelligence, *J. Comput. Syst. Sci. Int.* **33**, pp. 160–169.

Adamatzky, A. (1998b). Reconstruction of non-logical axioms from the propositions of multi-agent doxastic logic, *Kybernetes* **27**, pp. 952–958.

Adamatzky, A. (1998c). Master–slave algebra: on the binary compositions of distributed beliefs, *Appl. Math. Comput.* **95**, pp. 173–180.

Adamatzky, A. (1999). Nonconstructible blocks in 1D cellular automata: minimal generators and natural systems, *Appl. Math. Comput.* **99**, pp. 77–91.

Adamatzky, A. (2000). Hot choosey sand: reflection of grain sensitivity on pattern morphology, *Int. J. Mod. Phys.* **11**, pp. 47–68.

Adamatzky, A. (2001a). Pathology of collective doxa. Automata models, *Appl. Math. Comput.* **122**, pp. 195–228.

Adamatzky, A. (2001c). Chemistry of belief — experiments with doxastic solutions, *Kybernetes* **30**, pp. 1199–1208.

Adamatzky, A. (2001d). Space–time dynamic of normalized doxatons: automata models of pathological collective mentality, *Chaos, Solitons Fractals* **12**, pp. 1629–1656.

Adamatzky, A. (2002b). Affectons: automata models of emotional interactions, *Appl. Math. Comput.* **146**, pp. 579-594.

Adamatzky, A. (2002c). On dynamic of affective liquids, *Dyn. Psychol.* **1** (2002). [`http://www.goertzel.org/dynapsyc/2002/emot2708.html`]

Adamatzky, A. (2005). Non-linear dynamics in affective solutions: analysis of massive collectives of emotional agents, *Kybernetes*, in press.

Adamatzky, A., Holland, O. and Melhuish, C. (1999a). Hierarchies of structured aggregation in simple swarms, *Proc. 11th Int. Congr. Cybernetics and*

Systems, 23–27 August 1999, Brunel University, Uxbridge, UK, pp. 287–291.

Adamatzky, A., Holland, O. and Melhuish, C. (1999b). Lazy + Busy + Sensitive = Structure, *Proc. Eur. Conf. Artificial Life, 1999.*

Adamatzky, A., Melhuish, C. and Holland, O. (1999c). Morphology of patterns of lattice swarms: interval parameterization, *Math. Comput. Modelling* **30**, pp. 35–59.

Alcott, L. M. (2000). *Little Woman* (American Literature Classics Library) [http://www.americanliterature.com/lw/lwindx.html]

Aleksander, I. (1997a). Neuroconsciousness: a fundamental postulate. In: *Neural Network Perspectives on Cognition and Adaptive Robots*, ed. A. Browne (Institute of Physics, Bristol), pp. 153–166.

Aleksander, I. (1997b). *Impossible Minds: My Neurons, My Consciousness* (World Scientific).

Allport, F. H. (1924). *Social Psychology* (Houghton Mifflin, Boston, MA). Cited in [McPhail (1991)].

Alves, S. G., Oliveira Neto, N. M. and Martin, M. L. (2002). Electoral surveys' influence on the voting processes: a cellular automata model, *Physica A* **316**, pp. 601–614.

Amelie, R. O. (1980). *Explaining Emotions* (University of California Press).

Andersen, P. A. and Guerrero, L. K. (Eds.) (1998). *Handbook of Communication and Emotion* (Academic Press).

Saint Augustine. (2000). *The City of God* (Modern Library, 2000); quotation obtained using http://www.concordance.com.

Saint Augustine. (2002). *The Confessions of Saint Augustine*, Book 9, Chap. XII, transl. E. B. Pusey (Project Gutenberg, 2002). [ftp://ibiblio.org/pub/docs/books/gutenberg/etext02/tcosa10.txt]

Axelrod, R. (1986). An evolutionary approach to norms, *Am. Polit. Sci. Rev.* **80**, pp. 1095–1111.

Axelrod, R. (1997). *The Complexity of Cooperation: Agent-Based Models of Competition and Collaboration* (Princeton University Press).

Baader, F. (1996). Using automata theory for characterizing the semantics of terminological cycles, *Ann. Math. Artif. Intell.* **18**, pp. 175–219.

Babinec, P. (1997). Stochastic resonance in the Weidlich model of public opinion formation, *Phys. Lett. A* **225**, pp. 179–181.

Bainbridge, W., Brent, E., Carley, K., Heise, D., Macy, D., Markovsky, B. and Skvoretz, J. (1994). Artificial social intelligence, *Annu. Rev. Sociol.* **20**, pp. 407–436.

de Balzak, H. (1998). *The Lily of the Valley* (Project Gutenberg). [ftp://sailor.gutenberg.org/pub/gutenberg/etext98/tlotv10.txt]

de Balzak, H. (1972). *The Chouans*, transl. M. A. Crawford (Penguin, London, 1972) (Project Gutenberg, 1999). [ftp://ibiblio.org/pub/docs/books/gutenberg/etext99/choun10.txt]

Barbalet, J. M. (2000). *Emotion, Social Theory, and Social Structure* (Cambridge University Press).

Barr, A. E. (1995). *Remember the Alamo* (Project Gutenberg). [ftp://sailor.

gutenberg.org/pub/gutenberg/etext95/alamo10.txt]

Bates, J. (1994). The role of emotions in believable agents, *Commun. ACM* **37**, pp. 122–125.

Bateson, G., Jackson, D. D., Haley, J. and Weakland, J. (1956). Toward a theory of schizophrenia, *Behav. Sci.* **1**, pp. 251–264.

Beattie, J. (1998). My Mary. In: *Bulchevy's Book Of English Verse*, Verse No. 471 (Project Gutenberg). [ftp://ibiblio.org/pub/docs/books/gutenberg/etext90/pgbev10.zip]

Beckmann, M. J. (1971). Market share, distance and potential, *Reg. Urban Econ.* **1**, pp. 3–18.

Belnap, N. D. (1971). How a computer should think. In: *Contemporary Aspects of Philosophy*, ed. G. Ryle (Oriel Press, London).

Bergstra, J. A., Bethke, I. and Rodenburg, P. (1995). A propositional logic with four values: true, false, divergent and meaningless, *J. Appl. Non-Class. Logics* **5**, pp. 199–218.

Berry, G. and Boudol, G. (1992). The chemical abstract machine, *Theor. Comput. Sci.* **96**, pp. 217–248.

Bochvar, D. A. (1939). On a three-valued calculus and its application to analysis of paradoxes of functional calculus of classical reasoning, *Mat. Sb.* **4**, pp. 287–308 (in Russian).

Bolc, L. and Borowik, P. (1992). *Many-Valued Logics* (Springer, Berlin).

Bonabeau, E. (1997). From classical models of morphogenesis to agent-based models of pattern formation, *Artif. Life* **3**, pp. 191–211.

Bonabeau, E., Theraulaz, G., Fourcassié, V. and Deneubourg, J.-L. (1998a). The phase-ordering kinetics of cemetery organization in ants, *Phys. Rev. E* **57**, pp. 4568–4571.

Boutilier, C. (1996). Abduction to plausible causes: an event-based model of belief update, *Artif. Intell.* **83**, pp. 143–166.

Breazeal, C. and Scassellati, B. (1999). How to build robots that make friends and influence people, *Proc. IRO99, Kyonjiu, Korea.* [http://citeseer.nj.nec.com/breazeal99how.html]

Burns, T. R. and Gomolinska, A. (2001). Socio-cognitive mechanisms of belief change: applications of generalized game theory to belief revision, social fabrication, and self-fulfilling prophesy, *Cognitive Syst. Res.* **2**, pp. 39–54.

Burstedde, C., Klauck, K., Schadschneider, A. and Zittartz, J. (2001). Simulation of pedestrian dynamics using a two-dimensional cellular automaton, *Physica A* **295**, pp. 507–525.

Butz, M. R. (1997). *Chaos and Complexity: Implications for Psychological Theory and Practice* (Taylor & Francis, London).

Callen, E. and Shapero, D. (1974). A theory of social imitation, *Phys. Today*, July, pp. 23–28. Cited in [Stauffer (2002)].

Carstensen, L. L., Gottman, J. M. and Levenson, R. W. (1995). Emotional behavior in long-term marriage, Psychol. Aging **10**, pp. 140–149.

Castelfranchi, C., Conte, R. and Paolucci, M. (1998). Normative reputation and the costs of compliance, *J. Artif. Soc. Soc. Simul.* **1**, p. 3. [http://www.soc.surrey.ac.uk/JASSS/1/3/3.html]

Castellano, C., Marsili, M. and Vespignani, A. (2000). Nonequilibrium phase transition in a model for social influence, *Phys. Rev. Lett.* **85**, p. 3536.

Chadwick, P., Birchwood, M. and Trower, P. (1996). *Cognitive Therapy for Delusions, Voices and Paranoia* (John Wiley).

Chalmers, D. (1996). *The Conscious Mind: In Search of a Fundamental Theory* (Oxford University Press).

Chandra, A. (1997). A computational architecture to model human emotions, *Proc. Intelligent Information Systems (IIS'97)*, ed. H. Adeli, pp. 86–89.

Chemical Kinetics Simulator 1.01, IBM Almaden Research Centre. [http://www.almaden.ibm.com/st/msim/ckspage.html]

Chua, L. (1998). *CNN: A Paradigm for Complexity* (World Scientific, Singapore).

Clements, R. R. and Hughes, R. L. (2004). Mathematical modelling of a mediaeval battle: the Battle of Agincourt, 1415, *Math. Comput. Simul.* **64**, pp. 259–269.

Colby, K. M. and Gilbert, J. P. (1964). Programming a computer model of neurosis, *J. Math. Psychol.* **1**, pp. 405–417.

Collins, W. (1999a). *The Legacy of Cain* (Project Gutenberg, 1999). [http://www.gutenberg.config.com/etext99/lcain10.txt]

Collins, W. (1999b). *The New Magdalen* (Project Gutenberg, 1999). [http://www.ibiblio.org/gutenberg/etext99/nmgdl10.txt]

Conlisk, J., Gong, J.-C. and Tong, C. H. (1997). Social interaction and the dynamic of norms, submitted to *J. Econ. Theory* (1997) (see http://weber.ucsd.edu/~ctong)

Conrad, J. (1998). *Tales of Unrest* (Project Gutenberg, 1998). [http://sailor.gutenberg.org/etext98/tnrst10.txt]

Coville, W. J., Costello, T. W. and Rouke, F. T. (1960). *Abnormal Psychology* (Barnes and Noble, New York).

Dawkins, R. (1976). *The Selfish Gene* (Oxford University Press).

Del Val, A., (1993). Syntactic characterizations of belief change operators, *Proc. 13th Int. Joint Conf. AI (IJCAI-93)*, Vol. 2, ed. R. Bajcsy (Morgan Kaufmann, San Mateo, 1993), pp. 540–545.

Dennet, D. (1991). *Consciousness Explained* (Penguin, London).

Derrida, B. (1987). Dynamical phase transition in nonsymmetric spin glasses, *J. Phys. A* **20**, pp. L721–L725.

Derrida, B. and Pomeau, Y. (1986). Random networks of automata: a simple annealed approximation, *Biophys. Lett.* **1**, 45–49.

Dittrich, P., Ziegler, J. and Banzhaf, W. (2001). Artificial chemistries — a review, *Artif. Life* **7**, pp. 225–275.

Doran, J. (1998). Simulation collective misbelief, *J. Artif. Soc. Soc. Simul.* **1**, p. 1. [http://www.soc.surrey.ac.uk/JASSS/1/1/3.html]

Dubois, D. and Prade, H. (1992). Evidence, knowledge, and belief functions, *Int. J. Approx. Reason.* **6**, pp. 295–319.

Dumas, A. (1998a). *Ten Years Later* (Project Gutenberg, 1998). [ftp://ibiblio.org/pub/docs/books/gutenberg/etext98/2musk10.txt]

Dumas, A. (1998b). *The Count of Monte Cristo* (Oxford University Press, 1998) (Project Gutenberg, 1998). [ftp://ibiblio.org/pub/docs/books/

gutenberg/etext98/crsto10.txt]

Ebeling, W. and Schweitzer, F. (2002). Self-organization, active Brownian dynamics, and biological applications, *Nova Acta Leopoldina.* [arXiv:cond-mat/0211606v1]

Ebeling, W., Schweitzer, F. and Tilch, B. (1999). Active Brownian particles with energy depots modeling animal mobility, *Biosystems* **49**, pp. 17–29.

Eckman, P. (1992). Are there basic emotions?, *Psychol. Rev.* **99**, pp. 550–553.

Eliot, G. (1996). *Adam Bede* (Project Gutenberg). [ftp://sailor.gutenberg.org/pub/gutenberg/etext96/adamb10.txt]

El-Nasr, M. S., Ioerger, T. R. and Yen, J. (2001). A web of emotions, *Workshop on Emotion-Based Agent Architectures, Seattle*

Epstein, J. M. and Axtell, R. L. (1996) *Growing Artificial Societies* (MIT Press, Cambridge, MA).

Fagin, R. and Halpern, J. (1988). Belief, awareness and limited reasoning, *Artif. Intell.* **34**, pp. 39–76.

Farkas, I., Helbing, D. and Vicsek, T. (2002). Crowd behaves as excitable media during Mexican wave, *Nature* **419**, pp. p. 131. See also http://angel.elte.hu/wave/.

Farkas, I., Helbing, D. and Vicsek, T. (2003). Human waves in stadiums, *Physica A* **330**, pp. 18–24.

Festinger, L., Pepitone, A. and Newcomb, T. (1952). Some consequences of de-individuation in a group, *J. Abnorm. Soc. Psychol.* **47**, pp. 382–389.

Fontata, W. and Buss, L. W. (1996). The barrier of objects: from dynamical systems to bounded organizations, Santa Fe Institute Working Paper No. 96-05-035.

Franceschi, P. (2003). An analytical view of delusion. [http://cogprints.ecs.soton.ac.uk/archive/00003208]

Frank, R. (1998). *Passions Within Reason: The Strategic Role of the Emotions* (Norton, New York).

French, P. A. and Wettstein, H. K. (1999). *Philosophy of Emotions* (University of Notre Dame Press).

Freud, S. (1921). *Group Psychology and the Analysis of the Ego* (Hogarth Press, London).

Friedman, N. and Halpern, J. Y. (1996). A qualitative Markov assumption and its implications for belief change. In: *Uncertainty in Artificial Intelligence*, eds. E. Horvitz and F. Jensen (Morgan Kaufmann, San Francisco), pp. 263–273.

Frijda, N. H. and Mesquita, B. (2000). Beliefs through emotions. In: *Emotions and Beliefs. How Feelings Influence Thoughts*, eds. N. H. Frijda, A. S. R. Manstead and S. Bem (Cambridge University Press), pp. 45–77.

Frijda, N. H., Manstead, A. S. R. and Bem, S. (2000). The influence of emotions on beliefs. In: *Emotions and Beliefs. How Feelings Influence Thoughts*, eds. N. H. Frijda, A. S. R. Manstead and S. Bem (Cambridge University Press) pp. 1–10.

Gaboriau, E. (1995). *The Count's Millions* (Project Gutenberg). [ftp://sailor.gutenberg.org/pub/gutenberg/etext95/cntmi10.txt]

Gaboriau, E. (1999). *Other People's Money* (Project Gutenberg). [`ftp://sailor.gutenberg.org/pub/gutenberg/etext99/opmny10.txt`]

Galam, S. (2002). Modeling rumors: the no plane Pentagon French hoax case. [`arXiV:cond-mat/0211571v1` (2002)]

Gärdenfors, P. (1990). *Knowledge in Flux: Modeling the Dynamics of Epistemic States* (Bradford Books).

Gaspar, G. (1991). Communication and belief changes in a society of agents: towards a formal model of an autonomous agent, *Decentralized A.I., Proc. 2nd Eur. Workshop Modelling Autonomous Agents in a Multi-Agent World*, eds. Y. Demazeau and J. P. Muller (North-Holland, Amsterdam), pp. 245–255.

Gerasimova, I. A. (1989). *Norms with Provisoes and Discursions in Lack of Information* (Nauka, Moscow) (in Russian).

Gilbert, N. and Conte, R. (1995). *Artificial Societies: The Computer Simulation of Social Life* (UCL Press, London).

Giunchiglia, F., Serafini, L., Giunchiglia, E. and Frixione, M. (1993). Non-omniscient belief as context-based reasoning, *Proc. 13th Int. Joint Conf. AI (IJCAI-93)*, Vol. 2, ed. R. Bajcsy (Morgan Kaufmann, San Mateo), pp. 548–554.

Goertzel, B. (1996). On the algebraic structure of consciousness, *Dyn. Psychol.* [`http://www.goertzel.org/dynapsyc/1996`]

Goldenberg, J., Libai, B., Solomon, S., Jan, N. and Stauffer, D. (2000). Marketing percolation, *Physica A* **284**, pp. 335–347.

Goleman, D. (1996). *Emotional Intelligence* (Bloomsbury, London).

Goles, E. and Hernández, G. (2000). Dynamical behavior of Kauffman networks with AND-OR gates, *J. Biol. Cybernet.* **8**, pp. 151–175.

Gottman, J. M. (1997). What should be the focus of emotion regulation in children? A nonlinear dynamic mathematical model of children's peer interaction in groups, *Dev. Psychopathol.* **9**, pp. 421–452.

Graumann, C. F. (1985). Crowd mind and behaviour: afterthoughts. In: *Changing Conceptions of Crowd Mind and Behaviour*, eds. C. F. Graumann and S. Moscovici (Springer, Berlin), pp. 217–228.

Graumann, C. F. and Moscovici, S. (1985). (Eds.) *Changing Conceptions of Crowd Mind and Behaviour* (Springer, Berlin).

Guastello, S. (1995). *Chaos, Catastrophe, and Human Affairs: Applications of Nonlinear Dynamics to Work Organizations, and Social Evolution* (Lawrence Erlbaum, Mahwah, NJ).

Gutowitz, H. and Langton, C. (1995). Mean field theory of the edge of chaos, *Lect. Notes Artif. Intell.* **929**, pp. 52–64.

Hadley, R. F. (1988). Logical omniscience, semantics, and models of belief, *Comput. Intell.* **4**, pp. 17–30.

Hadley, R. F. (1991a). The many uses of "belief" in AI, *Minds Mach.* **1**, pp. 55–74.

Hadley, R. F. (1991b). A sense-based, process model of belief, *Minds Mach.* **1**, pp. 279–320.

Hagen, E. H. (1995). Intraspecific exploitative mimicry in humans, *Human*

Behavior and Evolution Society Annu. Meet., Santa Barbara, CA, June. [http://cogprint.ecs.soton.ac.uk/archive/00000756/00/dd.html]

Hameroff, S. (1998). Quantum computation in brain microtubules? The Penrose–Hameroff Orch OR model of consciousness, *Philos. Trans. R. Soc. Lond. A* **356**, pp. 1869–1896.

Hameroff, S. (2001). Consciousness, the brain, and spacetime geometry, *Ann. N. Y. Acad. Sci.* **929**, pp. 74–104.

Hameroff, S. and Penrose, R. (1996). Conscious events as orchestrated space–time selections, *J. Conscious. Stud.* **2**, pp. 36–53.

Hameroff, S., Nip, A., Porter, M. and Tuszynski, J. (2002). Conduction pathways in microtubules, biological quantum computation, and consciousness, *BioSystems* **64**, pp. 149–168.

Hansen, C. H. and Hansen, R. D. (1988). Finding the face in the crowd: an anger superiority effect, J. Pers. Soc. Psychol. **54**, pp. 917–924.

Hardy, T. (1994). *Return of the Native* (Penguin, London, 1994). (Project Gutenberg). [ftp://ibiblio.org/pub/docs/books/gutenberg/etext94/nativ10.txt]

Hatfield, E., Cacioppo, J. T. and Rapson, R. L. (1992). Primitive emotional contagion, *Rev. Pers. Soc. Psychol.* **14**, pp. 151–177.

Hatfield, E., Cacioppo, J. T. and Rapson, R. L. (1994). *Emotional Contagion* (Cambridge University Press).

Hegselmann, R. and Flache, A. (1998). Understanding complex social dynamic: a plea for cellular automata based modelling, *J. Artif. Soc. Soc. Simul.* **1**, p. 3. [http://www.soc.surrey.ac.uk/JASSS/1/3/1.html]

Heise, D. R. (1998). Conditions for emphatic solidarity. In: *The Problems of Solidarity: Theories and Models*, eds. P. Doreian and T. Fararo (Gordon and Breach, Amsterdam), pp. 197–211.

Heise, D. R. and O'Brien, J. (1993). Emotion expression in groups. In: *Handbook of Emotions*, eds. M. Lewis and J. M. Haviland (Guilford Press, New York), pp. 489–497.

Heise, D. R. and Weir, B. (1999). A test of symbolic interactionist predictions about emotions in imagined situations, *Symb. Interact.* **22**, pp. 139–161.

Helbing, D. (1991). A mathematical model for the behaviour of pedestrians, *Behav. Sci.* **36**, pp. 298–310.

Helbing, D. (1992). A fluid-dynamic model for the behaviour of pedestrians, *Complex Syst.* **6**, pp. 391–415.

Helbing, D. (1993). Boltzmann-like and Boltzmann–Fokker–Planck equations as a foundation of behavioral models, *Physica A* **196**, pp. 546–573.

Helbing, D. (1995a). Theoretical foundation of macroscopic traffic models, *Physica A* **219**, pp. 375–390.

Helbing, D. (1995b). *Quantitative Sociodynamics* (Kluwer Academic, Dordrecht).

Helbing, D. and Molnár, P. (1995). Social force model for pedestrian dynamics, *Phys. Rev. E* **51**, pp. 4282–4286.

Helbing, D., Farkas, I. J. and Vicsek, T. (2000). Simulating dynamical features of escape panic, *Nature* **407**, pp. 487–490.

Helbing, D., Molnár, P. and Schweitzer, F. (1998). Computer simulation of pedes-

trian dynamics and trail formation. [xxx.lanl.gov/cond-mat/9805074]
Helbing, D., Hennecke, D., Shvetsov, V. and Treiber, M. (2002). Micro- and macro-simulation of freeway traffic, *Math. Comput. Modelling* **35**, pp. 517–547.
Hess, U. and Blairy, S. (2001). Facial mimicry and emotional contagion to dynamic emotional facial expressions and their influence on decoding accuracy, *Int. J. Psychophysiol.* **40**, pp. 129–141.
Hillman, J. (1992). *Emotion. A Comprehensive Phenomenology of Theories and Their Meaning for Therapy* (Northwestern University Press).
Hogg, T. and Huberman, B. A. (1998). Controlling smart matter, *Smart Mater. Struct.* **7**, pp. 1–14.
Hołyst, J. A., Kacperski, K. and Schweitzer, F. (2000). Phase transitions in social impact models of opinion formation, *Physica A* **285**, pp. 199–210.
Ilachinski, A. (2001). *Cellular Automata: A Discrete Universe* (World Scientific, Singapore).
Ilachinski, A. (2004). *Artificial War: Multiagent-Based Simulation of Combat* (World Scientific, Singapore).
Izard, C. E., Kagan, J. and Zajonc, R. B. (1998). *Emotions, Cognition and Behaviour* (Cambridge University Press).
Jager, W., Popping, R. and van de Sande, H. (2001). Clustering and fighting in two party crowds: simulating the approach avoidance conflicts, *J. Artif. Soc. Soc. Simul.* **4**. [`www.soc.surrey.ac.uk/JASS/4/3/7.html`]
Kabashima, Y. (2002). Propagating beliefs in spin glass models. [`arXiv: cond-mat/0211500v1`]
Kacperski, K. and Hołyst, J. A. (1999). Opinion formation model with strong leader and external impact: a mean field approach, *Physica A* **269**, pp. 511–526.
Kacperski, K. and Hołyst, J. A. (2000). Phase transitions as a persistent feature of groups with leaders in models of opinion formation, *Physica A* **287**, pp. 631–643.
Kauffman, S. A. (1969). Metabolic stability and epigenesis in randomly constructed genetic nets, *J. Theor. Biol.* **22**, pp. 437–467.
Kauffman, S. A. (1993). *The Origins of Order: Self-Organization and Selection in Evolution* (Oxford University Press).
Kaufman, B. E. (1999). Emotional arousal as a source of bounded rationality, *J. Econ. Behav. Organ.* **38**, pp. 135–144.
Kenny, A. (1994). *Action, Emotion and the Will* (Thoemmes Press, London).
Kirchner, A. and Schadschneider, A. (2002). Simulation of evacuation processes using a bionics-inspired cellular automaton model for pedestrian dynamics, *Physica A* **312**, pp. 260–276.
Kleene, S. C. (1938). On a notation for ordinal numbers, *J. Symb. Logic* **3**, pp. 150–155.
Klein, J. (1956) *The Study of Groups* (Routledge and Kegan Paul, New York).
Kraus, S. and Lehmann, D. (1988). Knowledge, belief and time, *Theor. Comput. Sci.* **58**, pp. 155–174.
Kraus, S. and Perlis, D. (1989). Assessing others' knowledge and ignorance, *Proc.*

4th Int. Symp. Methodologies for Intelligent Systems, pp. 220–225. [http://www.cs.umd.edu/projects/active/papers/know-ign.ps]

Kruse, L. (1986). Conceptions of crowds and crowding. In: *Changing Conceptions of Crowd Mind and Behaviour*, eds. C. F. Graumann and S. Moscovici (Springer, Berlin), pp. 117–142.

Lakemeyer, G. (1991). A computationally attractive first-order logic of belief, *Logics in AI: Proc. Eur. Workshop JELIA '90*, ed. J. Van Eijck (Springer, Berlin), pp. 333–347.

Lang, A. (1996). *Letters to Dead Authors* (Project Gutenberg). [http://www.ibiblio.org/gutenberg/etext98/letda10.txt]

Langton, C. G. (1990). Computation at the edge of chaos: phase transitions and emergent computation, *Physica D* **42**, pp. 12–27.

Lanzetta, J. T. and Englis, B. G. (1989). Expectations of cooperation and competition and their effects on observers' vicarious emotional responses, *J. Pers. Soc. Psychol.* **33**, pp. 354–370. Cited in [Hess and Blairy (2001)].

Le Bon, G. (!994). *The Crowd: A Study of the Popular Mind* (Traders Press, Greenville); first edition published in 1895.

Leppänen, J. M., Tenhunen, M. and Hietanen, J. K. (2003). Faster choice-related times to positive than to negative facial expressions, *J. Psychophysiol.* **17**, pp. 113–123.

Lettvin, J. Y. and Pitts, W. (1943). A mathematical theory of the affective psychoses, *Bull. Math. Biophys.* **5**, pp. 139–148.

Levenson, R. W. and Ruef, A. M. (1997). Physiological aspects of emotional knowledge and rapport. In: *Emphatic Accuracy*, ed. W. J. Ickes (Guilford Press, New York), pp. 44–72.

Levesque, H. J. (1984). A logic of implicit and explicit belief. In: *Proc. Nat. Conf. Artif. Intell. AAAI 84*, pp. 198–202.

Levy, D. and Nail, P. R. (1993). Contagion: a theoretical and empirical review and reconceptualization, *Soc. Gen. Psychol. Monogr.* **119**, pp. 183–235.

Lewis, M. and Haviland-Jones, J. M. (Eds.) (2000). *Handbook of Emotions* (Guilford Press, New York).

Ligomenides, P. A. (1991). Computation and uncertainty in regulated synergetic machines, *Uncertainty in Knowledge Bases (IPMU'90): 3rd Int. Conf. Information Processing and Management of Uncertainty in Knowledge-Based Systems*, eds. B. Bouchon-Meunier, R. R. Yager and L. A. Zadeh (Springer, Berlin), pp. 413–422.

Lindmark, K. and Heckmann, D. (2000). Interpreting symptoms of cognitive load and time pressure in manual input, *8th GI Workshop Adaptivity and User Modeling in Interactive Software Systems (ABIS-2000), Osnabrueck, Germany.*

Loring, M. T. (1994). *Emotional Abuse* (Maxwell Macmillan, Toronto, 1994).

Łukasiewicz, J. (1920). On three-valued logic, *Ruch Filos.* **3**, pp. 169–171 (in Polish).

Lundqvist, L. O. and Dimberg, U. (1995). Facial expressions are contagious, *J. Psychophysiol.* **9**, pp. 203–211.

Lyons, W. (1980). *Emotion* (Cambridge University Press).

Mahmassani, H. S. (1990). Dynamic models of commuter behavior: experimental investigation and application to the analysis of planned traffic disruptions, *Transp. Res. A* **24**, pp. 465–484.

Mahmassani, H. S., Jayakrishnan, E. and Herman, R. (1990). Network traffic flow theory: microscopic simulation experiments on supercomputers, *Transp. Res. A* **24**, pp. 149–162.

Manevitz, L. M. (1989). Knowledge automata, *Proc. 17th IASTED Int. Symp. Simulation and Modelling*, ed. M. H. Hamza (ACTA Press, Anaheim), pp. 353–356.

Marchant, K. (1999). A logic table of emotional functions, *International Workshop on Affect in Interactions.*

Marin, I. and Sappington, J. (1994). A machine with "feelings": system models of emotional behavior, *Proc. World Congr. Neural Networks, San Diego, CA*, Vol. 1.

Marsden, P. (1998). Memetics and social contagion: two sides of the same coin, *J. Memet.* **2** [`http://www.cpm.mmu.ac.uk/jom-emit/1998/vol2/marsden\_p.html`]

Martin, E. D. (1920). *Behavior of Crowds* (Harper & Brother, New York).

Martins, J. P. and Shapiro, S. C. (1988). A model for belief revision, *Artif. Intell.* **35**, pp. 25–79.

Marx, G. T. and McAdam, D. (1994). *Collective Behavior and Social Movements: Process and Structure* (Prentice-Hall).

Mayne, T. J. and Ramsey, J. (2001). The structure of emotions: a nonlinear dynamic systems approach. In: *Emotions: Currrent Issues and Future Directions. Emotions and Social Behavior*, eds. T. J. Mayne and G. Bonanno (Guilford Press, New York), pp. 1–37.

McCarthy, J. (1979). Ascribing mental qualities to machines. [`http://www-formal.stanford.edu/jmc`]

McCullock, W. S. and Pitts, W. H. (1943). A logical calculus of the ideas immanent in nervous activity, *Bull. Math. Biophys.* **5**, pp. 115–133.

McDougall, W. (1921). *The Group Mind* (Cambridge University Press).

McMullin, B. and Varela, F. J. (1997). Rediscovering computational autopoiesis, Santa Fe Institute Working Paper No. 97-02-012.

McPhail, C. (1991). *The Myth of the Madding Crowd* (Aldine de Gruyter, New York).

McPhail, C. (2001). *Acting Together: The Social Organization of Crowds* (Aldine De Gruyter, New York).

Melges, F. T. and Fougerousse, C. E. (1966). Time, sense, emotions, and acute mental illness, *J. Psychiatr. Res.* **4**, pp. 127–140.

Melo, F., Umbanhowar, P. B. and Swinney, H. L. (1995). Hexagons, kinks, and disorder in oscillated granular layers, *Phys. Rev. Lett.* **75**, pp. 3838–3841.

Meynell, A. K. (1999). *The Children* (Project Gutenberg). [`ftp://ibiblio.org/pub/docs/books/gutenberg/etext99/chldn10.txt`]

Milton, J. (1999). *Poetical Works* (Project Gutenberg, 1999). [`http://www.ibiblio.org/gutenberg/etext99/pmsjm10.txt`]

Minsky, M. L. (1988). *The Society of Mind* (Simon and Schuster, New York).

Molloy, J. F. (1999). *Royalty Restored* (Project Gutenberg). [http://www.ibiblio.org/gutenberg/etext99/rruc210.txt]

Montgomery, L. M. (1992). *Anne of Avonlea* (Project Gutenberg). [ftp://sailor.gutenberg.org/pub/gutenberg/etext92/avon10.txt]

Morgan, R. L. and Heise, D. (1988). Structure of emotions, *Soc. Psychol. Q.* **51**, pp. 19–31.

Morley, C. (1994). *The Haunted Bookshop* (Wildside Press, 2001) (Project Gutenberg). [ftp://ibiblio.org/pub/docs/books/gutenberg/etext94/hbook10.txt]

Moscovici, S. (1985). Introduction. In: *Changing Conceptions of Crowd Mind and Behaviour*, eds. C. F. Graumann and S. Moscovici (Springer, Berlin), pp. 1–4.

Moscovici, S. (1985). The discovery of masses. In: *Changing Conceptions of Crowd Mind and Behaviour*, eds. C. F. Graumann and S. Moscovici (Springer, Berlin), pp. 5–25.

Mullen, P. E. (1997). The mental states and states of mind. In: *The Essentials of Postgraduate Psychiatry*, eds. R. Murray, P. Hill and P. McGuffin (Cambridge University Press), pp. 3–40.

Murray, R. M. (1997). Schizophrenia. In: *The Essentials of Postgraduate Psychiatry*, eds. R. Murray, P. Hill and P. McGuffin (Cambridge University Press), pp. 281–309.

Nagatami, T. (2003). Chemical-reaction model for Mexican wave, *Physica A* **323**, pp. 677–685.

Nota, G., Orefice, S., Pacini, G., Ruggiero, F. and Tortora, G. (1993). Legality concepts for three-valued logic programs, *Theor. Comput. Sci.* **120**, pp. 45–68.

Nowak, C. and Eklund, P. W. (1994). On combinatorial possible worlds, *AI'94, Sowing the Seeds for the Future, Proc. 7th Australian Joint Conf. AI*, eds. C. Zhang, J. Debenham and D. Lukose (World Scientific, Singapore), pp. 187–194.

Nowak, A., Szamrej, J. and Latane, B. (1990). From private attitude to public opinion: a dynamic theory of social impact, *Psychol. Rev.* **97**, pp. 362–376.

Oatley, K. (1992). *Best Laid Schemes: The Psychology of The Emotions* (Cambridge University Press).

O'Hara, K., Reichgelt, H. and Shadbolt, N. (1995). Avoiding omnidoxasticity in logics of belief: a reply to MacPherson, *Notre Dame J. Formal Logic* **36**, pp. 475–495.

Ortega y Gasset, J. (1985). *The Revolt of Masses* (University of Notre Dame Press).

Paar, D. W. (1992). Introducing confusion to create change, *Psychother. Patient* **8**, pp. 93–102.

Paris, J. B. and Vencovska, A. (1993). A model of belief, *Artif. Intell.* **64**, pp. 197–241.

Partick, C. J. and Zempolich, A. (1998). Emotion and aggression in the psychopatic personality, *Aggress. Violent Behav.* **3**, pp. 303–338.

Paulus, P. B. and Nagar, D. (1989). Environmental influences on groups. In: *Psy-*

chology of Group Influence, ed. P. B. Paulus (Lawrence Erlbaum, Mahwah, NJ), pp. 111–140.

Picard, R. W. (197). *Affective Computing* (MIT Press, Cambridge, MA).

Planalp, S. (1999) *Communicating Emotion* (Cambridge University Press).

Plewczyński, D. (1998). Landau theory of social clustering, *Physica A* **261**, pp. 608–617.

Prentice-Dunn, S. and Rogers, R. W. (1989). Deindividuation and the self-regulation of behavior. In: *Psychology of Group Influence*, ed. P. B. Paulus (Lawrence Erlbaum, Mahwah, NJ), pp. 87–109.

Press, W. H., Flannery, B. P., Teukolsky, S. A. and Vetterling, W. T. (1993). *Numerical Recipes in C: The Art of Scientific Computing* (Cambridge University Press).

Proykova, A. and Stauffer, D. (2002). Social percolation and the influence of mass media, *Physica A* **312**, pp. 300–304.

Rashevsky, N. (1949). Mathematical biology of social behavior, *Bull. Math. Biophys.* **11**, pp. 105–113.

Read, S. J. and Miller, L. C. (Eds.) (1998). *Connectionist Models of Social Reasoning and Social Behaviour* (Lawrence Erlbaum, Mahwah, NJ).

Reicher, S. (1987). Crowd behaviour as social action. In: *Rediscovering the Social Group*, ed. J. C. Turner (Basil Blackwell, Oxford), pp. 171–202.

Reisenzein, R. (1996). Emotional action generation. In: *Processes of the Moral Regulation of Behavior*, eds. W. Battman and S. Dutke (Pabst Science, Lengerich), pp. 151–165.

Reisenzein, R. (1998). Outlines of a theory of emotions as metarepresentational states of mind, *Proc. 10th Conf. Int. Soc. for Research on Emotions*, ed. A. H. Fischer (ISRE, Amsterdam), pp. 186–191.

Rescher, N. (1969). *Many-Valued Logic* (McGraw-Hill, New York).

Rowe, N. (1989). *Rules and Institutions* (University of Michigan Press, Ann Arbor).

Russell, J. A. (1980). A circumplex model of affect, *J. Pers. Soc. Psychol.* **36**, pp. 1161–1178.

Saam, N. J. and Harrer, A. (1999). Simulating norms, social inequality, and functional change in artificial societies, *J. Artif. Soc. Social Simul.* **2**, p. 1. [`http://www.soc.surrey.ac.uk/JASSS/2/1/2.html`]

Schaller, M. and Svozil, K. (1996). Automaton logic, *Int. J. Theor. Phys.* **35**, pp. 911–940.

Scheeff, M., Pinto, J., Rahardja, K., Snibbe, S. and Tow, R. (2000). Experiences with Sparky, a social robot, *Proc. Workshop Interactive Robotics in Entertainment* (Carnegie Mellon University, Pittsburgh). [`http://citeseer.nj.nec.com/428152.html`]

Schelling, T. C. (1971). Dynamic models of segregation, *J. Math. Sociol.* **1**, pp. 143–186. Cited in [Stauffer (2002)].

Schimansky-Geier, L., Mieth, M., Rosé, H. and Malchow, H. (1995). Structure formation by active Brownian particles, *Phys. Lett. A* **207**, pp. 140–146.

Schweitzer, F. and Schimansky-Geier, L. (1994). Clustering of "active walkers" in a two-component system, *Physica A* **206**, pp. 359–379.

Shakespeare, W. (1997a). *The Taming of the Shrew* (Project Gutenberg, 1997). [http://www.ibiblio.org/gutenberg/etext97/1ws1010.txt]

Shakespeare, W. (1997b). *Love's Labour's Lost* (Project Gutenberg, 1997). [http://www.ibiblio.org/gutenberg/etext99/1ws1211j.txt]

Slesinger, J. A. (1968). Study of community opinions concerning the summer 1967 civil disturbance in Milwaukee (The University of Wisconsin-Milwaukee Office).

Smelser, N. J. (1962). *Theory of Collective Behaviour* (Free Press, New York).

Sobociński, B. (1952). Axiomatization of partial system of three-valued calculus of propositions, *J. Comput. Syst.* **11**, pp. 23–55.

Sociophysics, (2002). Abstract Booklet (University of Bielefeld). [http://ais.gmd.de/$\sim$frank/sociophysics]

Solomon, S., Weisbuch, G., de Arcangelis, L., Jan, N. and Stauffer, D. (2000). Social percolation models, *Physica A* **277**, pp. 239–247.

Snyder, D. M. (1991). Alternative view of schizophrenic cognition, *Speculat. Sci. Technol.* **14**, pp. 211–217.

Stauffer, D. (2002). Sociophysics simulations [arXiv:cond-mat/0210213v1]

Stauffer, D. and Kułakowski, K. (2002). Why everything gets slower? [arXiv:cond-mat/0210225v1]

Stein, B. D. and Myers, D. (1999). Emotional sequelae of disasters: a primary care physician guide, *J. Am. Med. Womens Assoc.* **54**, pp. 60–64.

Stoker, B. (1993). *Dracula* (Wordsworth Classics).

Strassburger, G. and Rehberg, I. (2000). Crystallization in a horizontally vibrated monolayer of spheres, *Phys. Rev. E* **62**, pp. 2517–2520.

Sulis, W. and Combs, A. (Eds.) (1996). *Nonlinear Dynamics in Human Behaviour* (World Scientific, Singapore).

Summers, C. and Markusen, E. (Eds.) (1999). *Collective Violence* (Rowman and Littlefield, Lanham)

Svozil, K. and Zapatrin, R. R. (1996). Empirical logic of finite automata: miscrostatements versus macrostatements, *Int. J. Theor. Phys.* **35**, pp. 1541–1548.

Tambe, M., Johnson, L. and Shen, W. M. (1998). Adaptive agent tracking in real-world multiagent domains: a preliminary report, *Int. J. Hum.-Comput. Stud.* **48**, pp. 105–124.

Taylor, J. A., Carletta, J. and Mellish, C. (1996). Requirements for belief models in cooperative dialogue, *User Modeling User Adapted Interact.* **6**, pp. 23–68.

The Holy Bible, Douay-Rheims version, both testaments (Project Gutenberg, 1998) [http://www.ibiblio.org/gutenberg/etext99/2drvb10.txt]

de Tocqueville, A. (1998). *Democracy in America*, Vol. 1, transl. F. Bowen (Wordsworth). Transl. H. Reeves (Project Gutenberg, 1997). [http://www.ibiblio.org/gutenberg/etext97/1dina10.txt]

Toffoli, T. and Margolus, N. (1987). *Cellular Automata Machines: A New Environment for Modelling* (MIT Press, Cambridge, MA).

Toffoli, T. and Margolus, N. (1991). Programmable matter, *Physica D* 47, pp. 263–272.

Tsetlin, M. L. (1973). *Automaton Theory and Modelling of Biological Systems* (Academic Press, New York).

Tuomela, R. (1996). Philosophy and distributed artificial intelligence. The case of joint intention. In: *Foundations of Distributed Artificial Intelligence*, eds. N. Jennings and G. O'Hare (John Wiley, New York), pp. 487–503.

Turner, J. C. (1987). *Rediscovering the Social Group. A Self-Categorization Theory* (Basil Blackwell, Oxford).

Ullman-Margalit, E. (1978). *The Emergence of Norms* (Oxford University Press).

Umbanhowar, P. B., Melo, F. and Swinney, H. L. (1996). Localized excitations in a vertically vibrated granular layer, *Nature* **382**, pp. 793–796.

Valente, A. and Breuker, J. (1994). A commonsense theory of normative systems, *Proc. ECAI'94: Workshop Artificial Normative Reasoning*, ed. J. Breuker.

Vallacher, R. R. and Nowak, A. (1994). *Dynamics Systems in Social Psychology* (Academic Press).

Varela, F. J., Maturana, H. R. and Uribe, R. (1974). Autopoiesis: the organization of living systems, its characterization and a model, *BioSystems* **5**, pp. 187–196.

Vicsek, T., Czirók, A., Ben-Jacob, E., Cohen, I. and Shochet, O. (1995). Novel type of phase transition in a system of self-driven particles, *Phys. Rev. Lett.* **75**, pp. 1226–1228.

Visser, A. and Nagel, K. (2001). Traffic simulation, *Future Generat. Comput. Syst.* **17**, pp. 625–626.

Volker, L. G. and Conrad, M. (1998). The role of weak interactions in biological systems: the dual dynamics model, *J. Theor. Biol.* **193**, pp. 287–306.

Walpole, H. (2003). *The Captives* (Project Gutenberg). [`http://www.ibiblio.org/gutenberg/etext03/cptvs10.txt`]

Weidlich, W. (1991). Physics and social science — the approach of synergetics, *Phys. Rep.* **204**, pp. 1–163.

Weidlich, W. (2000). *Sociodynamics: A Systematic Approach to Mathematical Modelling in the Social Sciences* (Taylor & Francis, London).

Wiedermann, J. (1998a). The cogitoid: a computational model of cognitive behaviour, Institute of Computer Science, Academy of Sciences of the Czech Republic, Tech. Rep. No. 743.

Wiedermann, J. (1998b). Towards algorithmic explanation of mind evolution and functioning, *Proc. MFCS'98, 1998*, ed. L. Brim *et al* (Lect. Notes Comput. Sci. **1450**), pp. 152–166.

Wild, B., Erb, M. and Bartels, M. (2001). Are emotions contagious? Evoked emotions while viewing emotionally expressive faces: quality, quantity, time course and gender differences, *Psychiatry Res.* **102**, pp. 109–124.

Winters, K. C. and Neale, J. M. (1983). Delusions and delusional thinking in psychotics: a review of the literature, *Clin. Psychol. Rev.* **3**, pp. 227–253.

Wolf, D. E. (1999). Cellular automata for traffic simulations, *Physica A* **263**, pp. 438–451.

Wuensche, A. (1994). The ghost in the machine: basins of attraction of random Boolean networks. In: *Artificial Life III*, ed. C. G. Langton (Santa Fe Institute Stud. Sci. Complexity) (Addison-Wesley, Reading, MA).

Wuensche, A. (1996). The emergence of memory; categorisation far from equilibrium. In: *Towards a Science of Consciousness: The First Tuscon Discussions and Debates*, eds. S. R. Hameroff, A. W. Kaszniak and A. C. Scott (MIT Press, Cambridge, MA).

Wuensche, A. and Lesser, M. (1992). *The Global Dynamics of Cellular Automata* (Addison-Wesley, Reading, MA).

Yager, P. R., Ford, K. M. and Agnew, N. A. (1992). A formal constructivist model of belief revision, *Int. J. Expert Syst. Res. Appl.* **5**, pp. 157–168.

Zak, M. (2000). Dynamics of intelligent systems, *Int. J. Theor. Phys.* **39**, pp. 2107–2140.

Zak, M., Zbilut, J. P. and Meyers, R. E. (1997). *From Instability to Intelligence: Complexity and Predictability in Nonlinear Dynamics* (Springer, Berlin).

Ziller, R. C. (1964). Individuation and socialization, *Hum. Relat.* **17**, pp. 341–360.

Zimbardo, P. G. (1969). The human choice: individuation, reason, and order versus deindividuation, impulse, and chaos, *Nebraska Symp. Motivation*, pp. 237–307.

Index

abuse
  emotion, 41
affecton, 48
  coupled, 58
  probabilistic, 54
  reflecting, 57
agent
  hyper-sensitive, 205
aggression, 42
aging
  emotion, 29
algebra
  doxastic, 73
anger, 25, 28, 32, 35, 48
anxiety, 48
anxious
  agent, 75, 80, 91, 94
  algebra, 76
  chemistry, 100
artificial chemistry, 11
artificial society, 9
attachment
  anxious, 42
automata
  emotional, 48
  state transition, 49

belief
  collective, 68
breather, 163

cellular automata, 3, 11
chemical machine, 10
circumplex model, 25
cogitoid, 9
complexity
  connectives, 174
  logic, 173
computational chemistry, 10
confusion, 25, 32, 35, 48
consciousness, 4, 10
conservative
  agent, 75, 80, 90, 94
  algebra, 76
contradicting
  agent, 76, 80, 91, 93
contrition, 42
crowd
  hyper-active, 183
  hypo-active, 183

deficiency
  emotion, 33
deindividuation, 5, 6, 68
delusion, 69
derationalization, 5
detachment
  emotion, 43
disaster, 34
dissolution, 188
domains
  emotion, 39
double bind, 182
doubt, 69

doxastic
  chemistry, 99
  composition
    irrational, 70
  state
    dominating, 144
    extinct, 144
    generative, 146
  word
    reactions, 97
  world, 96
    non-constructible, 97
    stable, 96
doxaton, 17, 73, 116
  normalized, 117
  reflecting, 118
  reflective, 77
  static complexity, 121
  transition graph, 117

emotional contagion, 24, 65
epistemic set, 69

fear, 25, 28, 32

generator
  doxastic, 73
glider, 165, 169

happiness, 25, 28, 32, 35, 42, 48
hostility, 218
hyper-sociality, 186

idempotent, 57
ignorance, 69
injunction
  negative, 183
interval
  sensitivity, 182
irrationality, 183

Kauffman network, 151
knowledge, 69

labyrinthine patterns, 91
Langton parameter, 121, 171, 210

logic
  Łukasiewicz, 154
  bifurcatory, 156
  Bochvar, 154
  Hallden, 180
  Kleene, 154
  multiple-valued, 152
  oscillatory, 156
  Sobociński, 180
  three-valued, 152

Markov chain, 54, 79
misbelief, 69
molecular dynamics, 1

naive
  agent, 75, 80, 90, 92
  algebra, 76
network
  Boolean, 152
  logical, 151
non-sense functor, 74
norm
  definition, 112
  principal, 117, 118
  social, 112

opinion formation, 2
oscillation
  emotion, 29, 33
  logic, 159
    chaotic, 166
outburst
  anger, 42
  emotion, 39

Pascal triangle, 124, 170
pattern
  condensed, 205
  granular, 205
  labyrinthine, 205
  porous, 205
  sparse, 205

quiescent state, 81, 120

rational reactions, 102
reaction set
  stable, 38
reactivity
  emotion, 33
reflective
  agent, 77
relation
  interpersonal, 51

sadness, 25, 35, 48
schizophrenia, 182
sensitivity set, 204
sociophysics, 3
stable neighborhood, 121
state
  doxastic, 69
stirred crowd, 78

threshold
  activation, 198
tolerance, 217
transition
  global, 58

unreachable
  emotion, 60
unrest, 201, 219

violence, 219

wave
  emotion, 31, 34, 45